Driver Behaviour Modelling in Disordered Traffic Systems: Vehicle-following and Filtering Scenario

Thesis submitted in partial fulfilment of the requirements

for the award of the degree of

Doctor of Philosophy

in

Civil Engineering

by

Sanhita Das

Under the supervision of

Prof. Akhilesh Kumar Maurya

Department of Civil Engineering

Indian Institute of Technology Guwahati

Guwahati – 781039 Assam India

June, 2020

Department of Civil Engineering
Indian Institute of Technology Guwahati
Guwahati – 781039 Assam India

Certificate

This is to certify that this thesis entitled "**Driver Behaviour Modelling in Disordered Traffic Systems: Vehicle-following and Filtering Scenario**" submitted by **Sanhita Das**, in partial fulfilment of the requirements for the award of the degree of Doctor of Philosophy, to the Indian Institute of Technology Guwahati, Assam, India, is a record of the bonafide research work carried out by her under my guidance and supervision at the Department of Civil Engineering, Indian Institute of Technology Guwahati, Assam, India. In my opinion, the thesis work has reached the requisite standard fulfilling the requirement for the degree of Doctor of Philosophy in Civil Engineering. To the best of my knowledge, no part of the work reported in this thesis has been presented for the award of any degree at any other institution.

Date: June 2, 2020
Place: Guwahati

(Prof. Akhilesh Kumar Maurya)
Thesis Supervisor
Professor
Email: maurya@iitg.ac.in
Phone: +91-361-258-2426

Declaration

I hereby declare that

- The work contained in this thesis is original and has been done by myself and under the general supervision of my supervisor.

- The work reported herein has not been submitted to any other Institute for any degree or diploma.

- Whenever I have used materials (concepts, ideas, text, expressions, data, graphs, theoretical analysis, results, etc.) from other sources, I have given due credit by citing them in the text of the thesis and giving their details in the references.

June 2, 2020

(Sanhita Das)

Department of Civil Engineering
Indian Institute of Technology Guwahati
Guwahati, Assam, India 781039

Acknowledgements

This thesis is the result of my four and half years of research in Indian Institute of Technology Guwahati. It has probably been the most exciting, challenging, productive and fruitful period of my life. Indeed the final phase of my dissertation was a very challenging and stressful period. But I must say despite all the highs and lows, I have enjoyed most of my time. And this would not have been possible without the help and support of many people who have contributed in many ways in reaching this point.

First and foremost, I would like to express my heartfelt gratitude to my supervisor Prof. Akhilesh Kumar Maurya for his trust, support, guidance and giving me the freedom in doing research independently. I am highly obliged to him for extending his help and support in collecting video data during the initial stage of my research work. His technical and practical insights into the problem and new ideas coming from our discussions always motivated me to continue the research.

I would also like to thank other members of my dissertation doctoral committee- Prof. Subashisa Dutta, Prof. Rajan Choudhary and Prof. Anil Kumar Mishra for their insightful comments, timely suggestions and inspiration that helped me to improve the quality of my research. I am also grateful to Prof. Partha Chakroborty of IIT Kanpur for his availability to discuss research problems and providing valuable insights into this work. I am also indebted to Dr. Avijit Maji of IIT Bombay for his valuable suggestions and also Dr. Abhishek Kumar and Dr. Laishram Boeing Singh for their constructive comments during my progress seminars.

As traffic data collection forms the basis for modelling driving behaviour realistically, this work would not have reached its conclusion without the engagement and generous help of my colleagues and friends who helped me in collecting data. I am truly grateful to CSIR-CRRI for providing the traffic data used in this thesis for modelling filtering behaviour, with special thanks to my supervisor and Arunabha Banerjee for their efforts in reaching out and collecting the data from them. I am also thankful to Dr. Anuj Budhkar, Kuldeep Kalita, Hariprasad, Dhanabhagyalakshmi, Suresh and Bhanu for their sincere efforts and extending their help in collecting traffic data using dynamic video tracking technique. I sincerely acknowledge Dr. Budhkar for his painstaking effort in collecting data from different locations and providing access to the collected data partly used in this thesis. I would also like to express my gratitude to Hariprasad, Bhagya, Anushree, Sunanda, Ashesh Choudhury, Porishmita and Ksheeraja for the precious help in assisting me with traffic data extraction.

The guidance and motivation from my friends, Rama, Sonia, Ekta, Madhulisha, Vinamra, Arunabha, Suresh and Alice deserve my heartfelt acknowledgements. The never-ending discussions, sometimes about traffic, sometimes about other things are indeed special moments to me. I am also grateful to Anshu, Geetimukta, Sneha, Ria, Pranab, Suvin, Bharat, Rahul, Akshita, Pratyasha, Rimi, Ankush, Nishant, Santanu, Saswati, Bhaskar, Iba, Subhadipto, Soumi, Pallavi, Reghulas, Arpita and all my colleagues who helped me directly or indirectly in

so many ways during this long process. My stays at the IIT Guwahati could not have been better without them.

I am grateful to IIT Guwahati for allowing me to use the available resources including travel support for the international and national conferences. My special thanks to the staff, students and faculty of the Department of Civil Engineering at IIT Guwahati for their consistent help and support throughout the period of this research.

Finally, I would like to take this opportunity to thank my parents, parents-in-law and all my family members for their unconditional support, endless love and encouragement throughout writing this thesis. I do extend my appreciation to my mother who always took a great interest in my research work and showed tremendous support during all my endeavours. My lovely nephews-Srish and Swapnil get special thanks who have been the source of my liveliness. At the end, I deeply thank Devaprasad for all unreserved love and care, and remarkable patience. Words cannot express how grateful I am for your support throughout my research career especially in difficult times.

I sincerely apologize if I have left anyone out, but my thanks goes to you as well!

--Sanhita Das

Abstract

Driver behaviour modelling entails realistic characterization of how drivers interact with the surrounding environment, how they control their vehicles in response to prevailing traffic conditions and how they perceive safety. With driver behaviour models forming the cornerstone of microscopic simulation tools, a realistic representation of such models is sought to have a knock-on effect in many practical applications including road safety evaluation, traffic operation and management studies, development of microscopic as well as macroscopic models, autonomous systems and intelligent transportation systems applications. Driving behaviour models have become a pivotal topic in traffic flow modelling and human factors research. While pioneering efforts were devoted to modelling driving behaviour in lane-based systems, an in-depth exploration is required to model the behavioural phenomena in disordered traffic systems, with proper quantitative substantiation. Drivers in disorderly traffic systems, often tend to evaluate opportunities for possible lateral movements while progressing longitudinally, either to have a better forward field of view or to initiate lateral shifts. Differences in driving style, sporadic driving behaviour, static and dynamic characteristics of varying vehicle types and weak-lane discipline traffic add even more complexity to modelling such disorderly traffic flow phenomena. This dissertation attempts to address some unresolved challenges on understanding and modelling driving behavioural phenomena of disordered traffic systems, by capturing both lateral and longitudinal interactions with the preceding vehicles simultaneously. Specifically, the objective is to attain a comprehensive investigation of different driving regimes in the vehicle-following scenario such as car-following, staggered-following and two-leader following; and filtering scenario to capture behavioural aspects of drivers realistically both from safety evaluation and behavioural modelling standpoint.

The dissertation begins with a description of different driving regimes, providing an extensive review of the behavioural models traditionally developed for both lane-based and disordered traffic systems, modifications made in the existing models and applicability of these models in describing the vehicle-following and filtering behaviour of drivers. The level of information required to describe the behavioural phenomena requires utilization of appropriate data collection schemes. To reproduce realistic driving behaviour, detailed trajectory data are obtained from video recorders utilizing static and dynamic video tracking techniques. Considering the flexibility of static video recorders in obtaining aggregate behaviour of different drivers interacting with diverse vehicle types, this technique is used to understand the staggered-following and filtering behaviour of different vehicle types at urban mid-block sections. Conversely, efforts are being directed in this research to establish an image-based in-vehicle trajectory data collection system for understanding detailed behavioural responses of drivers in a single leader and two-leader car-following scenario.

Utilizing the extracted trajectory data, this research work has illustrated that what has traditionally been thought to be a simple vehicle-following process depends, in fact, to a large extent on the lateral descriptor of traffic, making the lateral dimension or centerline separation (CS) an important concept in traffic flow modelling. This finding further facilitated the development of copula-based models to accommodate the dependence structure between the

lateral and longitudinal descriptors of traffic. Empirical evidence suggested that CS has a prominent effect on the drivers' selection of headways, on defining time-to-collision thresholds and also in modelling behavioural responses of drivers (in terms of acceleration) in the staggered-following scenario. In an attempt to model the structural and parametric uncertainties of human driving process in vehicle-following scenario, data-driven artificial neural network based single-leader and two-leader car-following models were developed. The developed models could explain the dynamic non-linear behavioural phenomena of drivers, much better than the classical car-following models both in terms of trajectory reproducing accuracy and generalization capability. The behavioural aspects of drivers in a two-leader car-following scenario, which has remained unexplored till date, has been attempted in this research. Specifically, symbolic emphasis has been laid to understanding the differences in drivers' behavioural characteristics with respect to different positional arrangement of the leaders, control actions of the subject drivers and modelling their dynamic non-linear responses. Driver's response in such two-leader following scenario depends on vehicle types, speeds of the interacting vehicles and lateral positioning of the vehicles. In this line, the concept of 'critical pore' has been introduced in this research to evaluate the transition regime from two-leader vehicle-following to filtering scenario. In particular, the performances of different methods were evaluated for classifying and predicting pore acceptance (filtering) and rejection (vehicle-following) decisions at urban mid-block sections.

To summarize, this dissertation has attempted to focus more on understanding the micro-level behavioural aspects of drivers and modelling drivers' responses in each driving regime. Having recognized the differences in driving behaviour in each driving regime, if the results obtained in this research are implemented in the microscopic simulation models, it would inherently augment the reliability and predictability of the simulation model more realistically. In the context of intelligent transport systems applications, this research can be the new impetus in the target of providing advanced collision warning system adaptation databases and real-time implementation of driver behaviour prediction models in a cognitive architecture, which will not only improve driver's safety but also optimize traffic flow.

Citation to Published Work

Chapter 3 is based on the following papers:

1. **Das, S**., Maurya, A. K., & Budhkar, A. K. (2019a). Dynamic data collection of staggered-following behaviour in non-lane-based traffic streams. *SN Applied Sciences*, 1(6): 591.

2. **Das, S**., Budhkar, A., Maurya, A. K., & Maji, A. (2019b). Multivariate Analysis on Dynamic Car-Following Data of Non-lane-Based Traffic Environments. *Transportation in Developing Economies*, 5(2): 17.

Chapter 4 is based on the following papers:

1. **Das, S**., & Maurya, A. K. (2018a). Multivariate analysis of microscopic traffic variables using copulas in staggered car-following conditions. *Transportmetrica A: Transport Science*, 14(10): 829-854.

2. **Das, S**., & Maurya, A. K. (2018b). Bivariate modeling of time headways in mixed traffic streams: a copula approach. *Transportation Letters*, 1-11.

3. **Das, S**., Maurya, A. K., & Budhkar, A. K. (2019c). Determinants of time headway in staggered car-following conditions. *Transportation Letters*, 11(8): 447-457.

4. **Das, S**., & Maurya, A. K. (2019d). Defining Time-to-Collision Thresholds by the Type of Lead Vehicle in Non-Lane-Based Traffic Environments. *IEEE Transactions on Intelligent Transportation Systems*, 1-11.

Chapter 7 is based on the following papers:

1. **Das, S**., & Maurya, A. K. (2018c). Modelling of motorised two-wheelers: a review of the literature. *Transport Reviews*, 38(2): 209-231.

2. **Das, S**., & Maurya, A. K. (2019e). Modeling maneuverability of motorized two-wheelers during filtering in urban roads. *Transportation Research Record: Journal of Transportation Research Board*, 2673(5): 637-647.

3. **Das, S**., & Maurya, A. K. (2020). Pore acceptance predictions of motorised Two-Wheelers during filtering at urban Mid-Block sections. *Journal of Intelligent Transportation Systems: Transport, Planning and Operations*, 1-13.

Table of Contents

List of Figures

List of Tables

List of Abbreviations

Terms	Abbreviations
2D	Two Dimensional
3W	Motorized three-wheeler
ACC	Adaptive Cruise Control
A-D	Anderson Darling
ADAS	Advanced Driver Assistance Systems
AIC	Akaike Information Criteria
AMH	Ali-Mikhail-Haq
ANN	Artificial Neural Network
ANOVA	A One-Way Analysis of Variance
AOVM	Asymmetric Optimal Velocity Model
BLM	Binary Logit Model
BP	Back Propagation
CA	Collision Avoidance
CaF	Comfort at Filtering
CDF	Cumulative Distribution Function
CF	Car Following
CFI	Comparative Fit Index
CS	Centerline Separation
CU	Common Unit
CvM	Cramer-von Mises
DF	Direct Front
DH	Distance Headway
FAR	False Alarm Ratio
FC	Frictional Clearance
FGM	Farlie-Gumbel-Morgenstern
FV	Following Vehicle
FVDM	Full Velocity Difference Model
GA	Genetic Algorithm
GFM	Generalized Force Model
GHR	Gazis-Herman-Rothery
GPS	Global Positioning Systems
HL	Hidden Layer
IDM	Intelligent Driver Model
IFM	Inference from Margins
ITS	Intelligent Transportation System
K-S	Kolmogorov Smirnov
LC	Lateral Clearance
LCV	Light Commercial Vehicle
LF	Left Front
LFV/RFV	Left Front Vehicle/Right Front Vehicle
LG	Longitudinal Gap
LL	Log Likelihood

LM	Levenberg-Marquardt
LS	Lateral Separation
LV	Leading Vehicle
MAE	Mean Absolute Error
MAPE	Mean Absolute Percent Error
MES	Maximum Escape Speed
MLE	Maximum Likelihood Estimation
MoRTH	Ministry of Road Transport and Highways
MPL	Maximum Pseudo-Likelihood Method
MSE	Mean Squared Error
MTW	Motorized Two-Wheeler
NGSIM	Next Generation Simulation
NN	Neural Network
OVM	Optimal Velocity Model
PDF	Probability Density Function
RF	Right Front
RMSE	Root Mean Square Error
RMSEA	Root Mean Square Error of Approximation
RS	Relative Speed
SEM	Structural Equation Model
SRMR	Standardized Root Mean Square Residual
SV	Subject Vehicle
SVM	Support Vector Machine
TDE	Traffic Data Extractor
TH	Time Headway
TTC	Time to Collision

Glossary of Terms

Terms	Description
Car-following	Driver in the following vehicle (car) assigns full leadership to the leading vehicle (car)
Centerline separation	Lateral difference between central positions (widths) of the leading and following vehicles
Critical pore	Minimum pore size accepted by subject vehicles to complete filtering manoeuvre between two leaders at a mid-block section
Disordered/non-lane based/weak-lane discipline traffic	Lanes are not well demarcated or lane discipline is not followed
Staggered-following	Driver in the following vehicle assigns partial leadership to the leading vehicle
Two leader following	Drivers in the following vehicle follow both the leading vehicles simultaneously
Vehicle following	Collective term used to describe the following behaviour of subject vehicles in the presence of single/two leader(s) involving similar/varying vehicle-pair interactions
Lateral clearance	Clear lateral distance between two adjacent vehicles

1

Introduction

1.1. Background

The rapid growth in urbanization and an expanding economy has dramatically increased travel demand in urban areas, thus putting enormous pressure on transport and road infrastructure. While India's real per-capita income has increased by almost 7 times (from ₹ 266.578 to ₹ 1981.26) between 1980 and 2017 (World Bank, 2018), the share of motorized two-wheeler and car transport in India rose from 2,117 to 1,87,091 and 1,059 to 33,688 respectively from 1980 to 2017 (MoRTH, 2019). The striking rise in motorization rates has generated serious transport problems leading to traffic fatalities and injuries, congestion, environmental pollution and lack of adequate mobility, which create an adverse effect on the social, economic and environmental health of our growing cities. The important question now is how to mitigate congestion and improve the effectiveness of urban transport systems. Perhaps, minimizing congestion involves increasing roadway capacity, either by adding new lanes, adopting effective traffic management strategies or by implementing proper safety measures. Although some amount of road expansion is still warranted to deal with specific bottlenecks or to connect rural settlements, but, given the societal and budgetary constraints, such efforts are not always practically feasible. Moreover, conducting field tests for the design of traffic control and congestion management measures are also pragmatically inconvenient. Therefore, for the real-time evaluation of traffic control strategies and demand management, microscopic simulation tools, which mimic individual driver behaviour explicitly in a controlled environment prove to be an essential solution in evaluating detailed traffic performance at different roadway sections.

Driving behaviour models, capturing both longitudinal and lateral movements of vehicles, form the cornerstone of microscopic traffic simulation tools. Modelling driver behaviour requires a detailed understanding of how drivers interact with the surrounding environment and how they control their vehicles in response to prevailing traffic/environmental conditions. The subject has recently garnered increased attention as the advent of advanced information and new technology in the form of intelligent transport systems (ITS) has begun to offer new and increasingly subtle ways in managing and controlling system operations. Indeed a realistic development of such models is sought to enhance the development of smarter and user-friendly autonomous cruise control systems, intelligent traffic operation studies, traffic safety evaluation, congestion mitigation, capacity estimation and so forth. Traditionally, pioneering efforts were devoted to model the driving behavioural phenomena by investigating longitudinal

(car following) and lateral interactions (lane changing) between vehicles separately and independent of each other. While development of two separate models can describe homogeneous traffic quite well, the prospect of these traditional models in representing driver's behaviour of disordered (or, non-lane based) traffic systems is still ambiguous.

1.1.1. Characteristics of disorderly traffic

A disordered traffic system is one where lanes are not well demarcated or lane discipline is not followed. Traffic patterns emerging in such disordered traffic systems are different from lane-based or ordered traffic systems. Traffic in developed countries is aptly described as homogeneous and lane-based traffic system because it predominately consists of passenger cars and is characterized by strict lane discipline with restricted movement across the lanes. Conversely, traffic in developing nations is essentially disordered where vehicles have the flexibility to occupy any lateral space on the roadway irrespective of lane markings. Differences in driving style, static and dynamic characteristics of a wide variety of traffic mix make the system disordered and heterogeneous, thereby adding more complexity to the traffic phenomena. Interactions among different vehicles and the resulting manoeuvres they undertake in disorderly traffic are exceptionally different and indeed much more complex than lane-based traffic scenario. A clear comparison of disorderly traffic in Indian conditions and that in homogeneous conditions of developed countries is depicted in Figure 1.1.

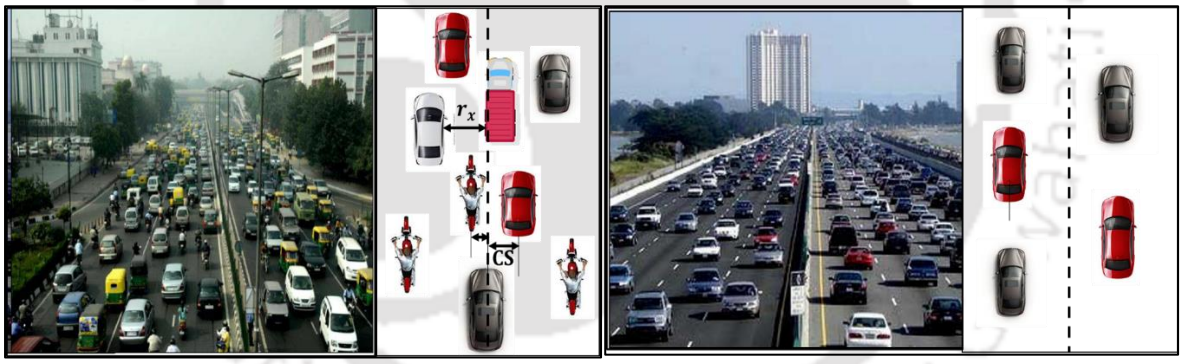

(a) **(b)**

Figure 1.1. Traffic stream with **(a)** disorderly traffic condition, and **(b)** homogeneous and orderly traffic condition

The line diagram presented in Figure 1.1(a) illustrates the disorderly traffic flow phenomena of non-lane based traffic systems. Smaller vehicles in such disordered systems often take advantage of compact widths and exhibit chaotic trajectories by traversing through the lateral gaps (or r_x, as depicted in the figure) described by surrounding vehicles. Even while progressing longitudinally, the following vehicles do not always assign full leadership to the vehicle in front. They, in fact, shift their vehicles from the centerline position of the preceding vehicle to the left or right side, either to have a better field of view of the forward scenario or to initiate lateral shifts. Vehicles in such traffic systems not only interact with the preceding vehicle longitudinally but also simultaneously look for possible gaps in the surrounding vehicles in the lateral direction. Once they identify it, they orient their vehicles and try to occupy the vacant space. Moreover, vehicles may not have only one but several leaders. Drivers

may not strictly follow a single leader, but may assign partial leadership with it by maintaining certain centerline separation (indicated as CS in Figure 1.1(a)), follow more than one leader or even may be in between the leaders. Certainly, there is always an integration of the longitudinal and lateral movements of vehicles and this integrated driving behaviour gives rise to various driving phenomena (Lee et al., 2009) like tailgating, moving abreast, swerving, vehicle following, multiple leader following, filtering and travelling according to the dynamic lanes formed by the vehicles.

1.1.2. Driving behaviour model for disordered systems

A suitable integrated driving behaviour model developed for disordered traffic environments should capture interdependencies between longitudinal and lateral movements, and subsequently model different driving regimes such as car-following, staggered following, following multiple leaders, filtering between vehicles and lateral shift process. In essence, while the term 'car-following' is commonly used for describing the following behaviour of cars in lane-based traffic, the same cannot be directly used for disorderly traffic as the degree of lateral movement is more prevalent in the latter. For such disorderly flows, 'staggered-following' is a more suitable term used to describe the following behaviour of vehicles when they prefer to follow the preceding vehicles by maintaining certain lateral separation or centerline separation (CS) with them. In a similar manner, vehicles in disorderly traffic may also follow more than one preceding vehicle (termed as 'multiple-leader following') or even they may attempt to pass in between two leading vehicles (commonly termed as 'filtering' in the literature) under prevailing traffic conditions. The choice of driver in maintaining a desired lateral position depends on the orientation of leading vehicles in the interaction regime, presence of surrounding vehicles, their relative longitudinal and lateral locations, speeds, desired path and driver characteristics. More specifically, vehicles may prefer assigning full leadership to a single leader in car-following scenario, however the driver's choice in selecting a lateral position may vary in staggered-following scenario. Even in a two-leader following scenario, they may prefer to position themselves in the middle by maintaining a safe longitudinal distance with the vehicles ahead. This justifies that the desired lateral position of any vehicle depends to a large extent on the relative positions (both longitudinal and lateral) with the interacting vehicles. However, integrating the lateral and longitudinal descriptors in the interacting regime has not been fully considered in the past.

A realistic development of an integrated driving behaviour model requires precise and elaborate understanding of different driving regimes and modelling behavioural responses of drivers in terms of longitudinal and lateral acceleration. On modelling vehicle interactions in the longitudinal direction (such as in car-following, staggered-following, multiple leader following and filtering), drivers' responses are modelled in terms of longitudinal acceleration considering relative speeds as the main stimulus. On the contrary, during lateral shift process of vehicles, the lateral acceleration behaviour needs to be modelled depending on the distance between current position and desired target position. Although different comprehensive models have been developed by researchers to represent disorderly traffic scenario, such models either

lack proper calibration and validation with empirical data or limited consideration of integrated longitudinal and lateral behaviour (Maurya, 2007; Ravishankar and Mathew, 2011). For the development of a realistic integrated driver behaviour model, a precise understanding and modelling of different driving regimes is essential so that it can capture both longitudinal and lateral dynamics of vehicles, and hence interdependencies among them.

1.2. Motivation

Although many research efforts have been done to model driving behaviour in disordered traffic systems, there is still a paucity of research in depicting the unique behavioural patterns of vehicles such as staggered following, multiple leader following, filtering/passing between two vehicles and swerving manoeuvres of various vehicle types. A detailed understanding and description of these driving regimes need to be attained first and if it can be duly incorporated into a single model, will improve the reliability and predictability of the simulation model more realistically. Considering complexity in non-lane based systems, it is thus imperative that an in-depth investigation of distinct manoeuvring patterns of vehicles is first carried out prior to the development of an integrated model. There is still a lack of attention in depicting the longitudinal control of vehicles, handling multiple leaders in the longitudinal direction and modelling interactions among different vehicles, with due consideration of the lateral descriptor of traffic. Indeed a comprehensive and detailed investigation of different driving regimes such as car-following, staggered-following, multiple leader following and filtering between vehicles, by capturing both lateral and longitudinal interactions with the preceding vehicles requires due cognizance from behavioural modelling standpoint. Capturing such interdependencies and driver behavioural responses will indeed contribute a step towards the development of a full-fledged integrated driving behaviour model of disordered traffic systems, by providing a realistic representation of the driver behaviour.

1.3. Research Challenges

Some of the research challenges in the development of an integrated driving model are described below:

- **Why is modelling different driving regimes important for the development of an integrated model?**
  An integrated driving behaviour model developed for disorderly traffic should provide a realistic representation of traffic flow phenomena and complex manoeuvring patterns of vehicles. As rightly pointed out by Asaithambi et al. (2016), the complex driving behavioural phenomena give rise to different driving regimes such as car-following, staggered-following, following between two vehicles, filtering in between vehicles and lateral shifts. If such driving regimes are defined, and subsequently drivers' behaviour phenomena are modelled realistically, it would contribute towards development of a comprehensive driving behaviour model for disordered traffic systems.

In particular, development of an integrated driver behaviour model requires realistic characterization of the driving regimes, drivers' responses while interacting with the leading vehicles (in their longitudinal direction of travel) and surrounding vehicles (lateral movement), deterministic values of regime boundaries such as transition from following to filtering and so forth. Modelling different driving regimes in the vehicle-following scenario[1] (such as car-following, staggered-following, following between two vehicles) and filtering scenario provides information on drivers' longitudinal acceleration, longitudinal and lateral distance keeping behaviour, etc. Conversely, understanding the lateral shift process entails modelling of lateral acceleration behaviour. Such detailed understanding is anticipated to constitute a step towards development of an integrated model, which is indeed an emerging yet challenging topic, entailing in-depth investigation with proper empirical substantiation.

- **Are the existing data collection techniques appropriate for modelling different driving regimes observed in disorderly traffic?**
  Appropriate data collection schemes play a dominant role in reproducing realistic driver behavioural phenomena. Owing to the non-intrusive nature and flexibility in obtaining visual data information, vehicle tracking scheme from static video recorders is commonly employed in the existing studies (Mallikarjuna et al., 2009; Munigety et al., 2014; Kanagaraj et al., 2015). Although it offers spatial limitation, information on the position of tracked vehicle and its relations with the surrounding traffic can be obtained. However, understanding the behavioural responses of drivers in car-following regimes (either a single leader or multiple leaders) requires dynamic position tracking for a longer period. Researchers claim that the estimation of such dynamic data from onboard Global Positioning System (GPS) receivers can be a suitable alternative. However, considering the prevalence of lateral dimension in the following regime of disorderly traffic systems, collection and estimation of such dynamic data put an additional constraint and pose a challenge to the modeller.

- **Data requirements for driver behaviour modelling are stringent. What attributes need to be selected for modelling?**
  Estimation of trajectory data is a demanding task. Information on surrounding traffic of the subject vehicle such as interacting vehicle types, presence of any surrounding vehicle just adjacent to the considered vehicle, longitudinal and lateral spacing with the surrounding vehicles, individual speeds, vehicle dimensions, etc. and geometric characteristics such as type and width of road, straight or curved sections, etc. are

[1] The term 'vehicle-following' is more commonly used to describe the following behaviour of different interacting vehicle types in disorderly traffic environments. Because of vehicle heterogeneity and disorderly traffic flow phenomena, a subject vehicle may follow either a single leader or more than one leader. In such scenario, 'vehicle-following' can be a more generic term used to describe the following behaviour in the presence of a single-leader (strict following, staggered-following) or more than one leader (two-leader or multiple-leader following). Concisely, 'vehicle-following' is a more suitable term for disordered traffic systems than 'car-following' of lane-based/ordered traffic systems.

important for understanding and modelling driving behaviour. Selection of appropriate attributes, however depends on the studied phenomena, level of information available and also on modeller's perspectives.

- **Why is the integration of longitudinal and lateral interaction important in traffic flow modelling?**
  Research conducted on modelling vehicle interactions in non-lane-based systems did not adequately consider the lateral descriptor of traffic. Besides, a series of works performed on the topic mainly involved partial consideration of lateral separation in car-following models (Gunay, 2007; Jin et al., 2010; Zheng et al., 2012). While the micro-level characteristics of traffic flow such as time headway, longitudinal gap and speed describe the longitudinal movement, little is known about the effect of lateral indicator in modelling the longitudinal descriptors of traffic. Investigating and modelling the inter-dependencies between longitudinal and lateral descriptors by itself is a research area. If a significant dependent relationship is found, integrating the longitudinal and lateral descriptors is sought to ameliorate the predictability of the microscopic simulation models more realistically.

- **Can the existing models be applied for modelling disorderly traffic flows?**
  Although researchers have acknowledged the effects of lateral separation in conventional models, the credibility of these models in describing the single-leader and multiple-leader following phenomena is still unresolved and undocumented. In parallel, the filtering behaviour of smaller vehicles in such traffic systems further needs detailed characterization. Human factor, in general, forms the major component in the operational and control process in a following and filtering driving regime. Accommodating complexity of human driving process in the model can advocate towards the development of a more realistic model. With proper estimation of reliable trajectory data, if a driver behaviour model with due consideration of lateral dimension, is developed and proved to outperform the existing models, it is believed to enhance the accuracy and reliability of micro simulation modelling. This in turn, would foster development of smarter and user-friendly autonomous vehicles, and a more safe and efficient transportation system.

- **Can the safety aspects of drivers be evaluated in such systems?**
  Close-following behaviour runs a significant risk and contributes to a higher percentage of rear-end collisions. Researchers proposed several safety indicators or warning thresholds to evaluate collision risks in lane-based scenario. Yet, the prospect of these defined thresholds in evaluating safety of non-lane based systems is another challenging area of research. Accurate characterization of an appropriate warning threshold can invariably enhance safety by distinguishing between safe and unsafe encounters.

To address such unresolved research challenges, this dissertation attempts to investigate the driving behavioural phenomena of disorderly traffic. In particular, suitable emphasis has been laid on understanding and modelling different driving regimes such as car-following, staggered-following, multiple leaders following and filtering behaviour which are commonly observed in such disorderly traffic environments. Achieving a detailed understanding of each driving regime entails collection of suitable data, utilization of appropriate data collection techniques, realistic characterization of driver's behavioural process, consideration of both the longitudinal and lateral descriptors of vehicle interactions in an interacting regime, predicting realistic responses of human driving behaviour, probable risks associated with them and so forth. In an attempt to accomplish such challenges efficiently, efforts are being directed in this research to establish a suitable data collection technique for understanding detailed behavioural responses of drivers in such disorderly traffic scenario. This research further attempts to investigate each driving regime in a comprehensive manner, by capturing the behavioural aspects of drivers realistically both from safety evaluation and behavioural modelling standpoint.

1.4. Research Aims and Objectives

The main objective of this research work is to provide a comprehensive understanding and investigation of vehicle-following and filtering behaviour in disordered traffic systems that can capture interdependencies between both longitudinal and lateral vehicle interactions simultaneously. The above stated objective can be achieved by the following sub-objectives as discussed below:

- Identification of microscopic traffic variables describing vehicle-following and filtering behaviour.
- Development of an experimental technique to collect and process reliable time-series data for the vehicle-following scenario.
- Evaluation of driver behaviour and safety assessment in staggered-following scenario.
- Development of a single leader vehicle-following model for non-lane based (or disordered) traffic systems and its comparison with different existing models.
- Modelling two-leader vehicle-following behaviour and its comparison with existing models.
- Modelling filtering behaviour of vehicles in disordered traffic systems.

1.5. Scope of the Research

The proposed research work aims to investigate vehicle-following and filtering behaviour of vehicles in disordered traffic systems. More specifically, three types of manoeuvre in the vehicle-following scenario including car-following, staggered-following and two-leader following are incorporated in this work. The scope of the research is limited to mid-block straight sections having no influence of gradients, bus-stops, parking lots, interactions with pedestrian movements, etc., with data being collected in the day hours only. In particular, driver

behavioural modelling of different vehicle-pair combinations are attempted, while the detailed dynamic behavioural processes in a single-leader and two-leader vehicle-following scenario are specifically investigated for only cars. Further, the filtering behaviour of motorized two-wheelers (MTWs) and cars are investigated for such traffic. The development of a comprehensive integrated driver behaviour model is however beyond the scope of the thesis.

1.6. Thesis Organization

A road map of the thesis is illustrated in Figure 1.2. The chapter-wise organization of the thesis is given below:

- **Chapter 1:** This chapter provides introduction, motivation, research objectives and overview of the thesis.

- **Chapter 2:** This chapter is devoted to the background knowledge required for better understanding of the driving behavioural phenomena in disordered traffic systems.

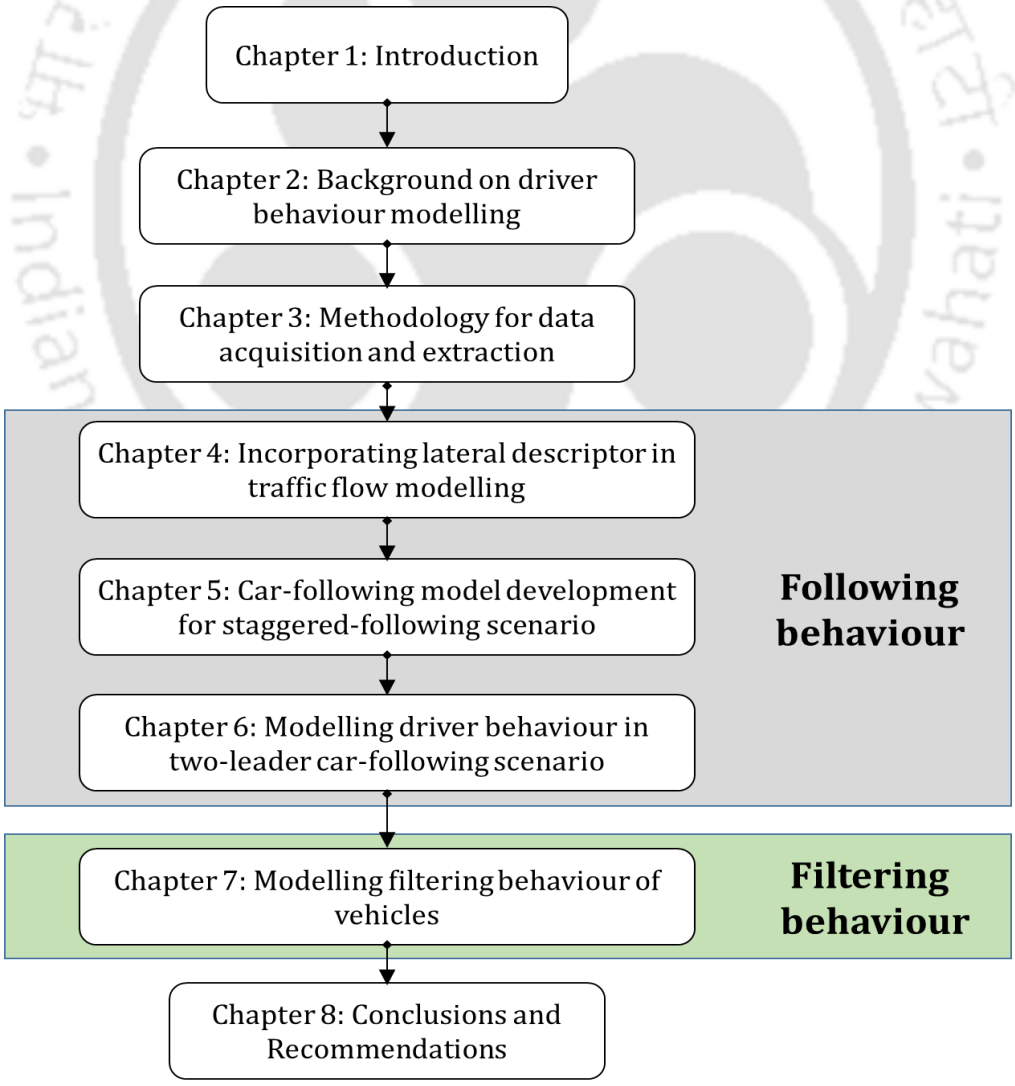

Figure 1.2. Structure of the thesis

- **Chapter 3:** This chapter presents the data collection techniques and methodological framework utilized in this work for understanding behavioural phenomena of drivers in real-world traffic conditions.

  Parts of this chapter have been partially presented in Das et al. (2019a) and Das et al. (2019b).

- **Chapter 4:** This chapter outlines the importance of lateral descriptor of vehicle interaction in traffic flow modelling and in evaluating safety, describing a methodological framework that can integrate both the longitudinal and lateral interactions in the staggered-following process simultaneously.

  The contents of this chapter are based on the published work reported in Das and Maurya (2018a, 2018b, 2019d) and Das et al. (2019c).

- **Chapter 5:** A data-driven based methodological modelling framework is presented in this chapter for a single-leader single-follower car-following scenario. The credibility of the developed model is compared with the existing car-following models and further substantiated from model stability standpoint and also from trajectory reproducing accuracy.

- **Chapter 6:** This chapter discusses the following process of drivers in a two-leader car-following scenario, with a detailed explanation on the behavioural differences of drivers in response to different positional arrangement of the leaders. A data-driven based two-leader single-follower car-following model is further presented to model the two-leader following behavioural phenomena of drivers.

- **Chapter 7:** This chapter introduces the filtering behaviour of vehicles (motorized two-wheelers and cars) in disordered traffic systems, describing how this choice is affected by different driver-vehicle characteristics and local traffic conditions. Proper emphasis has also been laid to the assessment and classification of lateral gap (or, pore) acceptance or rejection decision of drivers during the filtering and following manoeuvre.

  Parts of this chapter have been published in Das and Maurya (2018c, 2019e, 2020).

- **Chapter 8:** This chapter highlights the conclusions of this research. A summary of the main contributions is presented and new avenues for future research have also been discussed.

2

Review of Modelling Driver Behaviour

As already discussed, a realistic driving behaviour model developed for disordered systems should be able to capture both longitudinal and lateral movements of vehicles simultaneously. Presence of different vehicle types in non-lane-based traffic environments and their interactions with the surrounding vehicles give rise to different driving behavioural phenomena such as car-following, staggered following, multiple-leaders following and filtering between vehicles. Yet more realism can be embraced in the models only with prior understanding of these specific manoeuvring patterns of vehicles. A detailed understanding and modelling of each driving regime is pivotal in augmenting the reliability and development of a comprehensive microscopic traffic simulation model. Knowing the importance of such models in capacity estimation, safety operation studies, traffic management studies, congestion mitigation, autonomous systems and intelligent transport systems applications, transport modellers in developing nations have paid considerable attention in providing a comprehensive representation of different driver's behavioural phenomena in the microsimulation models.

This chapter provides an extensive review of these specific dynamic behavioural patterns of vehicles prevailing in disordered traffic systems, describing the modelling approaches and data collection methodologies used for understanding their behavioural patterns in both orderly and disorderly traffic systems. An outline of this chapter is presented in Figure 2.1.

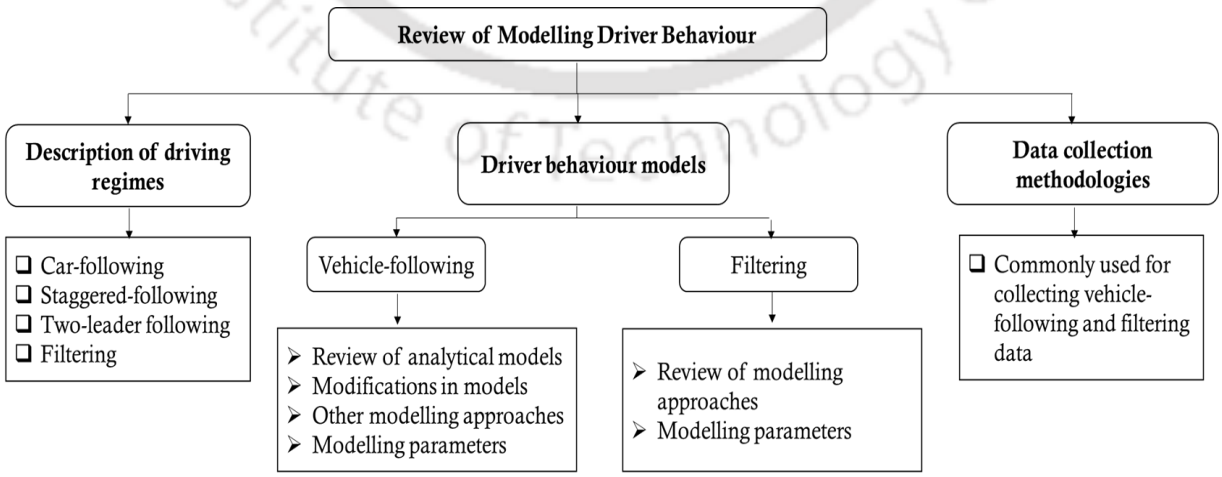

Figure 2.1. Outline of the presented literature review

2.1. Description of driving regimes in disordered systems

The development of a comprehensive microscopic simulation model entails succinct and realistic characterization of driving behavioural phenomena. Absence of lane discipline and presence of different vehicle types result in an integrated two-dimensional movement of vehicles, where vehicles often look for possible opportunities to make lateral movements while progressing longitudinally. This gives rise to complex manoeuvring patterns such as maintaining shorter headways, close following, swerving and filtering (Munigety and Mathew, 2016). While describing non-lane based motorized two-wheelers (MTWs) movements in Vietnam, Lee (2008) summarized some distinctive riding patterns of MTWs as '*travelling alongside another vehicle in the same lane, oblique following, moving to the head of a queue, filtering, swerving or weaving, tailgating, maintaining a shorter headway when aligning to the lateral edge of the preceding vehicle, travelling according to the virtual lanes formed dynamically by the vehicles in surroundings, and self-organization phenomena*'. Asaithambi et al. (2016), on the other hand, underlined that a wider range of driving regimes exist in disorderly traffic streams that need to be clearly defined and modelled for the development of a full-scale behavioural model. This includes driving regimes describing longitudinal interaction with the leaders such as car-following, staggered-following, following between two vehicles and passing; travelling abreast, lateral movement and lateral shift processes. As a first step towards the development of microscopic driver behaviour model, understanding and modelling such longitudinal interaction regimes with the leaders in disordered systems entails in-depth exploration. In particular, this includes interactions with the immediate leaders, partial leaders, multiple leaders and filtering between leaders, as illustrated in Figure 2.2.

***Note*: CS**: centerline separation; **LG**: Longitudinal gap; **LF**: Left-front; **RF**: right-front; $\mathbf{r}_x$: pore size

Figure 2.2. Following behaviours in disorderly traffic **(a)** Car-following **(b)** Staggered-following **(c)** Two-leaders following and **(d)** Filtering

Car-following or vehicle-following: The driver in the following vehicle (car) assigns full leadership to the leading vehicle (car). Considering wide variety of traffic mix in disordered traffic environments, the following behaviour is also observed for different combinations of leader-follower pairs. In such cases, when the following vehicle follows the leading vehicle of any vehicle type, such arrangement is then defined as vehicle-following scenario.

Staggered car-following or staggered vehicle-following (or, staggered-following): The staggered car-following behaviour refers to a scenario when the following vehicle (car) interacts with the leading vehicle (car) by assigning partial leadership with the leading vehicle. In such scenario, the following vehicle maintains certain extent of centerline separation with the leader and evaluates possible opportunities for lateral movements while progressing longitudinally, either to have a better field of view or to initiate lateral shifts for possible overtaking opportunities, if any. This gives rise to longitudinal as well as lateral interactions with the vehicle ahead. For mixed traffic environments, when the following vehicle of a particular vehicle type is staggered with the leading vehicle of similar or different vehicle type, such scenario is then referred as staggered vehicle-following or staggered-following.

Following two leaders: The driver in the following vehicle assigns partial leadership with both the leading vehicles. Because vehicles can avail any lateral space on the roadway in disordered traffic environments, the subject vehicle, in certain situations, prefer to follow between two leaders (left-front and right-front vehicles). This allows them to apperceive the forward visual field extended in between the leading vehicles, looking for possible opportunities to pass in between the leading vehicles.

Filtering: Filtering behaviour refers to the complex manoeuvring pattern of vehicles in dense urban heterogeneous traffic environments where they tend to utilize the available lateral spaces described by other vehicles (also defined as pores) on the road in order to achieve higher speeds and reduced travel times. Although this is a commonly observed phenomena for MTW riders, motorized three-wheelers and even cars are observed to filter through traffic in such heterogeneous disordered systems.

2.2. Driver behaviour models describing the following behaviour

Studies describing longitudinal interactions in heterogeneous disordered traffic systems suggest extensions of the car-following paradigm. Even when vehicles strictly follow the leaders, drivers may react differently depending on the interacting leader-follower vehicle pairs. The following behaviour further depends on the positioning of the leading vehicles. Absence of lane discipline and differences in static and dynamic characteristics of vehicles result in situations where drivers assign partial leadership with a single leader, by maintaining certain lateral separation with them. They can even follow two leaders simultaneously or filter in between them. These peculiar driving regimes make the traffic system complex, a detailed understanding of which deserves considerable attention. This section provides an extensive review of relevant academic studies related to longitudinal movement models developed for

lane-based as well as for disorderly traffic environments. A detailed review of each driving regime in the context of homogeneous and disorderly traffic is discussed in this section.

2.2.1. Car-following regime: A review of analytical models

Car-following literature divides into Newtonian (or engineering/analytical) versus psycho-physiological modelling frameworks (Brackstone and McDonald, 1999; Pariota et al., 2016). Over more than 60 years of modelling efforts, the complexity in car-following models grew, for characterizing the human constraints and preferences in the model. The rationale behind development of car-following models is to appraise how driver controls her/his vehicle with respect to the preceding vehicle precisely and realistically. The drivers indeed make a compromise between the urge to minimize trip duration but at the same time maximize safety (Brilon et al., 1999). Car-following models form an essential component in microscopic traffic simulation and is based on the assumption that drivers interact only longitudinally with the vehicle ahead i.e. the decision of a driver to accelerate/decelerate or to brake is influenced only by the leading vehicle immediately ahead, both travelling in the same lane. This presumption counts valid when drivers manoeuvre within well demarcated travel lanes, a follower responds to its immediate single leader and vehicles do not exhibit any lateral movement.

The concept of car following (CF) was first proposed by Reuschel (1950) and Pipes (1953). During 1958-1963, the core car-following theories and models were born. The essential issue was selecting the appropriate variables that the driver of the following vehicle responds to. Since then, a large number of analytical/engineering models were developed that subsequently embraced realistic behaviourism. Analytical car-following models involve a set of mathematical expressions that describe the dynamics of the subject vehicle following another vehicle in a single lane. A great deal of CF models has been developed such as Gazis-Herman-Rothery (GHR) model, safe distance or collision avoidance model, linear (Helly) model, optimal velocity model, intelligent driver model, psychological model, fuzzy logic model, cellular automata model, potential field model, etc. A detailed review of the CF models is discussed in Mahapatra et al.'s (2018) work. Among all the existing CF models, some of the most studied and influential ones such as Gazis-Herman-Rothery (GHR), safe distance model, optimal velocity model (OVM) and Intelligent Driver Model (IDM) are described in this section. A summary of the car-following models developed for lane-based traffic conditions is presented in Table 2.1.

2.2.1.1. Gazis-Herman-Rothery model

By the mid-1950s, the GHR model of traffic pursued by Chandler et al. (1958) at the General Motors research labs stated that the acceleration of the following vehicle was proportional to the relative speed between the lead and following cars with a time lag between the two quantities. This yielded the classic *stimulus-response frame* and the general formulation of the model is

$$\ddot{x}_{FV}(t+\tau) = \frac{\alpha_{l,m}[\dot{x}_{LV}(t+\tau)]^m}{[x_{LV}(t) - x_{FV}(t)]^l}[\dot{x}_{LV}(t) - \dot{x}_{FV}(t)]$$

where $\ddot{x}_{FV}(t+\tau)$ is the acceleration of the following vehicle (FV) at time $t+\tau$, $[\dot{x}_{LV}(t) - \dot{x}_{FV}(t)]$ is the relative speeds between leading vehicle (LV) and following vehicle (FV), τ is the driver's perception-reaction time, $x_{LV}(t) - x_{FV}(t)$ is the relative spacing between LV and FV, l and m are exponents and $\alpha_{l,m}$ is a constant whose dimensions depend on l and m.

Table 2.1. Summary of the car-following models developed for lane-based traffic conditions

	Gazis-Herman-Rothery Model (GHR model)	Safe distance model	Optimal velocity model (OVM)	Intelligent Driver Model (IDM)
Authors	Chandler et al. (1958) Gazis et al. (1959) Herman and Rothery (1965) Treiterer and Myers (1974)	Kometani & Sasaki (1959) Gipps (1981) Barceló (2002)	Bando et al. (1993) Helbing and Tilch (1998) Jiang et al. (2001) Ge et al. (2008)	Treiber et al. (2000a) Treiber and Kesting (2013) Jiang et al. (2014) Derbel et al. (2012)
Basic assumption	Acceleration of FV is related to • Relative speeds between the leader and the follower • Relative positions, and • Speed of FV	FV maintains a safe distance with LV in order to avoid collision and is related to • Speed of the LV at time *t* • Speed of the FV at $t+\tau$ τ is the reaction time	Acceleration of FV is related to • Difference between the driver's optimum velocity and the current velocity. • Relaxation time. Optimum velocity is a function of relative positions between the leader and follower.	Acceleration of FV is related to • Speed of FV • Maximum acceleration • Relative speeds • Desired gap and • Actual gap available The model combines both the free road acceleration and an intelligent braking strategy.
Modifications made	-Different calibration parameters were proposed in different studies. -Changes in the sensitivity term to account for free-flow and congested regions. -Accounted for acceleration and deceleration responses	FV's speed is minimum of accelerating stage (speed<desired speed) and emergency braking, (Gipps,1981)	-FVDM: an additional term is included taking both positive and negative velocity differences. -TVDM: included a weighing factor to indicate the influence of LV on FV motion	-Modified the desired minimum gap term. -Validation of the model has been done on a freeway considering trucks and cars.
Capabilities and issues	-Reasonable theory. -Simple to understand and use. -Considers reaction time. -No conclusive findings for the calibrated parameters. -Considers no change in relative positions when relative speed is zero	-Easy to use as it excludes calibration of parameters. -Considers reaction time in Gipps' model. -Drivers do not always keep the safe-distance	-Reasonable theory -Simple to understand the dynamics of traffic congestion, stop-go waves, etc. -Validation of the model has not been done.	-Suitable for traffic with road inhomogeneity -Replicates traffic quite well, validation still needs further consideration. -Does not consider risk factor explicitly.

Note: **LV**: Leading vehicle, **FV:** Following vehicle, **FVDM**: Full velocity difference model, **TVDM**: Two velocity difference model

Many authors have proposed different calibration parameters for these models. Chandler et al. (1958) calibrated the parameters considering l and m equal to zero using the dataset of eight test vehicles which drove a test track for over a 30-minutes period. Gazis et al. (1959) subsequently derived a macroscopic relationship between speed and flow using the microscopic equation as a starting point. But the mismatch in the results led them to introduce

a term $1/\Delta x$ into the sensitivity constant. This new model with *m=0, l=1* was confirmed by Herman and Potts (1959) who calibrated the new formulation using 11 subject vehicles on roads in New York. Edie (1960) applied the model proposed by Gazis et al. (1959) to match a new set of parameters. He introduced the velocity dependent term on the sensitivity constant leading to a new model with *m=1, l=1*. The sensitivity of their microscopic relationships for different $\dot{x}_{LV}(t+\Delta t)$ and $[x_{LV}(t)-x_{FV}(t)]$ terms was investigated by Gazis et al. (1961) and their investigation showed that two separate relationships could be used to describe the traffic flow, one for non-congested and the other for congested traffic. Afterwards, many other authors (May and Keller, 1967; Heyes and Ashworth, 1972; Treiterer and Myers, 1974; Ceder and May, 1976; Aron, 1988; Ozaki, 1993) calibrated the parameters to obtain the best combination of *m* and *l.*

Though a great deal of work has been performed on the calibration and validation of GHR model, no conclusive findings could be obtained for the correct values of *m* and *l.* Moreover the stimulus-response models consider that if the relative speed is zero then there is no change in the relative positions of vehicles. Furthermore, the model does not have any acceleration and deceleration limits. This is important in disorderly traffic conditions because accelerations and decelerations are restricted by vehicle characteristics.

2.2.1.2. Safe Distance models

Spacing models hypothesize that FV reacts to the spacing of LV than to the relative speed. The original formulation of the safe distance or collision avoidance models was by Kometani and Sasaki (1959) in which they specified a safe following distance within which a collision would be unavoidable when the leading vehicle acts unpredictably and the space headway in front of the subject vehicle is shorter than the safe distance. The next major development of this model was by Gipps (1981). Gipps' model assumed that the subject vehicle tends to choose the velocity that can avoid rear end collision if the leading vehicle performs emergency braking. This model is based on two constraints for the follower's velocity: (a) the speed never exceeds its desired speed and its free acceleration first increases with speed and then decreases to zero as the vehicle reaches its desired speed, (b) the FV must stop safely if the leading vehicle suddenly applies brakes. The speed attained by a vehicle at a given time instant (t+ τ) is formulated as

$$v_{FV}(t+\tau) = min\begin{cases} v_{FV}(t)+2.5a_{FV}\tau\left(1-\dfrac{v_{FV}(t)}{V_{FV}}\right)\sqrt{\left(0.025+\dfrac{v_{FV}(t)}{V_{FV}}\right)} \\ b_{FV}\tau+\sqrt{b_{FV}^2(\tau)^2-b_{FV}\left[2(x_{LV}(t)-s_{LV}-x_{FV}(t))-v_{FV}(t)\tau-\dfrac{v_{LV}^2(t)}{\hat{b}}\right]} \end{cases}$$

where a_{FV} is the maximum acceleration that the following vehicle (FV) driver wishes to undertake, b_{FV} is the most severe braking that the FV wishes to undertake, s_{LV} is the effective size (physical size + some margin) of the leading vehicle, V_{FV} is the desired speed of the

following vehicle, $\hat{b}$ is the estimation of b_{FV} employed by the driver of FV and τ is driver's reaction time. The first equation represents the driver's tendency to reach a desired speed and the second equation estimates the speed that needs to be maintained to avoid collision. Gipps' model does not involve calibration of parameters, which instead has led to widespread use of this model both in simulation packages (Barceló, 2002; Liu, 2010; Silcock, 1993, Ciuffo et al., 2008) and in different research studies. One of the reasons for the popularity of this model is the realistic behaviour reported for situations involving either a pair of vehicles or platoons. Although the base of Gipps' model is reasonable, in reality a driver cannot estimate the safe distance accurately. Many researchers have attempted to modify Gipps' model and it remains the most widely used model till date.

2.2.1.3. Optimal Velocity Models

The first optimal velocity model was proposed by Bando et al. (1993) based on the consideration that each FV moves at her/his own optimum/desired velocity depending on the relative spacing with the leader and the FV controls acceleration in a manner that the desired velocity is maintained according to the motion of LV. The acceleration of FV is related to the difference between the driver's optimum velocity and the current velocity of the FV and is formulated as $a_{FV} = c[V(\Delta x) - v_{FV}]$ where c is the calibration parameter representing driver's sensitivity to the difference between optimal and current velocities, V is the optimal velocity function of Δx and v_{FV} is the current velocity of FV. A $\tanh(x)$ type curve was adopted as a candidate for V and the velocity function was chosen as $V(\Delta x) = \tanh(\Delta x - 2) + \tanh(2)$. The optimal velocity (OV) function was defined differently by different researchers but all were based on the fact the FV accelerates or brakes maintaining a safe distance with the LV.

The potential velocity function was modified by Bando et al. (1995) for the convenience to fit the function with observed data. Helbing and Tilch (1998) calibrated OVM with the empirical data but the model produced too high accelerations and unrealistic deceleration. Therefore they proposed a generalized force model (GFM) which reached better agreement with field data than OVM. But GFM does not behave well in all aspects because the model does not take the effect of positive Δv on traffic dynamics. Taking the positive Δv factor into account, Jiang et al. (2001) developed the OVM by taking both positive and negative velocity differences into account and adding an additional term $\lambda \Delta v$ into the car-following equation, λ is sensitivity constant and they called it a Full Velocity Difference Model (FVDM). The model is then applied to several traffic simulations and the results reveal that FVDM predicts correct delay time of car motion and the car in FVDM accelerates more quickly than the car in GFM. In another study, Lenz et al. (1999) incorporated multi-anticipative driving behaviour into the model to predict traffic flow on highways. Considerable research in the Intelligent Transportation Systems are nowadays performed to improve the efficiency and safety of the traffic system. Several car following models considering more than one leading car information provided by ITS have been proposed (Nagatani, 1999; Hasebe et al., 2003; Ge et al., 2004; Li and Zhang, 2013). The simulation results suggested that only the information of three cars ahead is enough for cooperative driving in Intelligent Transportation System.

The OVM has recently gained more attention by both applied mathematics and physicists due to its simple differential equation formulation and the single variable OV function. The model has also been developed for non-lane based traffic by considering lateral separation effects and time-to-collision (TTC) variable. Recent modifications in the OVM are due to its simplicity in understanding dynamics of the evolution of traffic congestion, stop and go waves, etc.

2.2.1.4. Intelligent Driver Model

Treiber et al. (2000a) developed a continuous microscopic single lane model, Intelligent Driver Model (IDM) for describing the congested traffic forming near road inhomogeneities on German freeways. The model combines both free-road acceleration and deceleration strategies of the following vehicle and is a function of the velocity, gap and the velocity difference to the preceding vehicle. The acceleration function is given by

$$a_n = a_{max}\left(1 - \left(\frac{v_n}{v_n^0}\right)^{\delta} - \left(\frac{s^*(v_n, \Delta v_n)}{s_n}\right)^2\right)$$

Where a_{max} is the maximum acceleration of vehicle *n*, v_n^0 is the desired velocity of *n*, δ is a parameter of the model (fixed as 4) which is used to characterize how the maximum acceleration of a vehicle decreases with increase in speed, s_n is the actual gap available between the front bumper of the following vehicle and the rear bumper of the leading vehicle, s^* is the desired minimum gap. In this model, the free road acceleration term is defined by $a_{max}\left(1 - \left(\frac{v_n}{v_n^0}\right)^{\delta}\right)$ while the deceleration term is $-a_{max}\left(\left(\frac{s^*(v_n,\Delta v_n)}{s_n}\right)^2\right)$. When a vehicle *n* comes too close to the preceding vehicle, the tendency to decelerate will depend upon the actual gap available and the desired minimum gap. The desired minimum gap is a function of $v_n \; and \; \Delta v_n$ and is given by

$$s^*(v_n, \Delta v_n) = s_n^0 + T_n v_n - \frac{v_n \Delta v_n}{2\sqrt{a_n b_n}}$$

where b_n is the desired deceleration of the vehicle *n*, s_n^0 is the jam distance of the vehicle *n* and $T_n$is the safety gap of the vehicle *n*.

The validation of the model was done by Treiber et al. (2000b) on a Dutch freeway for different percentage of cars and trucks. The flow-density diagram of heterogeneous traffic (cars and trucks) for congested flow looked reasonable than that for homogeneous traffic. Treiber and Kesting (2013) made an improvement in the model considering the situation that when the desired space gap exceeds the actual gap in the high speed range, drivers tend to be more defensive. The desired minimum gap in IDM is different from the reaction time used in other models. Some researchers (Jiang et al., 2014; Derbel et al., 2012) modified the desired time gap T by adding some additional term and considering it as a stochastic quantity changing its value at each simulation step rather than a constant value.

Although this model has been primarily used for single lane traffic with road inhomogeneity, the applicability of the model for disorderly traffic has not yet been fully explored. The model does not consider risk explicitly, though some aspects are handled in the deceleration factor and time gap implicitly. Most of the parameters are unobservable in real car-following situations, making the estimation more challenging.

2.2.1.5. Applicability of CF models in vehicle-following scenario

Early assumptions in CF modelling were rooted in the behaviouristic perspective of car drivers interacting with each other. However vehicle following behaviour of different leader-follower vehicle pairs may differ from cars due to differences in static and dynamic characteristics of vehicles, positioning of vehicles and different characteristics of their drivers. Yet, the extent to which the traditional models would be applicable to disordered traffic environments has recently been reported in a number of studies. Researchers have focused on studying responses between drivers driving different vehicle types and even for the same driver under different stimulus framework.

Ossen and Hoogendoorn (2011) compared five CF models to identify differences in the following behaviours of two cases: car following car and car following truck. Their findings indicated differences in their behaviours and the desired time headways of cars were found to be smaller when following a truck than following another passenger car. A study by Siuhi and Kaseko (2016) incorporated vehicle mix in *stimulus-response* CF model. Two separate models were estimated for acceleration and deceleration responses for different vehicle pairs including cars following cars, car following trucks and trucks following cars on a single lane. Results of the study demonstrated the need to separate the models for different vehicle-pairs. The findings were further substantiated by Aghabayk et al. (2016), Tordeux et al. (2010), Durrani et al. (2016), Ponnu and Coifman (2015), Chand et al. (2016), Sarvi (2013), Raju et al. (2019). Rakha and Wang (2009) evaluated Gipps' model and showed that it overestimated speeds for heavy vehicles. This indeed indicates that the capability and manoeuvring ability of different vehicle types existing in disorderly traffic streams could influence on their traffic stream characteristics. Ravishankar and Mathew (2011) modified the Gipps' equation to incorporate vehicle-type dependent parameters for different combinations of cars, trucks, motorized three-wheelers (3W) and buses on a single lane traffic. The model parameters were estimated using trajectory data collected using global positioning systems (GPS) devices in Mumbai. Kanagaraj et al. (2013) evaluated the performance of different CF models namely Gipps' model, IDM, Krauss and Das and Asundi models for disordered traffic conditions. In describing the longitudinal movement, they included strict following scenario, staggered following and non-overlap following as well, to capture some extent of disordered traffic characteristics in the models. In their study, Gipps' model was found to replicate field conditions better than other models. Recently, Anand et al. (2019) compared the suitability of GHR and Gipps' model for different leader-follower vehicle pairs using trajectory data collected in Chennai. Calibration of the vehicle-following models indicated that Gipps' model was more suitable for car-car and car-MTW pairs, while the GHR model was appropriate for MTW-MTW, MTW-car, MTW-

3W and 3W-MTW vehicle pairs. They further suggested the need to develop a hybrid model to capture the following behaviour of different combinations of vehicle pairs.

In summary, the presented literature showed the impacts of mixed vehicle types on traffic stream behaviour. Conventional models have been directly utilized to represent vehicle-following scenario of disordered systems, without incorporating the lateral separation effects. Although Gipps' model has been considered as the most influential and widely-used CF models both in lane-based and non-lane based systems, most of the researchers suggest development of separate vehicle-type dependent car-following models for vehicle-following scenario.

2.2.2. Staggered-following regime: modifications in conventional models

Moving from the car-following behavioural models to the emergence of staggered-following models, there is a growing body of literature that has enabled betterment of the existing models by incorporating lateral separation effects in the following scenario. In pursuit of realistic representation of staggered-following behaviour, the core CF models including GHR model, Gipps' model and optimal velocity model were predominantly investigated in the recent studies. Specifically, this section presents an overview of the modifications made in existing conventional models for a better representation of the staggered-following behaviour.

2.2.2.1. Modified GHR model

Jin et al. (2011) proposed a non-lane-based car-following model using time-to-collision information on a single lane highway. By taking lateral separation effects and visual angle observation, TTC is defined and accordingly introduced in the GHR model as the following driver's stimulus. The introduction of visual angle and lateral separation in the model was found to increase the capacity than that without lateral separation effect. Later Tao et al. (2015) improved the GHR model by considering generalized expectation time headway as stimulus in the model. The expectation headway is the headway that the following driver prefers to maintain with the leading vehicle at a certain lateral separation between them. Considering the differences between the actual and expected headway, the following driver decides whether to speed up or slow down. Numerical results suggest that the improved model strengthens model stability and enhances the function of the typical model.

2.2.2.2. Modified safe distance model

Lane-based driving discipline is defined by Gunay (2003) as the tendency of a vehicle to drive at the center of a lane as much as possible. Data for central positions of vehicles from multilane highways in Germany indicated that lateral positions of vehicles follow a normal distribution. A similar analysis was conducted in Turkey and it was found that vehicles move laterally along the entire road space, irrespective of lane markings (Gunay, 2004). The increase in center-line separation between two consecutive vehicles results in a decrease in headway.

With a view to incorporate the lateral separation effects in car-following models, Gunay (2007) considered that if a LV suddenly decelerates or applies brakes, the FV may not necessarily come to a complete stop; rather the follower may have the opportunity to move laterally and pass the stopped leader through the escape corridor, just to avoid a rear-end collision with the LV. Using this concept, the author modified the Gipps' car-following model where the maximum allowed speed of FV at the end of the reaction time is determined by the most restrictive of the two factors: (1) Maximum Escape Speed (MES)- the speed at which FV decelerates at the time of passing to the maximum speed allowed by the width of the escape corridor, and (2) speed which allows FV adequate time to veer laterally (t_{veer}) so as to avoid a rear-end collision (Figure 2.3).

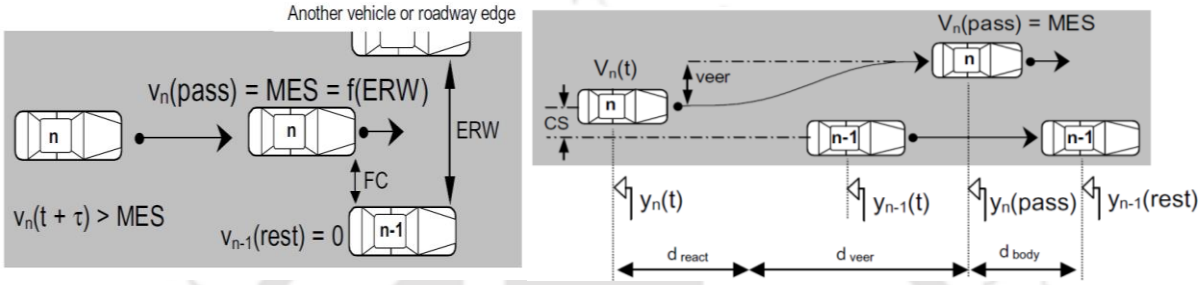

(a) **(b)**

Figure 2.3. (a) MES governed following in non-lane based **(b)** Partial lane change (Gunay, 2007)

The simulation updates the speed of the following vehicle according to the following equations (1 or 2), whichever governs the situation.

(1) $v_n(t+\tau) \leq b_n\tau + \sqrt{(b_n\tau)^2 + 2b_n\left\{v_n(t)\frac{\tau}{2} + \frac{MES^2}{2b_n} + \frac{v_{n-1}^2(t)}{2b_{n-1}} + y_n(t) - y_{n-1}(t) + s_{n-1}\right\}}$

(2) $v_n(t+\tau) \leq 2\frac{y_{n-1}(rest) - y_n(t) - 0.5\tau v_n(t) - \frac{t_{veer}}{2}MES - d_{body}}{t_{veer}+\tau}$

where b_n, b_{n-1} are the deceleration rates of the FV and LV respectively, d_{react} is the distance travelled during the reaction time, d_{veer} is the distance travelled during veering manoeuvre. The simulated space-time trajectories of follower-leader pairs for various frictional clearances (FCs) indicated that FV prefers to follow LV when FC is less than 0.5m. When both the LVs are separated in 0.5m-1.5m, the subject vehicle is no longer a follower instead it slows down speed while passing. However, FC greater than 2m leads the subject vehicle to pass the escape corridor without much fluctuations in speed. Similarly the results indicated that when CS is less than 2m, the interaction is a basic car-following case. The development of this model is a potential breakthrough of all the pre-existing car-following models, essentially for non-lane-based disciplined traffic. The validation of the model for describing the speed, flow and density diagrams of a three-lane carriageway in Istanbul was extended by Gunay (2009) for a simulation time of 60 min considering light and heavy vehicles. The proposed model produced closer results when compared with that of homogeneous traffic conditions.

A similar type of study was conducted by Xu et al. (2015) giving full considerations to the effect of FC on car-following behaviour. They have considered two conditions: when the subject vehicle is influenced by the two front vehicles in different lanes, and when the subject

vehicle is not influenced by the adjacent vehicle. The first condition only involves MES (veering is ignored) whereas in the second condition, the lateral drift of the vehicle for overtaking action due to the absence of adjacent vehicle is considered by taking veering time. Accordingly the safe minimum following distances required by the subject vehicle in both the cases are obtained and a numerical simulation study was carried out to verify the model. The verification of the model indicated that frictional clearance is proportional to the escape speed but is inversely proportional to the following time and minimum safe distance. Results on centerline separation of vehicles showed that when CS<1.9, subject vehicle follows LV, CS=1.9m: subject vehicle desires to surpass the LV and when CS>1.9m: subject vehicle drives at the maximum expected speed without any influence from the adjacent vehicle.

Lenorzer et al. (2015) modelled disordered traffic conditions of the entrance sections of Cadbury junction, Thane at evening peak hours by modifying the Gipps's car-following model. They considered that the subject vehicles follow the most restrictive leader while if there is a possibility of swerving and the duration of swerving is less than the reaction time, there is a reduced gap to avoid collision. They modified the Gipps' model by taking the reaction time as the minimum of reaction time and time required for swerving. The effect of LC into the model has also been considered (Gunay, 2007). The model was then made to run on a software package AIMSUN and the results on traffic counts indicated that there was less variation in the simulated and the observed counts (less than 5%).

2.2.2.3. Modified optimal velocity model

Taking into account the lateral separation characteristics between the leader and the follower on a single lane, Jin et al. (2010) modified the full velocity difference (FVD) model and proposed a non-lane based full velocity difference car-following model (Figure 2.4).

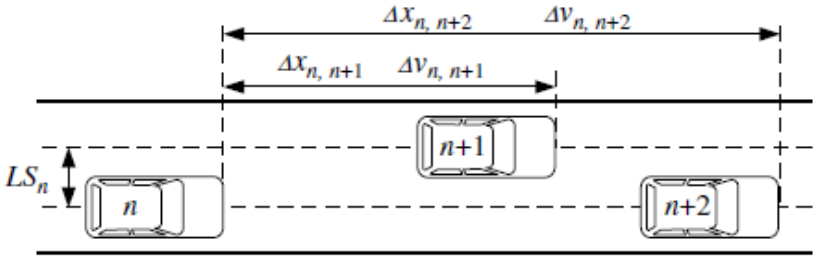

Figure 2.4. Staggered pattern of vehicles (Jin et al., 2010)

The dynamics of FV is a function of lateral separation effects of its leader and is formulated as

$$a_n(t) = \alpha\{V[\Delta x_{n,n+1}(t), \Delta x_{n,n+2}(t)] - v_n(t)\} + \kappa G[\Delta x_{n,n+1}(t), \Delta x_{n,n+2}(t)]$$

$$V[\Delta x_{n,n+1}(t), \Delta x_{n,n+2}(t)] = V[(1-p_n)\Delta x_{n,n+1}(t) + p_n \Delta x_{n,n+2}(t)]$$

$$G[\Delta x_{n,n+1}(t), \Delta x_{n,n+2}(t)] = [(1-p_n)\Delta x_{n,n+1}(t) + p_n \Delta x_{n,n+2}(t)]$$

$$V[\Delta x] = 0.5 v_{max}[\tanh(\Delta x - h_c) + \tanh(h_c)]$$

where $\alpha = {}^{1}/_{\tau}$ is the sensitivity coefficient of a driver to the difference between the optimal and the current velocities, $\kappa = {}^{\lambda}/_{\tau}$ is the sensitivity coefficient of response to the stimulus G(.), the lateral separation effect of the leader and follower is incorporated in $p_n = \frac{LS_n}{LS_{max}}$; LS_n is the lateral separation distance between car *n* and *n+1,* and LS_{max} is the maximum lateral separation distance that the leading car has no impact on the following car. $p_n = 0$ corresponds to the FVD model where *n* only follows *n+1*; whereas $p_n = 1$ indicates that *n* follows *n+2* as *n+1* is on another lane. The numerical simulation results showed that the effects of the lateral separation stabilized the traffic flow and lowered the critical distance headway.

Jin et al. (2012) developed a staggered car-following model using time to collision (TTC) variable into the optimal velocity model to describe the lateral separation effects of a pair of consecutive vehicles maintaining the same lateral distance and moving on a steady state on a single lane highway. A similar work was carried out by Zheng et al. (2012) to study the impact of lateral friction on two-lane unidirectional traffic flow. Visual angle is considered as one type of stimulus of a following driver to reflect the imperfect perception of distance, speed and acceleration. The FVD model is modified by replacing the original headway distance and relative velocity term with the visual angles and their changing rates respectively. The proposed model incorporated the lateral separation effect parameter p_n and the visual angles of driver *n* at time *t* for the two preceding vehicles in both the lanes were related to the lateral separation of vehicle *n,* LS_n, relative headway spacing, length of the vehicles and its width.

In a later date, He et al. (2015) extended the optimal velocity model by taking into consideration the effects of lateral separation and overtaking expectation through the escape corridor (Gunay, 2007). The study mainly focused on the effect of overtaking expectation on car-following behaviour. It does not necessarily guarantee the overtaking manoeuvre. An overtaking parameter is introduced considering the width of the escape corridor and the width of the FV expecting to overtake. When the width of the escape corridor is less than the width of the vehicle, parameter is zero; if it is greater, value is one and if it lies in between, the value is $\frac{Width_{escape\ corridor} - Width_{Car}}{Width_{lane} - Width_{Car}}$. The new model is developed with the lateral separation parameter and the overtaking parameter. The stability analysis of traffic flow is then performed to determine the effects of different factors on the traffic flow. Results indicated that increase in lateral separation and overtaking expectation increased the stability at a lower density and decreased for a high density. Calibration of the model is done using the trajectory data set from NGSIM (a program funded by the Federal Highway Administration of USA) using Genetic Algorithm approach. Further the model was validated using data on an urban road section in Guangzhou, China. The overall simulation results demonstrated that the proposed model performed better than Optimal Velocity model and Intelligent Driver Model. Xu (2015) extended the FVD model by including driver's reaction time delay into the equation to understand the mechanism of traffic jams because driver's reaction time may lead to unstable traffic flow (Zhou et al., 2014). A summary of the work related to staggered-following behaviour is presented in Table 2.2.

Table 2.2 Summary on the modifications made in basic CF models for mixed traffic conditions

Authors	Basic CF model		Vehicle types	Type of study	Parameters added	Data modelled	Calibration	Simulation platform	Final model representation
Jin et al. (2011)	Modified GHR model		C	Staggered-following with right-front leader	Visual angle information defined by TTC as stimulus	Single lane	Trial and Error	Numerical simulation	Flow and density variation with lateral separation
Tao et al. (2014)	Modified GHR model		C	Staggered car-following One Right front leader	Generalized expectation time headway (preferred time headway at a certain lateral separation) as stimulus	Single lane	Trial and Error	Numerical simulation	Headway and speed evolution with time
Jin et al. (2012)	Modified optimal velocity model	OVM	C	Staggered car-following One Right front leader	Time-to-collision variable using visual angle and visual gap angle.	Single lane	Trial and error	Numerical simulation	Headway and speed evolution with time
Zheng et al. (2012)	Modified optimal velocity model	FVD	C	Staggered car-following Two leaders : • Direct front vehicle • Left front vehicle	• LS effect between the leader and the follower • Visual angles	Single lane	Trial and error	Numerical simulation	Headway and velocity variations for different lateral separation parameter
He et al. (2015)	Modified optimal velocity model	OVM	C	Staggered car-following Two leaders : • Direct front vehicle • Left front vehicle	• LS between the subject and the leader • Escape corridor	NGSIM 25-min data	Genetic Algorithm	Numerical simulation	Comparison of Gap, velocity variations with time for proposed model, OVM and IDM
Gunay (2007, 2009)	Safe distance approach	Gipps	C	Staggered car-following • One right front leader	• LS, FC • Maximum Escape speed (speed required for passing through the escape corridor) • Veering distance	Multilane highway in Istanbul, Turkey	Assumptions of Gipps' model	C++	Space-time trajectories, Gunay (2007) Speed, Flow, Density diagrams (Gunay, 2009)
Lenorzer et al. (2015)	Safe distance approach	Gipps	C, 3W, T, B	Staggered car-following considering swerving manoeuvre (when duration of swerving is less than the reaction time)	• Lateral clearances of LV and FV • Maximum lateral speed of FV	Near Cadbury Junction, Thane at evening peak hour	Assumptions of Gipps' model	AIMSUN simulator	15-minutes traffic counts were compared

Note: **C**: Cars, **3W**: Motorized three-wheelers, **T**: Trucks, **B**: Buses**; LS**: Lateral Separation, **FC**: Frictional Clearance, **CS**: Centerline Separation; **TTC:** Time-to-collision; **FVD:** Full Velocity Difference Model**; OVM:** Optimal Velocity Model; **IDM**: Intelligent Driver Model; **NGSIM**: Next Generation Simulation (US Highway 101 dataset)

2.2.2.4. Other modelling approaches

Extending the concept of Jin et al. (2010), Peng et al. (2011) developed a non-lane based lattice hydrodynamic model considering the lateral separation effects in traffic flow. Numerical simulation results indicated that incorporation of lateral separation improves the stability of traffic flow. Gupta and Dhiman (2014) argued that the consideration of lateral separation not only stabilizes traffic flow, but also shrinks the critical region. Using potential attention field of drivers, Tao et al. (2014) established a driving behaviour model by reflecting driver's perception of the surrounding traffic environment with the changing field intensity value. The field intensity is a function of driver's own characteristics and motion state of its vehicle. Numerical results indicated that the model could simulate traffic flow operations quite realistically. In another study, Papathanasopoulou and Antoniou (2018) developed a locally weighted regression based data-driven model to describe car-following behaviour of disorderly traffic using trajectory data from Chennai. They concluded that data-driven model performed better than Gipps' model in predicting speeds and also highlighted the need for vehicle-dependent models. This finding is also consistent with Mathew and Ravishankar's (2012) work. Utilizing GPS trajectory data for six different vehicle-pair combinations (including car following car, motorized three-wheeler following car, car following motorized three-wheeler, motorized three-wheeler following another motorized three-wheeler, car-following bus and bus following car), Mathew and Ravishankar (2012) modelled vehicle-type dependent following behaviour using neural network approach. They found that in addition to leading vehicle's speed and space headway, interacting vehicle type needs to be considered to predict follower's speed in a single-leader following regime. A comparison of the developed model with the conventional Gipps' model further demonstrated improved performance of the data-driven based neural network model.

The lateral effect was further embodied in several works in which the lanes were classified into 'sublanes' or 'strips'. Mathew et al. (2015) proposed a strip-based modeling approach to model disordered traffic environments using trajectory data collected in Mumbai, in which a lane is divided into a number of strips. Depending on the width of vehicle, vehicles can occupy multiple number of strips. Such modelling approach however fails to capture the lateral movements of MTWs. The variable lateral clearance maintaining behaviour on mixed bicycle dynamics was introduced in cellular automata models (Feng et al., 2016) with an occupancy rule involving lateral gap information. Similar concept was also utilized in Luo et al.'s (2015) work considering interactions between bicycles and cars. Although the lateral gap maintaining behaviour between different vehicle combinations has been investigated in several studies empirically (Mallikarjuna et al., 2013; Pal and Chunchu, 2019; Budhkar and Maurya, 2017a; Siddique, 2013), they do not deal with any driver behaviour model.

To summarize, several researchers have proposed modifications in the conventional car-following models (such as GHR model, Gipps' model and optimal velocity model) by incorporating the effects of lateral separation. Yet, these models still lack validation against real-world data base. Conversely, the strip-based or sub-lane based approaches could capture heterogeneity in vehicles quite precisely (Mathew et al., 2015; Luo et al., 2015), but deciding a strip size or a cell size is more crucial. More precisely, there has been a growing attention

towards consideration of lateral separation effects in recent years. Howbeit, the inter-dependence between longitudinal and lateral separations in a staggered-following scenario and the applicability of the conventional models in such disordered systems still remain unexplored

2.2.3. Research on handling multiple leaders in the following regime

Recently, transport modellers have acknowledged that drivers in disorderly traffic environments often follow multiple leaders simultaneously. Although many advancements have been made in the existing conventional CF models to model staggered-following behaviour, a series of models have now emerged to incorporate more than one leader case, mainly in the context of behavioural modelling of non-lane based systems. This section therefore provides a systematic review of ongoing research work conducted for modelling multiple-leaders following behaviour in non-lane based disordered systems.

Research on multiple-leaders following dates back to the early 2000s. Cho and Wu (2004) developed a motorcycle traffic flow model based on the concept of thrust and repulsion. The desired speed of the following vehicle gives the thrust to proceed while the leading vehicle gives repulsion to the subject vehicle. The model considered in this study is a function of its desired speed, current speed, leader's speed, space headway and a minimum safe headway. It is based on the assumption that only the nearest left-side leader and right-side leader offer repulsion to the subject vehicle. A weight function is accordingly used to capture the lateral separation effects in the model. This model can handle single-leader as well as two-leaders following behaviour in the longitudinal movement models. However, calibration and validation of the model has not yet been reported. In a later date, Nguyen (2012) proposed a safety space model to describe the dynamic behaviour of MTWs in the presence of surrounding vehicles. This model assumes that the vehicle will be the most influential if the subject vehicle responds to it with the maximum magnitude of acceleration. The following angle and the width of route to follow a leader were also considered to affect the selection of the most influential vehicle (Nguyen et al., 2014). The proposed non-lane-based model was calibrated by regression analysis and the validation of the model resulted in low root mean square error (RMSE) values on speed. It could correctly describe more than 61% of swerving manoeuvres to the left or right. A comparison on the fundamental diagrams showed that non-lane-based behaviour makes traffic volume decrease to a greater extent than lane-based behaviour in traffic congestion.

According to Mathew et al. (2015), the leader is identified as the vehicle among all possible leaders that is closest in distance to the subject vehicle and if it is a tie, the one that has been identified first is considered as the leader. But in such situations, both the leaders may have similar impact on the subject vehicle and may be considered as the critical leaders. Choudhury and Islam (2016) argued that in the presence of multiple leaders (left-front, direct-front and right-front) in disordered traffic streams, the driver in the following vehicle is subjected to multiple sources of stimulus for acceleration and reacts only to the stimulus of the governing leader. The GHR modelling framework was used for the acceleration component of the leader and calibration of the model was done using trajectory data of Dhaka. They found that the

probability of a given front vehicle of being the governing leader is dependent on space headway, amount of lateral overlap, type of subject vehicle and relative speed. On the other hand, Papathanasopoulou and Antoniou (2018) argued that the closest vehicle according to the direction of motion is chosen as the most critical leader. Asaithambi et al. (2018) defined the governing leader as the vehicle that overlaps laterally with the subject vehicle within the look ahead distance. Similar to the concept of Cho and Wu (2004), a data-driven locally weighted regression model was developed by Papathanasopoulou and Antoniou (2019) to estimate vehicle speeds for disordered traffic conditions. In a recent study by Raju et al. (2018), on the basis of visual assessment, they first assumed leader-follower pairs as the ones that are separated laterally by 1.5m from the edge of the leading vehicle. Subsequently, based on relative distance versus relative speed plots of the assumed pairs, those vehicle combinations are identified as the true leader-follower pairs that exhibit hysteresis phenomenon (common characteristic of vehicle-following process) among different combination of vehicles.

Recent literature has systematically highlighted the historical advancements made in conventional CF models to model disorderly traffic behaviour. In the context of handling multiple-leaders, the optimal velocity model proved to be the most prominent one amongst all. Li et al. (2015a) proposed a full velocity difference model considering the effects of two-sided lateral gaps on the behaviour of the following vehicle (Figure 2.5). The proposed model considers three leaders: left front, direct front and right front vehicles and accordingly, two-sided lateral gaps (one with the LF vehicle and the other with RF vehicle) are only considered in the model.

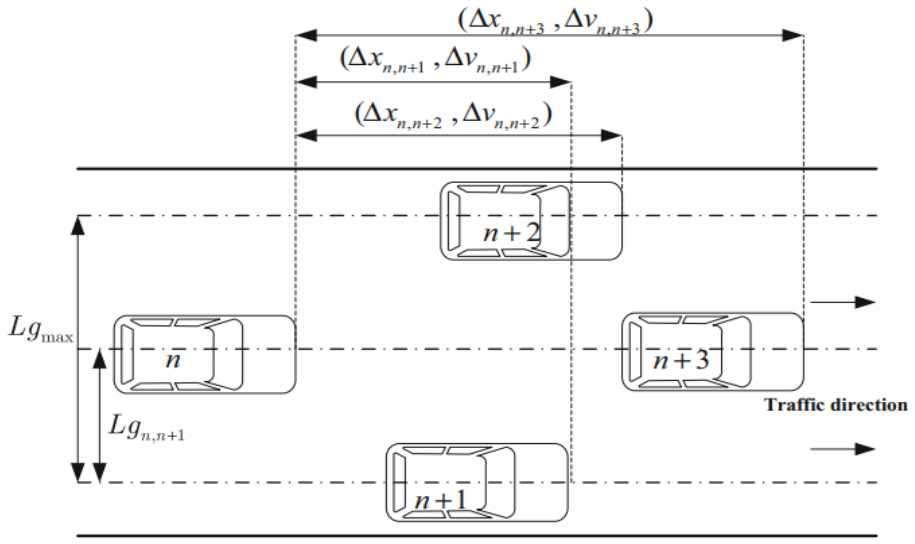

Figure 2.5. Representation of multiple-leaders following scenario (Li et al., 2015a)

Based on the FVD model, the two-sided lateral gap model takes the following form:

$$a_{FV}(t) = \alpha\{U[\Delta x_{n,n+1}(t), \Delta x_{n,n+2}(t), \Delta x_{n,n+3}(t)] - v_n(t)\} + \kappa G[\Delta v_{n,n+1}(t), \Delta v_{n,n+2}(t), \Delta v_{n,n+3}(t)]$$

$$U\left[\Delta x_{n,n+1}(t), \Delta x_{n,n+2}(t), \Delta x_{n,n+3}(t)\right] = \begin{cases} V\left[(1-2p_n)\Delta x_{n,n+1}(t) + 2p_n \Delta x_{n,n+3}(t)\right] \\ Lg_{n,n+1} \in [0, 0.5Lg_{max}\,] \\ V\left[(2p_n - 1)\Delta x_{n,n+2}(t) + 2(1-p_n)\Delta x_{n,n+3}(t)\right] \\ Lg_{n,n+1} \in [0.5Lg_{max}, Lg_{max}] \end{cases}$$

$$G\left[\Delta v_{n,n+1}(t), \Delta v_{n,n+2}(t), \Delta v_{n,n+3}(t)\right] = \begin{cases} (1-2p_n)\Delta v_{n,n+1}(t) + 2p_n \Delta v_{n,n+3}(t) \\ Lg_{n,n+1} \in [0, 0.5Lg_{max}\,] \\ V\left[(2p_n - 1)\Delta v_{n,n+2}(t) + 2(1-p_n)\Delta v_{n,n+3}(t)\right] \\ Lg_{n,n+1} \in [0.5Lg_{max}, Lg_{max}] \end{cases}$$

$$V(\Delta x) = 0.5 v_{max}[\tanh(\Delta x - h_c) + \tanh(h_c)]$$

Where α is the sensitivity parameter to the difference between optimal and current velocities; κ is the sensitivity coefficient related to the stimulus; $\Delta x(t)$ and $\Delta v_{n,n+1}(t)$ are the longitudinal space headway and speed difference between the leading vehicle n+1 and the following vehicle n at time t; $V(\Delta x)$ is the optimal speed function with respect to spacing Δx; the lateral separation effect is incorporated in $p_n = \frac{Lg_{n,n+1}}{Lg_{max}}$; p_n is the parameter representing the effect of lateral gap and Lg_{max} is chosen as 3.6m; v_{max} is the maximum speed of vehicle; and $\tanh(.)$ is the hyperbolic tangent function. The numerical simulation results indicated that this model could rapidly dissipate the effect of a perturbation such as a sudden acceleration or deceleration of a leading vehicle. The similar model was also used to investigate the energy consumption in electric vehicles traffic stream (Li et al., 2015b). Simulation results demonstrated that electric vehicles under non-lane discipline traffic streams consume more energy than lane-based discipline traffic. They suggested that regularizing lane-discipline might contribute to the improvement in energy efficiency.

Later, Li et al. (2016) proposed a new car-following model considering the effect of visual angle and lateral gap with the left-front and right-front vehicle. Numerical simulation results verified the impacts of lateral gap on traffic flow with respect to the smoothness and stability. More recently, Li et al. (2017a) considered the effects of the electronic throttle dynamics to capture the characteristics of connected autonomous vehicular traffic flow with two leading vehicles. Results from numerical experiments demonstrated that the model could represent the characteristics of connected and autonomous vehicular flow in terms of responsiveness, smoothness and stability. The effects of bilateral gaps were further considered in a macroscopic lattice hydrodynamic model proposed by Li et al. (2017b). The two-sided lateral gap model proposed by Li et al. (2015a) was further extended by considering the effect of gradient in addition to the lateral gaps (Li et al., 2018). Numerical results indicated that with the increase in gradient, the stability region enlarged in uphill scenario while it reduced in downhill scenario. Moreover, with the increase in gradient, the average space headway of traffic flow increased in uphill scenario while it decreased in downhill scenario. The bilateral gaps model proposed by Li et al. (2015a) could not capture the lateral separation with the direct front vehicle. Later, Xu et al. (2018) addressed the lateral gaps with left-front, right-front and also with direct front leaders and proposed a new car-following model. Linear stability analysis

illustrated that the proposed model had an enlarged stable region as compared to the two-sided lateral gap car-following model.

A synthesis of the literature illustrates that consideration of multiple leaders has received considerable attention in recent years for modelling the longitudinal movement of vehicles in non-lane based traffic environments. Most of the research has focused on the identification of a single governing leader among multiple vehicles ahead; lateral overlap and longitudinal gap being considered as the influential criterion in most of the work. Yet, the presence of more than a single leader may have a combined behavioural effect on the following process of vehicles. Indeed this aspect has been acknowledged in the series of modifications made in the optimal velocity models, in which the lateral gaps with each possible group of leaders were incorporated in the models. However, empirical calibration of the developed models has not yet been explicitly undertaken, which still requires validation against real data base.

2.2.4. Microscopic variables considered in vehicle-following models

Over the past decades there has been a gradual advancement in the car-following models, with an aim to embrace more realism in describing the following behaviour of vehicles in lane-based as well as in disorderly traffic environments. Various researchers have considered different parameters in the conventional car-following models to explain responses of the following vehicle. Most of the core car-following models employ vehicle speeds, relative speeds and distance headway (or, longitudinal gap) as significant input variables in describing the car-following behaviour. These variables can also be regarded as longitudinal descriptors of traffic as it describes vehicle interactions in the longitudinal direction of traffic flow. Conversely, other engineering models consider maximum operating characteristics of the following vehicles (such as acceleration/braking), desired speed, desired minimum spacing, jam distance, safety gap, etc. as relevant input variables in the car-following models. Over the years, there has been a historical betterment of each engineering car-following model, with inclusion of various aspects of driver heterogeneity, reaction time, driving error, prediction in different conditions such as congested, free-flow and transition phases, and so on.

While research shows that different CF models are available in the literature, there have also been notable advancements in the existing models for describing the vehicle-following behaviour of disorderly traffic. But, selection of input variables proves to be even more challenging because of complex vehicle interactions and vehicle-heterogeneity in such traffic. Several improvements, modifications and integration were made in the core CF models, by incorporating new input variables, for a realistic representation of vehicle-following behaviour. An overview of the microscopic traffic variables used in the modified car-following models for describing the staggered-following and multiple-leader following behaviour of vehicles is presented in Table 2.3.

It is evident from Table 2.3 that various research attempts have been undertaken in recent years by incorporating vehicle heterogeneity and lateral separation effects in the vehicle-following models. In the context of vehicle-following model development, different

Table 2.3 Summary of microscopic variables used in vehicle-following scenario of disordered traffic environments.

Authors	Modelling approach		Vehicle type	Microscopic traffic variables																
				Commonly used						Additional variables/parameters										
				V_{FV}	V_{LV}	RS	d_{FV}	A/D	LG	a_{LV}	CS	FC	t_{veer}	O_{exp}	θ	H_{exp}	L	W	TTC	I	Δ
Gunay (2007)	Staggered-following	Gipps' model	C	✓	✓		✓		✓			✓	✓				✓				
Ravishankar and Mathew (2011)			3W, C, T, B	✓	✓			✓	✓								✓				
Mathew et al. (2015)			MTW, 3W, C, T, B	✓	✓			✓	✓								✓	✓			
Lenorzer et al. (2015)			MTW, C, 3W, T, B	✓	✓			✓	✓			✓	✓				✓				
Xu et al. (2015)			C	✓	✓		✓		✓		✓	✓	✓				✓				
Anand et al. (2019)		Gipps and GHR	MTW, 3W, C	✓	✓	✓	✓	✓	✓			✓					✓	✓		✓	
Tao et al. (2014)		GHR Model	C			✓	✓		✓							✓	✓				
Sun et al. (2016)						✓	✓		✓	✓											
Siuhi and Kaseko (2016)				✓		✓	✓		✓								✓				
Jin et al. (2010)		FVD				✓	✓		✓		✓							✓			
Jin et al. (2012)						✓	✓		✓		✓							✓	✓		
Zheng et al. (2012)						✓	✓		✓		✓				✓			✓			
He et al. (2015)		OVM				✓	✓		✓		✓			✓				✓			
Mathew and Ravishankar (2012)		Neural network model	3W,C, B	✓	✓				✓											✓	
Asaithambi and Basheer (2017)		Discrete choice	MTW, C, B, T	✓	✓				✓			✓					✓	✓		✓	

(Contd.)

Authors	Modelling approach		Vehicle type	Microscopic traffic variables																
				Commonly used						Additional variables/parameters										
				V_{FV}	V_{LV}	RS	d_{FV}	A/D	LG	a_{LV}	CS	FC	t_{veer}	O_{exp}	θ	H_{exp}	L	W	TTC	I	Δ
Choudhury and Islam (2016)	Multiple leader-following	GHR	MTW, 3W, C, LCV, B, T	✓		✓	✓		✓		✓						✓			✓	
Li et al. (2015a), Xu et al. (2018)		FVD	C			✓	✓		✓		✓							✓			
Li et al. (2016)						✓	✓		✓		✓				✓			✓			
Li et al. (2018)						✓	✓		✓		✓							✓			✓
Papathanasopoulou and Antoniou (2018)		Locally weighted regression	MTW, 3W, C, LCV, B, T	✓	✓				✓		✓										
Cho and Wu (2004)		Concept of thrust and repulsion	MTW	✓	✓				✓		✓						✓	✓			
Nguyen (2012)		Safety space model	MTW, C	✓	✓	✓	✓		✓			✓					✓	✓			
Nguyen et al. (2014)				✓	✓	✓	✓		✓			✓			✓		✓	✓			

Note: **V:** Speed; **FV**: Following vehicle; **LV**: Leading vehicle; **RS**: Relative speed; **d**: Deceleration; **a**: acceleration; **A/D**: Maximum acceleration/deceleration of following vehicle; **LG**: Longitudinal gap; **CS**: Centerline separation; **FC**: frictional clearance or clear lateral clearance between two interacting vehicles;

t_{veer}**:** Veering time; O_{exp}: overtaking expectation of the subject/following vehicle; **θ:** visual angle perceived by the driver with respect to movement of its preceding vehicle;

H_{exp}**:** Generalized expectation headway and is defined as the headway that the subject vehicle hopes to maintaining with the preceding vehicle with certain centerline separation;

L: Vehicle length; **W:** Vehicle width; **TTC:** Time-to-collision; **I:** Type of interacting vehicles; **Δ:** Gradient of road (both uphill and downhill scenario)

GHR: Gazis-Herman-Rothery model; **OVM:** Optimal Velocity Model; **FVD:** Full Velocity Difference model;

MTW: Motorized two-wheeler; **3W:** Motorized three-wheeler; **C:** Car; **LCV:** Light Commercial Vehicle; **B:** Bus; **T:** Truck

researchers have underlined the need to develop vehicle-type specific models (Ravishankar and Mathew, 2011; Mathew and Ravishankar, 2012; Lenorzer et al., 2015; Choudhury and Islam, 2016; Asaithambi and Basheer, 2017; Papathanasopoulou and Antoniou, 218; Anand et al., 2019). Yet, the cognizance of lateral separation in describing disorderly traffic was highlighted in Gunay's (2007) work. Since then, the lateral separation was incorporated in optimal velocity model and in its subsequent modifications (such as full velocity difference model, two velocity difference model, etc.) to describe staggered-following (Jin et al., 2010, 2012; Zheng et al., 2012; He et al., 2015) as well as multiple-leader following behaviour (Li et al., 2015a, 2016, 2018; Xu et al., 2018). In a similar manner, the extent of lateral overlap was considered in Aaithambi and Basheer's (2017) work to classify car-following and staggered-following behaviour of different interacting vehicle pairs. An interacting leader-follower pair considered as an input in neural network model was found to significantly improve the performance of the model in predicting vehicle speeds (Ravishankar and Mathew, 2012). Moving beyond vehicle heterogeneity and lateral separation effects, different researchers have also attempted to include several input variables such as acceleration of leading vehicle (Sun et al., 2016), time-to-collision (Jin et al., 2012), visual angle (Zheng et al., 2012; Li et al., 2016), overtaking expectation (Hi et al., 2015) and headway expectation (Tao et al., 2014) in the conventional car-following models. Although time-to-collision and visual angle are related to driver's perception, selecting an appropriate visual angle threshold can be challenging (Saifuzzaman and Zheng, 2014). Moreover, drivers in general, cannot perceive leading vehicle's acceleration precisely and as such acceleration of leader as input in the car-following model may not represent realistic behaviour.

Research, however suggests that the surrounding environment or presence of more than one leader can have a significant influence on driver's confidence and behavioural phenomena (Muhrer and Vollrath, 2011). To address multiple-leader phenomena, researchers have predominately modified the full velocity difference model by considering relative spacing, relative speed and centerline separation with each set of leader, although empirical verification of the models is still lacking (Li et al., 2015a, 2016, 2018; Xu et al., 2018). Even, Li et al. (2018) considered road gradient into two-sided lateral gap model (modification of full velocity difference model). Although different input variables have been considered in the models, selection of adequate variables remains an issue for transport modellers. Variables that are easy to implement, more interpretable, easy to extract from collected data, realistic, simplify calibration process and at the same computationally efficient, can be a good alternative. Having incorporated lateral descriptors (centerline separation or frictional clearance) in the vehicle-following models, it is still not clearly known how the longitudinal and lateral descriptors of traffic are related, and also whether the effect of lateral separation changes with different roadway sections (single lane/multilane). Prior to driver behaviour modelling, suitable information related to interdependencies between longitudinal and lateral traffic flow descriptors needs to be attained first for a more realistic representation of driver behaviour, which indeed needs further exploration.

2.3. Driver behaviour models describing filtering behaviour of vehicles

Considering complex dynamic manoeuvring patterns of vehicles in non-lane based systems, recently there has been a great emphasis on understanding the filtering behaviour of smaller vehicles. Smaller vehicles, in such traffic systems, often take advantage of their compact sizes and high intuitive steering method to navigate through road traffic in a completely different way than any other vehicle. They are often observed to engage in complex manoeuvres where they tend to proceed through a series of available lateral spaces described by the vehicles in-front, commonly termed as filtering in the MTW-oriented literature. In essence, the filtering behaviour (also termed as seeping, creeping, percolation, Agarwal and Lämmel, 2016; Oketch, 2000, 2003) is a commonly observed phenomenon for motorized two-wheelers (MTWs).

A previous study by Nikias et al. (2012) highlighted that filtering is the most frequent manoeuvre of MTWs in urban arterials. Such nature of riding offers many purported benefits such as travel time saving, increased speeds and capacity, congestion and emission reduction, reduction in the risk of rear-end collisions, improved visibility of hazards and traffic (Hurt et al., 1981), etc. On the contrary, filtering behaviour has also been argued to pose several safety concerns as other vehicles fail to detect the presence of MTWs in the traffic (Rogé et al., 2010; Hublart & Durand, 2012) due to its compact size. Rogé et al. (2010) highlighted that one of the primary reasons for MTW-involved accidents is lack of attention and/or perception on the part of car driver to detect the MTW in time. Indeed they concluded that MTWs adopting filtering manoeuvre run a significant risk, as this behaviour makes them less visible to drivers, especially older drivers. In a study conducted by Clabaux et al. (2017) on urban areas in France, they found that the risk of MTW riders being involved in injury crashes is 3.94 times higher while filtering as compared to cases when they do not filter. Later, Clabaux et al. (2019) found that filtering by MTW is also associated with a higher risk of collision with a pedestrian.

The widespread adoption of MTWs in many countries and the risks involved with them while filtering have spurred a growing interest in transport modellers to model their manoeuvres. In a recently published research, Vlahogianni (2014) evaluated the determinants that significantly affect MTW riders' decisions to accept critical virtual lane widths during filtering. Critical lane width is defined as the minimum lateral clearance between any two vehicles which majority of MTW riders utilize while filtering. Some of the parameters that influenced riders' decisions were found as relative speed, spacing, heavy vehicles presence and occurrence of platoon of moving MTWs. However, research on the modelling of MTW traffic during filtering has been conducted in several ways. A review of the modelling approaches commonly employed for modelling the filtering behaviour in disordered traffic environments is discussed in this section.

2.3.1. Cellular Automata

Cellular automata model was first proposed by Nagel & Schreckenberg (Na-Sch) in 1992, wherein they depicted the basic features of traffic flows treating only cars on a single lane traffic stream. Since then, there has been a systematic advancement in the core Na-Sch model

to depict realistic behaviour of car-involved traffic (Nagel, 1996; Nagel et al., 1998; Kerner & Rehborn, 1996; Chowdhury et al., 1997; Knospe et al., 2000; Bham & Benekohal, 2004; Mallikarjuna & Rao, 2009).

Yet, during the early 2000s, a considerable number of cellular automata models have been employed by many researchers to explicate the interactions of MTWs with cars in urban mixed traffic streams. Lan & Chang (2003) first developed a particle-hopping model for describing the manoeuvreability of MTWs and their interactions with cars in mixed traffic streams on 2.5 m and 3.75 m lanes using each cell unit as 1.25x1.25m (Lan & Chang, 2005). Lan & Hsu (2005, 2006) introduced a common unit (CU) of squared grid 1.25x1.25 meters to represent a fine cell and a fine site for gauging the non-identical vehicle sizes and non-identical vehicle widths respectively to describe different vehicle types and their required clearances for safe movements on different lane widths. Based on their field observations in Taiwan, a MTW was represented by a particle of 1x2 cells, taking up 2 sites of road space whereas a car and bus were represented by 2x6 cells and 3x12 cells respectively. The same concept was further extended by Hsu et al. (2007) by reducing the CU size to a grid of 1.25x1.0m to precisely capture the realistic behaviours of MTWs. Another study by Meng et al. (2007) incorporated cars and MTWs into simulation by categorizing a single lane into three virtual sub-lanes in which each MTW occupied a cell of 3.75 m length (length of MTW and some safety distance).

However, in the context of modelling filtering behaviour of MTWs in mixed traffic streams, Lan et al. in 2009 proposed a refined CA model (1.25x1.0m) for cars using piecewise linear velocity variations to fix the abrupt deceleration behaviour of vehicles while approaching traffic jams or stationary obstacles. They introduced the concept of limited deceleration capability of vehicles into their simulations in order to ascertain safe distance with the front vehicles. They further proposed a sophisticated cellular automata model to elucidate the erratic MTW behaviours in mixed traffic conditions (Lan et al., 2010) which in addition to the conventional longitudinal movement and lane-change rules, can also explain the filtering behaviour of MTWs between two stationary cars.

Owing to the enhanced resolution of finer cell system, a precise representation of the traffic conditions can be attained but at the same time, it can significantly increase the computational burden, thereby reducing the simulation efficiency. In addition, deciding a proper cell size for simulating disorderly traffic is more crucial because the dynamic characteristics of vehicles such as speed, acceleration, and deceleration are highly affected by the length of the cell.

2.3.2. Porous flow approach

To address the filtering phenomena of smaller vehicles and dynamics of different vehicle classes in heterogeneous queues of disordered traffic systems, Nair et al. (2011) developed a continuum model using an equilibrium speed-density relationship, considering that vehicles traverse through a series of pores defined by other vehicles on the traffic stream. In this approach, the complex interactions of vehicular traffic are assessed on the basis of pore space distribution for each vehicle-class since all vehicle types cannot utilize the same pore space (larger vehicles cannot use the same pore that smaller vehicles can) and each vehicle class is

assumed to have an independent fundamental diagram. To account for the lateral dynamics of vehicles, the overall speed of traffic stream for each vehicle class is considered to consist of free vehicles $u_f(v,x,t)$ and restrained vehicles $u_r(v,x,t)$:

$$u\,(v,x,t) = u_r(v,x,t)\int_0^{r(v)} f_p\big(r_{p,}x,t\big)dr_p + u_f(v,x,t)\int_{r(v)}^{\infty} f_p\big(r_{p,}x,t\big)dr_p; \qquad \forall v = 1,2\ldots n$$

where

$$u_r(v,x,t) = u^f(v)\left(1 - \int_0^{r(v)} f_p\big(r_{p,}x,t\big)dr_p\right)^{\alpha_r}$$

$$u_f(v,x,t) = u^f(v)\left(1 - \int_0^{r(v)} f_p\big(r_{p,}x,t\big)dr_p\right)^{\alpha_f}$$

$f_p\big(r_{p,}x,t\big)dr_p$ indicates the fraction of pores with pore size r_p, r and f indicates restricted and free vehicles, $\alpha_r \geq \alpha_f$, $u^f(v)$ is the free flow speed of vehicle class *v*. A full description of the model can be found in Nair et al.'s (2011) research work.

This model was verified by Ambarwati et al. (2013) using empirical data from Indonesia. In their study, the pore size was found to be dependent on vehicle dimensions and type of vehicles they interact with. The authors further extended their work in 2014 with a view to analyze vehicle type-specific critical pore sizes, develop pore size density distribution and to produce the vehicle type specific speed-density and flow-density diagram for MTW-MTW, MTW-car and car-car (Ambarwati et al., 2014). Results of the study indicated that the pore size distribution depends on traffic composition and density; traffic composition also affects the fundamental relationships for mixed traffic flows. Later, an enhanced porous flow model was developed by Gashaw et al. (2018) considering mixed flow of cars and MTWs. Unlike Nair et al.'s (2011) work, Gashaw et al. (2018) provided a closed-form analytical expression for the pore size distribution and applied a consistent discretization method for the approximation of the conservation equations. Simulation results showed that a gradual replacement of cars with MTWs increase the traffic flow capacity by 9.3% already with 10% MTW penetration. The results further indicated that creeping through slow car traffic at traffic light actually impacts queue clearance time and as such should be considered by traffic light where the cycle length is set according to queue clearance time.

The proposed approach cannot implement more than two vehicle classes because the analysis becomes cumbersome for the multi-dimensional case. The pore size distribution for each vehicle class is expected to remain stationary which may not always hold true, especially in the case while approaching a signalized intersection. The porous flow model considers equilibrium speed-density relation where transitions in stationary traffic states are only allowed. The equilibrium assumption however induces uncertainty in describing the stationary state as there exhibits heterogeneity in driver behaviour and vehicular characteristics even within the stationary state.

2.3.3. Agent based modelling approach

Agent based modelling is a powerful microscopic simulation modelling technique in which the actions and interactions of a cluster of computational agents (Franklin & Graesser, 1997; Langton, 1989) in the traffic flow are simulated repeatedly over time. An agent has specific characteristics, memory and goals to identify its neighbourhood and meet the design objectives. This modelling is appropriate when agents are heterogeneous, interactions of agents are complex, nonlinear and agents exhibit complex behaviour (Bonabeau, 2002).

Substantial research work exist to model the filtering behaviour and complex interactions of MTWs using agent-based modelling technique. Lee (2008) described the characteristic behaviour of MTWs in which the author integrated the swerving/unswerving manoeuvre of MTWs moving behind another vehicle in a lane, the safety distance maintained by a vehicle while following obliquely and the path choice model to choose a desired path (left, straight or right). In a later date, Lee et al. (2009) integrated the path choice model, oblique and lateral headway model to describe the characteristic behaviour patterns of MTWs and the safety distance maintained by a MTW rider while following obliquely and laterally. Agarwal et al. (2015) used multi-agent transport simulation framework, MATSIM to simulate cars and MTWs near a signalized intersection. MATSIM is based on a queue model which employs the earliest-link-exit-time approach to simulate the mixed traffic conditions. The queue model however takes into account only the vehicles at the entry or exit of the link without considering any dynamics. At lower densities, speeds of MTWs and cars were found to be consistent whereas at higher densities, there was a reduction in the speed of cars while MTWs' speed remained unaffected. Filtering of smaller vehicles in the congested regime was modelled by Agarwal & Lämmel (2015) in which they introduced the concept of backward travelling holes that results inherently due to the creeping of smaller vehicles while all the large-sized vehicles are essentially in stationary mode. This work was extended by Agarwal & Lämmel (2016) to validate the filtering behaviour with real-world data of Patna, India. The agent-based technique was further used by Lee & Wong (2016) to simulate the queue formation process of MTWs in heterogeneous traffic near a signalized intersection using the BikeSim simulator. The simulator could represent the lateral position choice and longitudinal movements of MTWs while approaching a queue. They further demonstrated that the agent based simulator could integrate the discrete choice models for the microsimulation of heterogeneous traffic.

The widespread use of agent-based approach to simulate complex systems is due to its simplicity in the programming technique, ability to recognize and distinguish the attributes of other agents and ease in decision making process. Simulating a large number of agents at a lower level to describe the aggregate behaviour can however prove to be extremely computational intensive. Hence a proper balance between computational power and execution speed need to be attained to account for an improved performance of the model.

Combining increased vulnerability of MTW riders with their widespread utilization in urban areas, there has been an abundance of research work focusing more on safety-related studies and modelling approaches used to depict the dynamic behaviour. Literature has also underlined the heightened risks associated with MTW riders while filtering through traffic. While some

researchers have attempted to model the filtering behaviour considering mixed flow of cars and MTWs, a detailed investigation of the underlying factors affecting the filtering choice is still lacking. More importantly, cars also exhibit filtering behaviour in mixed traffic disordered traffic systems. This has not yet been represented in the literature, but deserves further exploration.

2.3.4. Microscopic variables used for modelling filtering behaviour

As indicated in the literature, filtering behaviour has been mostly studied for MTWs in urban heterogeneous environments. Most of the research work focusing on filtering manoeuvre consider speed difference with the leading vehicles and relative spacing between vehicles as the most contributing factors (Lan et al., 2010; Ambarwati et al., 2014; Vlahogianni, 2014; Agarwal et al., 2015, 2016; Lee and Wong, 2016). The diagonal opening (or pore size) between the front vehicles (Ambarwati et al., 2014; Lee and Wong, 2016), lateral gap between the vehicles (Vlahogianni, 2014; Lee and Wong, 2016) and speed of the subject vehicle (Nikias et al., 2012; Ambarwati et al., 2014; Agarwal et al., 2015; Lee and Wong, 2016) have also been demonstrated as significant variables. In addition, Nikias et al. (2012) and Vlahogianni (2014) concluded that involvement of trucks in either left or right lane and existence of a platoon of MTWs also affected riders' decision to filter. More specifically, they found that involvement of a heavy vehicle in the right lane is significant while the likelihood to filter is not dependent on the presence of heavy vehicle in the left lane. Moreover, differences in subject vehicle type (that is, motorcycle and moped) were also considered in Vlahogianni's (2014) work but results of binary logit model indicated no significant effect of two-wheeler vehicle type in the filtering choice.

The decision of the MTW driver to perform a filtering manoeuvre may depend on several factors such as driver characteristics (age and gender), vehicle characteristics (type and dimensions of interacting vehicles), current traffic conditions (speed, spacing, surrounding traffic, density, etc.) and history of past trajectories. Although speed of interacting vehicles, longitudinal and lateral spacing between vehicles and relative speed have been considered in the existing literature, details of surrounding traffic conditions such as presence of vehicles adjacent to the subject vehicle (either to the left or right side) and vehicle characteristics such as presence of heavy vehicles as an interacting left-front or right-front vehicle, vehicle dimensions of the interacting vehicles can be further explored. More determinants such as helmet usage, age, gender, occupancy of MTW and number of lateral movements made by MTW drivers in the past trajectories may have a significant influence on the filtering decision. The effect of two-wheeler vehicle type (motorcycle or moped) has no influence on the filtering choice (Vlahogianni, 2014). Yet, it is still unexplored how the filtering choice is affected by different subject vehicle types (say, MTWs, 3Ws and cars) and what traffic variables affect their decision to filter in between the leading vehicles. To address these concerns, an in-depth exploration investigating differences in the filtering behaviour according to subject vehicle type, with due consideration of variables explaining different driver-vehicle characteristics and local traffic conditions, still needs to be conducted in detail.

2.4. Methodologies used for collecting vehicle-following and filtering data

Several data collection methodologies are available to capture driving behavioural phenomena, some of which operate on-board and others off-board or roadside. Roadside data collection techniques enable identification, tracking and recording of vehicle trajectories for a shorter road stretch, the most popular being video cameras fixed at a high vantage point near roadside. This technique is also referred as static video tracking technique as it allows tracking vehicle trajectories from static cameras via video image processing. Owing to the non-intrusive nature and flexibility in obtaining detailed information on vehicle trajectory data for a wide variety of interacting vehicle types, video-recording technique has received considerable attention for the collection of microscopic traffic data for different vehicle-pair interactions. On the other hand, on-board data collection techniques involve monitoring trajectories of vehicles for a longer time, under more flexible and controlled experimental conditions. An instrumented vehicle is essentially equipped with sensors (GPS receivers, video cameras, etc.) whose kinematics is recorded for the analysis purposes. Because the instrumented vehicle travels along the road and provides a dynamic set of video data for a longer period of time, this technique is referred as dynamic video tracking technique.

In general, static video tracking technique provides visual information on different interacting vehicle types and their vehicle trajectories, thus making it suitable to investigate vehicle-following and filtering behaviour of different vehicle-pair interactions along a selected road section. Most of the car-following literature on disorderly traffic has employed static video tracking technique for obtaining detailed vehicle trajectory data (Kanagaraj et al., 2013; Choudhury and Islam, 2016; Anand et al., 2019; Raju et al., 2019). In the context of modelling disorderly flows, an open-source detailed trajectory data of Chennai has been made available by Kanagaraj et al. (2015). The video data were collected on a six-lane divided urban arterial in Chennai and trajectory data were extracted using trajectory extractor (Lee et al., 2008). The data included 3,005 vehicle trajectories with 111,629 observations obtained at a resolution of 0.5s. Asaithambi et al. (2016) evaluated the performance of different car-following models such as Gipps' model, IDM model, Krauss model and Das and Asundi model, using trajectory data of Chennai. Similarly, Papathanasopoulou and Antoniou (2018) used the open-source mixed trajectory data (Kanagaraj et al., 2015) to evaluate the feasibility of locally weighted regression car-following model. Siuhi and Kaseko (2016) incorporated vehicle heterogeneity (interactions of cars and trucks) in the GHR model using detailed trajectory data (obtained from static video recorders) of next generation simulation study (NGSIM). Choudhury and Islam (2016) utilized static video tracking technique to model multiple-leader following behaviour. They obtained detailed trajectory data of 895 vehicles with 5507 observations, consisting of a wide range of vehicle types (MTWs, 3Ws, cars, LCVs, trucks, buses, bicycle and cycle rickshaw), with data being collected from Dhaka, Bangladesh. Using trajectory data collected by static cameras from eight-lane divided mid-block section of Delhi, Raju et al. (2019) further evaluated the validity of different car-following models in describing vehicle-following (single-leader following) behaviour of disorderly traffic. Even for modelling filtering behaviour, existing studies have utilized trajectory data obtained from static video recorders. To name a few, Vlahogianni (2014) employed static video-based trajectory extraction method

to collect kinematic characteristics of MTWs and all vehicles involved, from an urban arterial. The dataset involved 1375 cases of MTW traffic, extracted at a resolution of 0.5s. Similarly, Ambarwati et al. (2014) collected trajectory data using static video cameras from two different sections of Indonesia for an empirical calibration and validation of porous flow model.

On modelling vehicle-following and filtering behaviour of disorderly traffic, literature has demonstrated the widespread consideration of static video tracking techniques. Information on vehicle trajectories of different vehicle types and their interactions with surrounding traffic can be suitably obtained for limited stretch lengths. However, calibration and validation of car-following or vehicle-following models requires detailed dynamic time-series information on the driver's responses for as long a period as desired. Although many studies have made notable advancements in the conventional car-following models to describe vehicle-following behaviour, an empirical calibration of the models have led to serious difficulties with both collection and processing of accurate time-series data in a common space-time reference system (Punzo and Simonelli, 2005; Punzo et al., 2005). The staggered-following behaviour in disordered traffic systems add even more complexity in obtaining reliable time-series vehicle-following data. In the domain of on-board data collection techniques or instrumented vehicles, the dynamics of the following vehicle can be thoroughly analyzed for long stretches along a route. On one hand, instrumented vehicles can adequately capture the relative spacing and speeds using sensors; while on the other hand, an accurate positional data of the equipped vehicles can be obtained with the satellite-based GPS technology (Gurusinghe et al., 2002). In the context of car-following theories, Hatipkarasulu et al. (2000) and Jiang and Li (2001) have underlined the flexibility of vehicle-mounted GPS receivers to collect the position and speed data with a positional accuracy of 1 to 5m and speed accuracy of 0.16km/h. Additionally, by utilizing time-series data for a platoon of 10 vehicles in a probing field, Gurusinghe et al. (2002) demonstrated the superiority of the GPS technology in accurately estimating data than other conventional methods. Punzo and Simonelli (2005) used kinematic differential GPS instruments to investigate the methodological issues of car-following model calibration and validation by accurately monitoring the trajectories of four vehicles in a platoon under real traffic conditions. The peer-reviewed literature has also elucidated the efficacy of real-time differential GPS receivers in suitably modelling the vehicle-following behaviour of disorderly traffic (Mathew and Ravishankar, 2012). Despite the high expected accuracy of kinematic GPS in vehicle tracking, the estimation of time-series trajectories in describing vehicle-following behaviour is indeed challenging. Having recognized the importance of lateral descriptor in describing vehicle-following behaviour, estimation of lateral separation from GPS receivers may produce unreliable results.

To summarize, the static video tracking technique has been utilized in many research work to capture vehicle heterogeneity, interactions between different vehicles, information on surrounding traffic as well as aggregate behaviour of drivers, in describing vehicle-following and filtering behaviour. Conversely, instrumented vehicles using dynamic video recorders and GPS receivers, were considered to describe detailed dynamic responses in vehicle-following behaviour of disorderly traffic. But such techniques cannot estimate relative spacing (both longitudinal and lateral separation) in vehicle-following scenario efficiently. Because proper

evaluation of detailed drivers' responses requires an accurate characterization of microscopic traffic variables and reliable experimental data, a suitable image-based on-board data collection technique still needs to be developed for understanding detailed driving behaviour in vehicle-following scenario of disordered traffic environments.

2.5. Gaps in the existing literature

Research on driver behaviour modelling has proliferated over the past several decades. Studies have largely focused on understanding and modelling car-following behaviour in homogeneous lane-based traffic, which has been considered as one of the most researched areas in traffic flow modelling and safety related studies till date. With time, researchers have duly acknowledged the distinct characterization of disorderly traffic flows from lane-based traffic. Interest in understanding driving behaviour in non-lane based traffic has progressively emerged, with a growing body of literature underlining the differences in behavioural patterns emerging in such disordered systems. While longitudinal interactions between vehicles in lane-based traffic are described by traditional car-following models, researchers have highlighted that modelling such interactions in non-lane based traffic systems involve considering interactions with immediate leader, partial leader, multiple leaders and filtering between leaders. The peer-reviewed literature detailing such driver behavioural aspects is still limited and there are important questions that are yet to be examined in detail.

Having provided an extensive review on the behavioural patterns of vehicles in both lane-based and non-lane based traffic scenario, a synthesis of the literature showed that there are key gaps in research methods, modelling parameters and data collection and processing methodology to describe driving behaviour accurately in such disordered systems. Specific gaps in the available literature and certain major issues are summarized below:

1. *Research methods*: A number of driving regimes describing the following behaviour need to be suitably investigated and modelled to describe driving behaviour in non-lane based disordered systems. First, a plethora of literature is available to describe the longitudinal descriptors of traffic flow in the car-following process. Yet, little is known about the effect of the lateral indicator in describing the integrated driving behaviour of non-lane based traffic systems. Second, several researchers have proposed modifications in the conventional car-following models to describe staggered-following (GHR, Gipps and OVM being widely used) and two-leader (or, multiple leader) following behaviour (one of the most prominent ones is extension of OVM). However, empirical calibration of the developed models have not yet been explicitly undertaken, which still requires validation against real data base. The applicability of these modified conventional models to describe non-lane based traffic flows further remain unexplored. Third, the transition from two-leader following regime to filtering in between them involves a series of parameters that affect the decision choice in undertaking such manoeuvre. Combining increased vulnerability of MTW riders with their widespread utilization in urban areas, researchers have focused more on modelling the filtering behaviour of MTWs. But, cars are even

observed to exhibit such behaviour in disordered traffic systems, which deserves considerable attention from driver behavioural modelling standpoint.

2. *Modelling parameters*: Literature has demonstrated the need to develop vehicle-type specific car-following models for mixed traffic scenario (Ravishankar and Mathew, 2011; Aghabayk et al., 2016; Durrani et al., 2016; Raju et al., 2019). Yet an in-depth exploration of the surrounding traffic and geometric conditions is required to describe the following behaviour in different driving regimes. Information on surrounding traffic involves description of interacting vehicles, presence and type of surrounding vehicle adjacent to the subject vehicle, lateral movement of vehicles, acceleration/deceleration of vehicles, vehicle dimensions, driver characteristics (where applicable), etc. On the contrary, information on geometric conditions involve type of road (urban arterials, highways, rural roads), width of road, straight or curved sections, etc. Although the lateral separation has been considered in some of the vehicle-following models, it is still not clearly known how the longitudinal descriptors of traffic are related to the lateral descriptor (or, centerline separation) and whether the effect of centerline separation changes with different interacting vehicles and different roadway sections (single lane/multilane). These determinants, being poorly-represented in the existing literature, may affect the behaviour of drivers not only in vehicle-following scenario but also in the decision making process while filtering through traffic.

3. *Data collection and processing*: The use of appropriate data collection schemes plays a dominant role in reproducing the realistic behavioural phenomena. Trajectory data using static video recording technique has been mostly utilized in the calibration and validation of vehicle-following models (Kanagaraj et al., 2013; Choudhury and Islam, 2016; Anand et al., 2019; Raju et al., 2019) and also for understanding filtering behaviour of disordered traffic systems (Vlahogianni, 2014; Ambarwati et al., 2014). Yet, utilization of such trajectory data in understanding the behavioural patterns of different vehicles interacting with a wide variety of traffic mix as well as with the surrounding environment is still scarce.

   Conversely, dynamic video recording technique with kinematic differential GPS instruments has been utilized in Mathew and Ravishankar's (2012) work to collect single-leader vehicle-following data of disorderly traffic streams. But, the collection of dynamic time-series data from only GPS receivers may lead to inaccurate and unreliable results as the lateral descriptor of vehicle interactions needs to be suitably addressed for modelling vehicle-following behaviour in non-lane based traffic environments. To overcome this, a suitable data collection technique needs to be developed to gather and process dynamic time-series data for understanding the behavioural responses of drivers in vehicle-following regimes (either single leader or two-leaders) of disorderly traffic by considering both longitudinal and lateral separation between vehicles.

In closing, with technological advances and ever-increasing computing capabilities, more realism can be embraced in the models with collection of high-fidelity traffic data and prior understanding of dynamic movement patterns of vehicles in non-lane based traffic systems. A synthesis of the literature addresses the need to precisely and realistically characterize different driving regimes such as car-following, staggered-following, two-leader following and filtering

behaviour by capturing both longitudinal and lateral movements from driver behaviour modelling standpoint. Proper investigation of the driving regimes will direct to the development of a comprehensive driving behaviour model for such disordered systems. It will further augment the reliability of the existing simulation models, safety enhancement of drivers and also in autonomous systems and intelligent transportation systems applications.

3

Methodology for Data Acquisition and Extraction

A realistic representation of driver's behavioural phenomena depends to a large extent on the accuracy of data obtained. Improved accuracy in data collection not only provides an accurate reproduction of real traffic phenomena but also allows development, calibration and validation of traffic flow models or submodels from a microscopic perspective. With driver behaviour model forming the cornerstone in microscopic traffic simulation model development, achieving a detailed understanding of how drivers react with surrounding traffic of differing or similar vehicle types and how they manoeuvre through traffic, entails selection of suitable experimental data collection technique and processing of real-time traffic data. In particular, trajectory data has been mostly utilized in the calibration and validation of driving behaviour models for homogeneous traffic (Toledo et al., 2003; Choudhury, 2007) as well as for disorderly traffic (Lee et al., 2009; Kanagaraj et al., 2010; Sangole and Patil, 2014). Considering the importance of vehicle trajectory data in understanding distinct manoeuvring patterns of vehicles, this chapter aims to describe various data collection techniques used for obtaining vehicle trajectories. An elaborate description of the data collection and estimation processes to realistically model disorderly traffic phenomena has been discussed in this chapter. Essentially, this chapter is divided into three sections as described below:

1. *Data collection techniques*: This section provides an overview of video recording based data collection techniques (both static and dynamic video tracking methods), advantages and disadvantages of each method and the possible applications in understanding driving behavioural phenomena in non-lane based traffic environments.

2. *Methodological framework using static video tracking technique:* This section describes the data collection and extraction process for understanding interactions between different combinations of leader-follower pairs, with static video cameras being placed at elevated positions to record moving vehicles. Essentially, the methodological approach used for understanding and modelling the staggered-following and filtering behaviour of different vehicle types is discussed in this section.

3. *Methodological framework using dynamic video tracking technique:* Efforts are being directed to the development of an image-based data collection system for the estimation

of dynamic time-series data, using camera calibration and in-vehicle global positioning system (GPS) information. Vehicles are equipped with cameras and GPS to track targeted vehicles over a longer period of time. This section describes the data collection, estimation and calibration process for a detailed understanding of single-leader and two-leader car-following behaviour.

3.1. Data collection techniques

Obtaining reliable vehicle trajectory data in non-lane based disordered systems has proven to be a demanding task for the past few years. Vehicle tracking using video recording technique has received considerable attention for the collection of vehicle-following and filtering data of disorderly traffic streams (Kanagaraj et al., 2013; Choudhury and Islam, 2016; Anand et al., 2019; Vlahogianni, 2014). Specifically, video based vehicle-tracking technique has the flexibility in obtaining more accurate and detailed information on vehicle trajectory data, which can be extracted from the video sequences using proper image processing techniques. Although an image processing technique can extract traffic data from the collected video images, a suitable semi-automated trajectory extraction tool for vehicle tracking in mixed traffic environments is still under development.

TRAZER (Mallikarjuna et al., 2009) and traffic data extractor (TDE) (Munigety et al., 2014) are the commonly used tools for trajectory extraction in mixed traffic scenario till date. However, lower accuracy in providing microscopic and macroscopic parameters and limited length of vehicle tracking (50m) have led to scanty use of TRAZER in vehicle tracking applications. On the contrary, the TDE tool offers advantages in capturing accurate trajectory data for a length of 250m depending on the video resolution. But, at the same time vehicle tracking using this tool proves to be a laborious and time-consuming task, which involves tracking of a single vehicle one at a time; meaning that multiple vehicles cannot be tracked in a single video frame. To overcome this limitation, Budhkar and Maurya (2017) has recently developed a more advanced version of a semi-automated trajectory extracting system based on vanishing point technique devised by Fung et al. (2003). The system is designed in a MATLAB platform to collect multiple information including information on targeted vehicle, driver characteristics, surrounding traffic environment, etc. in a single still image, thereby reducing considerable time and effort and subsequently providing a more detailed information on the trajectory of multiple vehicles in a single frame.

In particular, detailed trajectory data from video recorders can be obtained by static as well as dynamic video tracking techniques. While the static technique employs video cameras fixed at a static elevated position to record vehicle movements, the dynamic technique involves video cameras attached at the vehicles which keeps a continuous track of the targeted vehicles. A detailed description of both the video-based vehicle tracking techniques and their suitability in processing detailed trajectory data for understanding different driving scenario of non-lane based traffic environments are discussed in this section.

3.1.1. Static video tracking technique

This technique refers to video tracking of vehicles from the static background. In particular, the video footage is collected from the camera mounted at fixed or any preferable elevated locations that records moving traffic during acquisition (Bovik, 2010). A static camera mounted at a high vantage point, in an unobtrusive and undistorted manner, can record the naturalistic driving behaviour depending on the field of view and video resolution of the mounted camera. An arrangement of a static video recording technique and an example of the video image of a traffic stream captured from the static camera mounted at a high-rise building is presented in Figure 3.1.

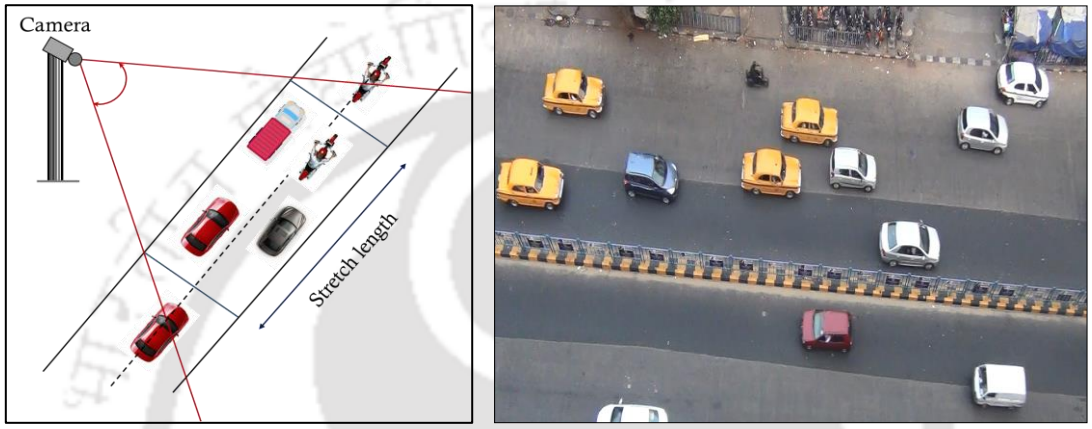

(a) **(b)**

Figure 3.1. (a) An arrangement of static video-recording technique and **(b)** snapshot of traffic stream captured from a static camera fixed in a high-rise building

In the context of data collection in disordered traffic environments, a few studies have utilized this approach to extract vehicle trajectory data. Yet, most of the studies differ either in the section length considered or the amount of trajectory data extracted. Mallikarjuna et al. (2009) considered a 25m section in Delhi to extract trajectories using TRAZER while Munigety et al. (2014) collected 3173 vehicle trajectories from a 320m section in Mumbai. Recently, Kanagaraj et al. (2015) collected trajectories of 3005 vehicles at a time resolution of 0.5s on a 200m section of a six-lane urban arterial in Chennai. The short surveyed length in obtaining trajectories due to limited field of view of cameras has been presumed to be the major disadvantage of this technique. The observation and driving behaviour analysis can be affected by the spatial limitation.

Having known its limitations, this technique offers certain advantages that has led to the widespread adoption in collecting trajectory data. Video footage obtained from this technique can be processed to extract multiple interactions between/among a wide variety of vehicle types, within the field of view of the camera. Information on the surrounding traffic mix, type of vehicles interacting, driver characteristics (MTW riders, cycle rickshaws, bicycle riders) along with the vehicle trajectories can be extracted simultaneously and visually assessed from the collected video footage. Extracting trajectory data however involves position tracking of considered vehicles using frame-by-frame analysis. Because this technique involves a static camera, the position coordinates of tracked vehicles in sequential video frames can provide

useful information on the actual vehicle positions, from which the kinematic characteristics of the tracked vehicles (actual speeds, acceleration/deceleration) can be attained. While a fixed time-resolution of 0.5s has mostly been considered for trajectory data extraction in the existing studies, the level of detailed information (say, every 0.1s or 0.2s information) required to understand drivers' responses in different driving regimes has not been appraised yet.

Data extraction using image processing technique is a labor-intensive process, still a detailed trajectory data carrying information of a wide variety of vehicles can be obtained from the video footage, but only along a limited stretch of road. Considering the flexibility of this method in obtaining trajectory data of a wide mix of vehicles, interactions of different vehicle types with surrounding traffic mix, drivers' characteristics (MTW riders) and so on, this technique is utilized in this research to provide a detailed understanding of the staggered-following and filtering behaviour of different combinations of interacting vehicle pairs.

3.1.2. Dynamic video tracking technique

Unlike static camera based video-recording technique, the dynamic approach envisages the use of instrumented vehicles (Brackstone et al., 2002). It essentially consists of equipping all the vehicles (either in a platoon or in a particular arrangement) with receivers and video cameras, and simultaneously monitoring their trajectories for long stretches along a road. Because the instrumented vehicles travel along the road, the video footage obtained from the camera provides a dynamic set of experimental data. Improved accuracy in the estimation and collection of reliable dynamic time-series data is indeed essential to achieve a detailed information on the driver's response and enhance the realism of vehicle-following models. Figure 3.2 illustrates the experimental setup used in dynamic video recording technique and snapshots of the front vehicle(s) captured from the camera fixed at the following vehicle.

The literature demonstrates several techniques for gathering time-series data which include, static laboratory simulators (Van Winsum and Heino, 1996), and instrumented vehicles equipped with radar sensors (Brackstone and McDonald, 2007; Brackstone et al., 2002, 2009) or onboard Global Positioning System (GPS) receivers. Driving simulator-based experiments lack the flexibility of representing real traffic phenomena. Howbeit, in the domain of instrumented vehicles, on one hand, instrumented vehicles can adequately capture the relative spacing and speeds using sensors; while on the other hand, an accurate positional data of the equipped vehicles can be obtained with the satellite-based GPS technology (Gurusinghe et al., 2002). On the modelling of vehicle-following behaviour of disorderly traffic streams, Mathew and Ravishankar (2012) collected data using vehicles equipped with GPS receivers along multilane highways of Mumbai. However, while inter-vehicle spacing can be obtained from the recorded vehicle positions, estimating lateral separation between the interacting vehicles from the GPS receivers may produce unreliable results.

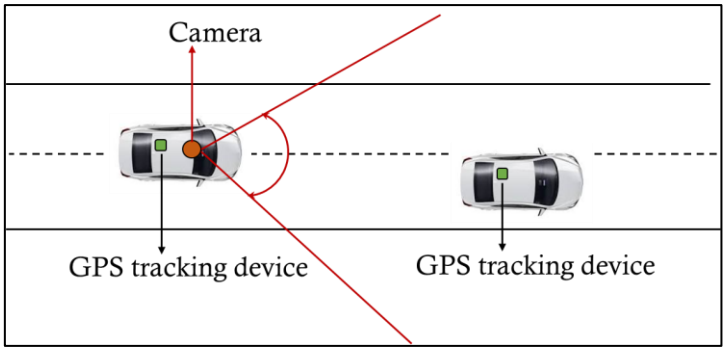

(a)

(b)

Figure 3.2. (a) Arrangement of experimental setup in dynamic video recording technique and **(b)** a typical single-leader and two-leader following scenario captured from the camera attached to the following vehicle

In essence, a proper evaluation of detailed car-following (or, vehicle-following) behaviour in non-lane based traffic environments requires an accurate characterization of both the longitudinal and lateral descriptors of traffic, and reliable experimental data. In this light, an image-based in-vehicle trajectory data collection technique is developed in this work to process continuous time-series data for understanding the car-following as well as multiple-leader (or, two-leader) following scenario of disordered traffic environments. A detailed description of the proposed methodology is elaborated in the subsequent sections. The methodological framework considered in the research work to fulfil the defined objectives is illustrated in Figure 3.3.

3.1.3. Errors in vehicle trajectory data reported in existing literature

The reliability of traffic flow studies and its applications depend inherently on the quality of trajectory data. Although many studies have performed experimental analyses and supported theoretical findings, few efforts have been devoted to report errors in vehicle trajectory data. Datasets with unknown accuracy values can be actually hazardous (Punzo et al., 2011) as credibility of the results will be questionable. Punzo et al. (2011) defined consistency conditions to inspect and quantify accuracy of Next Generation Simulation (NGSIM) trajectory datasets. Internal consistency analysis revealed average errors in spacing as 51cm, 8cm, 5cm, 3cm, 2cm, 2cm, 165cm, 36cm, 322cm and 33.5cm for I80-1, I80-2, I80-3, US101-1, US101-

2, US101-3, Lank-1, Lank-2, Peach-1 and Peach-2 NGSIM trajectory datasets respectively. They reported that more than 75% of vehicles revealed a systematic error (mean error lies beyond [-100, 100] interval, in cm) for arterial datasets (Lank and Peach). Houenou et al. (2013) predicted vehicle trajectories for lane change manoeuvres and reported mean errors in the range of 9cm to 45cm. They further underlined that the mean errors could fit the requirements of a collision detection system. A few studies have also attempted to provide rough positioning accuracy requirements for satellite based navigation systems on ITS applications. These have been reported as 500cm, 100-150cm and 50-100 cm that depends on the level of detail (Stephenson et al., 2011; Austroads Research Report, 2013), although no specific requirement has been set for specific ITS application. Concerning disorderly traffic conditions, the readily available online trajectory data (http://toledo.net.technion.ac.il/downloads) has been utilized in many studies in the area of traffic flow theory and its applications. Kanagaraj et al. (2015) reported an average error in spacing of 54.4 cm and 6.2cm in the longitudinal and lateral direction respectively.

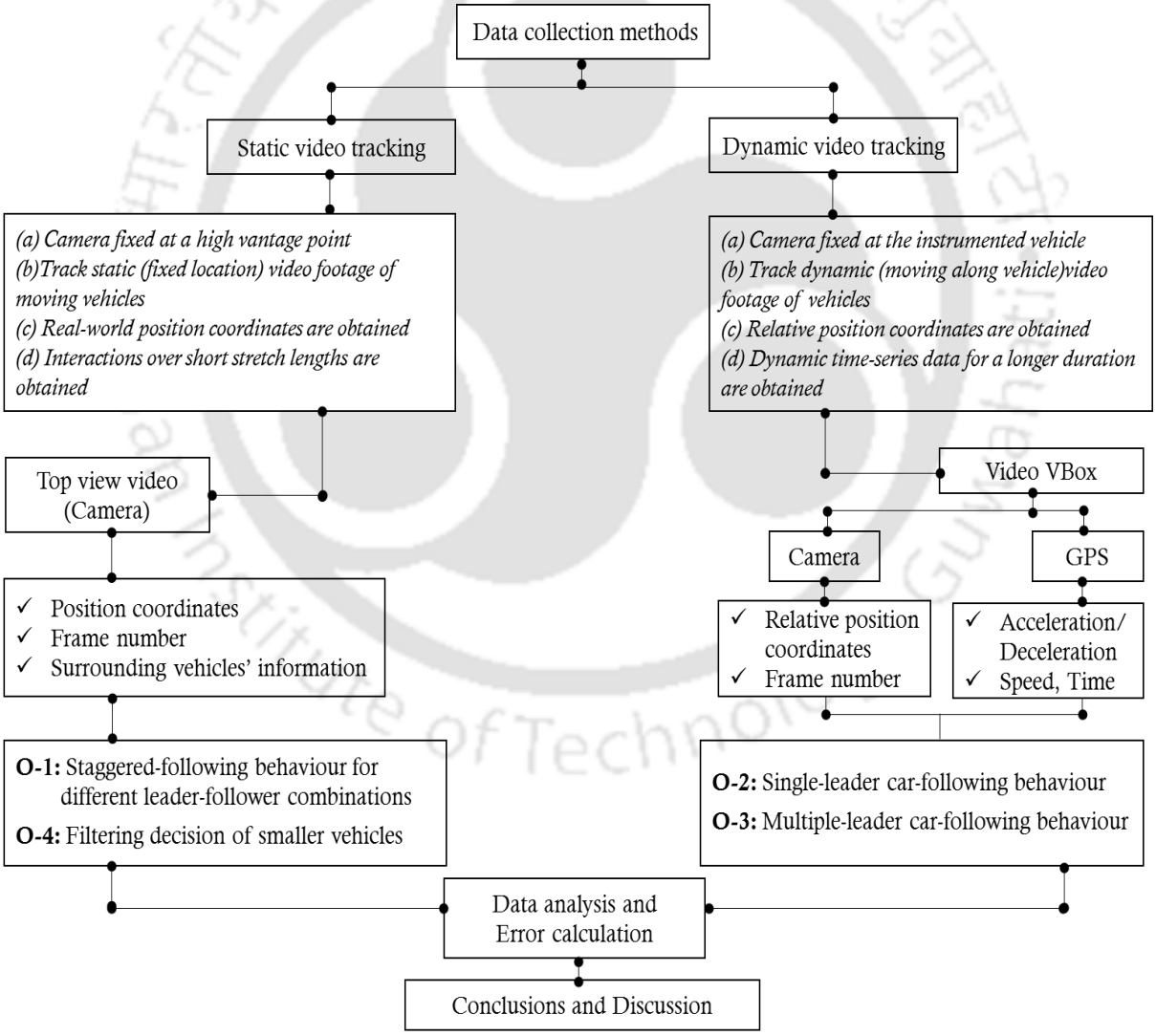

Figure 3.3. Data collection methodological framework utilized in the research work

3.2. Methodological framework using static video tracking technique

As discussed above, the static video recording technique offers advantages in obtaining the aggregate behaviour of different drivers and their interactions with diverse vehicle types from a fixed vantage point. Therefore, to capture multiple vehicle-pair interactions, this technique is used in this research to collect data on staggered-following and filtering behaviour of different vehicle types from a specific location. In particular, this section attempts to provide a detailed description of the data extraction methodology, calibration process used to transform image coordinates to real-world coordinates, locations of data collection and accuracy of the obtained data. First, the methodological approach adopted for staggered-following data estimation is elaborated, followed by a description on the data extraction methodology adopted for filtering scenario, and the last section discusses about the accuracy of data collection.

3.2.1. Staggered-following behaviour: Methodology and data estimation

The staggered-following behaviour refers to a scenario when the following vehicle interacts with the vehicle in-front (leading vehicle) by maintaining certain extent of off-centeredness or, by assigning partial leadership with the leading vehicle (as illustrated in Figure 2.2(b)). In such scenario, the following vehicle evaluates possible opportunities for lateral movements while progressing longitudinally, either to have a better field of view or to initiate lateral shifts. This gives rise to longitudinal as well as lateral interactions with the vehicle ahead, a better understanding of which requires detailed data collection and extraction methodology. While the longitudinal interactions between vehicles can be described by longitudinal gap, speed of individual vehicles and time headway, the lateral interactions can be indicated by measuring centerline separation between the interacting vehicles (Gunay, 2007). The details of data collection sites and methodology adopted to extract the microscopic traffic variables from the static video footage are described in this section.

3.2.1.1. Data collection locations

Data used for this study was collected by video recording technique in four different cities of India (Guwahati, Mumbai, Pune and Kolkata) at mid-block sections. The road sections considered were straight and far from the upstream (250-300m) and downstream (100-150m) of the signalized intersections. In all the days, weather was clear and the visibility was good (videos were collected in morning hours). The geometry of the road sections was uniform, and there were no nearby intersections, parked vehicles or other side friction that could affect driver's behaviour. Furthermore, there was no interaction between pedestrian and vehicle traffic as well. To capture naturalistic vehicular interactions over the subject study sections, videos of the traffic stream were recorded by placing the cameras at a high vantage point (high rise buildings). A total of five sections were considered in the study as presented in

Table **3.*1***.

Table 3.1. Details of video recording locations

Section	City	Road	Road width (m)	Trap length (m)	Duration (h)
1	Guwahati	Guwahati bypass	7.6	20	3
2	Mumbai	Western Express Highway	17.5	45	2.5
3		Jogeshwari-Vikhroli Link Road	10.8	20	2
4	Pune	Pune bypass	11.2	60	2.5
5	Kolkata	EM bypass	7.8	35	3

Two sections were selected in Mumbai: a three lane section on Jogeshwari-Vikhroli Link Road (width= 10.8m) and a five-lane section on Western Express highway (width= 17.5m). Two two-lane unidirectional carriageways were selected in Kolkata and Guwahati with road widths of 7.8m and 7.6m respectively; and a three-lane section was selected near Pune by-pass (11.2m width). The images of all the considered sections are presented in Figure 3.4.

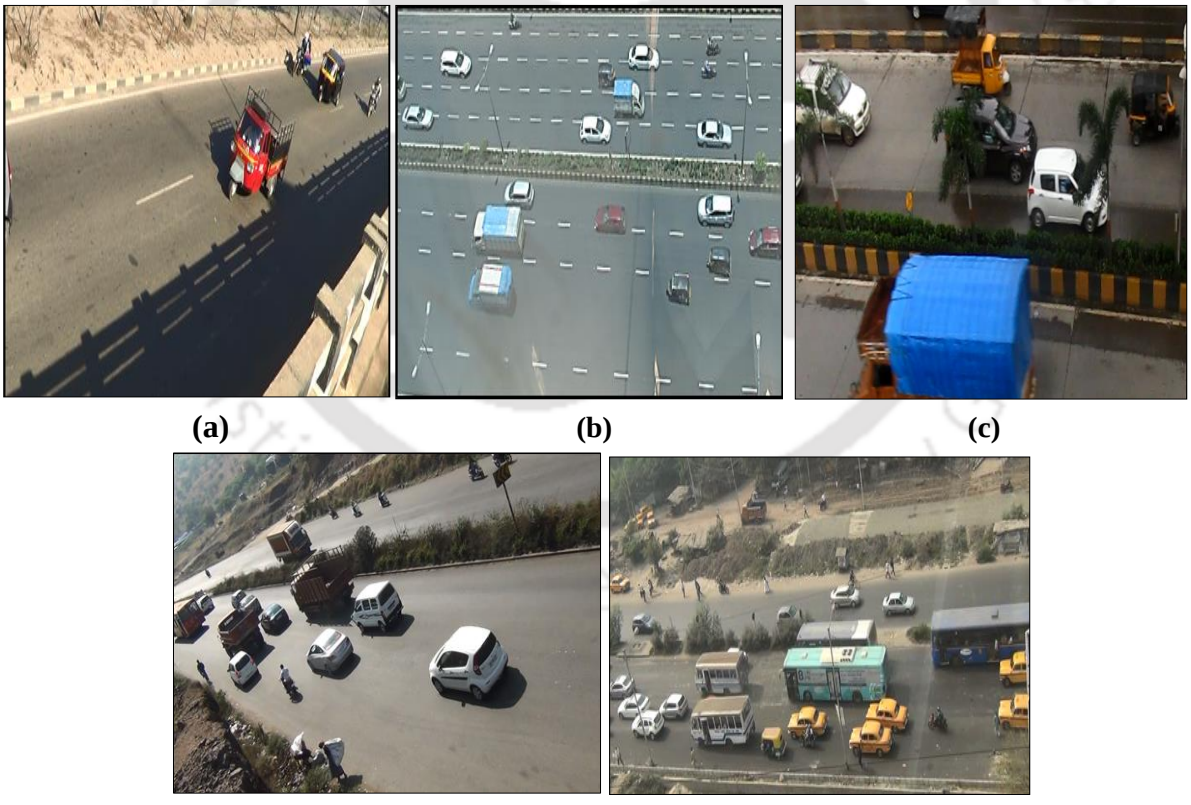

Figure 3. 4. Images of the traffic stream captured from the video recorders for **(a)** Section 1 (Guwahati) **(b)** Section 2 (Mumbai) **(c)** Section 3 (Mumbai) **(d)** Section 4 (Pune) and **(e)** Section 5 (Kolkata)

The considered road sections had predominant car traffic, followed by MTWs, motorized three-wheelers, light commercial vehicles and trucks. This indicates the presence of considerable longitudinal and lateral interactions between different vehicle types in the studied sections. The reason behind selection of different locations from four different cities lies in providing a detailed understanding of driver's behaviour while interacting with a variety of vehicle types and thereby, its variations across different road widths and cities.

3.2.1.2. Data extraction through trajectory tracking

A semi-automated trajectory extracting approach is utilized in this research to analyze video footage and extract microscopic data and vehicles' positions on the studied sections. Data on the basic kinematic parameters of vehicles such as speeds, relative spacing (or, longitudinal gap), lateral separation between the vehicles (centerline separation), etc., vehicular static characteristics such as length and width, and other information related to type of interacting vehicles (MTW, car, 3W, truck, LCV or bus) are collected from the trajectory extractor. The semi-automated trajectory extractor is developed in a MATLAB platform (Budhkar and Maurya, 2017) that has the flexibility to collect possible information on all the considered vehicles simultaneously at a given frame. The video sequences can be examined repeatedly (if required) by changing the frame number in the software itself to validate the level of information gathered.

The first step in data extraction lies towards identification of different leader-follower interacting vehicle pairs based on visual assessment of the video footage. Those vehicle pairs which were separated laterally within a distance of approximately 3.5m (based on visual inspection) were initially assumed to be interacting with each other. Once the vehicle-pairs are identified, the video footage is then loaded into the software for data extraction. A snapshot of the developed software and the screen view of the footage at a given frame is displayed in Figure 3.5.

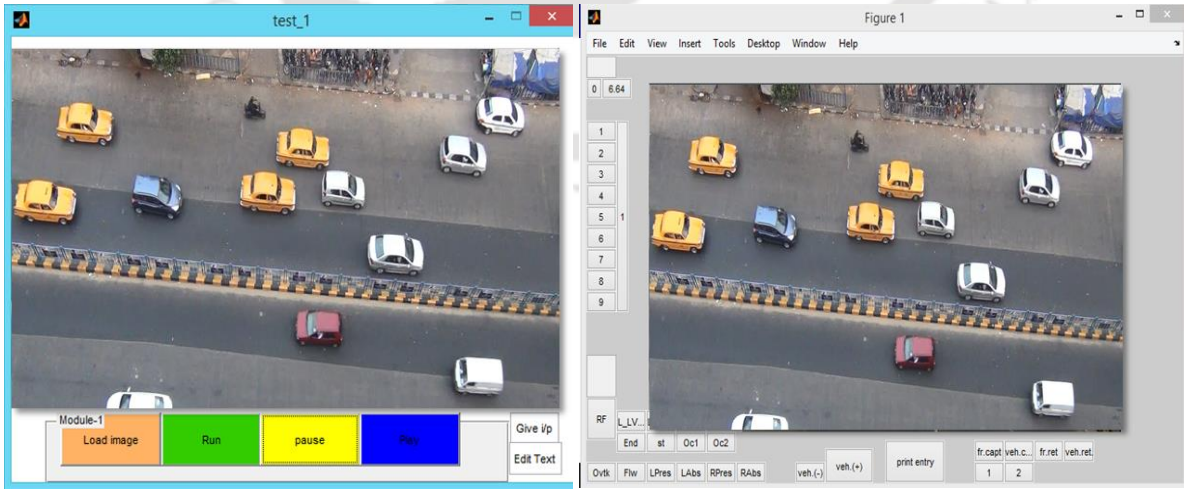

(a) **(b)**

Figure 3.5. Snapshots of the **(a)** semi-automated software and **(b)** displayed screen at each frame

In general, semi-automatic detection involves clicking on the identified vehicles manually where the system recognizes and tracks the position of each vehicle on the screen across multiple frames using frame-by-frame analysis as long as both the vehicles are visible on the footage. Essentially, a particular rear-end corner point of each considered vehicle is tracked at different frames to collect the trajectory data. On the other hand, for obtaining the dimensions of vehicles, any three visible edges of the vehicle are marked on the screen at any given frame, from which the lengths and widths can be estimated. The type of vehicles involved is also recorded by means of a vehicle code (appearing on the displayed screen of the software). Similarly, all prerequisite information on the surrounding traffic can also be stored. For each tracking, each vehicle's position on the screen is recorded and after suitable calibration process, the image coordinates of the mouse-clicks can be converted to real-world coordinates to obtain the desired microscopic traffic variables.

3.2.1.3. Camera calibration process

Camera calibration is an important step in visual traffic surveillance analysis, the purpose of which is to transform image coordinates extracted from the video footage to real-world coordinates. For the purpose of this research work, the camera calibration equations devised by Fung et al. (2003) are employed for conversion of the coordinates. It basically relies on obtaining four reference points in the video sequence and their respective coordinates in the real world. This process assumes a straight road surface, utilizes vanishing point technique, measuring the actual width of the fixed rectangle in the field. The coordinate conversion is conducted using camera calibration, which involves calculation of three angles of camera (angle the camera's axis makes with X, Y and Z axis), focal length, and distance of camera to plane along camera's axis (illustrated in Figure 3.6).

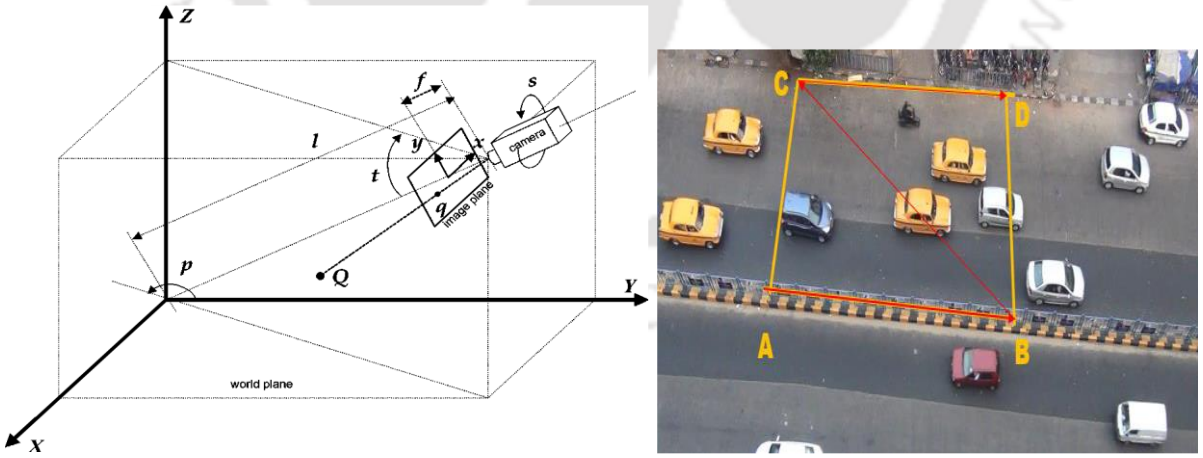

(a) **(b)**

Figure 3.6. (a) Employed camera model and **(b)** calibration pattern used for coordinates conversion

The camera parameter settings, including pan angle *p*, tilt angle *t*, swing angle *s*, focal length *f* and camera distance *l*, can be determined from the image coordinates (*x*, *y*) of the four reference points of the rectangle and the actual width of the fixed rectangle *w*. Subsequently,

based on the calculated camera parameters, the real-world coordinates of a point P (X_P, Y_P) can be estimated from the following equations as described in Fung et al.'s (2003) work.

$$X_P = \frac{l \sin p\,(x_P \sin s + y_P \cos s) + l \sin t \cos p\,(x_P \cos s - y_P \sin s)}{x_P \cos \mathrm{t} \sin s + y_P \cos t\ \cos s + f \sin t}$$

$$Y_P = \frac{-l \cos p\,(x_P \sin s + y_P \cos s) + l \sin p \sin t\,(x_P \cos s - y_P \sin s)}{x_P \cos \mathrm{t} \sin s + y_P \cos t\ \cos s + f \sin t}$$

$$l = \frac{w(f \sin t + x_A \cos t \sin s + y_A \cos t \cos s)\,(f \sin t + x_C \cos t \sin s + y_C \cos t \cos s)}{\begin{bmatrix} -(f \sin t + x_A \cos t \sin s + y_A \cos t \cos s) \\ (x_c \cos p \sin s - x_c \sin p \sin t \cos s + y_c \cos p \cos s + y_c \sin p \sin t \sin s) \\ +(f \sin t + x_C \cos t \sin s + y_c \cos t \cos s) \\ (x_A \cos p \sin s - x_A \sin p \sin t \cos s + y_A \cos p \cos s + y_A \sin p \sin t \sin s) \end{bmatrix}}$$

$$f = \frac{\chi_{BD} \cos p \cos t}{\beta_{BD} \sin p \cos s - \beta_{BD} \cos p \sin t \sin s + \alpha_{BD} \sin p \sin s + \alpha_{BD} \cos p \sin t \cos s}$$

$$\tan p = \frac{\sin t\,[(\beta_{BD}\chi_{AC} - \beta_{AC}\chi_{BD}) \sin s + (\alpha_{AC}\chi_{BD} - \alpha_{BD}\chi_{AC}) \cos s]}{(\alpha_{BD}\chi_{AC} - \alpha_{AC}\chi_{BD}) \sin s + (\beta_{BD}\chi_{AC} - \beta_{AC}\chi_{BD}) \cos s}$$

$$\sin t = \left[\frac{\begin{pmatrix} \sin s\,[(\alpha_{BD}\chi_{AC} - \alpha_{AC}\chi_{BD}) + (\beta_{BD}\chi_{AC} - \beta_{AC}\chi_{BD}) \cos s] \\ \sin s\,[(\alpha_{CD}\chi_{AB} - \alpha_{AB}\chi_{CD}) + (\beta_{CD}\chi_{AB} - \beta_{AB}\chi_{CD}) \cos s] \end{pmatrix}}{\begin{pmatrix} \cos s\,[(\alpha_{CD}\chi_{AB} - \alpha_{AB}\chi_{CD}) + (\beta_{AB}\chi_{CD} - \beta_{CD}\chi_{AB}) \sin s] \\ \sin s\,[(\alpha_{BD}\chi_{AC} - \alpha_{AC}\chi_{BD}) + (\beta_{AC}\chi_{BD} - \beta_{BD}\chi_{AC}) \cos s] \end{pmatrix}}\right]^{0.5}$$

$$\tan s = \frac{\begin{pmatrix} -\beta_{AB}\beta_{AC}\chi_{BD}\alpha_{CD} + \beta_{AC}\alpha_{BD}\beta_{AB}\chi_{CD} \\ +\beta_{CD}\chi_{AB}\beta_{BD}\alpha_{AC} - \beta_{AB}\chi_{CD}\beta_{BD}\alpha_{AC} \\ -\beta_{CD}\beta_{BD}\chi_{AC}\alpha_{AB} - \beta_{AC}\chi_{AB}\alpha_{BD}\beta_{CD} \\ +\beta_{AB}\chi_{AC}\beta_{BD}\alpha_{CD} + \beta_{CD}\beta_{AC}\chi_{BD}\alpha_{AB} \end{pmatrix}}{\begin{pmatrix} -\beta_{AB}\chi_{AC}\alpha_{BD}\alpha_{CD} + \beta_{AC}\chi_{AB}\alpha_{BD}\alpha_{CD} \\ -\beta_{AC}\alpha_{BD}\alpha_{AB}\chi_{CD} - \alpha_{AC}\chi_{BD}\beta_{CD}\alpha_{AB} \\ -\alpha_{CD}\chi_{AB}\beta_{BD}\alpha_{AC} + \beta_{AB}\alpha_{AC}\chi_{BD}\alpha_{CD} \\ +\alpha_{AB}\chi_{CD}\beta_{BD}\alpha_{AC} + \alpha_{BD}\chi_{AC}\beta_{CD}\alpha_{AB} \end{pmatrix}}$$

Where

$$\alpha_{AB} = x_B - x_A, \quad \alpha_{AC} = x_C - x_A, \quad \alpha_{BD} = x_D - x_B, \quad \alpha_{CD} = x_D - x_C$$

$$\beta_{AB} = y_B - y_A, \quad \beta_{AC} = y_C - y_A, \quad \beta_{BD} = y_D - y_B, \quad \beta_{CD} = y_D - y_C$$

$$\chi_{AB} = x_A y_B - x_B y_A, \chi_{AC} = x_A y_C - x_C y_A, \chi_{BD} = x_B y_D - x_D y_B, \chi_{CD} = x_C y_D - x_D y_C$$

$(x_A, y_A), (x_B, y_B), (x_C, y_C)$ and (x_D, y_D) represent the image coordinates of the four ends of the rectangle A, B, C and D respectively.

Based on the formulations, the real-world coordinates of a tracked position P (X_P, Y_P) can be evaluated from the image coordinates of that point (x_P, y_P). These transformed real-world position coordinates are then processed further to obtain desired static and kinematic

parameters of the trajectories such as longitudinal gap, centerline separation, vehicle speeds, time headway and vehicle dimensions, from which the interacting vehicle pair combination is identified.

3.2.1.4. Selection of data for 'steady-state staggered car-following' behaviour

Before performing the analysis, it is important for the purpose of this work to exclude any cases of free-flowing conditions and select only those data (obtained from the trajectory software) that represent staggered-following behaviour of the interacting vehicles. The extent of influence of the leader on the following vehicle can be ascertained by longitudinal gap, relative speed, maximum time headway and centerline separation. It is believed in this work that the subject vehicle will be more likely governed by the stimulus of the front leader if the longitudinal gap lies within 20m (Siddique, 2013). Moreover, a maximum relative speed difference of 1.5m/s (5.4km/h) between the leading and the following vehicles was suggested by Sayer et al. (2003) and Zhang and Bham (2007) to represent steady state car-following conditions. In addition time headway data more than 4s are excluded from all analysis because those headways are not considered to be interacting with the lead vehicles (Wasielewski, 1979; Michael et al., 2000). Further, all centerline separation values lower than 2m are assumed to represent lateral interactions in staggered-following processes.

3.2.2. Filtering behaviour of vehicles: Methodology and data estimation

Filtering behaviour refers to the complex manoeuvring pattern of smaller vehicles in dense urban heterogeneous traffic environments where they tend to utilize the available lateral spaces or diagonal distances described by other vehicles (also defined as pores, as indicated in Figure 2.2(d)) on the road in order to achieve higher speeds and reduced travel times. Although this is a commonly observed phenomena for MTW riders, smaller vehicles such as motorized three-wheelers and even cars are observed to filter through traffic in such heterogeneous disordered systems. Understanding such behaviour still deserves considerable attention from driver modelling standpoint, a detailed comprehension of which is discussed in the research work.

3.2.2.1. Data collection locations

For understanding the filtering behaviour of vehicles, those mid-block sections were selected that had predominantly MTW traffic, followed by cars and motorized three-wheelers. Data utilized in the research work were collected by video-recording technique from three midblock sections on urban arterials: two sections in Mumbai, India having road widths of 17.5m (Section 6 and Section 7) respectively, and one section in Pune having road width of 10.5m (Section 8). Videos of the traffic stream were collected from the top of a high rise building near the study sites for a period of 3hours (9:00-12:00 am) during good weather conditions and clear visibility. The video covered the day time data when the levels of congestion were moderate and the roadway quite far from the upstream and downstream of the nearby intersections. The

videos for both sections in Mumbai were captured for a stretch length of 40m while the trap length of the Pune section was 35m. A screenshot of the traffic streams from the video footage is presented in Figure 3.7.

(a) **(b)**

Figure 3.7. Snapshots of the traffic stream for the considered mid-block sections of **(a)** Mumbai (Section 6) and **(b)** Pune (Section 8)

As marked in Figure 3.7, MTWs can be observed to filter through the spaces described by the left and right-front vehicles. The selected sections exhibited filtering behaviour of mostly MTWs and cars, with smaller numbers of 3Ws' filtering manoeuvres. As a result, the filtering behaviour of MTWs and cars and their interactions with different left-front and right-front vehicles are only considered in the work. Moreover, the sections were characterized by varying speed ranges (average vehicle speeds for the three-lane and five-lane sections were obtained as 30km/h and 60km/h respectively). Particularly, the reason for choosing different midblock sections was the difference in their traffic and geometric characteristics, which will help in understanding the filtering behaviour of MTWs and cars riding at different speeds.

3.2.2.2. Methodology for data extraction

A concise understanding of the filtering behaviour of MTWs and cars requires an exhaustive trajectory dataset tracked over a period of time. This involves extraction and processing of data on the basic kinematic parameters such as vehicle speeds, longitudinal and lateral separation between the subject vehicles with the interacting leading vehicles, and surrounding traffic conditions (type of interacting vehicles, presence of surrounding vehicles, etc.). Other attributes of MTW riders such as age, gender and helmet usage are however approximated from the obtained video recordings. Data extraction mainly focused on identifying such cases when the subject vehicle intended to filter through or accept the lateral space circumscribed by the two leading vehicles (or, pore) and also when the vehicle preferred to follow the leading vehicles due to its incapability to pass through the available pore.

For the estimation of pore acceptance (or, filtering) and rejection (following) decisions, the subject vehicles performing the filtering and following manoeuvres at different time stamps were initially identified from the video footage and the trajectory data were extracted for each filtering and following case. As discussed in section 3.2.1.2, the similar semi-automated

trajectory extracting software was used for data extraction. The process involved tracking the position coordinates of both the left-front and right-front vehicles as well as the subject vehicle at each 0.5s time interval. For estimating pore size in a filtering scenario, the trajectories of all the three vehicles were extracted, starting from the time the subject vehicle has come under the influence of both the leading vehicles to the time it has left either of them. Out of all the tracked position coordinates of a particular interaction, the minimum pore size that was accepted by the subject vehicle during the filtering process was considered as the accepted pore. Similarly, all the vehicle-following events (when the subject vehicle preferred to follow the front vehicles due to its incapability to accept the available pore size) were identified and extracted from the video footage using frame-by-frame analysis. The maximum pore size that was rejected by the subject driver in the vehicle-following event was considered as the rejected pore. In particular, all the observations made on the rider's decision to accept or reject a pore were independent, with the extracted data containing implicit information on the aggregate behavioural decision of a variety of drivers in such urban traffic streams. Interactions of the subject drivers with different combinations of left-front and right-front vehicle types were considered in the research work. The raw trajectory data extracted from the video recorders are then transformed to real-world coordinates according to the calibration equations (discussed in section 3.2.1.3). These position coordinates are then analyzed further to derive the desired kinematic and static parameters such as vehicle speeds, spacing, pore sizes, type of the leading vehicles involved, etc.

3.2.2.3. Selection of data

For the purpose of the study, only those interactions were considered for which the available pore sizes (both lateral and diagonal, as illustrated in Figure 2.2(d)) between the leading vehicles were lower than 3m (Vlahogianni, 2014) for MTWs and 4m (Ambarwati et al., 2014) for cars. Because of bigger dimensions of cars, a larger threshold of pore size is considered for cars as compared to MTWs. The minimum pore size accepted by the subject vehicle to pass in between the left-front and right-front vehicles is defined as accepted pore. On the contrary, the rejected pore is defined as the maximum pore size which the subject vehicle rejects while following the leading vehicles for a minimum interaction period of 4s. Moreover a maximum longitudinal gap of 20m was considered to describe the interactions between the subject vehicles with the interacting vehicles. Filtering and following behaviour of MTWs and cars with several combinations of leading left front and right front vehicles (passenger cars, MTWs and trucks) were considered in this work.

3.2.3. Accuracy of data extracted

While extracting data from the video, an extractor may make an erroneous mouse click with a fixed standard deviation (in pixels) on the screen. For estimating accuracy of the extracted data utilized in modelling staggered-following behaviour, a sample of 100 cars belonging to a particular model of known width was initially taken for clicking two extreme points of the car's

width. The pixel values indicated a standard deviation of 5.03 pixels for one mouse click (Budhkar, 2017). Since length is calculated by two mouse clicks, variance of error of one mouse click will be halved. These 5 pixels on screen may correspond to different lengths in the field, depending on the zooming of camera lens as well as captured trap lengths.

As discussed in the previous sections, the system calibration was performed according to the methodology devised by Fung et al. (2003) where the four end-points describing a fixed rectangle A, B, C, D marked on the screen need to be converted to real-world coordinates (as shown in Figure 3.6(b)). Considering the two-lane unidirectional carriageway of 7.8m selected in Kolkata (Section 5,

Table **3.*1***) for modelling staggered-following behaviour, the image coordinates of the fixed rectangle are marked as $A\ (490.5, 390.5), B\ (1008.5, 615.5), C\ (923.5, 207.5)$ and $D\ (1515.5, 431.5)$. Therefore AC can be estimated as 470.08 pixels and BD can be obtained as 539.35 pixels and converting it in pixels/m we get $ac = 60.26$ and $bd = 69.15$. As discussed earlier, an error of 5.03 pixels was obtained due to erroneous mouse clicks therefore errors in measuring ac and bd have been found as 0.086 and 0.075 respectively, making an average of 8.08 cm. In a similar manner, the errors in distance for other sections are obtained as 5.7cm, 14.6cm, 9.4cm and 8.9cm for sections 1, 2, 3 and 4 respectively. On average, the error in distance measurement of the extracted data used for modelling staggered-following behaviour can be estimated as 9.34 cm. Similar methodology was further utilized for estimating error in the extracted data used for modelling filtering behaviour of vehicles. Accordingly, the average error of the extracted trajectory data was obtained as 6.94cm for all the sections considered for filtering study.

3.3. Methodological framework using dynamic video tracking technique

The dynamic video tracking technique is used to collect dynamic time-series data on the detailed car-following behavioural process of drivers over as long a period of time as desired. Such data collection process provides a detailed information on the control processes of drivers in response to different actions of leading vehicles. Considering the staggered-following scenario prevailing in non-lane based traffic environments, collection of time-series data from only GPS receives may lead to inaccurate and unreliable results. While reliable information on vehicle speeds and acceleration can be obtained from GPS receivers, relative distance measurements (both in longitudinal and lateral directions) prove to be inadequate for understanding detailed car-following behaviour as the longitudinal and lateral separation between the vehicles cannot be directly obtained from the GPS receivers.

Efforts are therefore being directed in this work to establish an image-based in-vehicle trajectory data collection system to process the microscopic variables (such as longitudinal gap, centerline separation, vehicle speeds, accelerations, etc.) using camera calibration and in-vehicle GPS information on straight roads. This data collection technique is developed to

gather and process dynamic data for understanding the detailed behavioural responses of drivers in a single-leader as well as in two-leader car-following regime. This section begins with a detailed description of the data-collection methodology, extraction and calibration process for a single-leader car-following scenario. In the subsequent section, the methodological framework used for multiple-leader (or, two leader) following scenario is described and the last section discusses the accuracy in extracted data obtained using the proposed methodology.

3.3.1. Single leader-car following process: Methodological framework

Details of dynamic time-series data used in understanding and modelling the single-leader car-following behavioural process of drivers is discussed in this section. This section further provides a comprehensive discussion about the experimental setup, data collection details, calibration process and the issues regarding data collection.

3.3.1.1. Instrumented vehicle setup and data collection

The data used were collected from a series of experiments conducted in March 2018 along straight sections of the NH-27, a four-lane divided carriageway in Guwahati, India, under real traffic conditions. Experiments were conducted by driving two vehicles simultaneously in the car-following state along rural highway covering a total stretch length of 37.33km during the afternoon hours, 2:00 to 4:30 pm. Both the vehicles were equipped with GPS receivers (Racelogic Video V-box) that recorded the position of each vehicle at 0.1-s interval, and a video-system attached to the windshield of the cars, allowing a complete visual record of the experiment (Figure 3.2(a)). From the positional data of GPS receivers, vehicle speeds, longitudinal/lateral acceleration are calculated through successive derivations of the space travelled; while inter-vehicle longitudinal and lateral gaps are evaluated from the synchronized recorded video by a semi-automated trajectory extracting system [detail discussion in Section 3.3.1.2.]

In the process of data collection, careful attention was devoted to the experimental setup. The drivers of both the vehicles were familiar with the travelled path but were not aware of the purpose of experimental design. The driver of the leading vehicle was instructed to maintain different speeds in the range of 30kmph to 90kmph at an interval of 10kmph each (that is, 30kmph, 40kmph, 50kmph, 60kmph, 70kmph, 80kmph and 90kmph) based on prevailing traffic conditions of the considered road stretch. On the other hand, the driver of the following vehicle was asked to follow the leading vehicle maintaining a safe distance based on his perception. In response to the actions of the leading vehicle, the following process of the subject vehicle was then captured based on the proposed data collection technique. As the aim of the experiment was to collect car-following data, the lane-changing manoeuvre and intrusions of other vehicles were avoided. Data for any unimpeded intrusions in unavoidable circumstances were discarded. In particular, the car-following data were processed for only such scenarios when the subject vehicle was under the influence of the leading instrumented vehicle. Moreover, the study was conducted for only straight sections where the effect of external

factors such as curves and gradients affecting the traffic flow were not considered. An example of a car-following scenario and a staggered-following scenario recorded from the camera attached to the following vehicle is presented in Figure 3.8.

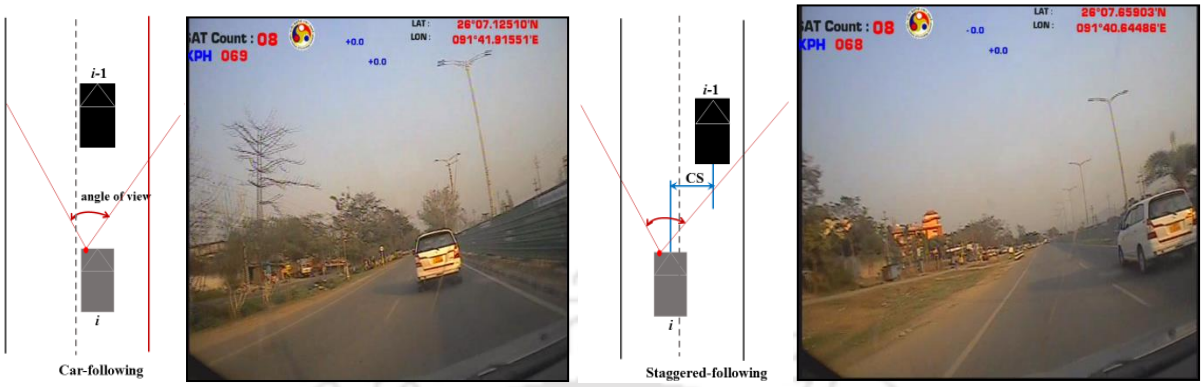

(a) **(b)**

Note: Red dot indicates the position of the camera attached to the following vehicle, *i*

Figure 3.8. A typical **(a)** car-following and **(b)** staggered-following scenario recorded from the camera attached to the following vehicle

The underlying assumptions of the experimental setup process are (a) the road under surveillance should be reasonably straight such that both the vehicles rest on the same plane and (b) careful attention should be paid to the fixture of the camera on the vehicle since any change in the camera orientation may result in improper data estimation. Such assumptions were carefully considered during data collection processes for obtaining reliable time-series data. To ensure this, the camera calibration exercise was conducted before and after the experiment by parking the test vehicle at the same location where it was kept during calibration. The image coordinates of the marked end-points on the road were then compared to validate the consistency of the measured road coordinates. As long as camera orientation remains fixed, image co-ordinates from frame of reference of test vehicle remain consistent.

3.3.1.2. Calibration process

In an attempt to extract and analyze the inter-vehicle spacing (both longitudinal and lateral) from the video footage, a semi-automated trajectory system is employed in this research where each vehicle's location on the screen is recognized and tracked at different time stamps using frame-by-frame analysis. The screen coordinates of the vehicle's position recorded at each tracking are then transformed to real-world coordinates by employing the camera calibration equations devised by Fung et al. (2003). The detailed process is discussed in Section 3.2.1.2.

For the dynamic video tracking method, the calibration process is slightly different from that in static technique. Although the transformation equations remain same in both the techniques, the calibration pattern used in dynamic technique requires measurement of other fixed distances in addition to the road width. It is quite imperative that the four reference points in the video sequence and their respective coordinates in the real world need to be captured and based on the calculated camera parameters (pan angle, tilt angle, swing angle, focal length and distance of the plane from the camera lens) and screen coordinate of each point, the real-world

coordinate of the respective point can be estimated. However, the calibration process involved in this dynamic technique requires selection of four endpoints of the road edge markings (as illustrated in Figure 3.9) to form a calibration pattern of rectangle ABCD.

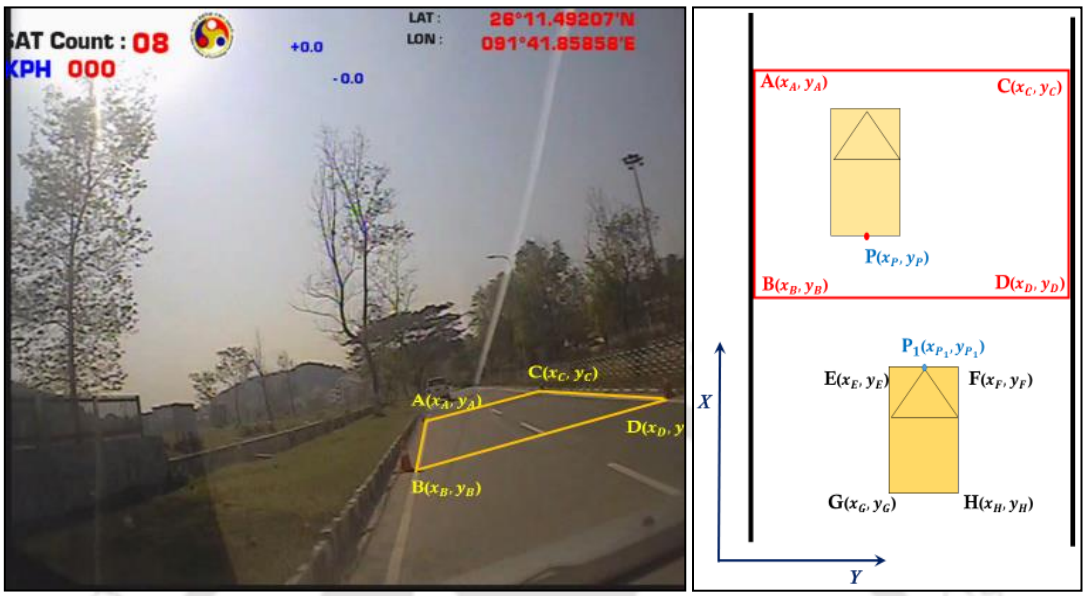

(a) **(b)**

Figure 3.9. Camera calibration technique considered in the study **(a)** rectangle ABCD viewed from the camera **(b)** top view of the calibration pattern along with the lead vehicle

With reference to Figure 3.9, four endpoints representing an exact rectangle in the world coordinates of known dimensions (AB=CD and AC=BD) are selected and using the semi-automated trajectory extractor, the corresponding end-point is traced to obtain its respective screen coordinates. Each end-point is however clicked several times on the screen, and for further data estimation and processing, the average pixel value for each point is considered to reduce errors in manual mouse-clicks. For the estimation of inter-vehicle spacing, it is considered that the edge of the test vehicle (EG or FH) is parallel to the road edge (AB or CD), and the longitudinal and lateral distance of the end-point (either B or D) from one front corner of the test vehicle (either E or F) is known. For any point P representing the mid-point of the rear bumper of the leading vehicle, the transformed real-world coordinates are estimated similar to the methodology described above. With all known measured distances and transformed real-world coordinates, the longitudinal and lateral spacing with the leading vehicle can be accurately estimated according to the following equations described below.

$$\text{Longitudinal gap} = (x_P - x_B) + (x_B - x_E)$$
$$\text{Centerline separation} = |y_P - y_B - (y_E - y_B) + (y_{P1} - y_E)|$$

Where the distances $(x_B - x_E)$, $(y_E - y_B)$ and $(y_{P1} - y_E)$ are accurately measured in the field during the calibration exercise (that is, before the start of experiment when the vehicle is stationary).

The real-time of sampling, the global coordinates and speed of each vehicle involved in the experiment are directly obtained from the GPS receivers at 10Hz frequency while the positional data of the vehicle in-front are extracted from the video recorders at each 5Hz frequency level.

After suitable transformation, the GPS data and the extracted video-data are then synchronized to obtain acceleration/deceleration and speed of both the vehicles, global time, longitudinal gap and centerline separation at every 0.2s-intervals.

3.3.1.3. Selection of staggered car-following data

The trajectory dataset resulted in a maximum longitudinal gap of 30m, which justifies that the dataset covers an entire spectrum of a close-following behaviour (Zheng et al., 2012). Data containing implicit information on car-following interactions during the observation period, that is, relative speeds in between -10kmph and 10kmph and centerline separation within 2m are considered. Only the absolute values of centerline separation are considered, irrespective of the positions of the leading vehicle (left or right side of the subject vehicle). Further, those trajectory data are considered for which both the cars involved in the process corresponding to each vehicle speed can be observed jointly during a period of at least 15s. Such information are usually considered to own significant car-following characteristics (Zheng et al., 2015) of the interacting vehicle pairs.

3.3.2. Multiple leader-car following process: Methodological framework

Besides modelling of single leader car-following process, due cognizance has recently been given towards the understanding of multiple-leader car-following behavioural process, commonly observed in non-lane based traffic environments. While interactions of the subject vehicle with different number of leaders in the interaction zone can be observed in urban roads, this research work specifically attempts to model the following process of cars in the presence of two leaders that is, both left-front (LF) and right-front (RF) leaders. This early phase of research first sought to understand the two-leader following process of cars interacting with the leading cars. In light of this, a detailed dynamic time-series data collection methodology, the experimental setup and calibration process are discussed in this section. In particular, the data collection methodology similar to the one described for single leader car-following scenario is adopted in the work. That is to say, the similar image-based trajectory extracting system (as discussed in Section 3.2) is used to collect and process reliable time-series data. Details of the instrumented vehicle set-up, data collection procedure and location details, along with the calibration pattern are discussed in the section.

3.3.2.1. Instrumented vehicle setup and data collection

An experiment similar to that carried out for single-leader car-following scenario was performed under real traffic conditions along straight roads of NH-37 in the month of April, 2019. The trajectories of left-front car, right-front car and the following car were collected with GPS receivers, along with the camera fixed to the windshield of the following car. All the three vehicles involved in the process were of similar static characteristics and models to eliminate the effect of vehicle characteristics in the study. The GPS receivers provided data on vehicle speeds, acceleration/deceleration of all the three vehicles at 0.1s time interval. Conversely,

longitudinal and lateral spacing with the left-front and right-front cars were extracted from the video footage by the semi-automated trajectory extracting system at every 0.2s interval. Essentially, experiments were conducted by driving the vehicles in a two-leader car-following state along rural highway during good visibility conditions, 8:00am to 4:00 pm in a weekend pertaining to low flow traffic conditions. A picture of the instrumented vehicle used in the data collection process is presented in Figure 3.10.

(a) **(b)**

Figure 3.10. A depiction of the instrumented vehicle and video VBox placed in the dashboard of the following car

The aim of the experiment was to collect two-leader car-following data under different positional arrangements of the leaders in real traffic conditions, for a better understanding of the dynamic behavioural process of following cars in response to different actions of the leading vehicles. To examine the behavioural characteristics of the followers, three specific cases of leaders' orientations are considered:

- *Case I*: when the leaders are moving parallel to each other, with a maximum 2m clear lateral gap in between and there is approximately 85-100% overlap in length of the leaders [Figure 3.11(a)]

- *Case II*: when the right-front vehicle is ahead of the left-front vehicle with 0% (rear-bumper of the RF vehicle is parallel to front-bumper of LF vehicle with 0m longitudinal gap between them) to 50% (rear-bumper of the RF vehicle is in the midway width of the LF vehicle) overlap in length of the leaders, separated by a maximum of 2m clear lateral gap [Figure 3.11(b)]; and

- *Case III*: when the left-front vehicle is ahead of the right-front vehicle with 0%-50% overlap in length, separated with a maximum 2m lateral gap in between [Figure 3.11(c)]. A pictorial representation of three different cases is presented in Figure 3.11.

The experiment was performed in a controlled environment in which both the drivers of the front vehicles were instructed to maintain a specified speed, with significant overlap (in length) between the leading vehicles. Based on the leading vehicles' orientation, the subject driver was to follow the vehicles ahead by maintaining a safe and comfortable desired spacing with them

based on his perception. The drivers were informed of the path to be taken, but they were unaware of the aim of the experiment. The instructors sitting on the three vehicles were coordinating among themselves through proper messaging application.

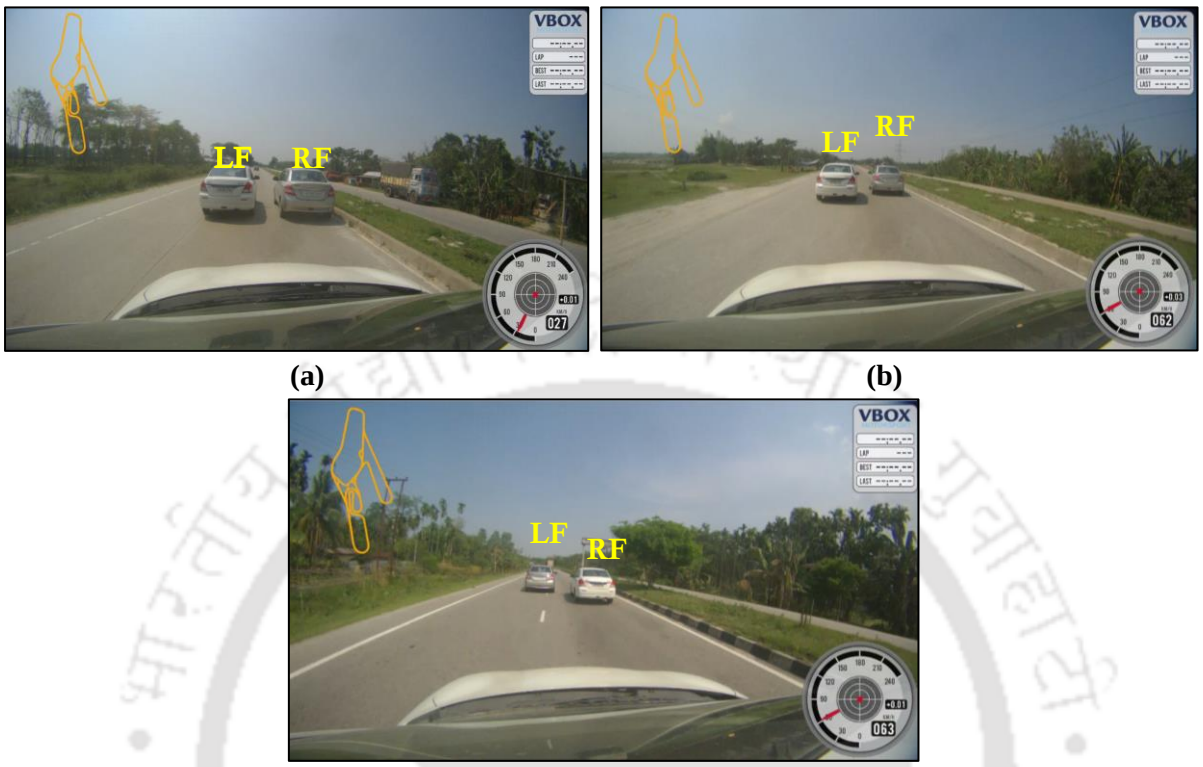

Figure 3.11. Illustration of different cases of leaders' positional arrangement viewed from the camera corresponding to **(a)** Case I **(b)** Case II and **(c)** Case III

Accordingly, for each positional arrangement, the drivers of the leading vehicles were instructed to maintain similar speeds lying in the range of 20kmph to 90kmph at an interval of 10kmph for a minimum of 30s time period. For each specified speed and positional arrangement of the leaders, the car-following process of cars was recorded and estimated. Typically, the total duration of interaction for a specified scenario is dependent on how long the subject driver wished to remain behind the vehicles and following that, a range of interactions were captured for a wide variety of speeds. The recorded data also involved detailed behavioural responses of following cars when there was transition in leading vehicles' speeds. It was further ensured that the lateral clearances between the leading vehicles are small enough such that the following driver cannot attempt to pass or filter through them. The two-leader following data were processed for such scenarios when the subject vehicle was only under the influence of both the leaders.

3.3.2.2. Calibration process

Once the video footage is collected, it is imperative to initially identify the two-leader following process of cars corresponding to each speed and positional arrangement of leaders. With this respect, three different cases of leaders' positional arrangements are identified from the footage

and then the extracting system is employed. The semi-automated trajectory extracting system is utilized to extract the position coordinates of each leading vehicle using frame-by-frame analysis. The positions of both the left-front and right-front vehicles are tracked at every 0.2s time intervals. This procedure is repeated for different leaders' speeds and orientations, until sufficient data are obtained. Moreover, the dynamic control process of followers in response to transitions in the speeds of leading vehicles (transitions in speeds until both the leaders maintain a stable speed) are also extracted and processed. Similar to the camera calibration equations devised by Fung et al. (2003), the screen coordinates of the vehicle's position recorded at each tracking are then transformed to real-world coordinates, the detailed process being discussed in Section 3.2.1.2.

The calibration process for a two-leader car-following scenario is similar to the singe-leader staggered car-following case as discussed in section 3.2.1.2, except the formulations of centerline separation between interacting vehicles. This process requires selection of four endpoints of the road edge markings (as illustrated in Figure 3.12) to form a calibration pattern of rectangle ABCD.

For any point P and Q representing the right-end point and left-end point of the rear bumper of the left-front and right-front vehicles respectively, the transformed real-world coordinates are estimated similar to the extraction methodology described in the previous sections. The screen coordinates of the four end-points of the fixed rectangle are obtained from the software and the distances $(x_B - x_E)$, $(y_E - y_B)$ and $(y_{P1} - y_E)$ are accurately measured in the field during the calibration exercise (that is, before the start of experiment when the vehicle is stationary).

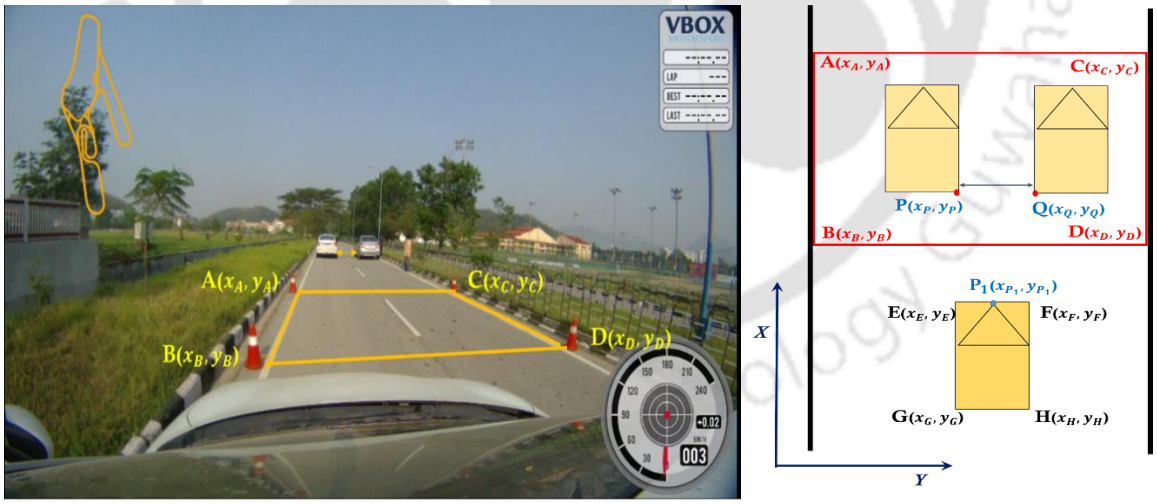

(a) **(b)**

Figure 3.12. Camera calibration technique considered in the study **(a)** rectangle ABCD viewed from the camera **(b)** top view of the calibration pattern along with the lead vehicle

With all known measured distances and transformed real-world coordinates, the longitudinal and lateral spacing with the left-front and right-front vehicles can be accurately estimated according to the following equations described below.

$$LG_{LF} = (x_P - x_B) + (x_B - x_E)$$

$$LG_{RF} = (x_Q - x_B) + (x_B - x_E)$$

$$CS_{LF} = (y_E - y_B) - (y_P - y_B) + 2 * (y_{P1} - y_E)$$

$$CS_{RF} = (y_Q - y_B) - (y_E - y_B)$$

Where LG_{LF}, LG_{RF}, CS_{LF} and CS_{RF} are the longitudinal gaps with the left-front and right front vehicles, centerline separation with the left-front and right-vehicles respectively. The distances $(x_B - x_E)$, $(y_E - y_B)$ and $(y_{P1} - y_E)$ are measured in the field and the factor 2 in the formulation is because both the subject vehicle and the left-front cars are of same model with same static characteristics.

The lateral clearance between the leading vehicles were also measured during the calibration exercise and this measurement was used to validate with the real-world coordinates obtained from the trajectory extractor. Such information is used further to estimate the accuracy of data extraction. The real-time of sampling, the global coordinates and speed of each vehicle involved in the experiment are directly obtained from the GPS receivers at 10Hz frequency while the positional data of the vehicle in-front are extracted from the video recorders at each 5Hz frequency level. After suitable transformation, the GPS data and the extracted video-data are then synchronized to obtain acceleration/deceleration and speed of all the vehicles, global time, longitudinal gap and centerline separation with left-front and right-front vehicles at every 0.2s-intervals.

3.3.2.3. Selection of two-leader following data

Initial data acquisition resulted into a complete set of multi-leader following time-series data for a wide range of vehicles speeds, with prerequisite information on the following behaviour of the subject drivers, from the start to the termination of the following process. The starting criteria was defined as being when the subject vehicle approached to either of the front vehicles with less than a 2s-time headway. This '2s-time headway' is commonly assumed as the starting criteria of a stable car-following event (Reiter, 1994). Conversely, the following process was defined to have reached the termination criteria when the subject driver either initiated an overtaking manoeuvre or headway is more than 2s. Moreover, only those trajectory data were considered to own significant multi-leader following characteristics for which all the three interacting vehicles were jointly observed for a time period of at least 15s (Zheng et al., 2015). Further, to ensure that the dynamic following behavioural process is preserved, the processed data with more than 2m lateral clearance between the LF and RF vehicles are discarded, such that the following vehicle (having 1.8m car width) cannot filter/pass in between the front vehicles by utilizing the lateral clearance maintained by them.

3.3.3. Accuracy of data extraction

While extracting data from the video, an extractor may make an erroneous mouse click with a fixed standard deviation (in pixels) on the screen, and an average extractor makes mouse-

clicking with an accuracy of 6 pixels. These 6 pixels correspond to different distances in the field, and error in calculating longitudinal gap will increase as field distance from point B increases. In case of single-leader car-following scenario, the maximum error (normally distributed, 3σ) was found to increase from 1.2% for a point exactly on point B (Figure 3.9(b)), to 11.7% for a point 30 m ahead of B for the experiment conducted on Guwahati roads (when point B was 8m ahead of test vehicle's front edge). Similarly, for two-leader car-following scenario, the error on point B (Figure 3.12(b)) was 0.8% and it increased to 5.12% for the point A (that was 10m ahead of B). Moreover, the accuracy in the speed measurement is 0.16kmph. To estimate the errors in lateral distance measurement, the screen coordinates of the two opposite ends of lane markings (of known width) were extracted from the software at different longitudinal positions on the road (as viewed from the camera). The conversion into real-world coordinates at different road sections resulted in an average estimated error of 8.76cm for the single-leader car-following data and 6.21cm for two-leader car-following data.

3.4. Chapter summary

The research work described in this thesis utilized the static video recording technique for understanding the vehicle-following and filtering behaviour of different vehicle types commonly observed in non-lane based traffic environments. Considering the advantage of static technique in recording the real traffic stream from an elevated fixed vantage point, longitudinal and lateral interactions of different combinations of vehicle-pairs could be obtained using this technique. However, it lacks flexibility in providing a detailed information on the driver's behavioural response for a longer period of time, specifically in the car-following regime. The dynamic video recording technique described in this chapter, sought to make a contribution to the problem of single-leader car-following and two-leader car-following data collection and estimation. The stringent requirements of data for the car-following regime were described, followed by a detailed description on the data collection and extraction methodology. The problem of GPS based systems in collecting car-following data for disordered systems is highlighted, with justification on the importance of developing an image-based in-vehicle trajectory extracting system for reliable estimation of dynamic time-series data.

Data utilized for an understanding of the staggered-following behaviour for different combinations of leader-follower vehicle pairs were primarily collected on urban roads in four different cities of India namely, Guwahati, Mumbai, Pune and Kolkata having road widths varying from 7.6m to 17.5m. In all the cases, data were collected in good visibility conditions (in morning hours) for a duration of 2h to 3h. While for the filtering behavioural study of MTWs and cars, three urban mid-block sections in Mumbai and Pune with varying geometric and traffic characteristics were considered, with data being collected in the morning hours from 9:00 to 12:00 noon. Conversely, a detailed dynamic time-series data for the single-leader and two-leader car-following regime were collected with the instrumented vehicle (cars) along a four-lane divided national highway (NH-37) in the city of Guwahati in morning hours. The time-series data were collected in a controlled environment during low-flow conditions such

that interactions with the leading vehicles could be observed for a wide range of speeds and different leaders' arrangements. Finally, the errors estimated in data extraction for both the static and dynamic data collection techniques were discussed in the chapter.

4

Incorporating Lateral Descriptor in Traffic Flow Modelling

Precise understanding of microscopic traffic variables provides a succinct characterization of the stochastic features of traffic flow phenomena. A comprehensive apprehension of how drivers interact with the surrounding traffic environment, how they control their vehicles during vehicle-following processes and how substantial the safety problem associated with drivers is, has been a subject of interest since decades. Traditionally, pioneering efforts were devoted to model driving behavioural phenomena by investigating the longitudinal and lateral interactions between vehicles separately and independent of each other. While modelling the longitudinal interactions between vehicles in car-following regime has gained considerable attention over years, an in-depth exploration is required, above and beyond the traditional car-following assumption, to describe the following behaviour in disordered traffic environments, with proper quantitative substantiation. Certainly, the behavioural phenomena of drivers in lane-based traffic is different from disordered traffic environments as the extent of lateral movement is more prevalent in the latter. In essence, vehicles in non-lane-based traffic scenario exhibit higher extent of lateral movements because of varying static and operational characteristics, sporadic driving behaviour, as a result of which they seldom follow their immediate vehicles in-front and often, they tend to evaluate opportunities for possible lateral movements while progressing longitudinally, either to have a better forward field of view or to initiate lateral shifts. This frequent lateral adjustment in positions within the interaction regime gives rise to scepticism regarding the suitability and selection of the commonly used traffic flow descriptors to describe the staggered-following processes of non-lane-based traffic environments. Although a plethora of literature is available to describe the longitudinal descriptors of traffic flow in the vehicle-following process, the applicability of lateral descriptor of traffic in understanding the behavioural phenomena of such traffic environments, still remains a matter of further exploration.

This chapter aims to underline the importance of lateral descriptor of traffic in traffic flow modelling, describing how this indicator can integrate the longitudinal and lateral interactions in the staggered-following process of non-lane-based traffic environments. The lateral traffic flow descriptor, being poorly represented in the existing literature, has indeed a knock-on effect in a better prediction of realistic driver behaviour, both in terms of augmenting the reliability

of microsimulation models and enhancing driver's safety. The chapter is essentially divided into three main sections, a brief description being provided below:

1. *Identification of microscopic traffic variables describing the integrated driving behaviour*: This section begins with an overview of the microscopic traffic variables describing the longitudinal and lateral interactions in the staggered vehicle-following process. This is followed by an investigation of a number of situational variables affecting the choice of driver's following behaviour.

2. *Methodological approach to accommodate dependence between the variables for different vehicle-pairs*: For a suitable representation of the integrated driving behaviour, this section provides a copula based methodological framework to model the dependence structure between the longitudinal and lateral descriptors for different leader-follower vehicle combinations.

3. *Evaluation of safety in staggered-following scenario:* This section highlights the safety aspects of the drivers in staggered-following events using surrogate safety indicators. Drivers' selection of minimum headways and the rear-end collision risks associated with them are assessed in this section.

4.1. Identification of microscopic traffic variables describing the integrated driving behaviour

The dynamics of traffic flow is essentially formed from the underlying interactions between different vehicles. Considering the two-dimensional movement of vehicles in non-lane-based traffic environments, this section discusses the fundamental variables of traffic flow from a microscopic perspective and introduces a micro-level indicator to describe lateral interactions in the staggered-following scenario. It further investigates the inter-relationship between the considered variables and the effect of endogenous as well as exogenous factors on the vehicle-following behavioural processes of drivers.

4.1.1. Longitudinal and lateral descriptors of traffic

The most important microscopic variables that are commonly used to describe the longitudinal interactions between vehicles are time headway, distance headway and speed of individual vehicles. Time headway (TH) is a *local* microscopic variable, describing the inter-arrival time difference between the front bumpers of the leading and following vehicles at a section across the road width (Dubey et al., 2012). The importance of time headway stems from the fact that it bears an inverse relationship with the flow rate and has important applications in estimating capacity (Chang and Kim, 2000; Suweda, 2016), passenger car unit (Saha et al., 2009), safety evaluation (Ayres et al., 2001; Duan et al., 2013; Taieb-Maimon and Shinar, 2001), traffic operation studies (Yin et al, 2009; Moridpour, 2014) and so on. Distance headway (DH), on

the other hand, is an *instantaneous* microscopic variable, measuring the longitudinal distance between the front bumpers of the successive vehicles at a given instant of time. The net distance headway or, longitudinal gap (LG) is more commonly used to describe the distance between the rear-bumper of the preceding vehicle and the front bumper of the subject vehicle. This measure is essentially important for analyzing and modeling the minimum safe distance required in the following processes to avoid a rear-end collision. In particular, distance headway and time headway are strongly correlated. Given the speed of the following vehicle, time headway can be obtained as the distance headway divided by the speed of the following vehicle.

These micro-level characteristics describing the longitudinal movement of vehicles are contemplated as dominant input parameters for generating vehicles in microscopic simulation models. These variables are important for microscopic driving behaviour analysis and they reflect the rudimentary uncertainties in vehicle-following manoeuvres. While the longitudinal interactions between the vehicles are described by time headway, longitudinal gap and speed, the consideration of the lateral descriptor of traffic can further augment the predictability and reliability of the microscopic simulation and traffic flow models developed for disordered traffic streams. One such fundamental indicator of non-lane-based traffic describing the lateral interaction in the following scenario is defined as centerline separation (CS), coined by Gunay (2007). It is a measure of the off-centeredness or staggeredness between the interacting vehicles in the vehicle-following process. This indicator has been considered in many car/vehicle-following studies to describe the lateral interaction in non-lane-based traffic environments (Gunay, 2007; Jin et al., 2010; Zheng et al., 2012; Li et al., 2015a). Centerline separation is estimated from the lateral positional difference between central positions (widths) of the leading (W_{LV}) and following vehicle (W_{FV}). A graphical representation of all the considered microscopic traffic variables is presented in Figure 4.1.

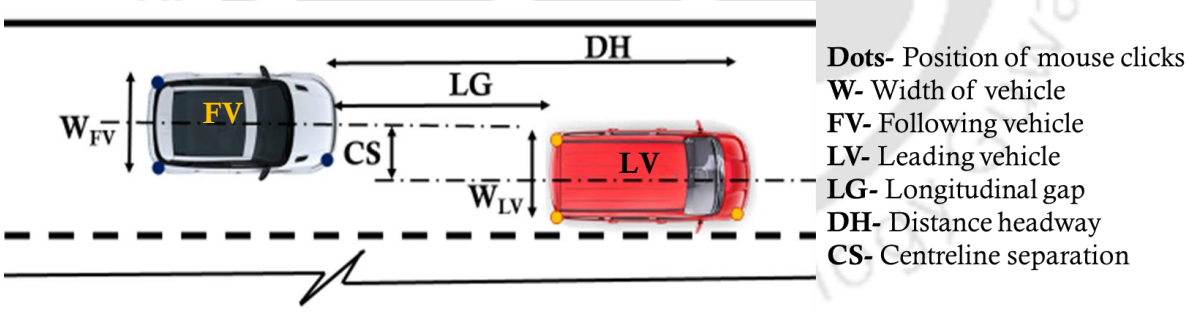

Figure 4.1. Sketch of variables considered for each interacting vehicle-pair

Among all the micro-level longitudinal characteristics of traffic flow, time headway and speed are considered as the most important parameters used to characterize traffic flow phenomena and for generating vehicles in microsimulation models. Considering the importance of such parameters and understanding that vehicles in non-lane-based traffic exhibit an integrated two-dimensional manoeuvring pattern (that is, both longitudinal and lateral), the inter-relationship between the longitudinal and lateral descriptors of traffic are further investigated in this research. Certainly, a better understanding and modelling of the longitudinal and lateral movement simultaneously would result in a better and realistic illustration of the driving behaviour in such disordered systems.

4.1.2. Dependence among the considered microscopic traffic variables

In the context of car-following studies, the relationship between TH and speed was investigated by several researchers. Fuller (1986) found negative correlation between speed and TH while Ota (1994) found no effects of speed on TH when drivers were instructed to follow the lead vehicles at a comfortable and safe distance for varying speeds of 50, 60 and 80km/h. The findings of Ota (1994) indeed suggested consistency of THs over speeds at steady-state car-following conditions. This hypothesis was further supported by Van Winsum and Heino (1996) results, obtained in a driving simulator over speeds of 40, 50, 60 and 70km/h, as well as with results of Taieb-Maimon and Shinar (2001) obtained in a field study. However, in a later date, Brackstone et al. (2009) suggested a gradual decrease in the following headways for speeds below 15m/s (54km/h) while it was constant above that threshold. Similarly, a study conducted by Piao and McDonald (2003) on time gap data of European countries found a decreasing trend of time gaps at speeds less than 60km/h and stable time gaps at speeds above 70km/h. The hypothesis of constant headways over a range of speeds (each at an interval of 5km/h) is further validated in this research work and the statistics of the time headway data for each speed group in a car-following scenario is illustrated in Figure 4.2.

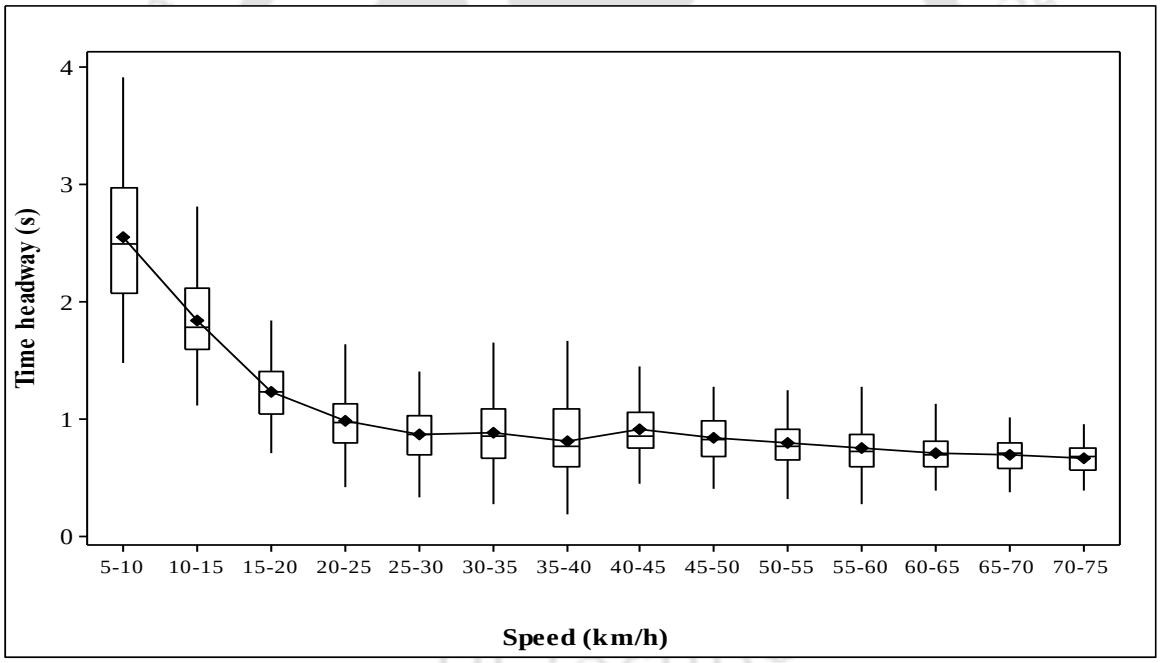

Note: Connecting line indicates mean time headways

Figure 4.2 Box-plot showing variations of time headways with speeds

Clearly, the figure depicts an inverse relationship between mean time headways and speeds. The following headways are found to follow a gradual decreasing pattern till 40 km/h while the variations in headways become minimal for speeds above 40km/h. To investigate the variability in following headways between two successive speed groups, F-tests were performed at α=0.05, the test results of which indicated no statistical difference for speeds above 60km/h. A one-way Analysis of Variance (ANOVA) test also corroborated that drivers' selection of headways are consistent at speeds above 60km/h [F (2, 287) = 0.87 < $F_{critical}$=3.03, p=0.41]. This envisages that the concept of constant THs that is more predominantly used in

driver assistance systems (Piao and McDonald, 2003), might be true for car-following conditions with speeds higher than 60 km/h, but is not true for lower speeds.

Moving beyond the dependence relationship between both the longitudinal descriptors (time headway and speed), the nature of association of the longitudinal descriptors with the lateral descriptor of traffic was further evaluated. The distributions of time headways and speeds for different levels of CS are presented in Figure 4.3.

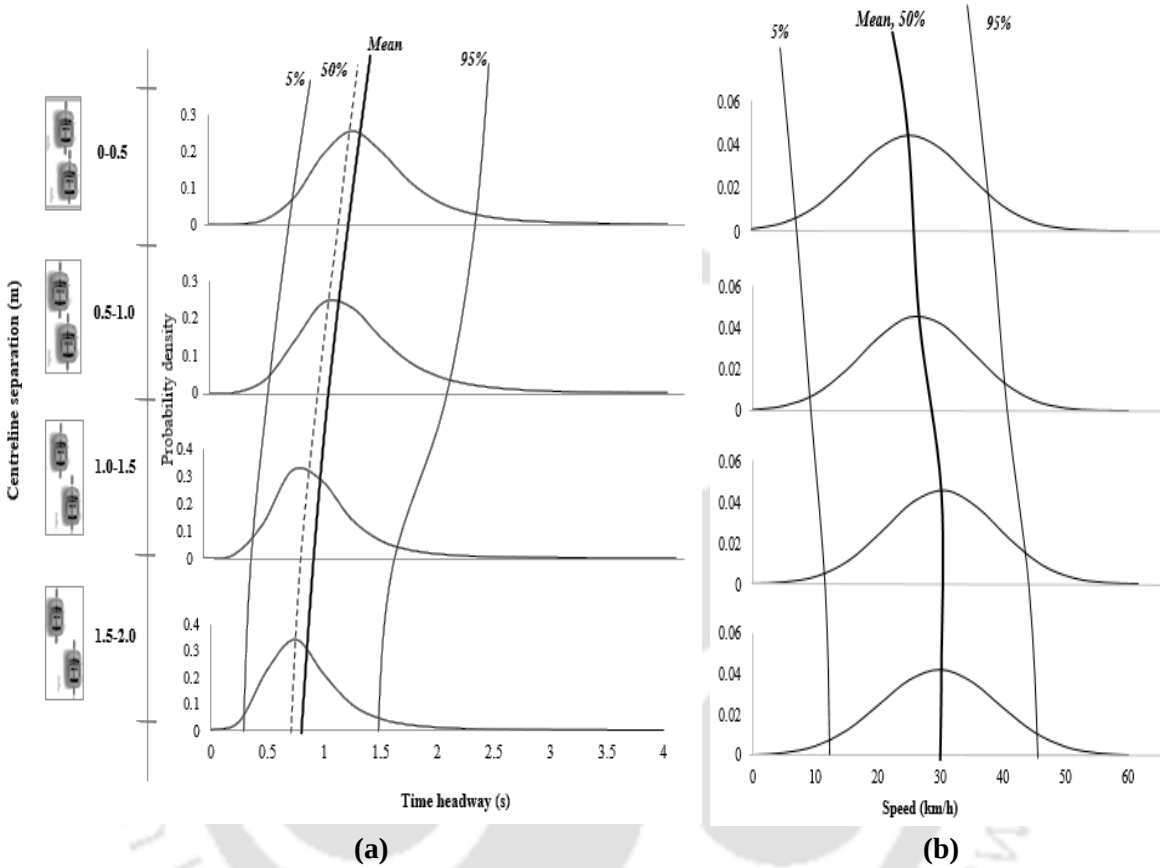

Figure 4.3. Contour plots of **(a)** time headways and **(b)** speeds with its distributions for different centerline separations

The contour lines that are overlaid on top of the distributions represent 5 percentile, 50 percentile (median), mean and 95% headway values. Interestingly, the pattern of the contour lines for different sets of CSs illustrates that time headways exhibit a decreasing relationship with the increase in CS while the reverse trend follows for speeds of following vehicles. This indicates that as the extent of staggeredness increases between the interacting vehicles, the following vehicles perceive a wide forward visual field of view, little obstruction of the vehicle in-front, more opportunities to perform lateral shifts and can anticipate the actions of the leading vehicles more confidently, as a results of which they tend to follow the preceding vehicles closely maintaining lower mean time headways. The inverse trend of the following headways with CS is consistent with the findings of Gunay's (2007) work. Although no clear correlation between TH and CS was obtained for Britain and Germany data in Gunay's (2007) study, datasets collected from Turkey indicated the decline in time headways for all considered sections.

4.1.3. Determinants of longitudinal descriptors in staggered-following conditions

The following headways maintained by the drivers during close-following scenario and its relationship with the rear-end collision risks involved are intuitively appealing. Anecdotal evidence supports the hypothesis that a considerable percentage of the crashes occur as a result of rear-end collisions during close car-following events (McGehee et al., 1992). The role of human (mis-) perception towards the prevailing traffic conditions has been deemed as a vital factor to the design and operation of traffic systems (Brackstone et al., 2009), and also to traffic flow processes such as traffic flow breakdown (Treiber et al., 2006). Therefore, examining drivers' selection of headways during the car-following scenario and understanding how this choice is affected by a number of local traffic variables, will not only enhance safety in the car-following scenario but also augment the design and operation of traffic systems.

Several determinants affecting the driver's choice of time-headways in car-following scenario are mainly characterized by driver characteristics, vehicle attributes and local traffic conditions. Research on the effect of exogenous (weather, geometric characteristics) and endogenous variables (flow rate, proportion of heavy vehicles) on time headways are well-documented in the literature. For the same level of traffic flow, Rossi et al. (2014) found that mean time headways increase with the increase in the proportion of heavy vehicles. Headway maintained by vehicles at specific lane positions during high flow conditions indicated that drivers maintain lower mean headways in passing lane than than in middle lane (Abtahi et al., 2011). The effect of weather conditions on mean time headways was further studied by Alhassan and Ben-Edigbe (2012) and Rahman and Lownes (2012) in car-following state. Amongst all determinants, one such endogenous factor that predominately affects time headways is the flow rate, which actually bears a reciprocal dependent relationship with time headways. In essence, a great deal of literature prevails that essentially concerns to the impact of differing traffic flow conditions (free-flow, congested, peak-hour, off-peak hour) on time headway distributions (Al-Ghamdi, 2001; Jin et al., 2009; Yin et al., 2009; Dubey et al., 2013; Rossi et al., 2014). Despite anecdotal evidence that headways decrease with increase in traffic flow levels, the impact of traffic flow on headways in car-following state has been only examined by Brackstone et al. (2009). In their study, they found no effect of traffic flow level on the choice of headways in car-following scenario when both the leading and following vehicles have less relative speeds.

The research work described in this section provides an in-depth exploration of several determinants that may affect driver's choice of time-headways in staggered-following scenario of non-lane-based traffic environments. In light of this, four research hypotheses are investigated that may provide a detailed understanding of drivers' choice of following headways in staggered-following case.

1. *Road width affects driver's selection of headways*. Although there is substantial evidence in the car-following literature that the following behaviour of drivers remains invariant with the type of road (urban arterials, motorways and urban streets), yet the effect of road width in staggered-following behaviour of drivers is still lacking.

2. *Choice of time headways varies with the amount of off-centeredness.* Understanding that the car-following behaviour in non-lane-based traffic is completely different from that in lane-based traffic environments, drivers' selection of headways are anticipated to vary considerably with the amount of off-centeredness between the interacting vehicles, as the lateral movement of vehicles is more prevalent in the former.

3. *The following behaviour varies with the type of leading vehicle*. Many studies have provided a preliminary assessment of the statistical properties of headways for different leader-follower pairs both for homogeneous (Ye and Zhang, 2009*;* Qingyi et al., 2010) and heterogeneous conditions (Kanagaraj et al., 2011), but the effect of leading vehicle type on the following headways has not been investigated in detail for different staggered positioning of vehicles.

4. *Drivers' choice on minimum time headways varies in staggered following scenario.* TH is a well-recognized safety indicator that represents the propensity of risks associated with drivers in close-following processes. For an assessment of rear-end collision risks, the peer-reviewed literature recommends different minimum TH thresholds mainly for lane-based scenario (Ayres et al., 2001; Duan et al., 2013; Taieb-Maimon and Shinar, 2001), but what remains still unclear lies in the choice of drivers in selecting minimum headways in staggered-following scenario.

4.1.3.1. Impact of road width on driver's choice of time headways

To examine the impact of road width on time headways, headway data are initially categorized into three groups- Category I (corresponding to road widths of 7.6m and 7.8m), Category II (having road widths of 10.8m and 11.2m) and Category III (with 17.5m road width) (refer section 3.2.1.1.). The statistical properties of the segregated headway data are presented in Table 4.1.

Table 4.1. Summary of TH data for different categories of road width

	Category I	Category II	Category III
Mean (s)	1.16	0.81	0.75
Median (s)	1.02	0.77	0.70
Standard deviation (s)	0.59	0.32	0.19
Skewness (s)	1.85	1.73	0.25
Sample size	904	256	809

All the statistical parameters of THs including mean, median, standard deviation and skewness are observed to decrease with the increase in road widths. The distribution pattern of THs depicted in Figure 4.4 shows that a large number of drivers travels at shorter headways with increasing road width conditions (0.5-1.75s, 0.5-1.5s and 0.5-1.25s for Category I, II and III respectively). Considering all the statistical univariate models, although the distributions do not exhibit any distinct difference for headways above 2.5s, the right-skewed properties of the distribution from category III, category II to category I indicates a fat-tailed distribution with large accumulation of long headways when road width decreases.

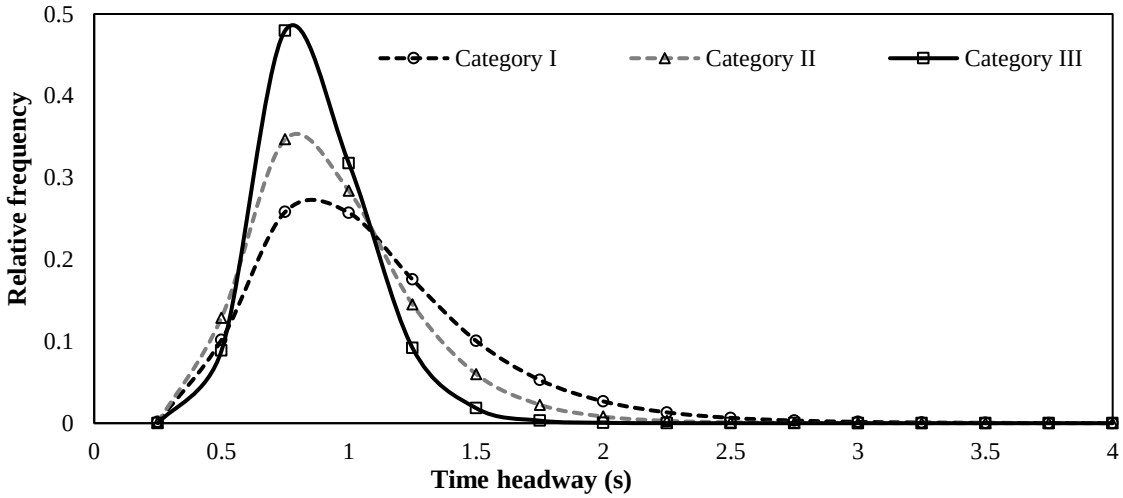

Figure 4.4. TH distribution patterns for different carriageway widths

To further support the hypothesis, the effect of vehicle speeds on time-headways is evaluated for different road width categories and the trend of mean headways for each speed group is presented in Figure 4.5.

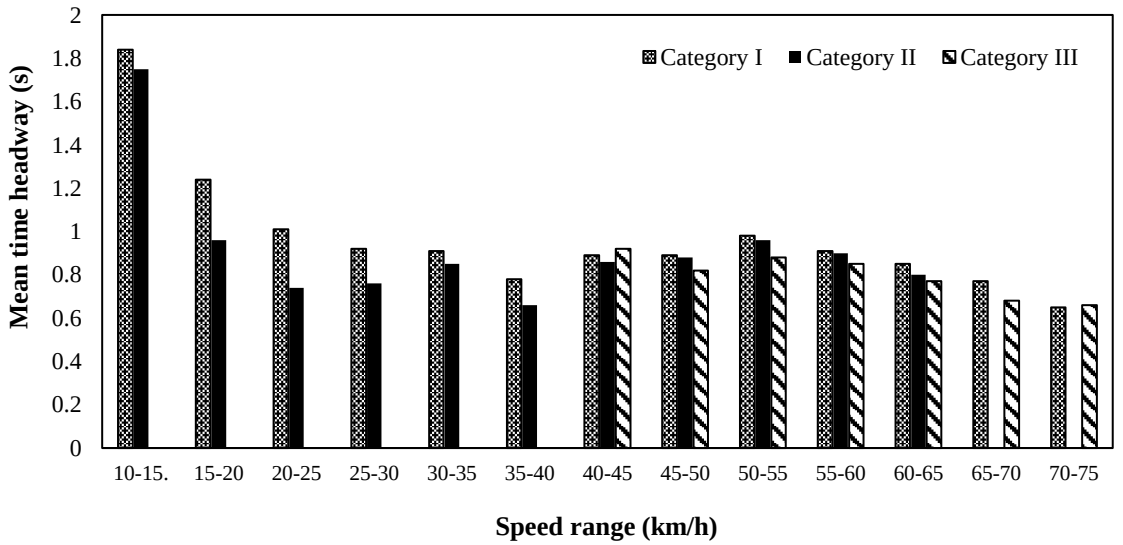

Figure 4.5 Variations in mean THs with increasing road widths for each speed range

In all the cases, a decreasing trend in following headways is observed as road width increases. This can be attributed to the fact that as road width increases, vehicles in the staggered-following interaction regime, tend to avail the free space by shifting laterally in order to avoid the lead vehicle, either to initiate lateral shifts or to follow the leading vehicle closely with a clear field of forward view. This justifies the decreasing trend of mean time headways with increasing road widths.

Furthermore, *t*-test (equality of means) between two road width categories and analysis of variance (ANOVA) test for comparing the means of three categories were also conducted corresponding to each speed group. The statistical test results indicated a significant difference in mean headways for speeds below 30km/h at 5% significance level, while no statistical difference is observed for speeds exceeding 30km/h. This signifies that although mean time

headways in the staggered-following scenario reduce with the increase in road widths, the reduction in following headways is not statistically significant for speeds above 30km/h.

4.1.3.2. Effect of centerline separation on time headways

The headway-maintaining behaviour of vehicles for different lateral separations with the lead vehicles are examined for different ranges of CS [0-0.5m, 0.5-1.0m, 1.0-1.5m and 1.5-2m]. The statistical properties of time headways for car-car pairs are summarized in Table 4.2.

Table 4.2. Statistical properties of THs for different levels of CSs

CS (m)	Standard deviation (s)	Median (s)	Mean (s)	5 percentile (s)	95 percentile (s)	Sample
0-0.5	0.53	0.97	1.09	0.56	2.19	752
0.5-1.0	0.47	0.84	0.96	0.49	1.97	584
1.0-1.5	0.37	0.74	0.79	0.45	1.25	379
1.5-2.0	0.30	0.68	0.73	0.39	1.22	254

The descriptive statistics of THs in Table 4.2 depict an inverse relationship of THs with increasing CS levels. In all the cases, the median values are found to be lower than 1s, which is considered as the preferred time headway of drivers for steady-state car-following conditions in rush hour traffic (Ayres et al., 2001) while 95% values are found to be lower than 2.19s. The 2s-criteria is often recommended as safe headway requirement for car-following in driving manuals of lane-based traffic. This tendency of the drivers in maintaining lower headways can be attributed to the fact that the following vehicles in staggered-following scenario of non-lane-based driving environments often tend to follow the leaders by maintaining certain extent of off-centeredness between them, either to have a better field of view or to avoid the encumbrance of the leaders. This allows the followers to make considerable lateral shifts as a result of which they tend to follow the leading vehicles closely maintaining lower longitudinal gap and thereby lower time headways.

An ANOVA test was also conducted to check the statistical significance in the mean headways for all the considered ranges of CSs. The results reveal significant different difference in the mean headways across different CS levels [$F(3, 1963) = 24.684 > F_{critical}=2.612$, $p<0.001$]. Certainly, the findings signify that the centerline separation needs to be incorporated for the formulation of time headway related models of non-lane-based traffic environments.

4.1.3.3. Effect of the type of leading vehicle on time headways

Differences in driving style, static characteristics and manoeuvring capabilities of a variety of vehicles lead to complex vehicular interactions. Understanding the behavioural aspects of the followers while interacting with different leading vehicles in the staggered-following scenario provide a deeper insight in the behavioural differences of the following vehicle in maintaining headways with vehicles in-front. The headway maintaining behaviour of cars while interacting

with the leading vehicles for different levels of CSs is investigated and a summary of the descriptive properties of time headways is presented in Table 4.3.

Table 4.3. Descriptive statistics of THs for different leader-follower vehicle pairs

CS (m)	Statistics	MTW-Car	3W-Car	Car-Car	LCV-Car	Truck-Car
A [0-0.5]	Mean (s)	0.61	0.65	1.09	1.21	1.60
	Median(s)	0.51	0.59	0.97	1.11	1.53
	Std.dev (s)	0.45	0.18	0.53	0.47	0.64
	Sample	48	37	752	53	75
B [0.5-1.0]	Mean (s)	0.56	0.63	0.96	1.02	1.58
	Median (s)	0.47	0.60	0.84	0.90	1.46
	Std.dev (s)	0.26	0.19	0.47	0.43	0.52
	Sample	44	32	584	50	42
C [1.0-1.5]	Mean (s)	0.53	0.56	0.79	0.89	1.47
	Median (s)	0.47	0.49	0.73	0.76	1.41
	Std.dev (s)	0.25	0.12	0.37	0.46	0.49
	Sample	31	30	379	37	48
D [1.5-2.0]	Mean (s)	0.50	0.55	0.73	0.77	1.43
	Median (s)	0.41	0.53	0.68	0.69	1.38
	Std.dev (s)	0.45	0.17	0.30	0.27	0.74
	Sample	22	26	254	25	27

It can be observed from the table that for each level of CS, mean and median values of time headway show a gradual increasing pattern from MTW-car to 3W-car, car-car, LCV-car and truck-car. This indicates that as the dimensions of the leading vehicles increase, the followers (cars) prefer to maintain a large separation with the vehicles in-front because the bigger dimensions of the leaders cause more hindrance to the field of view of cars thus restricting the followers to perceive a clear view of the forward scenario, as a result of which they maintain larger separation or headways with the leaders. This is even evident from the probability density plot presented in Figure 4.6.

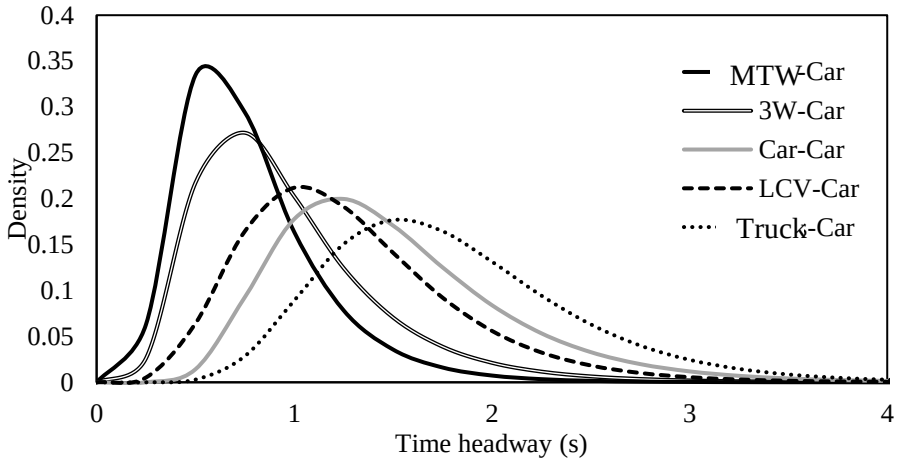

Figure 4.6 Distribution patterns of different leader-follower pairs across all centerline separation

Moreover, the decreasing tendency of time headways with the increase in CS for each leader-follower pair further justifies the behavioural pattern of the followers in maintaining even lower headways as the extent of off-centeredness between the interacting vehicles increases. The probability density plots of different leader-follower interacting vehicle pairs illustrated in Figure 4.6 clearly reveal a large accumulation of shorter time headways for MTW-car and the peaks of the distributions show a gradual rightward shift as the dimensions of the leading vehicles increase. For instance, the modes of the statistical models are observed as 0.5s, 0.75s, 1s, 1.25s and 1.5s for MTW-car, 3W-car, car-car, LCV-car and truck-car respectively. This shift in the distribution patterns justifies the differences in the headway maintaining behaviour of cars according to the type of lead vehicle. The results of ANOVA test also revealed significant difference in mean time headways across all the considered interacting vehicle pairs [F (4, 2588) = 28.464 > $F_{critical}$=2.312, p<0.001] for all CSs. To further examine the statistical difference in the mean headways for any two levels of CS corresponding to each vehicle-pair, *Z*-test for mean values of time headways was performed at 5% significance level and a summary of the obtained test-statistic results are presented in Table 4.4.

Table 4.4. Z-test results for headway means between any two CS ranges

CS	*Z*-statistic value [Significant difference?]																	
	MTW-Car			3W-Car			Car-Car			LCV-Car			Truck-Car		
	B	*C*	*D*	*B*	*C*	*D*	*B*	*C*	*D*	*B*	*C*	*D*	*B*	*C*	*D*
A [0-0.5m]	N	N	N	Y	Y	Y	Y	Y	Y	Y	Y	Y	N	N	N
B [0.5-1.0m]		N	N		Y	Y		Y	Y		Y	Y		N	N
C [1.0-1.5m]			N			N			N			N			N

Note: ***A***= 0-0.5m; ***B***= 0.5-1.0m; ***C***= 1.0-1.5m; ***D***= 1.5-2.0m; **Y**- Yes; **N**-No

It is evident form the *Z*-test results that the following headways of cars are not statistically different across different levels of CSs when they follow the leading MTWs and trucks. This can be adjudged from the fact that the compact sizes of MTWs provide a clear visual field of view to the following cars, hence the presence of MTWs as the leaders hardly affect the following behaviour of cars as a result of which the following headways are not statistically significant across all CSs for MTW-car pair. Conversely, for truck-car case, the larger dimensions of trucks obscure the view of the following vehicles for CS in between 0-2m. This implies that for any level of CS (0-2m), the following headways are dependent on the centerline separation with the leading trucks and therefore no statistical significant relationship was observed. While considering other leading vehicle pairs of moderate dimensions, the following headways of cars were found to be significantly different for different levels of CS. This indicates that the off-centeredness of the following vehicles with moderate-sized leaders (3Ws, cars and LCVs) significantly affect the following behaviour of cars. Interestingly, no statistical difference in mean time headways was obtained beyond 1.5m CS for all considered leader-follower vehicle pairs. This justifies that the effect of centerline separation in the following headways of cars is not prominent beyond 1.5m CS. Empirical evidence has therefore been made in support to the hypothesis that the type of leading vehicle significantly affects the following headway attributes of cars in staggered-following scenario of non-lane-based traffic environments.

4.1.3.4. Drivers' choice on minimum time headways varies in staggered-following scenario

Time headway is one of the typical risk indicators that represents the propensity of risks in car-following process. Understanding how close the following behaviour is requires more attention in the context of safe driving. Existing literature recommends different headway values as an indicator of criticality of a certain traffic situation, where most of the studies have been conducted in restricted simulated environments. The following behaviour however is different in real traffic than in simulator-based experiments where only a simplistic representation of traffic is created (Brackstone et al., 2009). This section is aimed to attain a comprehensive understanding of minimum time headways maintained by drivers in car-following conditions. Though quantifying safe headway is hard to acquire from the collected data, this section explores recent investigations on safe headway threshold and accordingly a comparative study is carried out based on previous investigations. Table 4.5 presents a list of some safe headway values that have been adopted by different researchers in homogeneous and lane-disciplined traffic conditions.

Table 4.5. Summary of some safe headway values used by different researchers

Study	Method	Following headway threshold (s)	Speeds (km/h)/ Conditions	Comments
Siebert et al. (2014)	Simulator	1.00	50, 100, 150	Unpleasant
		0.50		Dangerous
Purucker et al. (2014)	Simulator	0.75	50	Tailgating/ Dangerous
Ota (1994)	Simulator	0.60	50, 60, 80	Safe
Taieb-Maimon and Shinar (2001)	On road	0.66	50, 60, 70, 80, 90, 100	Safe
		1.40		Comfortable
Ayres et al. (2001)	On road	1.00	Rush hour	Safe
Duan et al. (2013)	Simulator	0.70	45	Safe
		0.92	90	

Background studies on safe THs recommend different threshold values in the range of 0.60-2s where '2s rule' for minimum safe distance following is more pronounced in Netherlands, Germany and Sweden. Most observations summarized in Table 4.5 have been made on lane-based flows, hence direct comparison of safe following behaviour on mixed traffic with the presented values (Table 4.5) can be acquired for only lower values of CS (say less than 0.5m) for car-car vehicle pair. This comparative study is hence performed for only car-car case with CS lower than 0.5m where percentage of riders with THs lower than the recommended thresholds are examined.

Taking the recommended thresholds as a base mark, the observed percentage obtained for CS lower than 0.5m is further extended for other CS ranges and the contour line plots of the recommended thresholds at different CS ranges are shown in Figure 4.7.

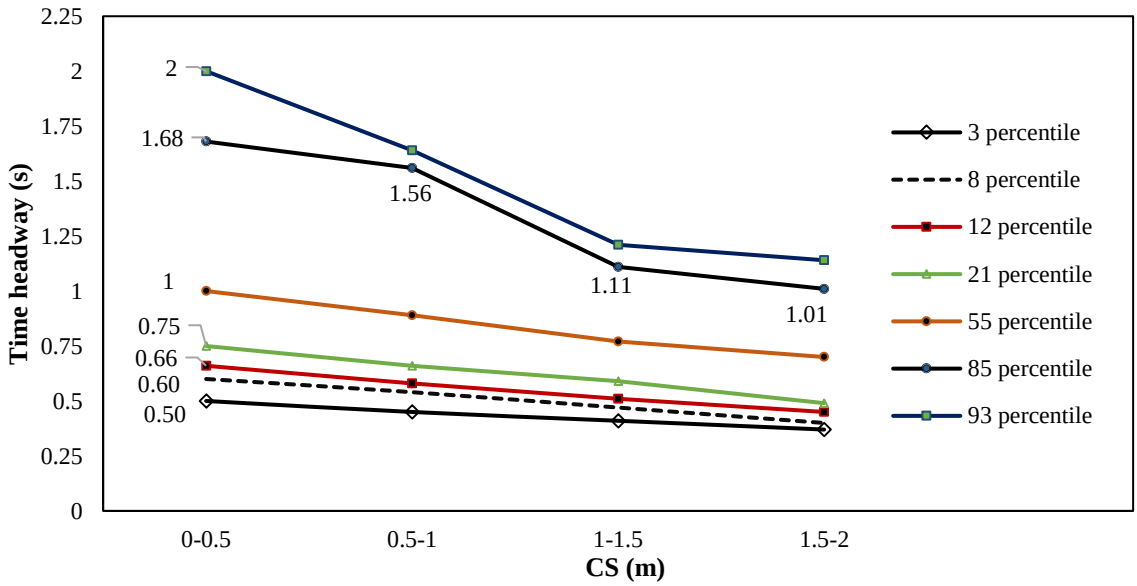

Figure 4.7 Contour lines of safe headway values at different centerline separations

The contour line plots of safe headway thresholds (suggested by various researchers) indicate that 93% of the drivers maintain headways less than 2s which is recommended as safe headway requirement for car-following in driving manuals. This percentage is considerably higher than Tennessee drivers' headways and Italian drivers' headway where 50.7% (Michael et al., 2000) and 62.7% (Bella et al., 2014) of the riders were not found to comply with the '2s-rule'. In our study, 55% of riders adopted headways less than 1s that is considered as the preferred time headway of drivers for steady state car-following conditions in rush hour traffic (Ayres et al., 2001). In a study by Taieb-Maimon and Shinar (2001), the average minimum close safe headway that drivers maintain with the lead vehicle on roads was found as 0.66 s across all speed ranges. Direct comparison of the value with our data indicated that 12 percentage drivers maintain headways lesser than 0.66s. Furthermore, almost 3 percent of the headways were lower than 0.5s which is considered as 'dangerous' in a simulator study (Siebert et al., 2014). Taking the value (TH=0.66m) suggested by Taieb-Maimon and Shinar (2001) as a safety criteria, it can be demonstrated from our study that 12% of drivers in car-following conditions show risky behaviour and with staggered car-following cases, the minimum TH threshold gradually decreases where it has been observed as 0.58s, 0.51s and 0.45s for 0.5-1m, 1.0-1.5m and 1.5-2m CS respectively. Furthermore 85% of the riders are observed to maintain headways less than 1.68s in car-following conditions and it gradually decreases to 1.01s at 1.5-2.0m CS. These findings demonstrate that the safe headway thresholds defined for lane-based traffic are different for the staggered-following scenario, indicating that the same safety thresholds may not define the actual risks associated with drivers in the following scenario of non-lane-based traffic environments. This justifies that the actual safety criteria for different staggered positions of vehicles needs further investigation for evaluating safety in such traffic streams.

To summarize, the choice of time headways in the staggered-following scenario is found to be strongly related with the lateral descriptor of vehicle interactions (or, centerline separation between vehicles). Although the following headways tend to decrease with the increase in road

widths, the reduction in headways is not found to be significant in TH modelling whereas the type of interacting leading vehicle indicated a prominent significant effect on the driver's selection of following headways. These obtained results, therefore, suggest the need to develop a methodological framework that can capture the dependence structure between centerline separation and time headways in the staggered-following scenario for combinations of leader-follower vehicle pairs, which can indeed enhance the predictability and reliability of the microscopic simulation models developed for non-lane-based traffic environments.

4.2. Methodological approach to accommodate lateral descriptor in time headway modelling for different vehicle-pairs

Understanding that the micro-level characteristic of traffic flow (that is, time headway) is inherently stochastic, many researchers have attempted to explore vehicle headway characteristics via independent univariate models. Traditional micro-simulation models assume the same headway distribution across all lateral separations of the interacting vehicles; but this assumption may not capture the variability in headways for different levels of CSs when traffic flow is essentially congested and vehicles do not follow lane discipline. Howbeit to ameliorate the realistic replication of drivers' behaviour in micro-simulation models for non-lane-based traffic environments, it requires an accurate characterization of the longitudinal (time headway) and lateral (centerline separation) descriptors of vehicle interactions as well as the potential dependence between CS and time headways for different combinations of interacting vehicle pairs. Constructing a joint bivariate distribution using copulas can be a more viable approach to account for the potential dependence structure between CS and TH in the staggered-following scenario. Therefore, in an attempt to better describe the integrated lateral and longitudinal behaviour, this section provides a methodological framework to accommodate the dependence of centerline separation and time headways in the staggered-following scenario for different combinations of leader-follower vehicle pairs. A step-by-step procedure concerning the theoretical background of copulas, development of the methodological approach and applicability of the methodological framework for time-headway model development has been discussed in detail.

4.2.1. Copula methodology for joint distribution modelling

4.2.1.1. Concept of copulas

Copulas have emerged as a flexible and powerful tool for multivariate stochastic analysis since decades (Bhat and Sener, 2009; Bhat and Eluru, 2009; Kim and Mahmassani, 2014; Zou et al., 2014; Zou and Zhang, 2016; Zou et al., 2017). A copula is a joint distribution function with margins uniformly distributed in [0, 1] that connects a stochastic multivariate relationship to its univariate marginal distribution functions of any dimension. The copula function offers a greater flexibility in correlating the dependence structure of several random variables through the choice of margins from different parametric families of univariate distributions. Sklar's

(1959) theorem forms the theoretical foundation of the copula theory. That is, for two continuous random variables (X_1, X_2) with marginal cumulative distribution functions $\big(F_1(x_1), F_2(x_2)\big)$, then by Sklar's (1973) theorem, a joint 2-dimensional cumulative distribution function (CDF) $F(x_1, x_2)$ can be generated as follows:

$$\begin{aligned} F(x_1, x_2) &= \mathbb{P}\,(X_1 < x_1, X_2 < x_2) \\ &= \mathbb{P}\left(F_1(X_1) < F_1(x_1), F_2(X_2) < F_2(x_2)\right) \\ &= C_\theta\big(F_1(x_1), F_2(x_2)\big) \end{aligned}$$

The equation shows that the joint CDF F can be described by the margins F_1, F_2 and the bivariate copula C, which captures the dependency structure between X_1, X_2. The 2-dimensional density function of X_1, X_2 in turn can be expressed in terms of copula density and marginal densities and can be obtained as:

$$\begin{aligned} f(x_1, x_2) &= \left(\frac{\partial^2 C\big(F_1(x_1), F_2(x_2)\big)}{\partial F_1(x_1)\partial F_2(x_2)}\right)\frac{\partial F_1(x_1)}{\partial x_1}\frac{\partial F_2(x_2)}{\partial x_2} \\ &= c_\theta[F_1(x_1), F_2(x_2)]\prod_{i=1}^{n=2} f_i(x_i) \end{aligned}$$

where $c_\theta[F_1(x_1), F_2(x_2)]$ is the density of the copula and is obtained by computing the second partial derivative of the copula on the two variables.

4.2.1.2. Measuring dependence structure

Because the dependence structures modelled through the copulas are independent of univariate margins, an appropriate copula function is the one which can suitably elucidate the dependence features of the data under consideration. In statistics, two commonly used measures of detecting dependence between the random variables have been formulated in the literature that are based on the concept of concordant and discordant pairs of observations: Kendall's τ and Spearman's ρ_S. Kendall's τ measure of dependence between the random variables (X_1, X_2) is defined as the probability of concordant pairs minus the probability of discordant pairs and is expressed as:

$$\tau(X_1, X_2) = \mathbb{P}\left(\big(X_1 - \tilde{X}_1\big)\big(X_2 - \tilde{X}_2\big) > 0\right) - \mathbb{P}\left(\big(X_1 - \tilde{X}_1\big)\big(X_2 - \tilde{X}_2\big) < 0\right)$$

where $\big(\tilde{X}_1, \tilde{X}_2\big)$ is an independent copy of (X_1, X_2). The second non-parametric measure of dependence i.e. Spearman's rank correlation coefficient ρ_S is three times the difference between the probability of concordance and the probability of discordance:

$$\rho_S(X_1, X_2) = 3\left(\mathbb{P}\left(\big(X_1 - \tilde{X}_1\big)\big(X_2 - \breve{X}_2\big) > 0\right) - \mathbb{P}\left(\big(X_1 - \tilde{X}_1\big)\big(X_2 - \breve{X}_2\big) < 0\right)\right)$$

where $\big(\tilde{X}_1, \tilde{X}_2\big)$ and $\big(\breve{X}_1, \breve{X}_2\big)$ are the two independent identically distributed random vectors of (X_1, X_2). It is to be noted that the distribution function for (X_1, X_2) is $F(.,.)$, while the distribution function for $\big(\tilde{X}_1, \breve{X}_2\big)$ is $F_1(.)F_2(.)$ since $\tilde{X}_1$ and $\breve{X}_2$ are independent vectors.

In addition to Kendall's τ and Spearman's ρ_S dependence measures, the traditional Pearson's-moment correlation coefficient r that is a measure of linear dependence between two variables has been investigated by many researchers, however at times, it can prove to be inappropriate and misleading. The rank-based measures of dependence are non-parametric techniques while the Pearson's correlation coefficient is a parametric method that largely depends upon the marginal distributions of the population and is affected by the shape of the distribution and outliers. It performs better than rank-based measures only for bivariate elliptical distributions. Because rank correlation measures are considered to be invariant with non-linear monotonic increasing transformations of the marginals and are easier to calculate for multivariate distributions possessing a simple closed-form copula (Embrechts et al., 2003), Kendall's τ and Spearman's ρ_S are commonly used to characterize the dependence structures in the copula literature, rather than the traditional Pearson's correlation coefficient.

4.2.1.3 Marginal distributions of the random variables

The estimation of a copula model requires optimal selection of marginal probability distribution functions. In this study, five univariate mathematical models lognormal (Das and Maurya, 2017), Burr (Maurya et al., 2015), log-logistic (Yin et al., 2009), gamma and Generalised Extreme Value (Dubey et al., 2012, 2013) are assumed for describing TH whereas for the CS data, five probability distributions- lognormal, logistic, Weibull, gamma and normal- were considered. The maximum likelihood method was used to estimate parameters of the univariate models while the validity of each distribution was evaluated based on log-likelihood and the Akaike Information Criteria (AIC) which is defined as follows (Akaike 1974):

$$\mathrm{AIC} = -2\sum_{i=1}^{n} \ln\left[f(u;\hat{\theta}\right] + 2\mathrm{k}$$

Where k is the number of parameters of the distribution function, $\hat{\theta}$ is a vector of estimated distribution parameters and n is the sample size of the data. The optimal model is selected as the one that corresponds to the largest log-likelihood value and minimum AIC.

Several statistical tests including Kolmogorov-Smirnov (K-S) test, Anderson-Darling (A-D) and Cramer-von Mises (CvM) tests were also conducted to assess the goodness-of-fit of the marginal distributions. The K-S test is a non-parametric and distribution free (critical values of the test statistic are independent of the specific distribution of the data being tested) goodness-of-fit test that measures the deviations of the observed cumulative distribution from a hypothesized continuous cumulative distribution function. On the contrary, the A-D test is a modification of the K-S test that is used to assess whether the data came from a specific distribution population. It is more sensitive to a specific distribution and tails of the distribution that is, it assigns more weight to the deviations in tails, than does the K-S test. A CvM test is also employed to verify the goodness of fit of the marginal distributions. This test is a measure of the squared deviations of the theoretical distribution and the empirical one over the whole range of data. This test has been proved to be more powerful than K-S test to a little deviation from the hypothesized distribution (Arnold and Emerson, 2011). The distribution was selected

as the best-fitted one when the AIC criterion and the K-S, A-D and CvM test statistics were minimal, rendering the null hypothesis unable to be rejected at α=0.05.

4.2.1.4 Selection of suitable bivariate copula models

Modeling the bivariate relationship of the considered 2D variables (TH, CS) requires prudent assessment of appropriate copula models. Because the dependence structures modelled through the copulas are separated from the univariate marginal distributions, an appropriate copula function is the one which suitably elucidates the dependence features of the data. A brief overview of the copula functions, that includes the Gaussian copula, the Farlie-Gumbel-Morgenstern (FGM) copula and various Archimedean copulas like the Gumbel-Hougaard copula, the Frank copula, the Clayton copula, the Ali-Mikhail-Haq (AHM) copula and the Joe copula, and dependence structures of each copula type is presented in Table 4.6.

In this study, the selection process of copula functions for bivariate analysis was performed by considering designated acceptable dependence domains and nature of association of the data under consideration. With a view to model the negative dependence structure between the considered micro variables, four copula functions namely, elliptical Gaussian copula, Farlie-Gumbel-Morgenstern (FGM) copula, Ali-Mikhail-Haq (AMH) copula and Frank copula were selected in this study. The primary argument for the choice of Gaussian copula stems from its capability to model all ranges of dependence (-1,1), whereas Archimedean class of copulas include a large set of closed-form copulas that cover a wide range of dependency structure. The Frank copula has nearly the full range (-1,1) in pair-wise correlation whereas AMH copula covers a moderate range (-0.182,0.333) of Kendall's τ. The FGM copula on the other hand provides an effective way for constructing a bivariate distribution if the correlation of the two variables is weak. The above-mentioned copula functions can be a more convenient choice to model the negative association of the selected variables and are hence employed in this study.

4.2.1.5 Parameter estimation of copula models

The most difficult problem in implementing copula theory is the estimation of unknown parameters of the copula. Some commonly used approaches that are mostly employed for estimating copula parameters are Inference from Margins (IFM) approach (Joe, 1997), maximum pseudo-likelihood method (MPL; Genest et al., 1995) and approach based on the rank correlation (Genest and Rivest, 1993).

The IFM method is a two-step parametric approach in which the parameters of the marginal probability distribution are estimated first and then the copula parameters are estimated based on the obtained marginal parameters (Joe, 1997). This method eases computational effort, especially when the maximum likelihood function becomes difficult to solve for a large number of parameters involved. Though this method is easy to employ, the IFM estimator depends largely on the choice of marginal distributions (Kim et al., 2007), and may run the risk of being unduly affected if selection of the margins turns out to be inappropriate (Zou and Zhang, 2016).

The maximum pseudo-likelihood method is another widely used approach that has proved to be an efficient yet accurate surrogate for likelihood estimation in a wide variety of probabilistic models (Strauss and Ikeda, 1990; Richardson and Domingos, 2006; Neville and Jensen, 2007), but fitting a highly non-linear functional form becomes relatively cumbersome.

Table 4.6 Characteristics and dependence measures of bivariate copulas

Copula type	Dependence characteristics	θ domain	Kendall's τ and domain	Spearman's ρ_S and domain
Gaussian	Captures full range of dependence, radially symmetric about the center, weak tail dependencies at extremes	$\theta \in [-1,1]$	$\frac{2}{\pi}\sin^{-1}\theta$ $\tau \in [-1,1]$	$\sin^{-1}\left(\frac{\theta}{2}\right)$ $\rho_S \in [-1,1]$
F-G-M	Allows for relatively weak dependence, radially symmetric	$\theta \in [-1,1]$	$\frac{2}{9}\theta$ $\tau \in \left[-\frac{2}{9},\frac{2}{9}\right]$	$\frac{1}{3}\theta$ $\rho_S \in \left[-\frac{1}{3},\frac{1}{3}\right]$
Gumbel	Only positive dependence structure of the bivariate data can be analyzed, strong right tail dependence, weak left tail dependence, radially asymmetric	$\theta \in [-1,\infty)$	$1-\frac{1}{\theta}$ $\tau \in (0,1)$	No closed form
Frank	No restriction on degree of correlation, radially symmetric, very strong central dependency, very weak tail dependency	$\theta \in (-\infty,\infty)$	$1-\frac{4}{\theta}[1-D_F(\theta)]$ $\tau \in (-1,1)$	$1-\frac{12}{\theta}(D_1\|\theta)-D_2(\theta)$ $\rho_S \in [-1,1]$
Clayton	Suitable for only positive dependence structure, radially asymmetric, strong left tail dependence, weak right tail dependence	$\theta \in (0,\infty)$	$\frac{\theta}{\theta+2}$ $\tau \in (0,1)$	Complicated expression $\rho_S \in (-1,1)$
A-M-H	Both positive and negative dependence can be analyzed; not appropriate for very large or very small Kendall's τ, radially asymmetric, strong dependence in the lower tails	$\theta \in [-1,1]$	$\frac{3\theta-2}{3\theta}$ $-\frac{2(1-\theta)^2}{3\theta^2}\ln(1-\theta)$ $\tau \in (-0.182, 0.333)$	$[[12(1+\theta)di\{\ln\}(1-\theta)$ $-24(1-\theta)\ln(1-\theta)]/\theta^2]$ $-\frac{3(\theta+12)}{\theta}$ $\rho_S \in [-0.271, 0.478]$
Joe	Account for only positive dependence, weak left tail dependence, strong right tail dependence	$\theta \in [1,\infty)$	$1+\frac{4}{\theta}D_J(\theta)$ $\tau \in [0,1)$	No simple form $\rho_S \in [0,1)$

$Note$: $D_F(\theta)=\frac{k}{\theta^k}\int_0^\theta \frac{t^k}{\exp(t)-1}dt,\ k=1,2;$ $di\{\ln\}(x)=\int_1^x \frac{\ln t}{1-t}dt$ is the Debye function

Another widely used method for estimating the dependence parameter resorts to the approach based on rank correlation. This approach utilizes the relationship between the dependence parameter θ and the two rank-based estimators Kendall's τ and Spearman's ρ_S. In

particular, for every parametric copula family, there exists a one-to-one correspondence between Kendall's τ and copula parameter (see Table 4.6) and solving the functional relationship between τ and copula parameter provides an estimate of the parameter. Although inversion of Spearman's rho is another alternative, literature has underlined the better performance of Kendall's τ than Spearman's ρ_S (Kojadinovic and Yan, 2010). Considering the popularity of inversion of Kendall's tau, mainly because of its explicit form and ease in computing parameters, this approach is used in the current study for parameter estimation of bivariate copulas.

4.2.2. Bivariate modelling of time headways for mixed traffic scenario

This section concentrates on integrating centerline separation in time-headway modelling for the staggered-following scenario of different interacting leader-follower vehicle pairs mostly prevalent in mixed traffic environments. For the identification of an interacting pair of vehicles in staggered-following scenario, the extent of influence of the leader on the following vehicle was ascertained by longitudinal gap, relative speed, time headway and centerline separation. The following vehicles with centerline separation lower than 2m, time headways less than 4s (Wasielewski, 1979; Michael et al., 2000) and longitudinal gap within 20m distance (Siddique, 2013) are assumed to interact with the vehicles in-front. Moreover, a maximum relative speed difference of 1.5m/s (5.4km/h) between the leading and the following vehicles was considered (Sayer et al., 2003; Zhang and Bham, 2007) to represent steady-state conditions.

Based on the methodology described above, the derived trajectory data resulted into a total of 3128 vehicle headways of different vehicle pairs. A summary of the descriptive statistical measures including asymmetry, peakedness and dispersion of TH and CS for all combination of interacting vehicles is presented in Table 4.7.

Table 4.7. Summary statistics of the microscopic traffic variables

Leader-Follower	Sample size	TH (s)					CS (m)				
		Mean	SD	Median	Skew	Kurt	Mean	SD	Median	Skew	Kurt
MTW-MTW	52	0.55	0.16	0.56	0.17	-0.52	0.82	0.56	0.81	0.34	-1.07
3W-3W	95	0.58	0.53	0.41	2.92	9.08	0.63	0.49	0.49	0.87	-0.34
Car-Car	1969	0.96	0.48	0.85	2.50	8.71	0.76	0.53	0.66	0.53	-0.76
LCV-LCV	42	1.09	0.26	1.09	0.04	-0.68	0.64	0.46	0.54	0.99	1.06
Truck-Truck	66	2.30	0.81	2.13	0.39	-0.64	0.57	0.45	0.47	1.23	1.08
MTW-Car	144	0.59	0.37	0.47	3.69	22.28	0.81	0.54	0.76	0.38	-0.88
Car-MTW	96	0.81	0.44	0.67	2.35	6.46	0.75	0.44	0.64	0.57	-0.20
3W-Car	125	0.58	0.17	0.55	1.09	2.23	1.08	0.56	1.08	0.02	-1.08
Car-3W	39	0.92	0.54	0.79	1.77	2.43	0.93	0.56	0.92	0.04	-1.09
LCV-Car	165	1.02	0.46	0.87	1.18	0.98	0.84	0.51	0.76	0.28	-0.97
Car-LCV	61	1.08	0.45	1.03	1.39	2.67	0.76	0.51	0.74	0.42	-0.92
Truck-Car	192	1.35	0.64	1.14	1.79	3.40	0.79	0.52	0.76	0.51	-0.63
Car-Truck	82	1.56	0.60	1.45	1.04	1.11	0.81	0.55	0.74	0.34	-1.07

Note: **SD**- Standard deviation, **Skew**- Skewness, **Kurt**- Kurtosis, MTW, 3W and LCV representing motorized two-wheeler, motorized three-wheeler and light commercial vehicle respectively.

The measures of central tendency presented in Table 4.7 of the microscopic variables that is, TH and CS show that THs are characterized by a wide range of mean headways varying from a minimum of 0.55s for MTW-MTW to a maximum of 2.30s for truck-truck. A large positive skewness of TH and CS indicates longer or fatter tail on the right side of the probability density function than that on the left side whereas a skewness near zero indicates a symmetric distribution. Skewness values of TH and CS indicate that the CS data are more symmetrically distributed than that of THs; a comparison of the mean and median values further corroborates this result. Positive kurtosis value of TH and CS indicates that the distribution has heavier tail and sharper peak than that of normal distribution. Most of the CS data are characterized by negative kurtosis values indicating that the tails of the distribution are lighter and have a flatter peak than a normal distribution. This information on the central tendency measures does not only provide a clear insight on the characteristics of the underlying data, but also forms the basis in the selection of suitable marginal statistical models. Clearly, the variations in the statistical properties of THs and CSs for different leader-follower vehicle pairs signify differences in the behavioural properties of a wide variety of vehicles, a detailed understanding and modelling of which requires further investigation.

4.2.2.1. Dependence between TH and CS for different vehicle pairs

To suitably elucidate the dependence relationship between the longitudinal and lateral descriptors, two rank-based dependence measures- Kendall's τ and Spearman's ρ_S are examined for different combinations of leader-follower pairs. The corresponding rank correlation coefficients between TH and CS are presented in Table 4.8.

Table 4.8. Correlation coefficients of TH and CS

Leader-Follower	Kendall's tau, τ	Spearman's rho, ρ_S
MTW-MTW	-0.079	-0.115
3W-3W	-0.225	-0.335
Car-Car	-0.238	-0.351
LCV_LCV	-0.059	-0.077
Truck-truck	-0.009	-0.021
MTW-Car	-0.094	-0.136
Car-MTW	-0.173	-0.250
3W-car	-0.135	-0.187
Car-3W	-0.487	-0.672
LCV-Car	-0.312	-0.441
Car-LCV	-0.274	-0.399
Truck-Car	-0.212	-0.339
Car-Truck	-0.061	-0.091

The correlation coefficients reveal negative dependence relationship between time headway and centerline separation for all leader-follower vehicle pairs. The underlying reason is that at large CS, the following vehicles encounter a wide forward view, little encumbrance of the lead vehicle, more opportunities to shift laterally and can anticipate lead vehicle's behaviour as a result of which followers maintain lower longitudinal gaps with the leaders, thereby resulting

in lower time headways. The field of view of the following vehicle is however, dependent on the size of the vehicle in-front. For instance, the behaviour of a car while following an MTW in-front will be different from that with truck as the leading vehicle. This is because the visual field offered by the leaders at different lateral positions of the interacting vehicle-pair governs the following headways or, in other words the extent of lateral separation between the interacting vehicles affects the headways maintained by the following vehicles. A detailed analysis of vehicle-type specific headway characteristics with the inclusion of lateral indicator will indeed provide a wider perspective in understanding the behavioural phenomena of different vehicles while interacting with the leading vehicles of different static and operational characteristics.

Kendall's τ values for all leader-follower combinations are observed to cover a wide spectrum lying in between -0.009 to -0.487, indicating inverse dependent relationships between TH and CS. Kendall's tau and Spearman's rho values for truck-truck indicate that TH and CS have negligible effect on each other because trucks due to their large dimensions and poor operating capabilities, often tend to follow the leading trucks and do not exhibit high lateral movement hence CS does not affect the following headways of trucks. On the contrary, because of small sizes and high intuitive steering method of motorized two-wheelers (MTW), they seldom follow other MTWs hence the headways maintained by them are also independent of the off-centeredness between the interacting vehicles (Kendall's τ for MTW-MTW is -0.079).

While considering the case of car-involved vehicle pairs, an intriguing feature observed is the dramatic increase in correlation values when the following vehicles interact with the vehicles in-front that are of larger dimensions than that of the subject vehicle. More concisely, Kendall's tau for car-3W is -0.487 which is comparatively higher than that of 3W-car (τ=-0.135). In a similar manner, the correlation values of car-MTW, car-3W, LCV-car and truck-car are observed to be quite higher than that of MTW-car, 3W-car, car-LCV and car-truck respectively. These findings can be attributed to the fact that when followers interact with leading vehicles of bigger sizes, they look for possible opportunities to avoid the encumbrance of the vehicles in-front and also to get a clear forward field of view so that they can initiate lateral shifts to perform the desired manoeuvre. For such vehicle-pair interactions, time headways maintained by the followers depend to a large extent on the lateral positions of the vehicles, justifying larger correlation values for such interacting pairs. Conversely, followers interacting with the vehicles in-front of relatively smaller sizes can easily perceive forward visual field even at lower CS, hence the effect of CS on THs is not that much prominent as found for other vehicle-pairs.

4.2.2.2. Selection of the best fitted univariate marginal models for TH and CS

The estimation of a suitable copula model requires proper selection of optimal marginal statistical models. The maximum likelihood method is used to estimate the parameters of the probability distribution models while the validity of each distribution is assessed based on log-likelihood, Akaike Information Criteria (AIC) and several goodness-of-fit tests (K-S, A-D, CvM). Based on the goodness-of-fit criterion, the best fitted model is chosen as the one for

which the test statistic values are the lowest, log-likelihood value is the largest and the corresponding AIC is the lowest. Table 4.9 presents the performance of the selected univariate marginal models for both TH and CS corresponding to car-car interactions.

Table 4.9. Comparison of performance measures for various TH distribution models for car-car

Traffic variables	Fitted marginal distributions	Log-likelihood	AIC	RMSE	Goodness-of-fit test statistic		
					K-S	CvM	A-D
TH	**Lognormal**	**-667.98**	**1341.97**	**0.028**	**0.017**	**0.078**	**0.748**
	Log-logistic	-693.07	1390.14	0.035	0.037	0.732	4.600
	Burr	-736.54	1477.08	0.040	0.061	2.026	12.625
	Weibull	-1078.01	2160.01	0.042	0.125	12.63	77.103
	GEV	-689.41	1384.82	0.033	0.027	0.364	4.077
CS	Lognormal	-1542.93	3089.86	0.021	0.106	7.606	47.518
	Gamma	-1262.40	2528.80	0.010	0.053	1.886	12.931
	Weibull	**-1228.76**	**2461.53**	**0.007**	**0.046**	**1.059**	**8.921**
	Beta	-1236.24	2476.48	0.009	0.049	1.296	9.686
	Normal	-1423.92	2851.84	0.018	0.087	6.140	39.215

***Note*:** Bold features indicate the best fitted theoretical probability distribution model.

Based on the goodness-of-fit test statistic indices, minimum AIC and large log-likelihood criterion, lognormal and Weibull distributions were selected as the best fitted ones for TH and CS data respectively. The same distributions also provided a good fit to the observed data for other leader-follower vehicle pairs, although with varying model parameter values. The results of goodness-of-fit tests for TH and CS data of all leader-follower vehicle pairs corresponding to lognormal and Weibull distributions are demonstrated in Table 4.10.

Table 4.10. Results of goodness-of-fit tests for different vehicle pairs

Leader-Follower	Time headway (LN*)				Centreline separation (WL**)			
	K-S	CvM	A-D	RMSE	K-S	CvM	A-D	RMSE
MTW-MTW	0.058	0.065	0.460	0.035	0.069	0.059	0.477	0.011
3W-3W	0.074	0.042	0.288	0.048	0.101	0.111	0.724	0.013
LCV-LCV	0.064	0.034	0.278	0.013	0.098	0.067	0.454	0.016
Truck-truck	0.088	0.084	0.528	0.019	0.071	0.058	0.382	0.011
MTW-Car	0.067	0.089	0.545	0.030	0.081	0.143	1.130	0.009
Car-MTW	0.047	0.034	0.254	0.022	0.067	0.062	0.406	0.014
3W-car	0.053	0.038	0.293	0.046	0.081	0.128	1.063	0.015
Car-3W	0.092	0.047	0.336	0.025	0.162	0.173	1.017	0.017
LCV-Car	0.058	0.088	0.687	0.011	0.095	0.189	1.382	0.011
Car-LCV	0.069	0.063	0.393	0.027	0.098	0.109	0.658	0.014
Truck-Car	0.041	0.051	0.427	0.014	0.093	0.301	2.097	0.010
Car-Truck	0.054	0.028	0.233	0.018	0.071	0.077	0.496	0.011

Note: * LN- Lognormal, **WL-Weibull

In all the cases, RMSE values were observed to be lower than 0.048, indicating a good fit to the observed data. The K-S, CvM and A-D statistical tests also failed to reject the goodness-of-fit hypothesis ($\alpha = 0.05$); test-statistic values were lower than the critical values for all. It

can thus be envisaged from Table 4.10 that lognormal and Weibull distributions provide satisfactory fitting performance to vehicle headway and CS data respectively for all vehicle pairs and are hence employed for development of copula models.

4.2.2.3. Estimation of bivariate copula models for TH and CS data

The construction of a 2D model for 2D variables (TH, CS) requires good assessment of suitable bivariate copula functions in comparison with their observations. Considering the negative dependent relationships between the 2D variables, four copula functions featuring a wide range of negative dependence were considered in this study representing Gaussian, FGM, AMH and Frank copulas. The dependence domain of the rank-based correlation measures for all the considered copula functions can be validated from Table 4.6. Considering one-to-one correspondence between the copula parameter and correlation measures, the inversion of tau's method was used for parameter estimation of the copula functions. The estimated parameter and performance measures of the copula functions in terms of log-likelihood and AIC values for different combinations of leader-follower vehicle pairs are presented in Table 4.11.

Table 4.11. Estimated parameter θ and their corresponding LL and AIC values for different copulas

Leader-Follower	Goodness of fit	Gaussian	FGM	AMH	Frank
MTW-MTW	θ	-0.124	-0.356	-0.390	1.064
	LL(AIC)	-179.79(361.59)	-174.19(350.39)	-174.09(350.18)	**-173.76(349.52)**
3W-3W	θ	-0.346	NA	NA	-2.112
	LL(AIC)	-42.47(86.94)			**-39.61(81.21)**
Car-Car	θ	-0.365	NA	NA	-2.246
	LL(AIC)	-8889.67(17781.34)			**-7707.78(15417.56)**
LCV-LCV	θ	-0.092	-0.266	-0.278	-0.532
	LL(AIC)	-696.28(1394.56)	-688.15(1378.30)	-689.70(1381.40)	**-688.13(1378.26)**
Truck-Truck	θ	-0.014	-0.041	-0.038	-0.081
	LL(AIC)	-826.30(1650.60)	-825.22(1648.44)	-825.14(1648.28)	**-824.05(1646.10)**
MTW-Car	θ	-0.147	-0.423	-0.474	-0.085
	LL(AIC)	-214.09(430.18)	-215.28(432.56)	-215.56(433.12)	**-213.93(429.86)**
Car-MTW	θ	-0.268	-0.779	-0.948	-1.596
	LL(AIC)	**-228.31(458.62)**	-235.32(472.64)	-237.69(477.38)	-239.65(481.30)
3W-Car	θ	-0.210	-0.607	-0.701	-1.233
	LL(AIC)	-739.26(1480.52)	-696.21(1394.42)	-695.03(1392.06)	**-692.90(1387.80)**
Car-3W	θ	-0.692	NA	NA	-5.505
	LL(AIC)	**-99.06(200.12)**			-138.15(278.30)
LCV-Car	θ	-0.471	NA	NA	-3.055
	LL(AIC)	-890.54(1783.08)			**-697.07(1396.14)**
Car-LCV	θ	-0.417	NA	NA	-2.629
	LL(AIC)	-450.56(903.12)			**-395.94(793.88)**
Truck-Car	θ	-0.327	-0.954	NA	-1.981
	LL(AIC)	-549.93(1101.86)	-493.21(988.42)		**-484.85(971.70)**
Car-Truck	θ	-0.095	-0.274	-0.295	-0.551
	LL(AIC)	-1754.48(3510.96)	-1724.27(3442.54)	-1722.48(3442.96)	**-1719.79(3441.58)**

Note-NA means parameter θ for the respective copula is not applicable because FGM and AMH copulas can model the correlation for only $\tau \epsilon [-0.22, 0.22]$ and $\tau \epsilon (-0.182, 0.333)$ respectively.

The similar criterion of large log likelihood and minimal AIC values were adopted to identify the best fitted copula model. Based on the dependence domains of the copula models, different copula functions were fitted for each leader-follower combination. From Table 4.11 it can be observed that the Frank copula showed the highest log-likelihood values and the lowest AIC values for almost all vehicle pairs, only exceptions are with Car-MTW and Car-3W where Gaussian copula is observed to provide a good fit to the observed data. On the basis of performance measures of the copula functions, it is thus decided that Frank copula and Gaussian copula with lognormal and Weibull distributions with different dependence parameters should be further investigated to examine the correlation of bivariate variables for different vehicle pair combinations.

4.2.2.3.1. Bivariate distributions for similar leader-follower vehicle pair

A visual assessment of the best fitted bivariate copula model in space (TH, CS, PDF) provides more insights into the integrated dependence structure of the measured traffic variables with respect to diverse vehicle type combinations. Figure 4.8 shows the best fitted 2D (TH, CS) distributions for same leader-follower vehicle pairs.

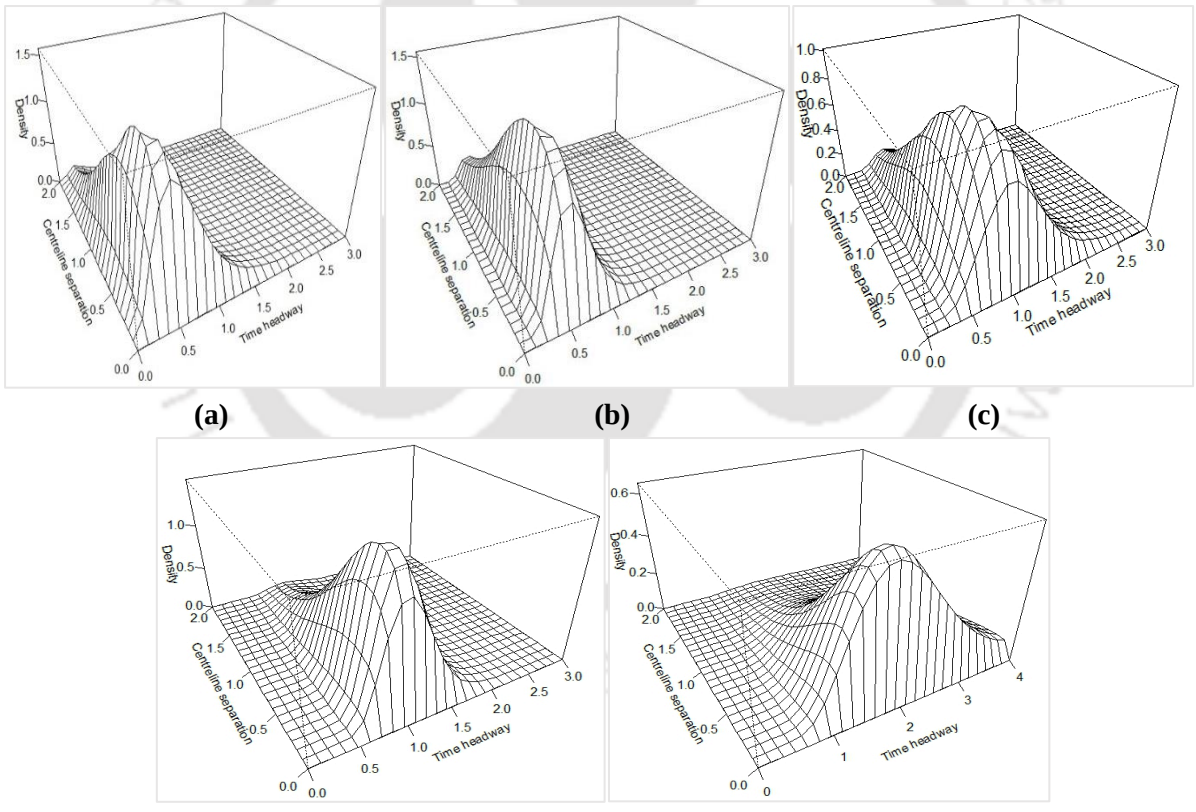

Figure 4.8 Fitted bivariate TH-CS distributions for **(a)** MTW-MTW, **(b)** 3W-3W, **(c)** car-car, **(d)** LCV-LCV and **(e)** truck-truck

The fitted TH-CS bivariate distributions clearly depict a reciprocal dependent relationship of 2D variables for each vehicle pair. Corresponding to 0.1m CS, the mode of the TH distribution is found to increase from 0.5s, 0.625s, 1s, 1.125s to 2s for MTW-MTW, 3W-3W, car-car, LCV-LCV and truck-truck pairs respectively. The gradual increase in the headway

values for a particular centerline separation can be related to the dimensions and operational capabilities of the interacting vehicles. This is because bigger-sized vehicles in-front usually have poor manoeuvring capabilities and they impose physical and psychological constraints to the followers; obscuring the forward view of the following vehicles, restricting them to look beyond the leading vehicles as a result of which the following vehicles maintain larger separation resulting in large headway values. On the contrary, small-sized vehicles boost confidence to the followers in maintaining a closer separation with them. Certainly, as the dimensions of the interacting vehicles increase, the drivers of the following vehicles perceive increased risks due to physical and psychological effects and therefore they prefer to maintain large separation or headways with the leaders at a particular centerline separation.

Moreover, the figure depicts a gradual rightward shift in the bivariate plots with the increasing dimensions of the interacting vehicles. In essence, the modes of the 2D plots for MTW-MTW, 3W-3W, car-car, LCV-LCV and truck-truck are observed at (0.375s, 0.5m), (0.5s, 0.5m), (0.875s, 0.5m), (1s, 0.3m) and (2s, 0.2m) respectively. The modal values reveal an interesting characteristic-although a majority of riders maintain larger headways with bigger dimensions of the interacting vehicles, the corresponding CS values indicate that most of the truck drivers maintain 0.2m CS with the leading trucks while 0.5m CS is mostly preferred when MTWs, 3Ws and cars interact with each other. Because of bigger dimensions and poor manoeuvring capabilities of trucks, they prefer to follow the leading trucks with lower CSs, without making large lateral shifts. This justifies the interpretation that the type of interacting vehicles, their static and dynamic characteristics influence the following behaviour of different vehicles in maintaining headways with certain extent of off-centeredness between them.

4.2.2.3.2. Fitted distributions for the same combination of vehicle pair

To further attain additional insights into the differences in vehicle headways for the same vehicle pair when the leading vehicle interchanges (for example the difference in headways for 3W-car and car-3W), the bivariate distributions are constructed for four different combinations of leader-follower pairs. Particularly, the interactions between MTWs and cars, 3Ws and cars, LCVs and cars, and trucks and cars are considered, the bivariate plots of which are presented in Figure 4.9.

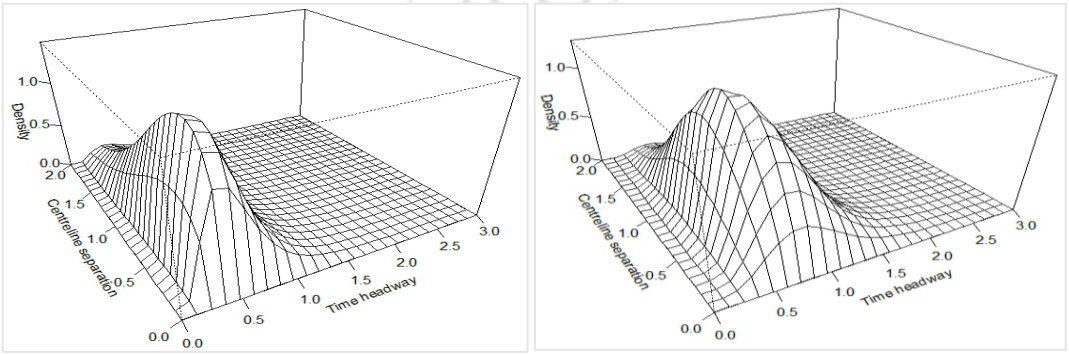

(a) **(b)**

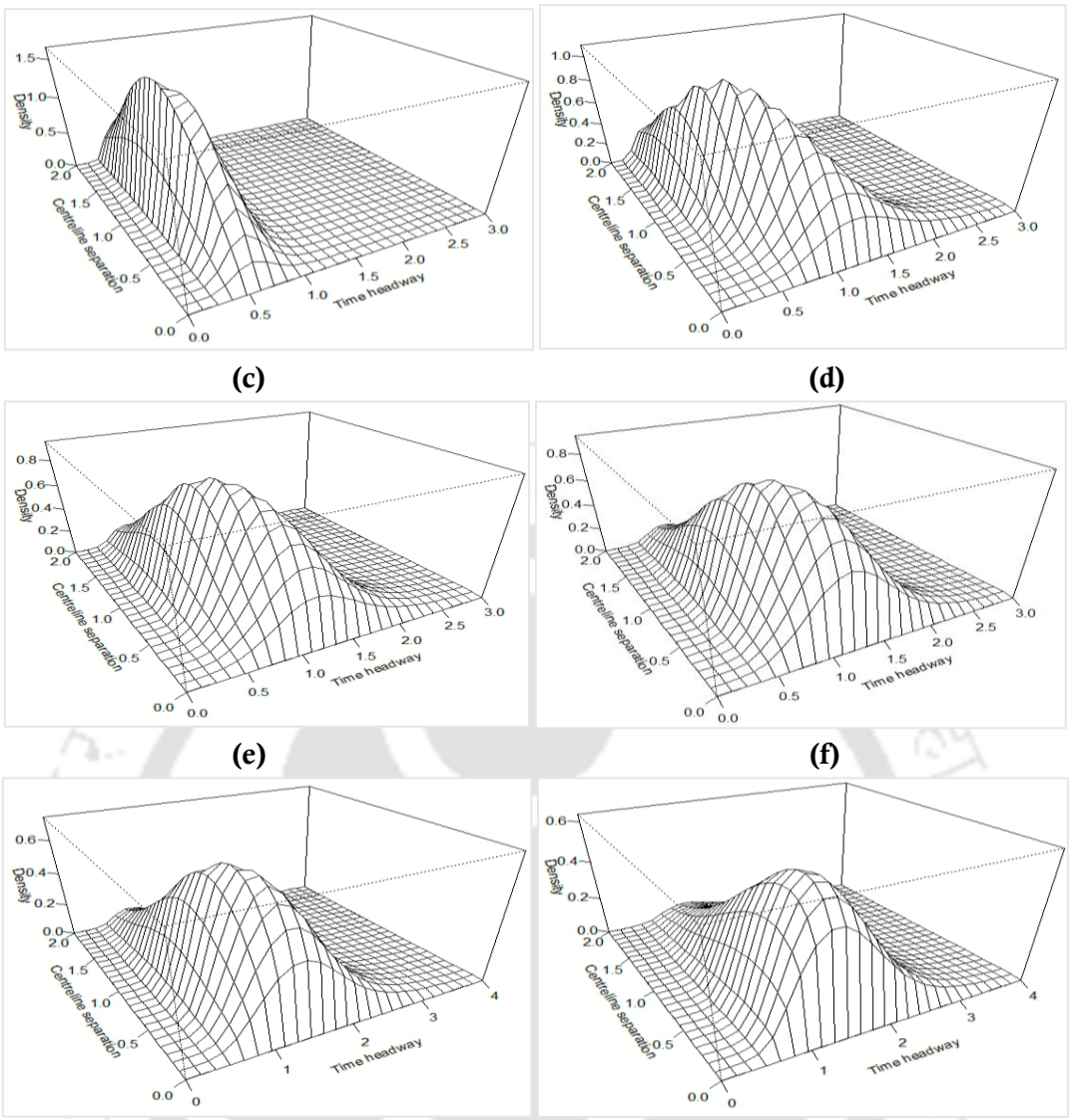

Figure 4.9 Bivariate distributions fitted for **(a)** MTW-car, **(b)** Car-MTW, **(c)** 3W-car, **(d)** Car-3W, **(e)** LCV-car, **(f)** car-LCV, **(g)** truck-car and **(h)** car-truck

The bivariate TH-CS distribution patterns exhibited in Figure 4.9 show that a significant number of drivers driving vehicles of better operating characteristics maintain lower headways with the lead vehicles. Considering the interactions of 3W-car and car-3W, the bivariate plots can be observed to be shifted more towards right when 3W follow the cars in-front. Moreover, the modes of TH distributions corresponding to 0.1m CS are observed to be 0.6s and 1.2s for 3W-car and car-3W interactions respectively. The increase in headways for car-3W case can be explained in two ways-while bigger dimensions of leading vehicles (say, car in this case) impose psychological impacts and obstruct the clear field of view of the followers, this increase in headway can also be related to the fact that 3Ws have poor operating characteristics than cars, which restrict them from attaining higher speeds even when the available gaps are large. Therefore, 3Ws as following vehicles maintain larger separation with the leading cars, thereby resulting in larger time headways.

Also it is to be noted that the peaks of TH-CS distributions for different vehicle pair occur at (0.4s, 0.4m), (0.6s, 0.8m), (0.5s, 1.2m), (0.7s, 0.8m), (0.825s, 0.8m), (1s, 0.625m), (1.125s, 0.625m) and (1.75s, 0.25m) for MTW-car, car-MTW, 3W-car, car-3W, LCV-car, car-LCV, truck-car and car-truck pairs respectively. The increase in peaks of TH distributions for the same combination of vehicle pairs further justify that the operating characteristics of following vehicles significantly affect the following headways while interacting with other leading vehicles. The modal values further imply that a majority of vehicles having poor dynamic characteristics maintain lesser extent of off-centeredness with the leaders. Cars can attain higher speeds and have high manoeuvring capabilities than 3Ws, LCVs and trucks; hence they can proceed at higher speeds with the availability of suitable longitudinal gaps and can make significant lateral shifts to avoid the encumbrance of the vehicles in-front, therefore they maintain lower headways and large CS with the lead vehicles. Trucks on the other hand have poor dynamic characteristics hence they progress at relatively lower speeds maintaining larger headways and lesser extent of off-centeredness with the leaders.

Enough empirical evidence has therefore been made to justify the interpretation that although the dimensions of the leading vehicles play a significant role in the selection of following headways and centerline separation, the operational capabilities of the following vehicles also affect the headway values and their (followers) preferences in maintaining certain amount of off-centeredness with the leading vehicles.

4.2.2.3.3. Conditional probability distributions using bivariate copulas

The conditional probability distributions for different combinations of the microscopic variables can be described via bivariate copula functions:

$$\mathbb{P}(TH \leq th|CS \leq cs) = \frac{C(v_1, v_2)}{v_2}$$

$$\mathbb{P}(TH \leq th|CS > cs) = \frac{v_1 - C(v_1, v_2)}{1 - v_2}$$

$$\mathbb{P}(TH \leq th|CS = cs) = \frac{\partial C(v_1, v_2)}{\partial v_2} \quad (2)$$

where $v_1 = F_1(x_{th}), v_2 = F_2(x_{cs})$; th and cs represent time headway and centreline separation respectively. The non-exceedance conditional probabilities of time headways given centerline separation exceeding/non-exceeding certain thresholds are presented in Table 4.12.

From the table, it is found that the conditional probability of TH increases with increasing vehicle headway thresholds and with the conditional factor (CS) increasing. For example, the probability for TH $\leq$ 1s in car-following state (CS $\leq$ 0.25m) for car-car is 0.3695 whereas for staggered car-following conditions with CS>1m, the conditional probability is 0.4715. The increase in conditional probabilities for large CS is also observed for other vehicle types. Because riders of the following vehicles encounter a wide forward field of view and less hindrance of the lead vehicle at large CS (CS>1m), there is an increased probability that they will maintain lower headways with the leaders whereas at CS $\leq$ 0.25m, the front leaders affect

the following behaviour of the lag vehicles as a result of which, the followers maintain large longitudinal separation and there is higher probability that vehicles will maintain larger time headways.

Table 4.12. Conditional probabilities of TH and CS

Leader-Follower	TH<1s		TH<2s	
	CS ≤ 0.25m	CS>1m	CS ≤ 0.25m	CS>1m
MTW-MTW	0.8255	0.9263	0.9857	0.9972
3W-3W	0.9409	0.9654	0.9996	0.9998
Car-Car	0.3695	0.4715	0.9932	0.9955
LCV-LCV	0.4075	0.7939	0.9536	0.9914
Truck-truck	0.0194	0.0206	0.4174	0.4328
MTW-car	0.9082	0.9135	0.9968	0.9971
Car-MTW	0.6317	0.8619	0.9819	0.9951
3W-Car	0.9553	0.9809	0.9998	0.9999
Car-3W	0.2082	0.9359	0.8769	0.9975
LCV-Car	0.2631	0.7894	0.9086	0.9904
Car-LCV	0.2508	0.7192	0.9105	0.9873
Truck-Car	0.2743	0.3279	0.8759	0.9011
Car-Truck	0.1553	0.1651	0.7978	0.8093

The conditional probability for TH ≤ 1s and CS ≤ 0.25m is found to be the highest for 3W-car and the least for truck-truck, meaning that there is a high chance of maintaining vehicle headways lower than the threshold value for cars interacting with the leading 3Ws while there is a very rare chance that THs will be lesser than 1s for trucks because trucks usually maintain larger headways which can also be observed from Figure 4.8(e). As discussed in subsection 4.1.3.4, the 1s- time headway threshold is considered as the most preferred headway for steady-state condition in rush-hour traffic (Ayres et al., 2001). Moreover, 2s-rule for minimum safe distance following is more pronounced in Netherlands, Germany and Sweden and is also recommended as safe time headway requirement for car-following in driving manuals of lane-based traffic. But the conditional probability values demonstrate considerable higher percentage of vehicles maintaining headways lower than 1s and 2s; although the probabilities vary with the type of interacting vehicles. These derived conditional probabilities illustrate that the TH thresholds defined for lane-based traffic vary with the type of interacting vehicles (even when the CS is lower) and also with different staggered positioning of the vehicles. Different thresholds values therefore need to be developed to evaluate the safe headway maintaining criteria of different vehicles in non-lane-based traffic environments.

Concisely, the bivariate joint distributions and the conditional non-exceedance probabilities of time headways and centerline separations for different vehicle pairs revealed an interesting finding- TH and CS are found to vary across different leader-follower vehicle pairs and they depend inherently on the operating characteristics of following vehicles and dimensions of the interacting vehicles. This finding clearly justifies the need to consider centerline separation in time-headway modelling and to develop bivariate vehicle-type specific behavioural models for a better representation of driving behaviour in disordered traffic environments.

4.3. Evaluation of safety in the staggered-following scenario

Close-following behaviour of vehicles is generally considered very risky and contributes to a high percentage of rear-end collisions. For example, in the US it accounts for approximately 32% of all crashes and 6% of fatal crashes (Traffic Safety Facts, 2013), in Japan it contributes to about 35% of all crashes (Watanabe and Ito, 2007), in China it is about 16% of all crashes (Duan et al., 2013) while in Germany rear-end crashes accounted for about 22% of all crashes (German Federal Statistical Office, 2009). According to MoRTH (2017), nearly 16.7% of all road traffic accidents are caused by rear-end collisions in Indian scenario. It accounted for 15.2% fatalities and 17.7% total injuries, clearly depicting the severity of risks associated with the drivers involved in road traffic accidents Rear-end collisions are usually attributed to insufficient headway, late brake response and insufficient brake force (Van Winsum and Heino, 1996). A thorough investigation of how drivers perceive associated risks in the following scenario and respond to a collision imminent situation is therefore required which can substantially improve the safety aspects of the drivers, design and performance of autonomous vehicle systems such as adaptive cruise control systems (ACC), safe traffic operations and in Intelligent Transportation Systems applications. In an attempt to provide a wider perspective in understanding the rear-end collision risks in disordered traffic environments, this section provides a copula-based methodological framework that will facilitate the application of temporal proximity measure for safety evaluation in vehicle-following events for different leading vehicle types. More specifically, the interactions of car drivers with the leading motorized two-wheelers (MTWs), motorized three-wheelers (3Ws), cars, light commercial vehicles (LCVs) and trucks are only considered in this work.

4.3.1. Working of adaptive cruise control systems in evaluating safety

Since decades, advanced driver assistance system (ADAS) has been a burgeoning topic within safety research. ADAS is designed to assist drivers during the primary driving task with an aim to improve safety, reduce the risks of accidents, increase capacity, benefit to traffic oscillations and enhance overall comfort level of drivers. The ADAS 'inform and warn the driver, provide feedback on driver actions, increase comfort and reduce the workload by actively stabilizing or manoeuvring the car' (PREVENT, 2006). The most prominent example of ADAS is the ACC system that became available in Japan, Europe and USA (Dickie, 2010), mainly on high-end vehicles and even in the near future, it is supposed to be accessible on lower grade vehicles as well (Young, 2012).

An ACC system aims toward partial automation of the vehicle's longitudinal control and the alleviation of driver's workload in a more efficient manner (ISO, 2010), that can not only modulate the desired speed but also maintain a safe headway to a preceding vehicle conforming to the settings predefined by the users. The steering wheel buttons or lever switches allow drivers to select an automation level mode by setting the desired speed and headway in ACC-equipped systems. In response to the settings imposed by the user, when a vehicle is detected

in its trajectory ahead, the system automatically controls the speed to keep safe distance with the vehicle in-front.

In particular, an ACC integrated with collision warning/collision avoidance systems can significantly reduce the severity of rear-end collisions by alerting drivers of upcoming potential threats and imminent collisions. In extreme events, whenever the driver fails to react and a collision is assessed to be unavoidable, the system performs an autonomous action in an appropriate manner. As a matter of fact, a consistent theme emerging from the peer-reviewed literature on the design of driver assistance systems requires an accurate characterization of an appropriate warning threshold to essentially distinguish between safe and unsafe encounters.

4.3.2. Temporal surrogate safety measure

Recent literature has systematically underlined temporal surrogate safety measure as an appropriate indicator for evaluating rear-end collision risks since they amalgamate both spatial proximity and speed. On one hand, surrogate events evince the potential crash causality and the intrinsic mechanism with evident probabilistic theories; while on the other hand, these measures are contemplated as a proactive approach, which assess safety before crashes actually eventuate.

Amongst all the temporal safety indicators, time-to-collision (TTC) and time headway (TH) are more commonly used. Time-to-collision is defined as '*the time that remains until a collision between two vehicles would have occurred if the collision course and speed difference are maintained*' (Hydén, 1996). A minimum TTC value (TTC_{min}) is often used as an indicator to ascertain the criticality of an encounter. In essence, lower the TTC_{min}threshold, higher will be the severity of a collision. Another well-recognized safety indicator for traffic conflicts namely, time headway is also considered as a measure of potential danger that can represent the propensity of risks associated with riders in close-following processes. Howbeit, literature has underlined TTC as an appropriate measure of conflict severity as compared to time headway. Laureshyn et al. (2010) have emphasized on the evaluation of several measures of conflict severities in which they presumed that TH has a weaker association with accidents than TTC, since TH considers only the temporal proximities between the road users rather than their relative speeds. A previous study by Vogel (2003) has related TTC with TH and demonstrated that TH could be considered as a potential safety measure criterion whilst TTC should be used to estimate the severity of a conflict situation because a small value of TTC_{min} (say, ≈ 0) represents actual danger in which a crash will occur. In particular, time-to-collision (TTC) has been widely considered as a potential parameter in defining warning threshold of an ACC/collision avoidance system (Li et al., 2017; Van der Horst and Hogema, 1993; Han et al., 2014; Hosseini et al., 2016) and in different traffic situations as well (Farah et al., 2009; Qu et al., 2014a, 2014b; Meng and Qu, 2012; Jin et al., 2011a) due to its simplicity and reliability. Considering the widespread acceptance of TTC indicator for evaluating rear-end collision risks, the applicability of TTC measure to describe the safety aspect of drivers in the staggered-following events of non-lane-based traffic environments is investigated in the following sections.

4.3.2.1. Concept of time-to-collision

In order to assess rear-end collision risks, many effective temporal proximity indexes were proposed, one of which was time-to-collision that has now been widely accepted as a beneficial and valid safety indicator for traffic conflicts (Farah et al., 2009; Vogel, 2003). The TTC indicator can be used to estimate the collision risk between two individual vehicles on the scale of seconds or even sub-seconds (Li et al., 2017).

The TTC notion denotes the time taken by the front end of the following vehicle to reach the rear end of the leading vehicle if both the vehicles proceed at their present speeds and on the same path, which can be determined as:

$$\mathrm{TTC_i(t)} = \begin{cases} \dfrac{x_{i-1}(t) - x_i(t) - l_{i-1}}{v_i(t) - v_{i-1}(t)}, & \text{if } v_i(t) > v_{i-1}(t) \\ \infty, & \text{if } v_i(t) \le v_{i-1}(t) \end{cases} \qquad (1)$$

Where $\mathrm{TTC_i(t)}$ denotes the TTC value of the following vehicle i at a time instant t, x and v denote the positions and velocities of the vehicles respectively, and l_{i-1} representing the length of the leading vehicle. The smaller TTC value indicates the higher risk of collision at a certain time instant.

4.3.2.2. Critical values of time-to-collision

To evaluate the risks associated with the vehicle-following processes, a threshold of time-to-collision should be determined which can discern unsafe vehicle-following events from the safe ones. Defining a standard TTC threshold has emerged as a contentious issue for evaluating collision risks. Table 4.13 presents a summary of minimum TTC thresholds recommended by many researchers for lane-based traffic scenario.

Table 4.13. Summary of TTC thresholds used by different researchers

TTC_{min} threshold (s)	Comments	Reference
5.0	Urban areas	Maretzke and Jacob (1992)
3.5	Non-supported drivers	Hogema and Janssen (1996)
3.0	Adequate	Van der Horst and Godthelp (1989); Svensson (1992); Minderhoud and Bovy (2001); Jin et al. (2011); Meng and Qu (2012); Qu et al. (2014a)
2.6	Safety concern	Hogema and Janssen (1996)
1.6-2	Low risk	Sayed et al. (1994)
1-1.5	Moderate risk	Sayed et al. (1994)
1.5	Desirable	Van der Horst (1990)
	Critical	Van der Horst (1990); Kraay and van der Horst (1985); Van der Horst and Hogema (1993); Sayed et al. (1994)
1.0	Critical	Hayward (1972); Van der Horst (1992)
0-0.9	High risk	Sayed et al. (1994)

A synthesis of previous work demonstrated different thresholds within the range of 0.90-5s, which have been propounded for varying traffic and driving scenarios. Generally, TTC values lower than the reaction time of drivers are considered unsafe. Maretzke and Jacob (1992) proposed a critical cut-off value of 5s for urban areas, while other researchers suggested a TTC-criterion of 4s for activating a collision avoidance system (Van der Horst and Hogema, 1993; Hirst and Graham, 1997) and for ascertaining the crash risk of a vehicle. Hirst and Graham (1997) and Brown et al. (2001) reported a TTC threshold of 3s for developing rear-end collision avoidance systems. Hirst and Graham (1997) indicated that a 4 or 5s TTC warning criterion resulted in too false alarms while a 3s criterion produced the least number of alarms even in some critical situations. In a later paper, Bella and Russo (2011) suggested the TTC thresholds of 2.5s and 3s to distinguish unsafe car-following manoeuvres. Besides, other researchers also recommended a critical threshold of 3s (Qu et al., 2014b; Meng and Qu, 2012; Jin et al., 2011; Van der Horst and Godthelp, 1989; Minderhoud and Bovy, 2001). A previous study conducted by Hogema and Janssen (1996) at the approach of a queue found the minimum values as 3.5s and 2.6s for non-supported and supported drivers respectively, where 2.6s TTC value was regarded as a safety concern. Several researchers have documented even lower critical values of TTC: 1s TTC threshold being considered as the critical conflict severity (Van der Horst, 1990); a TTC of 1.5s is considered as desirable (Van der Horst, 1990) while other studies suggested that encounters with TTC lower than 1.5s are critical (Van der Horst and Hogema, 1993; Van der Horst, 1990; Sayed et al., 1994; Kraay and Van der Horst, 1985).

A concoction of the peer-reviewed literature appears that the conflicts and the levels of severity depend to a large extent on the threshold value, where no definite clear-cut standard value has been established to distinguish conflicts and normal events. As indicated in the peer-reviewed literature, a TTC criterion of 3s has been recommended for developing rear-end collision avoidance systems (Hirst and Graham, 1997; Charly and Mathew, 2017), distinguish unsafe car-following manoeuvres (Bella and Russo, 2011) and for identifying the exposure to traffic conflicts (Qu et al., 2014b; Meng and Qu, 2012; Jin et al., 2011; Van der Horst and Godthelp, 1989; Minderhoud and Bovy, 2001). In accordance with the TTC values suggested by several researchers, a threshold of 3s is hence employed in this research work to investigate the joint crash-risk probabilities of drivers in vehicle-following cases of non-lane-based traffic environments.

4.3.2.2. Applicability of the warning threshold in staggered-following events

For the traffic safety assessment in car-following scenario, previous studies have proposed different methodologies (Jin et al., 2011; Jin et al., 2013), simulated environments (Van der Horst and Hogema, 1993; Qu et al., 2014a; Meng and Qu, 2012; Jin et al., 2011) and microsimulation software (Zhao and Lee, 2017) in order to validate the surrogate safety measures. Conversely, similar methodologies may not be suitable to define critical thresholds in disordered traffic environments, where vehicles often evaluate the opportunities to perform a lateral movement while making longitudinal progression, due to the differences in vehicle dimensions, performance capabilities and sporadic driver behaviour. Figure 4.10 depicts the following scenario of a vehicle *i* in lane-based and disorderly traffic environments.

As importantly, vehicles in lane-based traffic can even be observed to follow the leading vehicles with certain lateral separation between the leaders. In a research conducted by Gunay (2003), vehicles in lane-based driving discipline traffic were observed to maintain a mean distance of 1.78m from the left edge of the lane, with 0.34m standard deviation- a finding which can be contemplated as a threshold criterion for classifying a lane-based and non-lane-based car-following events. More specifically, CS≤0.34m can be assumed as a replication of actual car-following events while 0.34m<CS<3m can be considered as a typical staggered-following scenario of non-lane-based traffic environments.

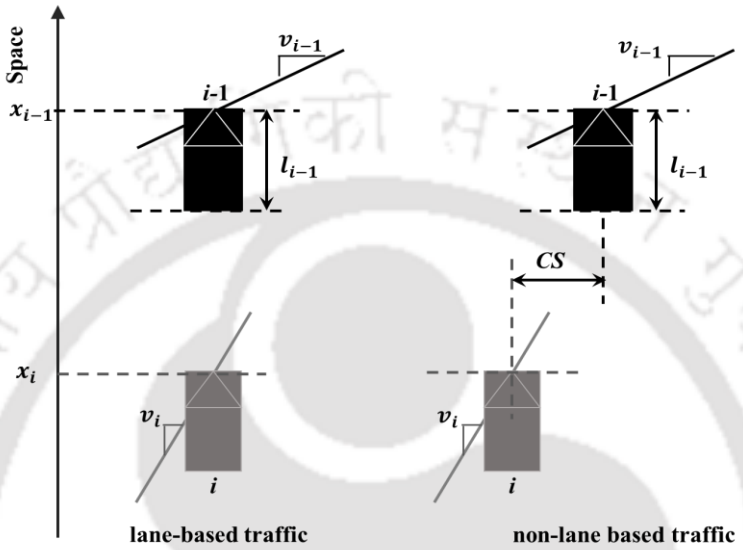

Figure 4.10 Prospect of rear-end collision occurrence in lane-based and non-lane-based traffic environments at a time t.

For the purpose of the analysis, any case of free-following conditions or other events with positive relative speed (leaders are faster) were excluded from the analysis. In addition, the following vehicles with centerline separation lower than 3m and longitudinal gap within 20m distance are assumed to interact with the vehicles in-front. However, considering the compact sizes of MTWs, the criteria of CS lower than 2.5m was employed to define the interaction between cars and motorized two-wheelers.

While TTC can be considered as a longitudinal descriptor of traffic, the lateral interaction can be well-described by centerline separation. Understanding that the utilization of TTC indicator in weak-lane discipline traffic requires an integration of the longitudinal and lateral descriptor, a copula-based methodology is utilized in this work to investigate the rear-end collision risks associated with the drivers in staggered-following scenario.

4.3.3. Development of bivariate copula models considering TTC and CS

This section describes the copula based methodological framework used for defining TTC thresholds in the staggered-following scenario for different vehicle-pair combinations. The following steps are involved in the development of copula models:

1) *Statistical analysis of TTC and CS according to lead vehicle type*- The first step entails investigation of the randomness or probabilistic properties of TTC and CS (for example: mean, median, standard deviation, skewness and kurtosis) that assist the selection of appropriate univariate marginal models. This analysis is useful in understanding the behavioural differences and the rear-end collision risks associated with the drivers according to lead vehicle type.

2) *Determination of dependence structure between TTC and CS*- To suitably explicate the dependence relationship between the random variables, two non-parametric rank-based dependence measures namely Kendall's τ and Spearman's ρ_S are considered.

3) *Models of probabilistic properties of TTC and CS for each lead-lag vehicle pair*- Five univariate probability distributions namely Burr, log-logistic, Weibull, Generalised Extreme Value (Chen, 2016) and lognormal were assumed to describe time-to-collision data whereas for the CS data, five mathematical models- lognormal, logistic, Weibull, gamma and normal- were considered. The best-fitted probabilistic distribution function was selected as the one for which the K-S, CvM and A-D test statistics and AIC criterion were minimal, failing to reject the null hypothesis at a nominal significance level of 5% (α=0.05).

4) *Selection of suitable bivariate copula models based on goodness-of-fit criteria*- Considering the negative degree of association between the 2D variables (TTC and CS), four copula functions namely Gaussian, Farlie-Gumbel-Morgenstern (FGM), Frank and Ali-Mikhail-Haq (AHM), rendering a wide range of negative pairwise dependence were considered in this study. The inversion of Kendall's tau method was used to estimate parameters of each copula model and the best fitted copula model is identified based on large log-likelihood and minimum AIC values.

4.3.3.1. Statistical analysis of TTC and CS according to lead vehicle type

The derived trajectory dataset resulted in 242 cases of MTW-car, 341 cases of 3W-car, 2801 cases of car-car, 289 cases of LCV-car and 401 cases of truck-car following events which would essentially elucidate the characteristics of the proximal safety indicator in non-lane-based traffic conditions. The descriptive statistics of the traffic variables (TTC and CS) including asymmetry, dispersion and peakedness for the processed data are summarized in Table 4.14. It is evident from the table that TTCs are specified by a wide spectrum of mean values ranging from 3.44s for MTW-Car to a maximum of 5.91s for truck-car. Because bigger sized vehicles impose physical and psychological effects on the subject vehicle, car drivers usually tend to maintain a longer longitudinal spacing with trucks than MTWs, hence the TTC values follow a decreasing trend from truck-car, LCV-car, car-car, 3W-Car to MTW-Car. Therefore, the results indicate that the risks associated with the car drivers are dependent on the type of lead vehicle ahead.

Table 4.14. Summary statistics of TTC and CS for different combinations of leader-follower pairs

	Time-to-Collision (s)					Centerline separation (m)				
	MTW-Car	3W-Car	Car-Car	LCV-Car	Truck-Car	MTW-Car	3W-Car	Car-Car	LCV-Car	Truck-Car
Mean	3.44	5.27	5.62	5.70	5.91	1.17	1.19	1.02	1.12	1.13
Median	2.91	3.79	4.07	4.27	4.36	1.11	1.14	0.85	1.04	1.02
Std. dev	2.40	4.60	4.56	5.03	6.26	0.75	0.71	0.76	0.74	0.77
Skew[a]	1.55	1.16	1.12	1.53	2.09	0.48	0.20	0.69	0.45	0.40
Kurt[b]	2.18	0.62	0.61	2.24	4.72	-0.52	-1.05	-0.46	-0.63	-0.83
Sample	242	341	2801	289	401	242	341	2801	289	401

[a]Skewness, [b]Kurtosis

The skewness and kurtosis values of TTC further indicate that the distributions have sharper peaks and heavier tails than that of a normal distribution; while lower positive skewness values of CS imply a more symmetrical distribution for CS data as compared to that of TTCs; minimal deviations in the mean and median values further substantiate this result. Kurtosis on the contrary, characterizes the outliers (or, heavy-tails) of a distribution. The negative kurtosis values for CS data signify a flat-peaked distribution with lighter tails than that of a normal distribution while positive kurtosis value for TTC data indicate a heavy-tailed distribution with sharper peak.

To provide additional insights into the statistical differences of TTCs according to lead vehicle type, a one-way analysis of variance test is conducted; the results of which indicated significant statistical difference among different vehicle pairs ($F_{(4,4074)} = 7.6 > F_{critical} = 2.60$, $p<0.001$). This finding justifies that the rear-end collision risks associated with car drivers varies by the type of vehicle in front.

Understanding that a precise characterization of the following processes of vehicles entails an integration of the longitudinal and lateral descriptors of vehicle interactions, the variation of TTCs with centerline separation for different leader-follower pair is further investigated in this section. The variations of time-to-collision for different level of centerline separations according to lead vehicle type are presented in Figure 4.11.

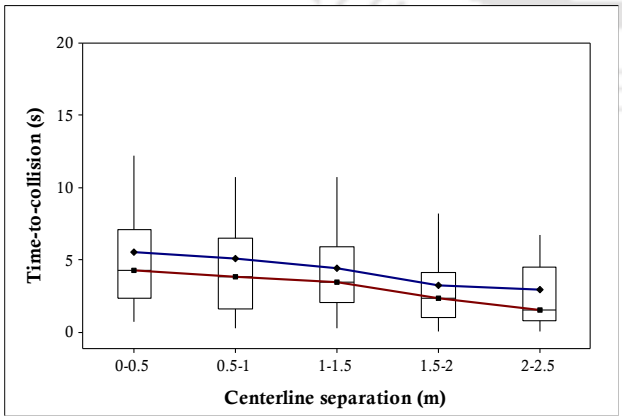

(a)

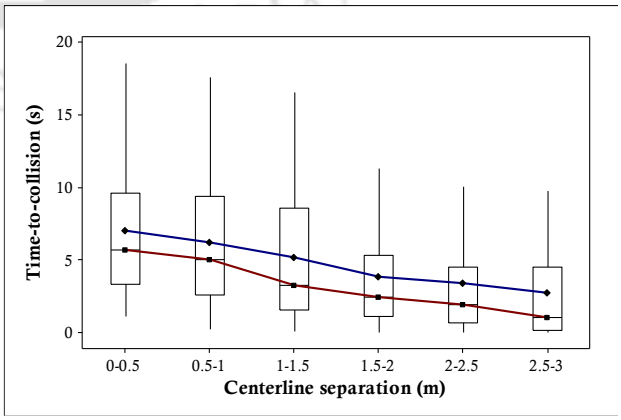

(b)

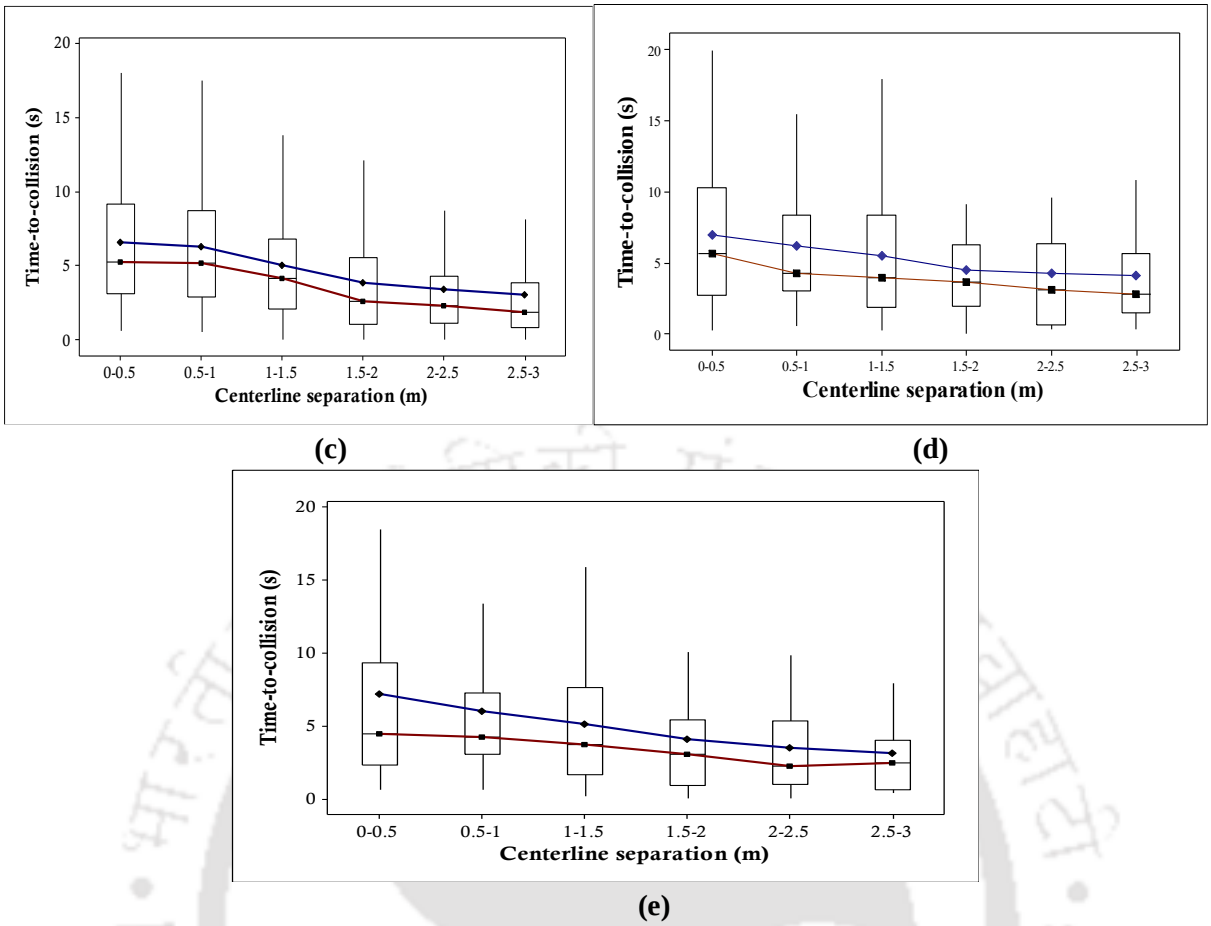

Note: Upper connecting line (blue line) and lower connecting line (red line) representing mean and median values respectively.

Figure 4.11 Plots of time-to-collision and centerline separation for **(a)** MTW-Car, **(b)** 3W-Car, **(c)** car-car and **(d)** LCV-car and **(e)** truck-car

The figure depicts that the mean and median values of time-to-collisions gradually decrease with the increase in CSs for all vehicle pairs. This observed trend is indicative of the fact that TTCs are dependent on the lateral positioning of vehicles in vehicle-following processes of disordered traffic streams. Because following vehicles at large CS, encounter a wide visual forward field of view and little encumbrance of the vehicles in-front, they tend to follow the leaders closely maintaining lower longitudinal spacing in staggered-following events and subsequently when they perceive increased risks, they can avoid the criticality of the situation by veering laterally beside the leader. The field of view is however dependent on the clear lateral separation between vehicles and the type of vehicle ahead.

Comparing the mean and median values at each CS range, TTC values can be observed to be increasing with the increase in the size of lead vehicle. This, indeed justifies the interpretation that the critical values of TTC suggested by different researchers for homogeneous and lane-based traffic cannot be directly applied for non-lane-based traffic environments as TTC depends to a large extent on the staggered positions of vehicles and type of lead vehicle in the latter. A small value of TTC represents a high-risk situation in car-following events but the same level of risk may not be perceived by drivers in staggered-following processes since in the latter, car drivers can maintain even smaller longitudinal gap at large centerline separation,

thereby having much lower TTC values.

As identified above, the risk level of drivers in staggered-following scenario varies by the type of front vehicle ahead and the lateral positioning of the vehicles. It therefore, justifies the need to propose a methodological framework that can address the bivariate relationship of proximal safety indicator with the lateral descriptor. This, in turn, will ascertain the propensity of crash risks at any lateral positioning of vehicle in vehicle-following scenario.

4.3.3.2. Determination of dependence structure between TTC and CS

The Kendall's τ and Spearman's ρ_S correlation coefficients computed between TTC and CS for different leader-follower vehicle pairs are found to be $\tau = -0.121, \rho_S = -0.183$; $\tau = -0.227, \rho_S = -0.333$; $\tau = -0.237, \rho_S = -0.347$; $\tau = -0.141, \rho_S = -0.214$ and $\tau = -0.151, \rho_S = -0.229$ for MTW-car, 3W-car, car-car, LCV-car and truck-car respectively. These values illustrate significant negative degree of association between time-to-collision and centerline separation. Kendall's tau and Spearman's rho values indicate that the rear-end collision risks show a weaker dependence relationship with CS when cars follow MTWs than the lead LCVs and trucks, 3Ws and cars. This difference is mainly attributed to the field of clear view available to the subject vehicle in the staggered-following events. Because of smaller widths and heights of MTWs, drivers in the following vehicles perceive the forward scenario more clearly which gives them more confidence about the anticipated actions of the lead vehicle. Conversely, for any CS (0-3m) LCVs and trucks obstruct the forward view of the following cars because of which car drivers maintain lower CS with the trucks, and no prominent dependent relationship was observed. On the other hand, car drivers tend to follow the leading 3Ws and cars (having moderate widths) closely in staggered-following events so as to have a broader front view, hence a moderate dependence relationship is observed for 3W-car and car-car.

4.3.3.3. Univariate models of TTC and CS for each combination of vehicle pair

Five statistical models-Burr, log-logistic, Weibull, Generalized Extreme Value and lognormal-are considered to select the best fitted univariate marginal probability distribution function for TTC whereas for the CS data, lognormal, logistic, Weibull, gamma and normal are considered. The best fitted distribution is selected as the one for which the K-S, CvM and A-D test statistics and AIC criterion are minimal, failing to reject the null hypothesis at a nominal significance level of 5% (α=0.05). Based on goodness-of-fit measures, log-likelihood and AIC criterion, lognormal and Weibull distributions were found to provide the best fits for TTC and CS respectively for different vehicle pair combinations. However, the estimated parameters of the lognormal and Weibull distributions were observed to vary according to lead vehicle type. The goodness-of-fit test results for the lognormal and Weibull distributions of TTC and CS data for all leader-follower vehicle pairs are presented in Table 4.15.

Table 4.15. Goodness-of-fit test results for different vehicle pairs

Variables	Leader-follower	Log-Likelihood	AIC	Goodness-of-fit measures		
				K-S	CvM	A-D
TTC (LN[a])	MTW-Car	-711.32	1426.62	0.084	0.470	3.007
	3W-Car	-1010.74	2025.48	0.089	0.926	6.126
	Car-Car	-1532.34	3070.67	0.021	0.047	0.349
	LCV-Car	-799.23	1602.47	0.068	0.266	1.971
	Truck-Car	-1117.31	2238.62	0.061	0.325	2.038
CS (WL[b])	MTW-Car	-286.51	577.22	0.056	0.218	1.489
	3W-Car	-435.04	874.08	0.095	0.632	4.341
	Car-Car	-716.30	1436.62	0.069	0.690	0.364
	LCV-Car	-302.72	609.44	0.072	0.215	1.464
	Truck-Car	-428.64	861.28	0.079	0.651	4.414

[a]Lognormal, [b]Weibull

In all the cases, estimated test statistics of the K-S, CvM and A-D tests were lower than the critical values, rendering the goodness-of-fit hypothesis unable to be rejected at α=0.05. Hence, lognormal and Weibull distributions were considered to be satisfactory for describing time-to-collision and CS data respectively for all vehicle-pair combinations and are therefore employed for bivariate distribution modelling using copula models.

4.3.3.4. Selection of bivariate copula functions based on goodness-of-fit measures

Constructing the bivariate relationship of the considered 2D variables (TTC, CS) requires prudent assessment of appropriate copula models. Considering the negative association between TTC and CS, four copula functions, namely Gaussian, FGM, AMH and Frank are considered in this study, and the inversion of Kendall's tau approach is utilized to estimate their corresponding parameters. The log-likelihood and AIC values of each copula model along with the estimated parameter are listed in Table 4.16.

Table 4.16. Goodness-of-fit test results of different copula models

Leader-follower	Estimated parameter & Goodness-of-fit	Gaussian	FGM	AMH	Frank
MTW-Car	θ	-0.188	-0.544	-0.623	-1.099
	LL	-996.57	-993.62	-993.83	-992.12
	AIC	1995.14	1989.24	1989.66	1986.24
3W-Car	θ	-0.348			-2.129
	LL	-1425.58	NA	NA	-1422.97
	AIC	2853.16			2847.94
Car-Car	θ	-0.364	-1.068		-2.240
	LL	-2217.78	-2220.36	NA	-2216.78
	AIC	4437.56	4442.72		4435.56
LCV-Car	θ	-0.221		-0.739	-1.296
	LL	-1098.81	NA	-1096.11	-1095.09
	AIC	2199.62		2194.22	2192.18
Truck-Car	θ	-0.235	-0.679	-0.803	-1.389
	LL	-1535.18	-1535.47	-1535.64	-1533.77
	AIC	3072.36	3072.94	3073.28	3069.54

The Frank copula exhibited the largest log-likelihood and the least AIC values for time-to-collision and centerline separation data for all vehicle pairs. Based on the performance measures of copula models presented in Table 4.16, it is thus adjudged that Frank copula model, with lognormal and Weibull distributions for TTC and CS respectively, should be further investigated to assess the collision risks in disordered traffic environments.

4.3.3.5. Evaluating rear-end collision risks from the developed copula model

This section is aimed to assess the applicability of the recommended TTC thresholds in staggered-following events of non-lane-based traffic environments. Firstly, this section discusses the crash-risk probabilities of drivers in vehicle-following scenario according to the lead vehicle type. Secondly, the variations in the minimum TTC thresholds across different centerline separations are investigated for different leader-follower pairs, and finally the prospect of crash-risk severities in staggered-following events is examined.

4.3.3.5.1. Associated crash-risks in vehicle-following events

Existing literature recommends different values of time-to-collision which could essentially distinguish safe and risky encounters, but those studies are mainly confined to lane-based homogeneous traffic streams. This subsection is aimed to attain a detailed understanding of the driver's prospect of having TTCs lower than the minimum recommended thresholds for actual vehicle-following events (that is, for lower CS values).

As discussed in the foregoing sections, CS≤0.34m can be assumed to replicate actual car-following events of lane-based traffic while 0.34m<CS<3m can be considered as a typical staggered car-following scenario of non-lane-based traffic environments. It can, therefore be contemplated that the recommended minimum TTC thresholds suggested by different researchers for lane-based traffic will be applicable to non-lane-based traffic environments only for lower values of lateral separations (CS≤0.34m). With an aim to apprehend the car drivers' probability of maintaining lower centerline separation (≤0.34m) with different leaders in non-lane-based traffic streams (for a minimum TTC threshold criteria), the conditional non-exceedance probabilities are estimated from the developed copula model using Equation 1.

$$\mathbb{P}(TTC \leq ttc | CS \leq cs) = \frac{C(v_1, v_2)}{v_2} \qquad (1)$$

Where $v_1 = F_1(x_{ttc}), v_2 = F_2(x_{cs})$ represent continuous univariate marginal distributions of TTC and CS; ttc and cs represent time-to-collision and centerline separation respectively, and C is the bivariate copula which captures dependence structure between the marginals TTC, CS. ttc is considered as 3s in this study.

As importantly, the conditional non-exceedance probabilities of drivers in actual vehicle-following events ($CS \leq 0.34\text{m}$) are initially estimated from the developed Frank copula model (with TTC<3s) for each vehicle-pair combination. These conditional probabilities corresponding to CS lower than 0.34m are obtained as 0.3913, 0.2871, 0.1992, 0.1649 and

0.1496 for MTW-Car, 3W-Car, car-car, LCV-car and truck-car respectively. It clearly implies that at lower CS (≤0.34m), the probability of car drivers maintaining lower than 3s-TTC threshold increases with decrease in the size of lead vehicle.

4.3.3.5.2. Defining TTC thresholds according to lead vehicle type

With an aim to entail a detailed characterization of time-to-collision thresholds, the conditional probabilities obtained for a 3s TTC threshold of actual vehicle-following events ($CS \leq 0.34$m, as discussed in Section 4.3.3.5.1) are further extended for different values of centerline separations. From the functional form of Equation 1, given a discrete non-exceedance probability value P and bivariate Frank copula model (with the estimated dependence parameter), the value ttc corresponding to any cs for the corresponding variables TTC and CS can be evaluated by solving the equation. In particular, for explicating the TTC thresholds according to lead vehicle type in staggered-following events (for different CS values), two cases are considered; (a) when a constant threshold of 3s is chosen for all vehicle pairs, and (b) when the same conditional probability of cars is chosen across all vehicle-pairs.

For the first case, a constant 3s-TTC threshold is considered across all leader-follower vehicle pairs. This constant TTC threshold corresponded to different vehicle-specific non-exceedance conditional probabilities (as already indicated in 4.3.3.5.1.). Corresponding to each vehicle-specific conditional probability (for 3s-TTC threshold and CS≤0.34m), the time-to-collision thresholds are further estimated for different values of centerline separations for all vehicle pairs as presented in Figure 4.12.

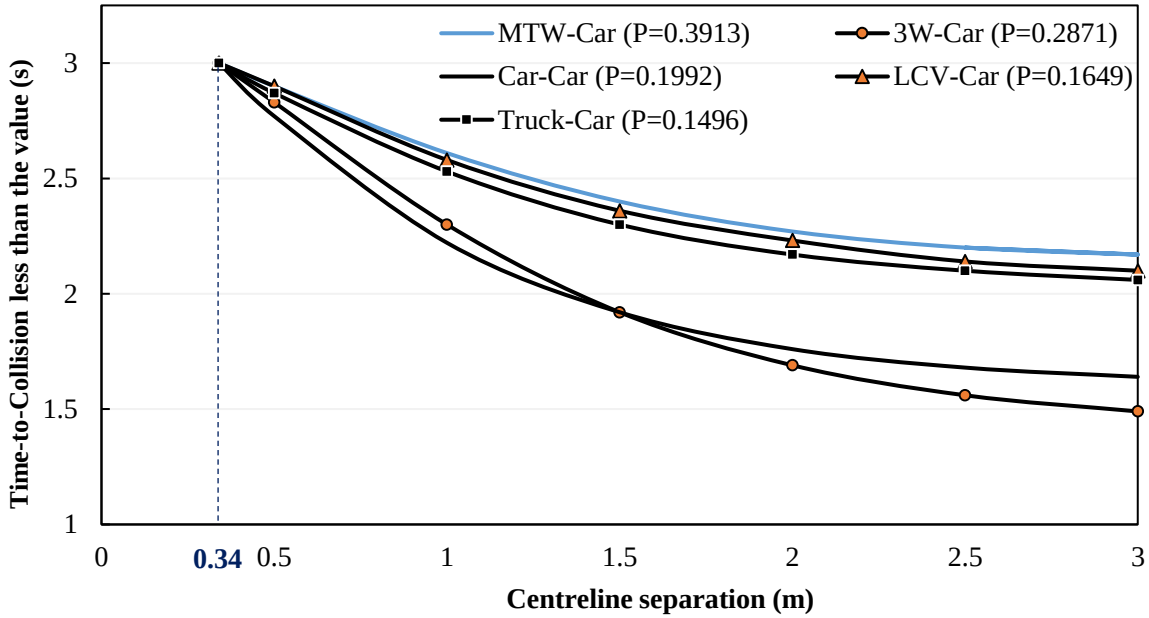

Figure 4.12 Estimation of minimum TTC thresholds at different CS values considering TTC as 3s for all the leader-follower pairs ($TTC \leq ttc | CS \leq cs$)

The contour plots signify a decreasing trend in TTCs with the increase in CS, which indeed manifests the driving behavioural pattern of a disordered traffic system as discussed in the foregoing sections. However, for a particular CS (say 2m), the TTC thresholds are observed to

be the highest for MTW-Car followed by LCV-car, truck-car, car-car and 3W-Car. But as identified previously, we expect the TTC thresholds to decrease from truck-car, LCV-car, car-car, 3W-Car to MTW-Car because car drivers usually tend to maintain larger spacing, thereby higher TTC values with the increase in lead vehicle size which eventually contradicts the obtained results. It is therefore evident that the consideration of a constant TTC threshold across all vehicle-pairs fails to represent the rear-end collision risks and the actual following behaviour of car drivers.

In an attempt to suitably elucidate the variations of TTC according to the type of lead vehicle, the conditional probability of $TTC \leq 3s$ for car-car pair is assumed to be consistent across all vehicle-pairs. Specifically, as the reported TTC thresholds are recommended for homogeneous traffic (mostly car-car case), the probability of $TTC \leq 3s$ for car-car interaction obtained in Section 4.3.3.5.1 is assumed to be constant irrespective of the lead vehicle type and the corresponding probability value is used to define the minimum TTC thresholds. Figure 4.13 represents the contour plots of minimum TTC thresholds across centerline separations according to the lead vehicle type considering equal probability as that of car-car.

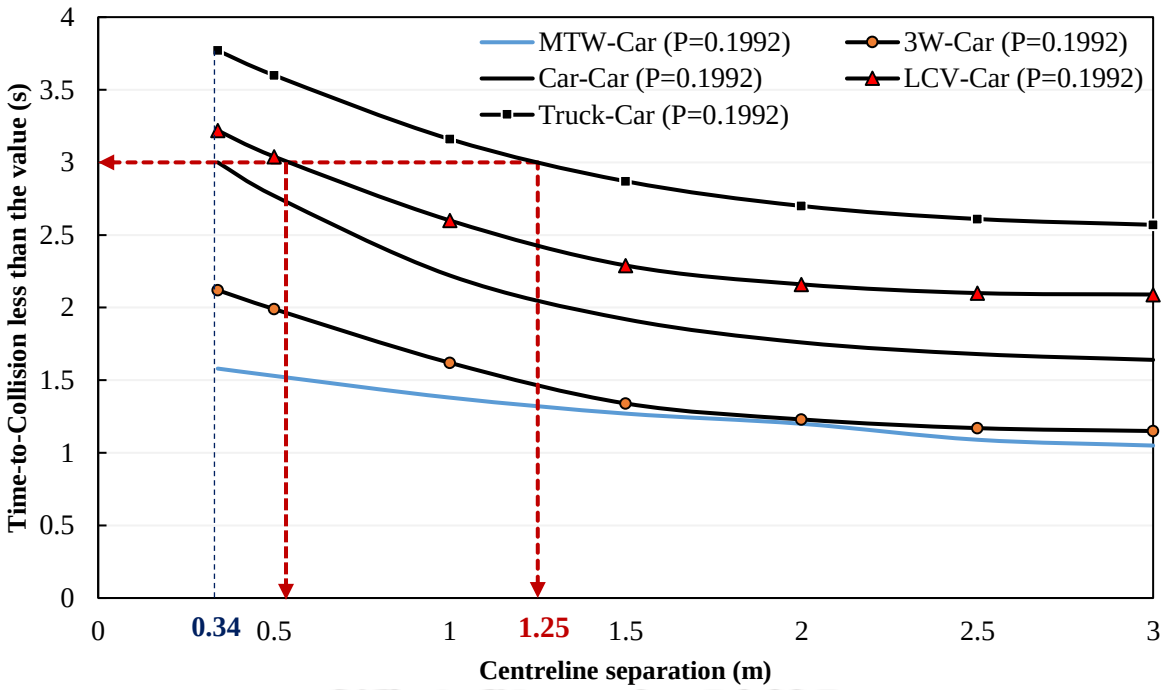

Figure 4.13 Estimation of minimum TTC thresholds at different CS values considering same probability (P=0.1992) for all the leader-follower pairs ($TTC \leq ttc|CS \leq cs$)

Considering 19.92% non-exceedance conditional probability value as constant across all vehicle pairs, the contour plots clearly demonstrate that at CS lower than 0.34m, time-to-collision values lie within a maximum threshold of 1.58-3.77s, the minimum and maximum values being observed for MTW-Car (TTC=1.58s) and truck-car (TTC=3.77s) respectively. The threshold range is further observed to follow a gradual decreasing pattern with the increase in CS, the minimum being obtained as 1.05-2.57s at CS=3m. As expected, the observed trend is indicative of the fact that TTCs decrease with increasing CS and decrease in size of the lead vehicle.

However, the severity of crash-risks evaluated for lane-based traffic appears to be somewhat different for non-lane-based traffic environments. For instance, the rear-end collision risk (TTC<3s) (Hirst and Graham, 1997; Brown et al., 2001) for car-following case may not represent the same level of risks in staggered-following case for car-car and even for other vehicle pairs. It can be envisaged from the figure that the rear-end collision risks associated with car drivers in actual car-following events (CS≤0.34m) are reflected by the same proportion of car-drivers when they follow LCVs and trucks at CS of 0.60m and 1.25m respectively. This observation further justifies that the 3s-TTC threshold does not remain consistent with CS as well as with the type of lead vehicle.

4.3.3.5.2. Safety enhancement with aid of variable TTC-thresholds

As identified in the peer-reviewed literature, the 3s-TTC threshold is often used as a warning criterion in collision avoidance systems (Hirst and Graham, 1997; Brown et al., 2009) and is considered as adequate for distinguishing dangerous encounters from safe ones (Hirst and Graham, 1997). Up to now, the research conducted did not yield concordant results regarding the assumption of a constant warning TTC-strategy in non-lane-based traffic environments. Contrary to previous studies, the current research however shows strong evidence that the rear-end collision risks vary with the lateral separation between the interacting vehicles and the type of vehicle ahead.

Compared to the TTC thresholds obtained in actual vehicle-following events (that is, TTC values corresponding to CS=0.34 from Figure 4.13), the results in Table 4.17 demonstrate that for each vehicle pair, the percentage reduction in TTC thresholds at different staggered positions of vehicles increase drastically with the increase in CS. This result is reasonable because at large CS, drivers usually have a wide visual field and can anticipate the behaviour of vehicles in-front with more confidence, therefore they tend to follow the leaders closely maintaining lower longitudinal gaps, thereby resulting in lower TTC values and higher percentage reduction in TTCs.

Table 4.17. Percentage decrease in TTCs with respect to the obtained minimum TTC values

Leader-follower	TTC (s) at CS=0.34m	Percentage reduction in TTC at different values of CS					
		0.5m	1m	1.5m	2m	2.5m	3m
MTW-Car	1.58	3.16	12.66	19.62	24.05	31.01	33.54
3W-Car	2.12	6.13	23.58	36.79	41.98	44.81	45.75
Car-Car	3.00	7.67	25.97	36	41.33	44	45.33
LCV-Car	3.22	5.59	19.25	28.88	32.92	34.78	35.09
Truck-Car	3.77	4.51	16.18	23.87	28.38	30.77	31.83

This outcome reveals that different TTC control threshold values should be considered in the ACC/CA system to reduce false warnings and enhance safety in staggered-following scenario. Based on the TTC values, CA systems can recognize the severity of an upcoming

hazard and provide real-time collision warning information to the drivers. Eventually, consideration of a constant TTC threshold across all CSs may generate frequent false alarms because the TTC thresholds are usually expected to decrease with the increase in lateral deviation between the vehicles. A system with a high false alarm rate can potentially annoy or distract the driver from real hazards and has often been proved to be a source of risk and irritation caused to the drivers (Lees and Lee, 2007). As highlighted by Baber (1994), false alarms often cause driver distractions, thereby diverting the operators away from the primary driving task. Although ACC/CA systems are already in the market since 1960s, the algorithms used in developing ACC/CA systems should consider the lateral descriptor of traffic in addition to the longitudinal dynamics to reduce high false alarm rates and enhance safety in vehicle-following events of such non-lane-based environments.

But there are some aspects which still requires elaboration. Based on this research work, the findings provide evidence of the variation in TTC thresholds according to the lead vehicle type. Interestingly, the percentage decrement in TTC thresholds for MTW-Car and 3W-Car with respect to 3s-TTC criteria (defined for cars) are obtained as 47.33% and 29.33% respectively while the TTC threshold increases by 7.33% and 25.67% when cars follow the lead LCVs and trucks respectively in actual vehicle-following events (CS≤0.34m). This corroborates that the rear-end collision risks associated with the car-drivers vary with the type of vehicle ahead. What is more critical is the imminent risk associated with the drivers when a constant warning criterion is chosen for cars following the leading trucks. Had a constant 3s-TTC threshold been considered for truck-car case, it would result in dangerous encounters if car drivers failed to avoid the criticality of the upcoming hazard by applying emergency braking. However, since driver assistance systems take over a part of the primary driving task by alleviating drivers' workload in a convenient manner, perfect ACC/CA systems would be required which minimizes drivers' intervention and warns the driver when a crash is imminent. This essentially necessitates the development of warning and intervention systems which can assist and support the drivers in detecting safety hazards or dangerous situations in disordered traffic systems.

The results from this study, henceforth, signify that the ACC/CA systems should incorporate different TTC-thresholds corresponding to the interacting lead vehicle type and the lateral deviation between the interacting vehicles, to evaluate and enhance traffic safety, rather than considering a constant TTC_{min} threshold across all centerline separations and lead vehicle types.

4.4. Chapter Summary

Up to now, the research conducted on modelling the staggered-following behaviour did not fully consider the lateral dimension of human driver behaviour. Besides, a series of works performed on the topic mainly involved partial consideration of lateral separation in car-following models (Gunay, 2007; Jin et al., 2010; Zheng et al., 2012) yet, little is known about the effect of the indicator in describing the integrated driving behaviour of non-lane-based traffic systems. This chapter has demonstrated that what has traditionally been thought to be a simple staggered-following process depends, in fact, to a large extent on the lateral descriptor

of traffic, making the lateral dimension an important concept that entails an in-depth exploration. The main contribution of this work therefore comes from its cognizance of considering the lateral separation of the interacting vehicles (centerline separation) in modelling the longitudinal descriptors of traffic- a proper consideration of which will augment the reliability of the existing models, safety enhancement of drivers and also help in detailed understanding and modelling of non-lane-based traffic streams.

Among all the longitudinal micro-level characteristics of traffic flow, time headway is considered as one of the most important parameters used to describe macroscopic traffic flow parameters (deterministic reciprocal relationship exists between flow rate and headway), microscopic car-following behaviour and also for generating vehicles in microsimulation software. To account for disorderly traffic environments, although the actual lane-based concept of time-headway has been modified by Dubey et al. (2012), the results of this work provided enough evidence that the lateral descriptor of traffic (that is, centerline separation) has a prominent significant effect on the driver's selection of following headways. Certainly, this lateral indicator should be integrated with time-headways to describe the staggered-following behaviour for a better predictability and reliability of the microsimulation models developed for such traffic systems. This facilitated the development of a copula-based methodological framework to essentially capture the integrated behavioural phenomena of drivers by accommodating both the longitudinal and lateral descriptors of traffic.

By considering driver's choice of time headways alongside a series of other explanatory variables, this chapter has further served to illustrate that the staggered car-following behaviour is far more complex than actually have been previously thought. The road width does not seem to significantly affect the choice of headways, although a decreasing trend in headways is observed with the increase in road width. The headway attributes of vehicles are found to be strongly associated with the interacting vehicle-pair characteristics, dimensions of the leading vehicles, operational capabilities of the following vehicles and also lateral positioning of interacting vehicles in the staggered-following scenario. As importantly, the proportion of drivers engaging in close car-following is found to be considerably higher than the safe-headway requirement recommended by different researchers and in driving manuals. While this would indicate higher exposure to increased risks, the relationship between close following time-headways and rear-end collision risks is indeed intuitively appealing. Close-following is considered as very risky contributing to higher percentage of rear-end collisions. For example, in India, it accounts for 16.7% of all road-traffic accidents (MoRTH, 2017). This entails a thorough investigation of how drivers perceive associated risks in the following scenario and respond to a collision imminent situation for enhancing safety in the staggered-following scenario of such traffic systems.

Recently, the temporal surrogate safety measure, time-to-collision has been considered as an appropriate indicator for evaluating rear-end collision risks as compared to time headway. In particular, TTC has emerged as an efficient variable to define operational criteria for collision-avoidance systems. Based on the minimum TTC thresholds recommended for lane-based traffic, this study corroborated a pragmatic decreasing relationship of TTC with increasing CS and decrease in lead vehicle size- a finding which indicates that the risk level of

drivers in staggered-following scenario varies by the type of front vehicle ahead and the lateral positioning of the vehicles. Specifically, the minimum TTC value recommended for lane-based traffic varies for non-lane-based traffic systems which indeed, leads to an over-prediction of the conflict-severities in staggered-following events. Eventually, the selection of a constant TTC threshold irrespective of all lead vehicle types was found to contradict the actual behavioural phenomena while the assumption of constant probability across all vehicle-pairs reflected the rear-end collision risks in accordance with the actual observations.

In congruence with the previous explanations, this work has therefore illustrated an important aspect in understanding the vehicle-following behaviour, by considering 'centerline separation' a salient lateral indicator to reliably and realistically model the driver behavioural phenomena. This chapter essentially provided a copula-based methodological framework to integrate the lateral and longitudinal descriptors of traffic, underlining the importance of centerline separation and characteristics of interacting vehicle types in modelling stochastic features of traffic flow phenomena, enhancing traffic safety and microsimulation model development.

5

Car-Following Model Development for Staggered-Following Scenario

The widespread adoption of traffic simulation models and advancement in intelligent transport systems have spurred a growing interest in traffic engineers and researchers to model the car-following behaviour. Car-following models were proposed to describe the interacting driver-vehicle units in a single lane, by obtaining a clearer understanding about how one driver follows her/his immediate preceding vehicle ahead in response to certain traffic environments/situations. Over the past decade, these models have systematically formed the cornerstone for microscopic simulation modelling, development of autonomous cruise control systems, intelligent transportation system applications, traffic safety evaluation and so forth.

Technological advances and the ever-increasing computing capabilities have led to the simulation of complex models in an effective yet efficient way, in terms of execution time and memory requirements. Recently, high-fidelity traffic data and availability of data-driven modelling approaches have enabled to stride over the modelling issues directly from a set of field data. More realism can therefore be embraced in the models with prior understanding of the actual driver behavioural phenomena. Although a plethora of literature has supported the development of a series of car-following models, there is currently a paucity of research concerning the applicability of the existing models to accurately represent staggered-following behaviour of non-lane-based traffic environments. What remains still unresolved and undocumented is the consideration of the lateral dimension in car-following model development and also the credibility of such models in describing the staggered-following behavioural phenomena. In particular, certain issues that have become increasingly apparent in the model development of staggered-following scenario mainly stem from the complexities in collecting and processing reliable time-series data, and inadequacy of the existing models in depicting the integrated 2D behavioural pattern of drivers. Indeed, proper estimation of dynamic time-series car-following data can ameliorate the realism of car-following models in the context of non-lane-based systems, which is still a demanding task requiring further exploration. By developing an integrated car-following model with due consideration of the lateral dimension, if such models are proved to outperform the existing models, it is believed that there would be a substantial improvement in the accuracy of traffic modelling, which in turn, would help in the development of smarter and user-friendly autonomous vehicles, and a more safer and efficient transportation system.

In light of this, this chapter aims to provide a methodological modelling framework to describe the 2D car-following behavioural phenomena of drivers during staggered-following conditions of disorderly traffic environments. Research findings from Chapter 4 illustrated that the following behaviour depends inherently on the lateral descriptor of vehicle interactions and interacting vehicle-type. However, it is the intent of the research work to develop a 2D model and compare its performance with the existing models; which can be done at its best, only for car-involved traffic. Considering such aspects, the objectives defined in this chapter mainly focus on car-following-car case. Knowing that the driver's control processes need to be accurately and realistically characterized in the model, a data-driven modelling approach is employed in this work, with its credibility being substantiated both in terms of real time-series testing dataset and from model stability point of view. To be more precise, this chapter is categorized into three sections as described below:

1. *Time-series data evaluation for understanding staggered car-following behaviour*: This section provides an overview of the car-following process in non-lane-based systems, followed by a detailed description of the processed time-series car-following data and nature of association between the microscopic traffic variables.

2. *Data-driven based single leader- single follower car following model:* A data-driven artificial neural network (ANN) based modelling approach is developed in this section in which the car-following task of drivers is elucidated. The structure of ANN model is first described, followed by estimation of reaction delay using different approaches. The credibility of the proposed model is then evaluated though a global sensitivity analysis and considering distinct features of car-following behaviour.

3. *Comparison of the proposed ANN-based model with existing models:* This section briefly describes the widely-used car-following models and estimation of the optimized parameter values. The performance of these existing models is then compared with the reference model (ANN model), confirming the suitability of the improved model in contributing to scientific research community.

5.1. Time-series data evaluation for understanding staggered car-following behaviour

The dynamic behavioural response of drivers in 'car-following processes' result in perturbations in traffic flow, thereby resulting in increased accident risks and reduction in capacity. Achieving a detailed understanding of such processes requires proper estimation and collection of reliable time-series dynamic data where drivers' responses in the control processes can be accurately and systematically measured over as long a period as desired. This section describes in particular, the car-following behaviour in disorderly traffic systems with a preliminary investigation of the statistical properties of the extracted data, obtained from the proposed image-based in-vehicle trajectory data collection system.

5.1.1. Car-following behaviour

The car-following behaviour is a control process in which each driver attempts to maintain a desired following distance behind the lead vehicle by accelerating or decelerating in response to the actions of the vehicle in-front. This continuous adjustment in vehicle speeds is governed by the drivers' perceptions of adjudging the leading vehicle speed as well as their own speeds, proximity to the desired following headway (or, longitudinal gap, LG) and response time delay which may overcompensate for small deviations from a target point (Braun et al., 1983; Schmidt, 1993), resulting in the following 'spirals' which can be expressed in the relative speed-relative spacing plane (Figure 5.1).

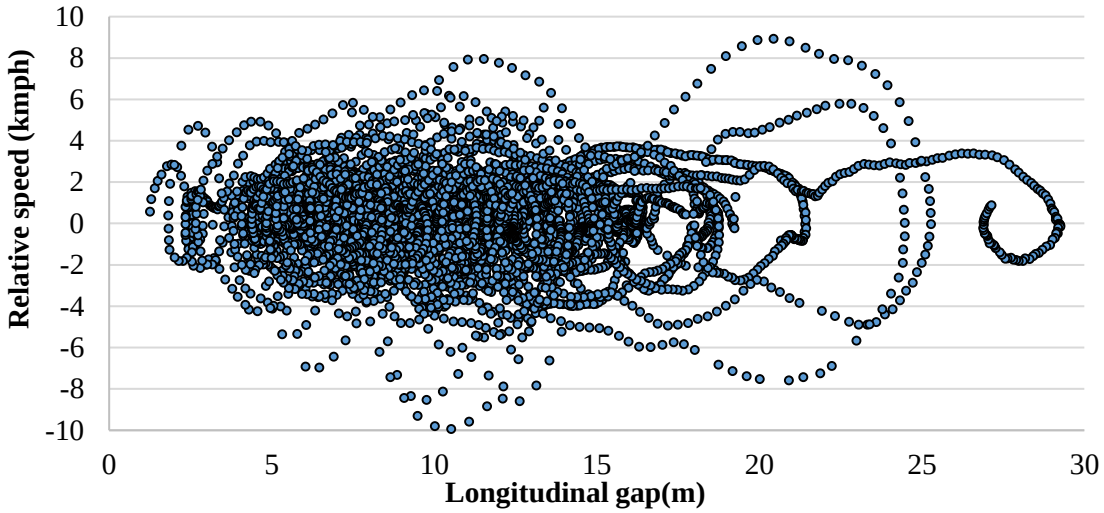

Figure 5.1. A typical car-following 'spiral' showing the variation of relative speed with longitudinal spacing

The observed range of longitudinal gap lying within 30m (*x*-axis of the spirals) justifies that the dataset covers an entire spectrum of a close-following behaviour (Zheng et al., 2012). The information on the behavioural processes of the following driver in response to the vehicle in-front is processed from the collected dynamic time-series data based on two criteria-

(a) Only those trajectories are considered that are likely to contain implicit information on the behavioural parameters pertaining to car-following regime. This indicates that data corresponding to only car-following interactions during the observation period, that is, relative speeds in between -10kmph and 10kmph and centerline separation within 2m are considered.

(b) As car-following models necessitate collection of continuous time-series interaction data over a period of time, those trajectory data are considered for which both the cars involved in the process can be observed jointly during a period of at least 15s, which usually own significant car-following characteristics (Zheng et al., 2015).

The spirals are indicative of the car-following processes of the driver across all speed ranges in staggered-following scenario and her/his perceptions in decision making, such as to maintain a safe desired headway. This behavioural phenomenon is more noticeable if the leading vehicle varies its speed; howbeit it is even apparent when the leading vehicle maintains a constant

speed. At large spacing, drivers cannot perceive relative speed precisely while at small spacing, there is a combination of relative speed and spacing in which the relative motion is so less that no response can be observed from the drivers at all. Nonetheless, the smaller the relative spacing is, the more perceptible the relative speed is. It therefore appears that the continuous adjustment in acceleration/deceleration responses of the drivers occurs when the actual spacing becomes smaller or larger than desired and drivers are unable to maintain that desired spacing. According to risk homeostasis theory (Wilde, 1982), the following drivers need to adjust their relative speeds in the car-following scenario to ensure an acceptable risk level. When the risk level is within the target risk level or desired safety margin, the driver may maintain a constant speed which can be adjudged as the steady car-following scenario. In conformity with the major findings of Chapter 4, it can also be speculated that the lateral indicator of vehicle interaction (namely, centerline separation) may provide a full understanding of the behavioural aspects of drivers in the following scenario of disordered systems- the consideration of which is anticipated to enrich the realism of car-following model development.

5.1.2. Car-following input parameters: selection and underlying variation

Early assumptions for car-following theories and models were rooted during 1958-1963. The essential issue was choosing the right input variables to model the stimuli that the following drivers respond to. After the core period, a number of prominent work enabled a sophisticated yet easy tracking of the historical betterment of each core model including aspects of driver heterogeneity (reaction time), spacing, speed, acceleration, time-headway, multiple vehicle interactions and notably, realism of the existing core models in replicating the car-following behaviour. Yet, the selection of input variables and behavioural process of drivers in car-following scenario of disordered systems still deserves broader examination, beyond the classical car-following framework. This section therefore provides a step-by-step procedure concerning preliminary investigation of the processed dynamic car-following data, selection of the input variables in car-following model development and behavioural adaptations of drivers in response to different considered variables.

The car-following data extracted to analyze how the immediate leading car's stimulus affects the following car's behaviour, resulted in a total of 9579 cases of car-following events (data being obtained at each 0.2s interval) for both the drivers during the entire observation period. As discussed in Section 5.1.1., for the purpose of analysis, the car-following condition is defined as a situation in which the driver follows the vehicle ahead with relative speeds between -10kmph and 10kmph, longitudinal gap and centerline separation lie within 30m and 2m respectively, ensuring that the vehicles interact with each other within the considered influence zone. The derived trajectory data contains information on speeds of interacting vehicles, acceleration/deceleration, longitudinal gap, centerline separation and relative speed between the interacting vehicles. A detailed description of the extracted trajectory data pertaining to the interaction regime is presented in Table 5.1.

.

Table 5.1. Basic statistical description of the extracted car-following data

Statistical measures	Speed (kmph)	LG (m)	CS (m)	Acceleration (m/s^2)	Deceleration (m/s^2)	Relative speed (kmph)
Range	[9.10,78.38]	[2.72,29.96]	[0,2]	[0,1.72]	[-3.19,0]	[-9.94,8.92]
Mean	47.60	12.16	1.08	0.45	-0.57	0.15
Median	45.10	11.61	1.21	0.37	-0.50	0.18
Std. dev.	10.15	4.31	0.59	0.25	0.34	1.93
5%ile	33.83	6.29	0.11	0.01	-0.81	-3.07
95%ile	65.59	19.90	1.94	0.81	-0.01	3.07
N*	9579	9579	9579	5250	4329	9579

Note: *Sample size

Statistics of the variables show that the car-following behaviour could be observed for a wide range of following vehicle's speeds lying in between 9kmph and 78kmph, with an average speed of 47kmph while only 5% speed data are below 34kmph. The acceleration and deceleration domains of the following vehicle observed in the data confirms that drivers are more sensitive to deceleration than acceleration as the maximum range of deceleration is much higher than that of acceleration, although the magnitudes of mean values are somewhat closer. More accelerations (N=5250) than decelerations (N=4329) occur overall as expected, considering real life acceleration/deceleration asymmetry (Ahmed, 1999). Although a maximum longitudinal gap of 30m suggests a close car-following behaviour, the lower bound of LG (2.72m) may not necessarily represent a high-risk situation because of the influence of lateral descriptor in the interaction process. In essence, the risk associated with the drivers in actual car-following scenario (CS=0m) corresponding to 3m LG may not represent the same level of risk at 2m centerline separation (as elaborated in detail in Section 4.3 of Chapter 4). The mean value of centerline separation is further observed as 1.08m which is comparatively higher than that mostly observed in car-following regime of lane-based scenario (<0.34m, Gunay, 2003); suggesting the staggered-following behaviour of cars, in which drivers are mostly observed to maintain certain amount of lateral separation with the leaders. On the other hand, the mean CS obtained in this study is similar to staggered-following scenario (1.08m versus 0.98cm) obtained in an Iranian study by Khansari et al. (2018).

Moving beyond preliminary statistical analysis of collected field data, the selection of input variables in a car-following model has mostly been conducted empirically based on sensible observation of underlying traffic phenomena. Yet, what remains still undocumented is proper judgement of input variables subjected to suitable theoretical statistical analysis. Clearly, modelling the staggered car-following behaviour requires consideration of both longitudinal and lateral descriptors of vehicle interactions, an in-depth statistical analysis of which will substantiate the selection of right input variables for a realistic representation of car-following process.

5.1.2.1 Factor analysis for selection of input car-following variables

Considering that no theoretical foundation is available in the literature related to the choice of input variables, a non-linear statistical method of factor analysis is investigated to extract useful information for understanding and modelling the staggered-following behaviour of disordered traffic systems. Most of the existing car-following models consider different aspects of driver heterogeneity, relative speed, relative spacing, acceleration and vehicle speeds, while the theoretical basis of the choice of lateral descriptor in model development has not yet been suitably validated. Utilizing factor analysis on the processed car-following data can provide a better understanding of the selection of considered input variables in the process of model development. In investigations in which a number of predictors are used, factor analysis is intended to reproduce suitable input variables that contain scientific parsimony or economy of description (Harman, 1976:4), with higher loaded information.

This section explores whether a list of considered variables reflect the car-following phenomena through exploratory factor analysis using principal components analysis and varimax rotation. The explanatory power of a factor can be conceptualized in terms of the factor's ability to explain the variance of a particular variable and accordingly, the total variance explained by a factor is termed as factor's eigenvalue. Factors with eigenvalues greater than or equal to one are considered as the interpretable ones. Several micro traffic variables that are commonly considered as inputs in the development of car-following models include relative speed, relative spacing (distance headway or longitudinal gap), vehicle speed and acceleration/deceleration characteristics of the interacting vehicles. Some researchers however argue that although relative speed and spacing are perceptible to the following drivers, they cannot apperceive relative acceleration between vehicles precisely. Consideration of relative acceleration as input in the model therefore proves to be ambiguous and unrealistic from driver behavioural modelling standpoint. The longitudinal descriptors (such as vehicle speeds, longitudinal separation between vehicles, relative speed) and lateral descriptors of traffic (such as centerline separation) are therefore considered for modelling car-following behaviour in disorderly traffic. Accordingly, all the five variables namely, speed of the following vehicle ($Speed_{FV}$), relative speed between the leading and the following vehicles (RS), acceleration of the following vehicle (acc_{FV}), longitudinal gap (LG) and centerline separation (CS) are utilized for exploratory factor analysis, the results being presented in Table 5.2.

Through the factor analysis, two factors (I and II) were retained satisfying the criterion of eigenvalue greater than one, which could collectively explain 63.5% of the total variance. Factor I accounts for 35% of the variance, amongst which speed of following vehicle, longitudinal gap and centerline separation showed high loading. For Factor II, which accounts for 28.5% of the variance, acceleration of the following vehicle and relative speed exhibited high loading. Rotation of factors reduce the factorial complexity of the variables so that each factor has a few high loadings while the rest approaches towards zero; without changing the overall amount of variance. The variables with a factor loading value greater than or equal to 0.5 obtained after rotation are represented in bold characters. These variables contain higher

information and contribute towards the explanatory power of each latent factor. Indeed, this justifies the importance of these variables in explaining the car-following phenomena of non-lane-based systems.

Table 5.2. Results of exploratory factor analysis

Variables	Factor structure matrix of principal component analysis					Factor structure matrix of first two factors rotated to Varimax criterion	
	Factor loadings						
	I	II	III	IV	V	I	II
$Speed_{FV}$	0.759	0.165	0.532	-0.138	0.309	**0.775**	0.052
RS	0.240	-0.806	0.112	-0.492	-0.193	0.119	**-0.833**
acc_{FV}	0.047	-0.851	-0.010	0.484	0.198	-0.079	**-0.849**
LG	0.617	0.014	-0.752	-0.159	0.169	**0.612**	-0.077
CS	-0.862	-0.116	-0.040	-0.346	0.350	**-0.869**	0.012
Eigenvalues	1.758	1.415	0.862	0.641	0.323	1.751	1.423
Total variance explained	0.352	0.283	0.172	0.128	0.065	0.350	0.285

Note: Bold values indicate higher information loaded

The rotated factor loadings reveal an interesting pattern: speed, longitudinal gap and CS are in general, commonly associated with drivers' intention/tendency to travel at a desired speed, maintain a desired longitudinal gap and off-centeredness based on the actions of the leading vehicle. There are certain assumptions in the existing car-following models which explain that follower drivers control their speeds to maintain a desired longitudinal gap with the vehicle ahead. But the lateral descriptor of vehicle interaction also exhibits a dependent relationship with following vehicle's speeds and available longitudinal gap. Even the results obtained in Section 4.1.2. indicate inter-dependencies among speed, LG and CS. To be more precise, these variables are attributed to drivers' perceptions or behavioural aspects towards maintaining a desired speed or spacing. On the contrary, the high loading variables in Factor 2 namely, acceleration and relative speed reflect the human sensory modalities because driver's control in accelerating/decelerating is based on her/his judgement of relative speed. This factor contributes more towards driver's judgement of relative speed and actions of the driver, which can be considered as a dynamic aspect. All the five variables including the response variable namely following vehicle's acceleration, longitudinal descriptors such as relative speed, longitudinal gap, speed, and lateral descriptor namely centerline separation, are therefore considered for understanding the staggered following behaviour of cars in non-lane based systems.

5.1.2.2. Adopted longitudinal gap and its variation

This section attempts to investigate the distance keeping behaviour of the drivers and its variations with followers' speeds as well as centerline separation between vehicles. In doing so, it is first necessary to divide the processed data according to centerline separation.

Accordingly, four CS ranges in steps of 0.5m were chosen such as 0-0.5m, 0.5-1m, 1-1.5m and 1.5-2m. Secondly, each CS set was divided according to the follower speed corresponding to an interval of 10kmph. The considered speed intervals in kmph were, [10, 20), [20, 30), [30, 40), [40, 50), [50, 60), [60, 70) and [70, 80). Once all the events were filtered, longitudinal gap data corresponding to each CS and speed interval were obtained.

Understanding the prospect of high crash risks associated with drivers in a dynamic car-following environment, maintaining a safe distance with the leading vehicle by controlling their speeds becomes a demanding task. The risk of engaging in a rear-end collision increases as the available longitudinal gap and centerline separation decrease. For a dynamic traffic environment, in car-following situations, drivers tend to adjust their speeds in order to maintain a safe or desired headway with the leader with certain extent of centerline separation, such that they are not exposed to crash risks if the leading vehicles suddenly apply brakes. Although speed observations provide information on driving style, risk perception and risk prone behaviour of drivers, the behavioural aspects of drivers in maintaining a preferred longitudinal gap for different speeds with certain CS require proper exploration. Accordingly, the 5^{th} percentile, 95^{th} percentile and mean longitudinal gap values maintained by the drivers at different speed groups for a certain range of staggeredness are evaluated and the corresponding variations are presented in Figure 5.2. The connecting line with red dots lying midway between the 5^{th} percentile line and 95^{th} percentile line represents the average values of longitudinal gap corresponding to different speed groups.

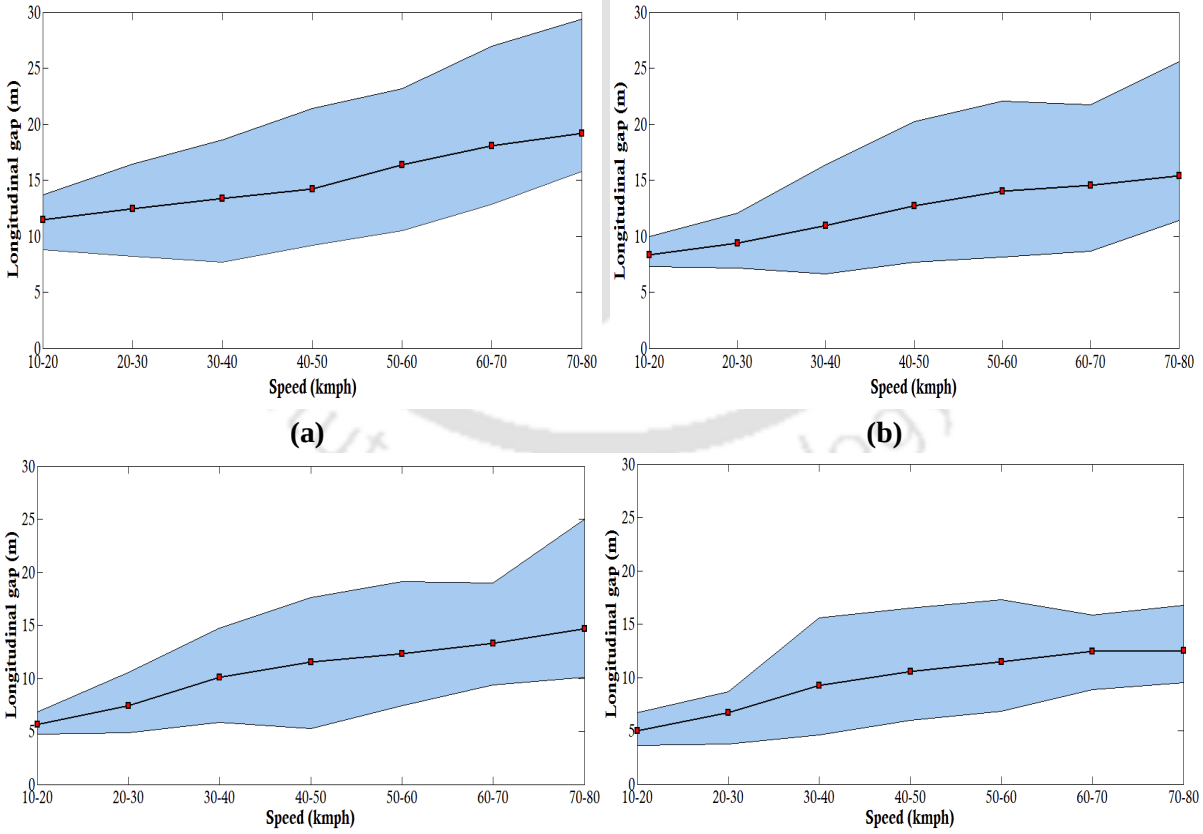

Figure 5.2. Statistical measures of longitudinal gap by speed level for CS levels of **(a)** 0-0.5m, **(b)** 0.5-1m, **(c)** 1-1.5m and **(d)** 1.5-2m.

It is clear from inspection of the above figures that with the increase in longitudinal gap between the vehicles, drivers proceed at comparatively higher speeds in order to maintain an acceptable desired distance with the leading vehicle. This is because drivers proceeding at higher speeds are exposed to higher crash-risks and therefore, they tend to maintain a safe larger acceptable gap with the leading vehicles taking into consideration the safety aspect of the car-following scenario. The same increasing trend of LG and speed is observed for all levels of centerline separation. A close investigation of the underlying statistical plots provide evidence that the range of longitudinal gap with speeds gradually decreases with the increase in off-centeredness between the vehicles. Because following vehicles at large CS, encounter a wide forward field of view, little encumbrance of lead vehicles, they tend to follow the leaders closely maintaining lower longitudinal gap. The minimum 5 percentile value corresponding to 1.5-2m CS is obtained as 2.94m, which can be considered as quite low for an actual car-following event. But such a value rather seems intuitively unsurprising because larger the CS between vehicles, the more lateral space is available to the driver to initiate lateral shifts and therefore lesser is the perceived risks. Conversely, the same LG at lower CS may represent a high risk prone behaviour. The results presented in this section are indicative of the fact that there is certain degree of dependence relationship among longitudinal gap, vehicle speeds and centerline separation in staggered car-following scenario.

5.1.2.3. Relative speed-acceleration mapping

In car-following situations, follower drivers are more sensitive to stimulus-variables from the vehicle in-front that determines their response (most often, acceleration or deceleration). This forms the basis of one of the most influential CF models, namely *stimulus-response frame* of GHR model (Chandler et al., 1958). Although the main stimulus drivers respond to in the GHR model is relative speed, there has been a continuous improvement in the CF models since decades including spacing, speed, acceleration, time headway, desired speed, memory (of speeds over a period of time), reaction time, asymmetries between acceleration and deceleration, traffic density and many more. The seed of *stimulus-response frame* that is, relative speed and acceleration mapping of the drivers involved in the CF process is sought to explore in this section.

According to Michael's theory (Michaels, 1965), drivers in the car-following process cannot perceive minute variations in relative speeds. They adjust their speeds based on the continually changing visual angle apperceived by the follower drivers in the course of car-following. Certainly, drivers have a threshold level below which they cannot have a precise estimation of relative speed. When the leading vehicle's speed is much higher than the follower, drivers become aware of the positive relative speed because it exceed their thresholds and therefore the driver makes the decision to accelerate in order to maintain certain desired spacing with the leader. On the other hand, when followers adjudge that they are moving at higher speeds than the leading vehicles, they start decelerating in order to maintain a minimum safe spacing with the vehicle in-front. The *stimulus* (relative speed)-*response* (acceleration/deceleration) mapping from the processed CF data is presented in Figure 5.3. The upper line represents the

95 percentile values of acceleration obtained for each relative speed, while the lower line depicts the lower 5 percentile values and the connecting line lying midway in between the upper and lower values represents the mean values of responses.

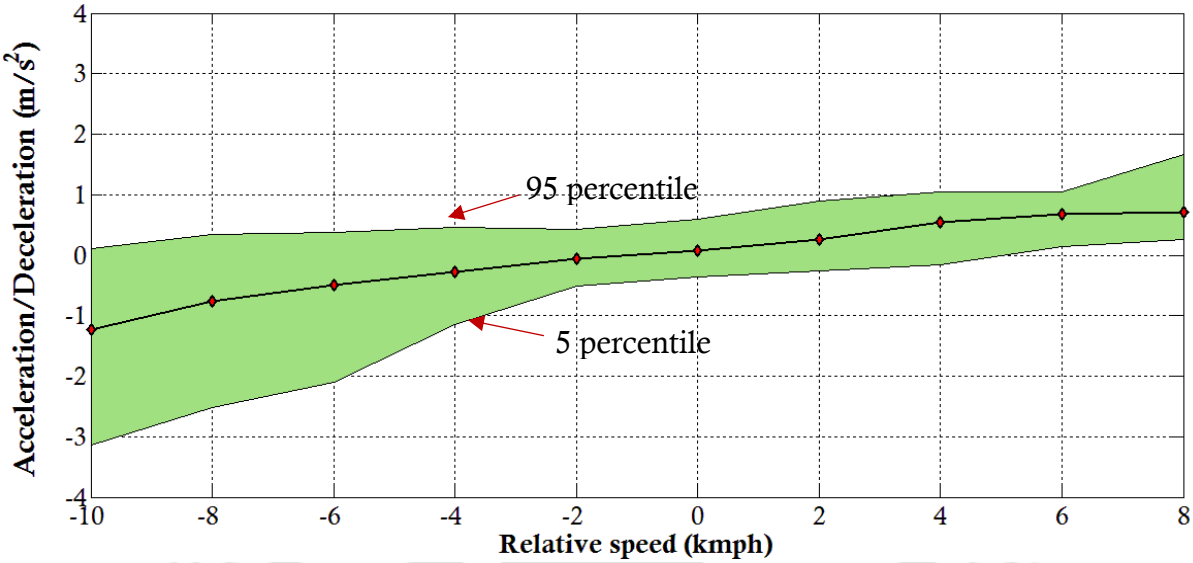

Figure 5.3. Mapping of acceleration/deceleration responses of the drivers with relative speed

The mean values of responses are in accordance with the assumptions-the larger the negative relative speed, larger is the magnitude of the deceleration response. The mean values of deceleration (in m/s^2) are obtained as 1.24, 0.77, 0.49, 0.28 and 0.06 for a range of negative relative speeds (km/h) -10, -8, -6, -4 and -2 respectively. Similarly, the mean acceleration values (in m/s^2) are estimated as 0.26, 0.54, 0.68 and 0.71 for relative speeds of 2, 4, 6 and 8km/h respectively. The higher deceleration rate offered by follower (say, 5 percentile value of -3.13 m/s^2 corresponding to a negative relative speed of 10kmph) as compared to the highest magnitude of acceleration response (that is, 95 percentile value of 1.67 m/s^2 at 8kmph speed) suggests that drivers are more sensitive towards deceleration response so as to decrease risk of possible collision with the vehicle in-front. In regard to drivers' responses, the average values of acceleration and deceleration are obtained as 0.453 m/s^2 and 0.568 m/s^2 respectively. The mean deceleration rate is somewhat similar to California drivers (that is, 0.568 m/s^2 vs. 0.58 m/s^2) whereas the acceleration rate is lower than that found in Siuhi and Kaseko's (2016) work (that is, 0.453 m/s^2 vs. 0.62 m/s^2) in the car-following state.

To summarize, the dynamic behavioural response of drivers in car-following scenario of disordered systems and her/his perceptions in decision making in response to actions of the leading vehicle have been investigated in this section. Statistical results substantiated the consideration of different variables including the response variable namely following vehicle's acceleration, longitudinal descriptors such as relative speed, longitudinal gap, speed, and lateral descriptor namely centerline separation, for understanding and modelling the staggered-following behaviour. Indeed the selection of these input variables are anticipated to enrich the realism and development of car-following models of disordered systems.

5.2. Development of single leader-single follower car-following model

The rationale behind development of car-following models is to appraise how driver controls her/his vehicle with respect to the preceding vehicle precisely and realistically. Characterizing human constraints and preferences in the model has become one of the major goals. Yet, many conventional engineering models are based on the assumption that driver's behaviour is *rational* and that she/he is perfectly able to perceive speed, spacing and acceleration. A *rational* driver is supposed to continuously correct the car motion to follow the optimal path (Simon, 1972). But in general, a driver cannot exactly compute the optimal path of motion and in no way, she/he can correct the car motion continuously. Or, to put it differently, drivers cannot simply evaluate and resolve small differences between a given value of spacing, speed, or acceleration and their desired values (Lubashevsky et al., 2003). While research shows that psychological plausible characterization of how drivers apperceive the driving situation has not been fully captured in engineering CF models, a richer representation of the cognitive processes in CF is still required to describe driver responses in an appropriate manner.

Given the importance of human factors in the operational and control processes, understanding and modelling the normative behaviour response of drivers are indispensable for the evaluation of performances of transportation systems. Drivers in a car-following regime are subjected to a multitude of complex driving tasks. For instance, drivers keep a track of the forward visual field and often maintain an awareness in order to safely control the vehicle involved in the decision-making process. The control process is associated with human factors such as driver state, visual conditionals and mental state and attention the driver is willing to pay to the lead vehicle (Van Winsum, 1999). Although drivers have preferred driving strategies, they cannot control this strategy sufficiently precisely because of the complex integrations associated with the perception and controlling processes of drivers in the car-following regime. This becomes even more complex in non-lane based systems because of the lateral dimension involved in vehicle interaction process. Drivers in such conditions, adopt a *satisficing strategy* in which they evaluate possible alternatives to maintain certain extent of off-centeredness in order to have a clear forward visual field and simultaneously maintaining a safe longitudinal spacing ahead. And based on the notion of *satisficing approach*, if the current situation is acceptable and adequate, then there is no need to look for other possible alternatives. Human factor, forming the major element of a car-following process along with all the involved driving tasks makes the action-control process really complex. A generalization of car-following in a block diagram is presented in Figure 5.4.

Considering such aspects of complex human driving processes, a modelling framework is advocated as a needed alternative that would adopt a driver centered perspective in characterizing car-following phenomena of non-lane based systems. The artificial neural network (ANN) can be a viable tool to model the structural and parametric uncertainties in the car-following processes. Understanding that ANN can inherently deal with indefinable nonlinearity (DeTienne et al., 2003) without intervention or inclusion of a priori knowledge of the data and functional form of any relationship, it can be considered as a powerful tool to deal with uncertainties and inaccuracies of human driving process. An ANN can map between variables that the driver can perceive and those that the driver can directly control with arbitrary

accuracy based on neural learning. This makes the system natural and suitable to model a human driving process in an appropriate manner. Therefore, this section provides an in-depth exploration of the development of ANN based car-following model for non-lane based systems considering both longitudinal and lateral descriptors of traffic.

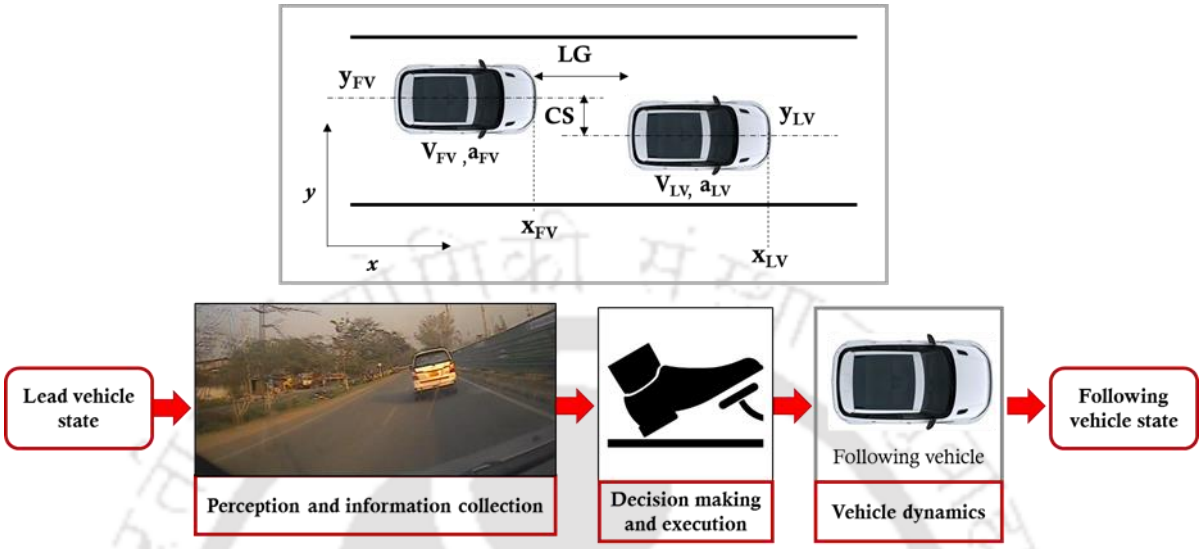

Figure 5.4. Representation of control process in a staggered-following scenario

5.2.1. Artificial Neural Network Methodology

Since 1990s, there has been an explosion of interest concerning development of neural networks in the field of transportation studies (Dougherty, 1995; Kalogirou, 2000; Karlaftis and Vlahogianni, 2011). The concept of neural networks, which forms the seed of artificial intelligence, has seen a meteoric rise in popularity typically because of their inherent propensity of storing massive empirical multi-dimensional data, their modelling flexibility, adaptability, learning and generalization ability and their good predictive ability (Bingham, 2001; Srinivasan et al., 2006). To be more elaborate, the widespread adoption of neural networks in decision making problems can be attributed to four main factors:

- *Model interpretation*- Neural networks (NN) are able to handle noisy and incomplete data with any degree of complexity in non-linear systems. They aim at providing an efficient representation of the underlying data, in terms of accuracy and development time, and offering good predictions on the underlying phenomenon.

- *Model development via learning process*- The functional form of NN model is approximated via learning the desired relations from the underlying data without intervention or inclusion of a priori knowledge (Flexer, 1996).

- *Model assumptions*- Unlike statistical models, neural networks do not require prior assumptions or knowledge of problem solving (Kalyoncuoglu and Tigdemir, 2004). Statistical models require a priori hypothesis regarding distribution of error term with

prior knowledge of the functional form of the model and they cannot effectively deal with nonlinearity. Contrarily, NN are inherently non-linear parametric models that can straightforwardly deal with indefinable non-linearity.

- *Multicollinearity*- Models in statistics are fairly inept at dealing with correlation between two or more independent variables, which is more efficiently dealt with in NN models as there is no assumption of uncorrelated independent variables (DeTienne et al., 2003) before model estimation.

Unlike statistical models, ANN models offer limited inherent explanatory power having hidden inference mechanism (many researchers call as 'black boxes'). However, development of such models provide an efficient representation of the underlying complex non-linear phenomenon, with good predictions and accuracy. Congruent to the car-following process described in this section, there exists significant multicollinearity between the longitudinal and lateral descriptors of vehicle interactions (speed, LG and CS, subsection 5.1.2.2.) which are considered as dominant input variables in a car-following model. Moreover, the control process of drivers or the human factors involved in car-following driving tasks makes the action-control process or *stimulus-response* frame essentially complicated, which simple statistical or mathematical models cannot inherently explain and predict the non-linear structure of the CF data. By virtue of the abovementioned features, NN models are believed to be a more flexible and adaptable approach in solving and predicting the complex and highly non-linear dynamics involved in the car-following process.

5.2.1.1. ANN architecture

According to McCulloch and Pitts (1943), artificial neural networks are intelligence algorithms inspired by the functioning of brain and nervous systems. Just like a human brain, the ANN demonstrates the 'ability to learn, recall and generalize from training patterns or data' (Riad et al., 2004). It has a massive interconnected element and parallel distributed processor that has a natural propensity for storing experiential knowledge and providing an approximate mapping between input and output by non-linear functional compositions (Srivaree-Ratana et al., 2002).

The architecture of a neural network elucidates the pattern of connection between nodes, method of determining inter-nodal connection strengths known as synaptic weights, and the activation functional form (Fausett, 1994). Neural networks are classified based on two criteria: *number of layers*- single (Hopfield nets), bilayer (Grossberg/Carpenter adaptive resonance networks) or multilayer (most backpropagation networks); and *direction of information flow and processing*- feed-forward network (information passes from input to output side and no connection exists between nodes within the same layer) and recurrent ANN (information flows from input to output and vice-versa, Govindaraju, 2000). Considering the simplicity and widespread usage of multi-layer feed forward neural network in diverse fields of transportation studies, this work concentrates on multilayer feed-forward ANN architecture, a schematic representation of which is displayed in Figure 5.5.

The network is composed of input layer, one hidden layer and an output layer. The *input layer* comprises of nodes representing various input variables x_1, x_2, x_3 that can influence the output y_1. It essentially receives the inputs and provides information to the network. Each neuron in an input layer is connected to every single neuron in the intermediate layer by links having an appropriate and adjustable connection weight, representing the relative connection strength of two nodes at both ends. That is, each input variable x_i is multiplied by a synaptic weight (w_{ij}^1) assigned for each connecting link to form a weighted input $w_{ij}^1 x_i$. The superscript in notation represents layers and subscripts represent neurons. The first subscript denotes the neuron in question and the second subscript refers to source of signal fed to the current neuron. The sum of the weighted inputs, $\sum_{i=1}^{3} w_{ij}^1 x_i$ along with the neuron threshold value or bias, b_j^1 then passes to the jth neuron in the hidden layer forming its own neuron output $p_j^1 = \sum_{i=1}^{3} w_{ij}^1 x_i + b_j^1$, often referred to as the net input. The net input then goes into the transfer function or activation function f^1 that produces jth neuron output r_j^1 in the first layer.

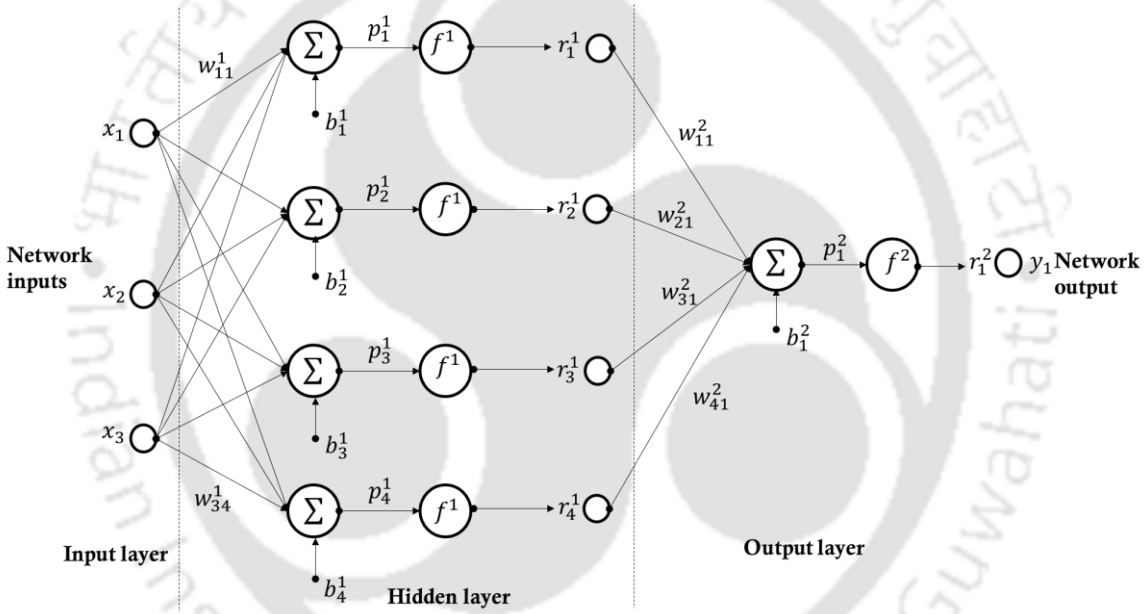

Figure 5.5. Configuration of three-layer feedforward ANN comprising of three network inputs, four neurons in hidden layer and one network output

Similarly, treating the outputs corresponding to inputs in the first layer, as the inputs of layer two, the input signals from hidden layer are then passed to second layer. The transfer function in the second layer f^2 can be completely different from that in the first layer. The output neuron can then be written as $r_1^2 = f^2\left((w_{11}^2 r_1^1 + w_{21}^2 r_2^1 + w_{31}^2 r_3^1 + w_{41}^2 r_4^1) + b_1^2\right)$. Thus in reality, the function of a neuron is to receive input from neighboring sources and compute an output signal that is propagated to other units.

5.2.1.2. Network training

The important step in the development of an ANN model involves determination of an optimal ANN architecture and selection of a suitable training algorithm. An optimal architecture can be considered as the one yielding the best performance in terms of error minimization, while retaining a simple yet compact structure. More often, a trial-and-error based procedure is employed to decide on the optimal structure. However, the ability of the NN to learn from its environment, and improve its performance through learning process is of prime importance. Training or learning is a process by which the synaptic weights and biases of a network are adapted through a continuous process of stimulation by the environment in which the network is embedded. This involves minimizing a predefined error function by iterative adjustment and optimization of connection weights and threshold values of each neuron such that the produced outputs are equal or very close to the targets.

Perhaps, backpropagation (BP) is one of the most popular training algorithms for multilayer feedforward neural networks (Wasserman, 1989; Fausett, 1994). It essentially attempts to improve neural network performance by minimizing network error through adjusting connection weights and biases. The mean squared error is often used as a measure to evaluate network performance,

$$E = \frac{1}{T}\sum_{t=1}^{T}\sum_{m=1}^{M}(r_m^2(t) - y_m(t))^2$$

Where M is the number of output nodes, T is the number of training patterns, $y_m(t)$ is a component of the desired output and r_m^2 is the corresponding ANN model output. The BP algorithm is a steepest gradient descent method in which the error is propagated backward through the network to each node. Accordingly the connection weights are adjusted based on equation

$$\Delta w_{ij}(s) = -\eta * \frac{\partial E}{\partial w_{ij}} + \xi * \Delta w_{ij}(s-1)$$

$$\Delta b_j(s) = -\eta * \frac{\partial E}{\partial b_j} + \xi * \Delta b_j(s-1)$$

Where $\Delta w_{ij}(s)$ and $\Delta w_{ij}(s-1)$ are the weight increments between node i and j during n^{th} and $(n-1)^{th}$ pass or epoch; $\Delta b_j(s)$ and $\Delta b_j(s-1)$ are the increments in bias values; η and ξ are the learning rate and momentum respectively. A learning rate is used to allow the training process reach the vicinity of a global minima without being trapped in the local minimum. The momentum factor on the other hand, speeds up training in very flat regions of error surface and help prevent oscillations in the weights. The weighted parameters are updated as long as the total network error is less than the acceptable desired level.

5.2.1.3. Mathematical model development

The development of the ANN prediction model entails creation and segmentation of a working database, proper design of neural network architecture, selection of training algorithms and validation and statistical comparison of ANN models. A graphical synthesis of the neural network methodology is illustrated in Figure 5.6.

The numerical iterative procedures involved in the design of ANN model are briefly described below.

(a) *Description of working database*- Based on the experimental time-series data collection procedure, speed of the interacting vehicles and acceleration/deceleration of the following vehicle were obtained from the GPS recorders, while the positional data of the leading vehicle (extracted from the video recorders) were processed to obtain longitudinal gap and centerline separation at each 5Hz frequency level. Prior to the training process, these time-series processed data were randomly divided into two segments: 80% input samples (constituting 7663 data) were used for training and 20% input samples (1916 data) for model validation. The data were segmented randomly in order to guarantee an accurate representation of the data distribution.

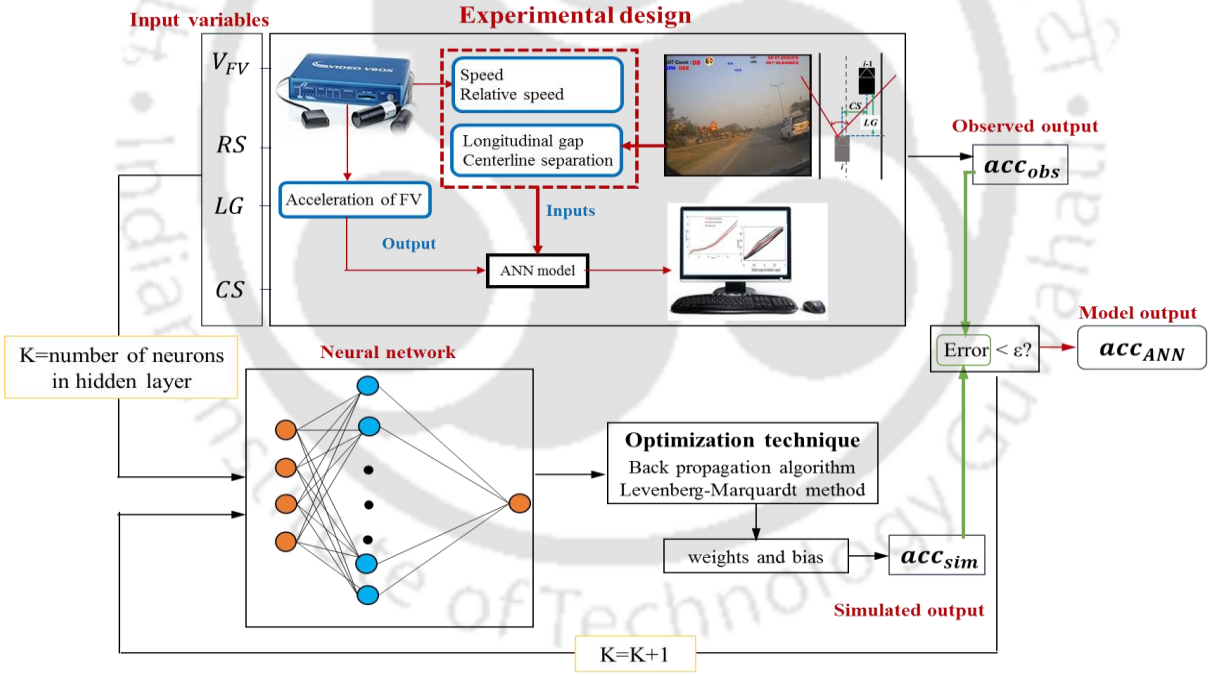

Figure 5.6. Iterative procedure designed for development of the data-driven ANN model

(b) *Selection of ANN architecture and training algorithm*- Several ANN architectures were evaluated to obtain reliable estimation of the response variable. The basic ANN architecture used consists of four neurons in the input layer corresponding to speed of the following vehicle (V_{FV}), relative speed (RS), longitudinal gap (LG) and centerline separation (CS); one/two hidden layer(s) and one neuron in the output layer given by acceleration of the following vehicle (acc_{FV}). To model the nonlinearity of car-following

behaviour, the transfer functions used are hyperbolic tangent sigmoid ($Tansig$) for the hidden layer and linear transfer function ($Purline$) for the output layer:

$$f^1 = Tansig(n) = \frac{1}{1+\exp(-2n)} + 1$$

$$f^2 = Purline(n) = n$$

n representing weighted sum of the inputs. An ANN architecture with two hidden layers (HLs) was also experimented to examine whether there is any significant improvement in the model performance for two HL ANN model as compared to network with one hidden layer. Moreover, considering higher convergence speed of backpropagation algorithms, the Levenberg-Marquardt (LM) algorithm was employed to obtain optimum weights and biases for the ANN models. The main strategy used to obtain the optimal ANN architecture was the progressive increment of neurons in the hidden layer, and checking for the minimum error criteria.

(c) *Evaluation metric*- To evaluate the performance of each ANN architecture, the empirical and simulated responses were statistically compared. Specifically, three criteria, mean squared error (MSE), root mean square error (RMSE) and correlation coefficient (R) are employed to validate the proposed architecture:

$$RMSE = \sqrt{\frac{1}{S}\sum_{s=1}^{S}\left(acc_{Exp(s)} - acc_{Sim(s)}\right)^2}$$

$$MSE = \frac{1}{S}\sum_{s=1}^{S}\left(acc_{Exp(s)} - acc_{Sim(s)}\right)^2$$

$$R = \frac{\sum_{s=1}^{S}\left(acc_{Exp(s)} - \overline{acc_{Exp}}\right)\sum_{s=1}^{S}\left(acc_{Sim(s)} - \overline{acc_{Sim}}\right)}{\sqrt{\sum_{s=1}^{S}\left(acc_{Exp(s)} - \overline{acc_{Exp}}\right)^2}\sqrt{\sum_{s=1}^{S}\left(acc_{Sim(s)} - \overline{acc_{Sim}}\right)^2}}$$

Where $acc_{Exp(s)}$ and $acc_{Sim(s)}$ are the measured or observed acceleration/deceleration value and the simulated ANN output respectively of the sample s, $\overline{acc_{Exp}}$ and $\overline{acc_{Sim}}$ are the mean values of the measured and simulated samples.

As it is highlighted in Figure 5.6, the same numerical procedure is followed by increasing the number of neurons in the hidden layer. The architecture is therefore modified and the training process is repeated to produce a new set of weighted coefficients. This process continues until the statistical criteria is fulfilled producing minimum RMSE, MSE error values and largest R value. For all combinations of ANN architecture, the maximum number of iterations, minimum performance gradient and learning rate are set to 1000, 1.0×10^{-5} and 0.01 respectively.

5.2.2. Consideration of driver's reaction delay

Reaction delay is an indispensable factor in operation and control process of drivers in car-following tasks. The inability of drivers to perceive and/or react to actions of the immediate vehicle in-front can lead to rear-end collisions, imprecise calibration of car-following models (Mehmood and Easa, 2009) and can contribute to traffic instabilities, thereby leading to traffic flow breakdown (Treiber et al., 2007). Delayed reaction times can eventually lead to the emergence of stop-and-go waves in a platoon of vehicles, especially under dense traffic situations. Clearly, this embodies how reaction delay affects traffic flow dynamics on a microscopic as well as on a macroscopic scale (Aycin and Benekohal, 2004).

Driver reaction time was defined as the summation of *mental processing time* and *movement time* (Green, 2000). *Mental processing time* is the time required to perceive a signal and decide on a response while *movement time* is the time taken to lift the driver's foot from the accelerator and then to touch the brake pedal. In psychological studies, reaction delay can be decomposed into three sequential components: mental processing time (including sensation, perception, response selection and programming), movement time and device response time. The cognitive uncertainties of drivers in CF processes involving perception and execution of a control strategy can be treated as a real-world human driving problem where reaction delay characteristics vary considerably with variations in stimuli, acceleration and deceleration asymmetry, surrounding environment, driver workload and fatigue, etc. Thus, a notable and plausible characterization of how drivers think about, react to the current stimuli and address the driving problem requires an in-depth investigation. More precisely, driver reaction delay is one such human behavioural aspect, a proper consideration and assessment of which is anticipated to significantly enhance the explanatory power of the developed CF models.

5.2.2.1. Adopted values of driver's reaction time

Many pioneering efforts devoted to the estimation of reaction delay have focused on driver specific and situational factors. Yet, selecting a suitable reaction time in CF models has emerged as a contentious issue since decades. Table 5.3 presents a summary of reaction times adopted by different researchers in varying driver and situational factors.

Various organizations have recommended 2.5s reaction time as the design value in the US and 2s in Europe while driver education manuals suggest the average reaction time as 1s with values ranging from 0.5-2s (Triggs and Harris, 1982). The 2.5s brake reaction time is valid only for normal car-road events in good weather conditions with high visibility. Korteling (1990) suggested mean reaction times of 0.62s and 0.709s for younger and older participants respectively. This is in congruence with the findings of previously conducted research by Hale et al. (1988). They concluded that reaction time of drivers aged between 50-60 years increased by 10% faster than those of younger drivers, while reaction time of elder drivers (65-75 years) increased about 30% faster. Recently, Mehmood and Easa (2009) underlined that although reaction time is slower with increased age, no significant relationship is observed between age and reaction time in normal car-following scenario. No slowing effect of reaction time with

age was also supported by many studies (Lerner, 1994; Olson and Sivak, 1986). Further, reaction time of female drivers (0.92s) were found to be slower than males (0.82s, Mehmood and Easa, 2009).

Table 5.3. Summary of driver reaction time

Research	Conditions	Reaction time (s)	Paradigm	Sample
Sivak et al. (1981a)	Light location	0.73	Road	12
Johansson and Rumar (1971)	Alertness	0.66*	Road	321
Korteling (1990)	Age	0.62 (Young)		40
	Road difficulty	0.709 (Old)	Road	225
Schweitzer et al. (1995)	Distance (6/12m) Speed (60/80kmph) Alertness	0.535	Road	45
Sivak et al. (1981a)	Brake light location	1.38	Naturalistic	277
Triggs and Harris (1982)		1.26**	Naturalistic	
Probst et al. (1984)		1.14	Road	
Törnros (1995)	Driving speed (70, 90, 110 kmph)	0.3-0.4	Naturalistic	24
Ma and Andréasson (2006)	Spectrum analysis	0.52-1.24	Naturalistic	10
Khashbat et al. (2012)	Age (18-30, 31-45, 46-60 years) Experience	0.623	Road	40
Brown (2012)	Age	1.148 (Young)	Simulator	27
	Complexity	1.270 (Old)		24
Kesting and Treiber (2008), Kesting (2008)	IDM CF model	1	Numerical Simulation	
Pekkanen et al. (2018)	IDM CF model	0.1	Simulation	
Zhang and Bham (2007)	Trajectory data	0.86	Naturalistic	157
Kometani and Sasaki (1959)	CF model	0.5	Road	
Subramanian (1996)	Acceleration GHR CF model	1.97	Road	
	Deceleration	2.29		
Mehmood and Easa (2009)	Age	0.82 (Male) 0.92 (Female)	Simulator	60
	Gender	0.65 (Young)		
	Driving Experience	0.75 (Middle)		
	Intensity	0.84 (Old)		

Note: *Median value, **85 percentile value

Different studies also showed enough evidence that reaction time increased with the increase in task complexity (Green, 2000; Cantin et al., 2009; Martinie et al., 2010; Brown, 2012). According to Brown (2012), the mean reaction time increased by 0.575s as the complexity of the task increased from simple (single stimulus) to complex stimuli (stimulus with other visual

or auditory input). In a similar study by Xing et al. (2015), the average simple and complex reaction times were obtained as 0.607s and 1.406s respectively.

A mean reaction time of 0.75s was suggested by the National Safety Council while Green (2000) considered 0.7s as the minimum reaction time for braking. These values are in agreement with many studies that consider 0.7-0.75s (0.5-0.55s perception time and 0.2s movement time) as the best mean reaction time that can be expected on the road (DeSilva and Forbes, 1937). Liebermann et al. (1995) and Schweitzer et al. (1995) found no effect of driving speed on reaction time, although drivers reacted slightly faster at 100kmph speed than that at 80kmph. Sivak et al. (1981a, 1981b) underpinned that longitudinal gap between the interacting vehicles had a significant effect on the reaction delay. With the presence of brake lights of the lead vehicle, the mean reaction delays at longer distances (0.67-0.83s) were 15% higher than that obtained at shorter distances (0.55-0.7s).

5.2.2.2. Estimation procedures

Evidently, the preceding discussion substantiates a plethora of literature, touching on the selected ranges of driver's reaction time and its variations with driver characteristics, driving scenario, traffic patterns, and road conditions and so on. The estimation of reaction delay in real car-following scenario indeed requires proper assessment. In light of this, several approaches were proposed. In essence, reaction delay based on fixed reaction time, and instantaneous reaction time are commonly employed in the existing research work related to CF model development.

- *Fixed reaction time*- In the development of car-following models, a constant reaction time in the range of 0.2-3s was considered in a large number of prominent work. The best performance of Gipps' model was achieved with apparent reaction time of 0.67s (Gipps, 1981; Gunay, 2007), 0.2s (Ravishankar and Mathew, 2011), 0.4s (Papathanasopoulou and Antoniou, 2015), 0.9s (Qu et al., 2014) and 1.2s (Kanagaraj et al., 2013). A reaction time of 0.5s was considered to demonstrate the dynamic performance of OVM model (Tang et al., 2011; Jin et al., 2010; Li et al., 2015a) and in other classical CF models (Papathanasopoulou and Antoniou, 2018) while 1s reaction time was considered in the development of fuzzy rule based car-following model and other work (Kikuchi and Chakroborty, 1992; Hoogendoorn and Ossen, 2006; Li et al., 2016; Zheng et al., 2012). Treiber et al. (2007) argued that crashes in a simulation run can be avoided if reaction time is less than 0.9s.

- *Instantaneous reaction delay*- Ozaki (1993) proposed a graphical technique to estimate reaction time based on relative speed and acceleration profiles. Utilizing freeway car-following data collected in Japan, he developed a piecewise linear function separately for acceleration and deceleration responses, considering longitudinal gap and leading vehicle's acceleration as independent variables. This model received considerable attention and was extended in a number of research work (Khodayari et al., 2011, 2012; Moghadam et al., 2016).

Based on NGSIM data, Khodayari et al. (2011) developed a neuro-fuzzy CF model based on instantaneous stimulus-reaction delay. They compared the model performance based on the proposed instantaneous reaction time and fixed reaction times of 0.1s, 0.3s and 0.6s. Results of the model provided better performance of instantaneous model, followed by 0.6s reaction time CF model. Later, Zheng et al. (2013) and Moghadam et al. (2016) extended the same concept and found better performance of car-following behaviour when instantaneous reaction time is considered.

While the peer-reviewed literature recommended a fixed reaction delay in the CF model development, it has been criticized by many researchers suggesting that a fixed delay often circumvents the realistic human behaviour in CF driving regime. Considering better prediction accuracy of instantaneous reaction time model (Khodayari et al., 2011; Moghadam et al., 2016; Zheng et al., 2013), a comparison of instantaneous reaction delay model, based on Ozaki idea and its modification (with consideration of lateral descriptor) and fixed reaction delay in intervals of 0.2s (0.4s, 0.6s, 0.8s and 1s), is made for the representation of realistic driver behaviour in the developed ANN-based CF model.

5.2.2.3. Evaluating reaction delay in staggered-following scenario

Based on the *stimulus-response* framework proposed by Khodayari et al. (2011), instantaneous reaction delay is specified by the time-interval between the *stimulus* (relative speed) and *response* (acceleration/deceleration) of the following vehicle. Figure 5.7 illustrates the relative speed and acceleration profiles of the following vehicle.

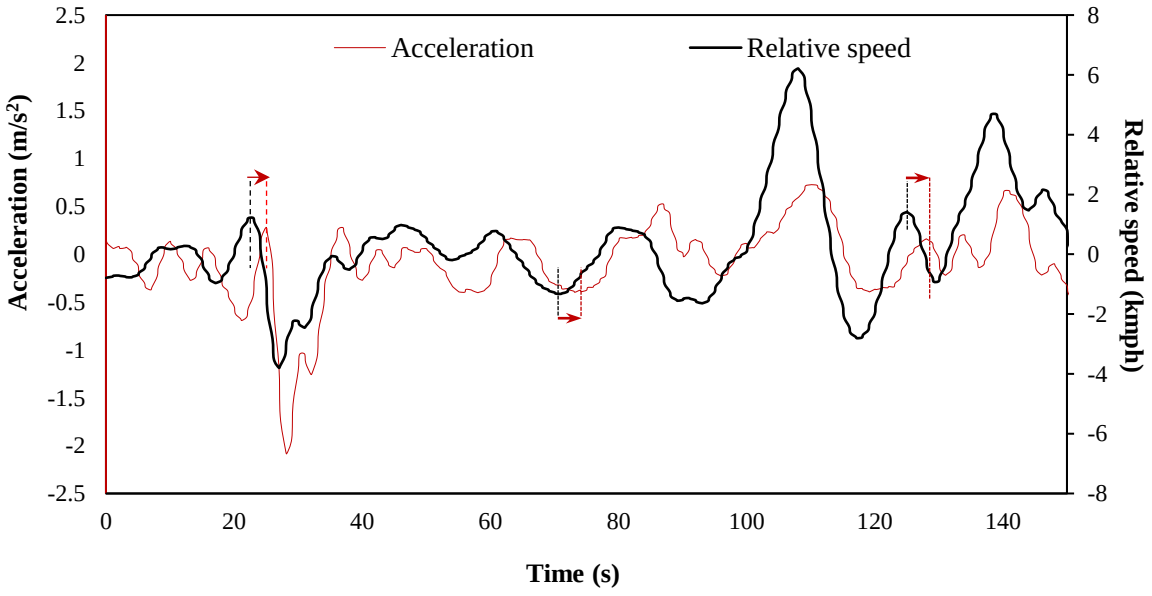

Figure 5.7. Relative speed and acceleration profile

It is clear that the changing tendency of following vehicle's acceleration is quite similar to the relative speed. Higher the acceleration rate offered by the leading vehicle, larger will be the relative speed between the vehicles and based on driver's perception, the following vehicle will

react accordingly after a certain time lag. This time lag is considered as driver's reaction delay (Khodayari et al., 2012) which can be obtained from the time difference between two subsequent variations in relative speed and acceleration, as indicated by arrows in the figure. The reaction delays appear to change during acceleration and deceleration responses because drivers, in general, are more sensitive towards deceleration response so as to decrease risk of possible collision with the vehicle in-front.

A thorough investigation of the complete relative speed-acceleration profile indicated some negative time-lags (response starts before changes in the stimulus), in which most of them occurred at smaller longitudinal gaps. This can be attributed to the fact that drivers in close CF regime respond in anticipation to the leading vehicles next action. Such negative time lags were not considered in the analysis. From the observed *stimulus-response* profiles, the relation delays corresponding to acceleration and deceleration responses resulted in a total of 364 samples. Table 5.4 summarizes the descriptive statistics of acceleration and deceleration instantaneous reaction delays.

Table 5.4. Basic statistical properties of the reaction delay

	Acceleration	Deceleration
Mean (s)	0.734	0.616
Median (s)	0.600	0.550
Std.dev (s)	0.321	0.280
Minimum (s)	0.30	0.20
Maximum (s)	1.50	1.30
Sample	163	201

The reaction delays are observed in the range of 0.2-1.5s, the maximum value being considerably lower than the acceleration (1.5s vs. 1.97s) and deceleration (1.3s vs. 2.29s) reaction delays suggested by Subramanian (1996) and design value recommended in US (2.5s) and Europe (2s). Comparing the mean values with the existing recommended values, the mean delays obtained in this study are found to be in congruence with the recommended ranges in some of the existing work (0.7-0.75s, DeSilva and Forbes, 1937; 0.55-0.83s, Sivak et al., 1981b; 0.52-1.24s, Ma and Andréasson, 2006). These values are however, slightly higher than the reaction time considered in some of OVM (0.5s, Tang et al., 2011; Jin et al., 2010), Gipps' model (0.4s, Papathanasopoulou and Antoniou, 2015) and lower than the apparent reaction time used in fuzzy-rule based models (1s, Kikuchi and Chakroborty, 1992; Hoogendoorn and Ossen, 2006) and Gipps' models (0.9s, Qu et al., 2014; 1.2s, Kanagaraj et al., 2013). Because drivers are more sensitive towards deceleration response than to acceleration taking into account safety concerns, mean deceleration delay is observed to be lower than mean acceleration delay. Comparing the means of acceleration and deceleration responses yielded significant differences in their mean values ($t_{stat}=2.64>t_{cri}=1.96$, $p<0.001$).

Clearly, this indicates that selecting a suitable reaction delay in CF model has been a contentious subject since long. For a proper and reliable estimation of instantaneous reaction delay, it is important to understand whether the lateral descriptor (or, CS) in staggered-following regime play any vital role in the driver's response time. In this context, based on the

idea proposed by Ozaki (1993), two separate linear piecewise models were developed. Similar to Ozaki delay, the first model (Model 1: Ozaki delay model) considers acceleration of the leading vehicle (acc_{LV}) and LG as independent variables for both acceleration and deceleration responses while the second model (Model 2: modified Ozaki delay model) incorporates CS as the third independent variable in addition to acc_{LV} and LG. The Ozaki model was re-calibrated using the observed sample data and the following equations were obtained for acceleration and deceleration responses:

Model 1: Ozaki delay model:

$$\text{Deceleration Delay} = 0.3928 + 0.1198\text{acc}_{LV} + 0.0116\text{LG}$$

$$\text{Acceleration Delay} = 0.5248 + 0.14422\text{acc}_{LV} + 0.0073\text{LG}$$

Model 2: Modified Ozaki delay model:

$$\text{Deceleration Delay} = 0.10339 + 0.14457\text{acc}_{LV} + 0.0205\text{LG} + 0.25324\text{CS}$$

$$\text{Acceleration Delay} = 0.34466 + 0.15930\text{acc}_{LV} + 0.0134\text{LG} + 0.16922\text{CS}$$

The constant terms in both the models justify that drivers' reaction delays for deceleration responses are lower than that when responding to an accelerating vehicle. This is quite evident because drivers respond faster to a decelerating vehicle and/or with the activation of leading vehicle's brake lights in order to avoid high risk situations or potential rear-end collisions. The magnitude of the parameter estimates of acc_{LV} and LG further confirm that drivers are more likely to respond faster during deceleration phase when the available gap is relatively lower and leading vehicle's acceleration is higher.

Interestingly, the parameter estimates of the modified Ozaki model (Model 2) indicated that in addition to acceleration and longitudinal gap, centerline separation is a significant parameter in explaining the reaction delay of drivers in staggered-following scenario. The positive coefficient of CS could be associated with the fact that drivers are less sensitive to the actions of the leading vehicle when they maintain certain extent of lateral separation with the leaders. This is because drivers encounter a wide forward visual field at large CS and can anticipate the lead vehicle's actions with more confidence, therefore the level of risk perceived by the following drivers at large CS are comparatively lower than the collision risks perceived in actual car-following scenario (CS=0). In such scenario, drivers respond a little slower at large CS as compared to that in CF regime. The magnitude of the parameter estimates further indicate that drivers' responses to deceleration phase are quite slower than that during acceleration phase.

Concisely, the developed instantaneous Ozaki reaction delay model, modified Ozaki delay model and fixed reaction delays of 0.4s, 0.6s and 0.8s and 1s are then further incorporated into a neural network based car-following model and the performance of all the models are evaluated for the design of a realistic CF model for non-lane based traffic environments.

5.2.3. The car-following model

5.2.3.1. Selection of ANN architecture

To design an ANN prediction model, it is assumed that the prediction model has four inputs (speed of the following vehicle, relative speed, longitudinal gap and centerline separation) and one output given by the acceleration of the following vehicle. Several model structure settings considering different set of neurons in the hidden layer(s) from 1 to 35 were trained by the back-propagation algorithm and compared. Consequently, the minimum error criterion were used to determine the optimal ANN architecture. For the selection of an optimal ANN architecture, the performance of several network configurations were compared assuming a constant reaction delay of 0.6s. Table 5.5 summarizes the results of the comparisons corresponding to varying ANN architecture and input variables.

Table 5.5. ANN architecture training results

Input variables	Neurons in HL	MSE	RMSE	R
RS, LG, V_{FV}	3-10-1	0.0897	0.2873	0.6841
RS, LG, V_{FV}, CS	4-10-1	0.0698	0.2653	0.7464
	4-15-1	0.0665	0.2554	0.7713
	4-20-1	0.0650	0.2528	0.7777
	4-25-1	0.0600	0.2438	0.7984
	4-30-1	**0.0570**	**0.2384**	**0.8105**
	4-35-1	0.0558	0.2361	0.8154
	4-10-5-1	0.0620	0.2475	0.7901
	4-20-5-1	0.0534	0.2315	0.8251

Note: Bold features indicate the final adopted model

Comparing the error criterion with 10 neurons in the hidden layer, the introduction of CS as input variable in addition to relative speed, longitudinal gap and current speed of following vehicle improved ANN performance significantly from R= 0.6841 to R=0.7464. Moreover, varying the number of neurons in the hidden layer(s) indicated that the configurations 4-35-1(one hidden layer with 35 neurons) and 4-20-5-1 (two hidden layers with 20 and 5 neurons in first and second layer respectively) exhibit similar performances; with very slight improvement when number of neurons in the hidden layer are increased from 30 to 35. Considering better computational efficiency, faster convergence to target functions and flexibility in learning rate of single hidden layer structure as compared to deep neural nets, the framework with a single hidden layer with 30 neurons is selected for the car-following prediction model.

To further evaluate the competence of the prediction model based on instantaneous and constant reaction delays, five other ANN prediction models were designed and simulated considering the same ANN structure [4-30-1]. Instantaneous reaction delays based on Ozaki idea (Ozaki delay model and modified Ozaki delay model) and constant delays of 0.4s, 0.6s, 0.8s and 1s were assumed for these models. Figure 5.8 shows the performance results of the prediction model considering Ozaki delay and modified Ozaki delay models.

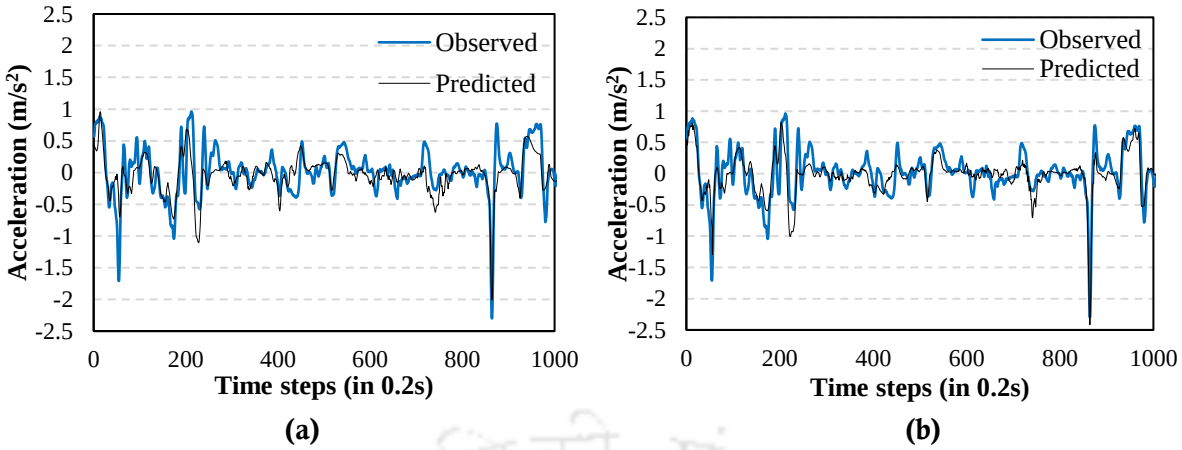

Figure 5.8. ANN estimation results based on **(a)** Ozaki delay model and (b) modified Ozaki delay model

As shown in the figure, the ANN model well represents the responses of the real driver but a close assessment of both the presented results signify a slight improvement in the predictions when the modified Ozaki reaction delay is considered. With the consideration of constant reaction delays, the model performances are further assessed, as illustrated in Figure 5.9.

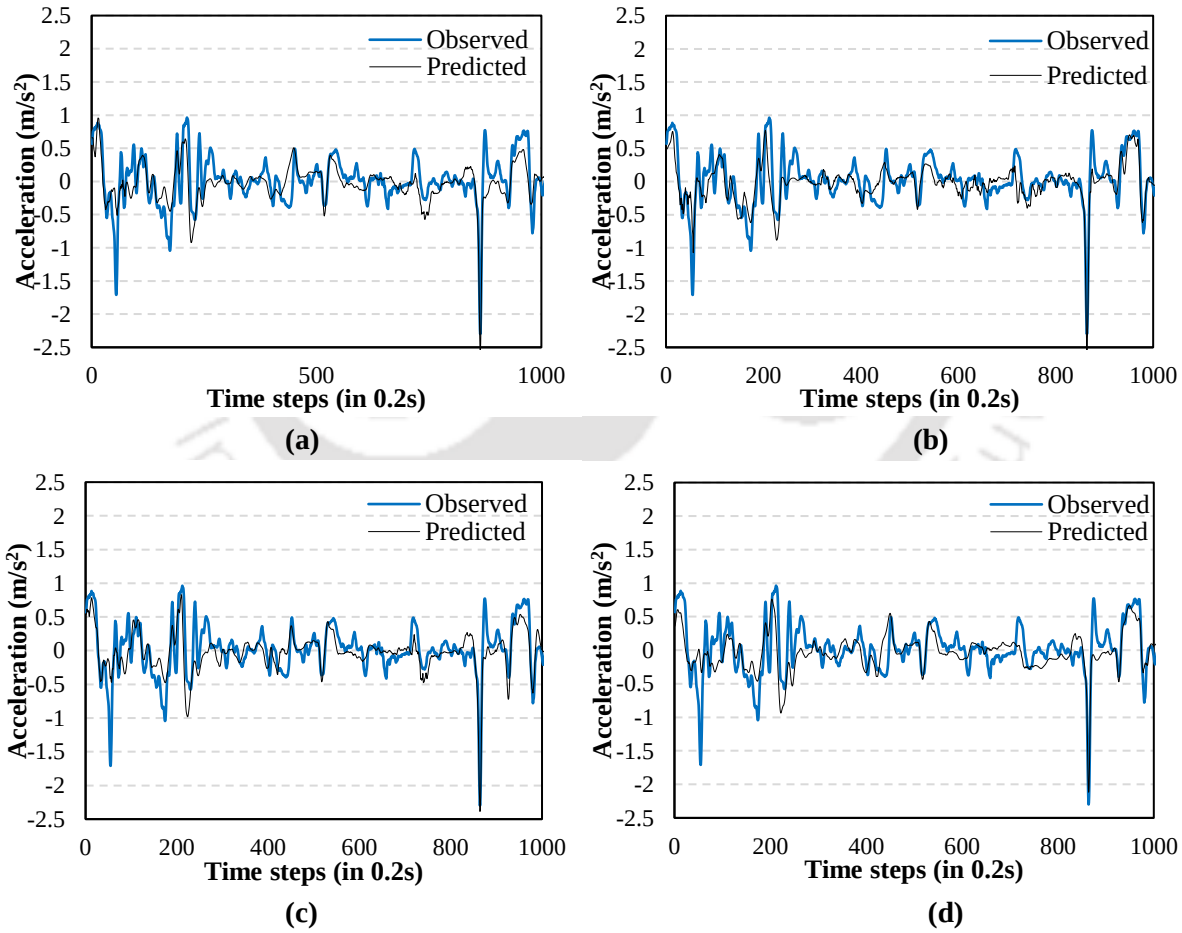

Figure 5.9. ANN prediction results considering constant reaction delays of **(a)** 0.4s **(b)** 0.6s **(c)** 0.8s and **(d)** 1s

The estimation results indicate good representation of the response variable (acceleration of the following vehicle) for a constant reaction delay of 0.6s. A comparison of all the estimation

results based on the considered error criterion will further substantiate the selection of the ANN based car-following model. Accordingly, errors in modelling of the six designed ANN car-following models are evaluated and summarized in Table 5.6.

Table 5.6. Performance measure for ANN car-following model with different reaction delays

ANN car-following model	MSE	RMSE	R
Ozaki delay model	0.0542	0.2326	0.8121
Modified Ozaki delay model	0.0519	0.2316	0.8164
Fixed reaction delay of 0.4s	0.0793	0.2516	0.6939
Fixed reaction delay of 0.6s	**0.0570**	**0.2384**	**0.8105**
Fixed reaction delay of 0.8s	0.0913	0.2774	0.7155
Fixed reaction delay of 1s	0.0963	0.2801	0.6807

Note: Bold features indicate the final adopted model

It is evident from Table 5.6 that the best ANN car-following model prediction was obtained based on instantaneous reaction delay using modified Ozaki delay model. Comparing the MSE values for Ozaki delay and modified Ozaki delay models yielded 4% reduction in prediction error when the lateral descriptor is considered in reaction delay estimation. Interestingly, the errors obtained in instantaneous reaction delay CF models are comparable with the ANN model with fixed delay of 0.6s while the prediction model with 1s reaction delay showed highest errors among all the designed models, followed by 0.8s reaction delay and 0.4s reaction delay. Although instantaneous reaction delay models yielded lowest errors, owing to enhanced computational simplicity and considerable prediction accuracy of 0.6s reaction delay based ANN model, the ANN car-following model with fixed reaction delay of 0.6s is further employed and considered to provide a good overall representation of realistic car-following behaviour. The predicted and observed responses presented in Figure 5.10 reveal a good correspondence between the data (as data lie close to the diagonal line), yielding a mean squared error of 5.70%.

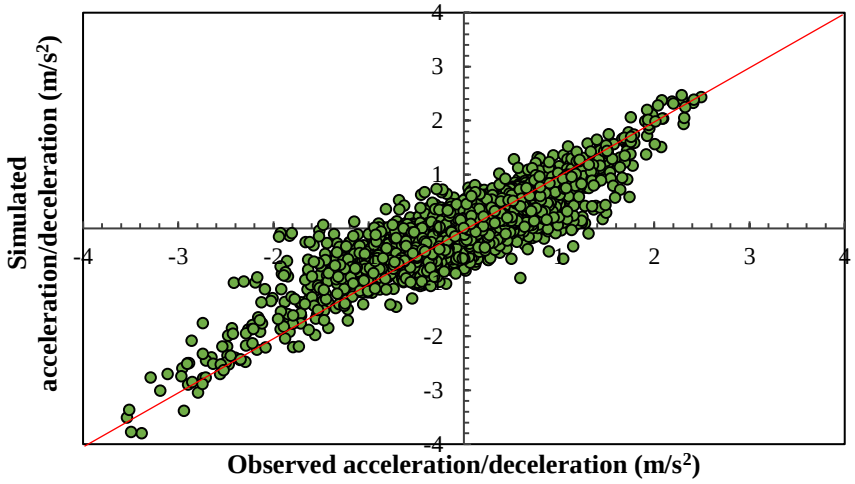

Figure 5.10. Observed and predicted responses based on ANN model with 0.6s reaction delay

Based on the proposed ANN architecture [4-30-1] and the transfer functions with hyperbolic tangent sigmoid and linear function in the HL and output layer respectively, the predicted

responses of 0.6s reaction delay-based car-following ANN model can be analytically represented by the following form

$$acc_{sim} = \sum_{j=1}^{30}\left[w_{(1,j)}^{2}\left(\frac{1}{1+exp\left(-2\sum_{i=1}^{4}\left(w_{ij}^{1}x_i + b_j^{1}\right)\right)}\right)+1\right] + b_1^2$$

where x_i is the input variable under consideration, w and b indicating synaptic weight and bias respectively; the superscript and subscripts in the equation representing layers and neurons (j) respectively. A more elaboration of the parameters can be found in 5.2.1.1.

5.2.3.2. Sensitivity analysis

Sensitivity analysis investigates the relative contribution of the uncertainty of the input variables x_i on the uncertainty of the output y. While local sensitivity analysis characterizes the effect of a small perturbation of input around a specific point, global sensitivity analysis considers the input variability within their entire feasibility space. In particular, global sensitivity analysis is more commonly used and well-documented in the academic literature because it is easy to implement, independent of the form of input-output functional relationship and provides more quantitative and detailed information on the output results based on different levels of conditioning in their entire feasible space.

The PAWN global sensitivity analysis is selected in the research work to understand the relative contribution of different input variables in the complex non-linear ANN-based computational models. This approach is based on measuring the distance between the unconditional cumulative distribution function (CDF) of y, obtained when all inputs vary simultaneously ($F_y(y)$) and the conditional cumulative distribution functions varying all inputs but fixed x_i, denoted by $F_{y|x_i}(y)$. The Kolmogorov-Smirnov (K-S) test statistic is used to measure the distance between unconditional and conditional cumulative distribution functions:

$$KS(x_i) = \underset{y}{max}\left|F_y(y) - F_{y|x_i}(y)\right|$$

As KS statistic depends on the fixed x_i value, the PAWN sensitivity index (T_i) is calculated considering a statistical measure (maximum or median) over all ranges of x_i

$$T_i = \underset{x_i}{stat}\left[KS(x_i)\right]$$

The PAWN sensitivity index is an absolute measure and its numerical value indicates the contribution of the considered input variables: the lower the value of T_i the less influential is the corresponding input variable. Based on the numerical approximation described in Pianosi and Wagener's (2015) work, sensitivity analysis was carried out considering 1000 random samples of input x, 100 random samples for each conditioning value for x_i and 20 random samples for the fixed input x_i. The random samples were generated within the entire feasibility space by considering the minimum and maximum values of each variable. Figure 5.11 depicts the unconditional and conditional CDFs of the response of the following vehicle (model output) for each input parameter. The red lines represent the unconditional CDFs and the transition of black to white lines represent the maximum to minimum values of conditionals.

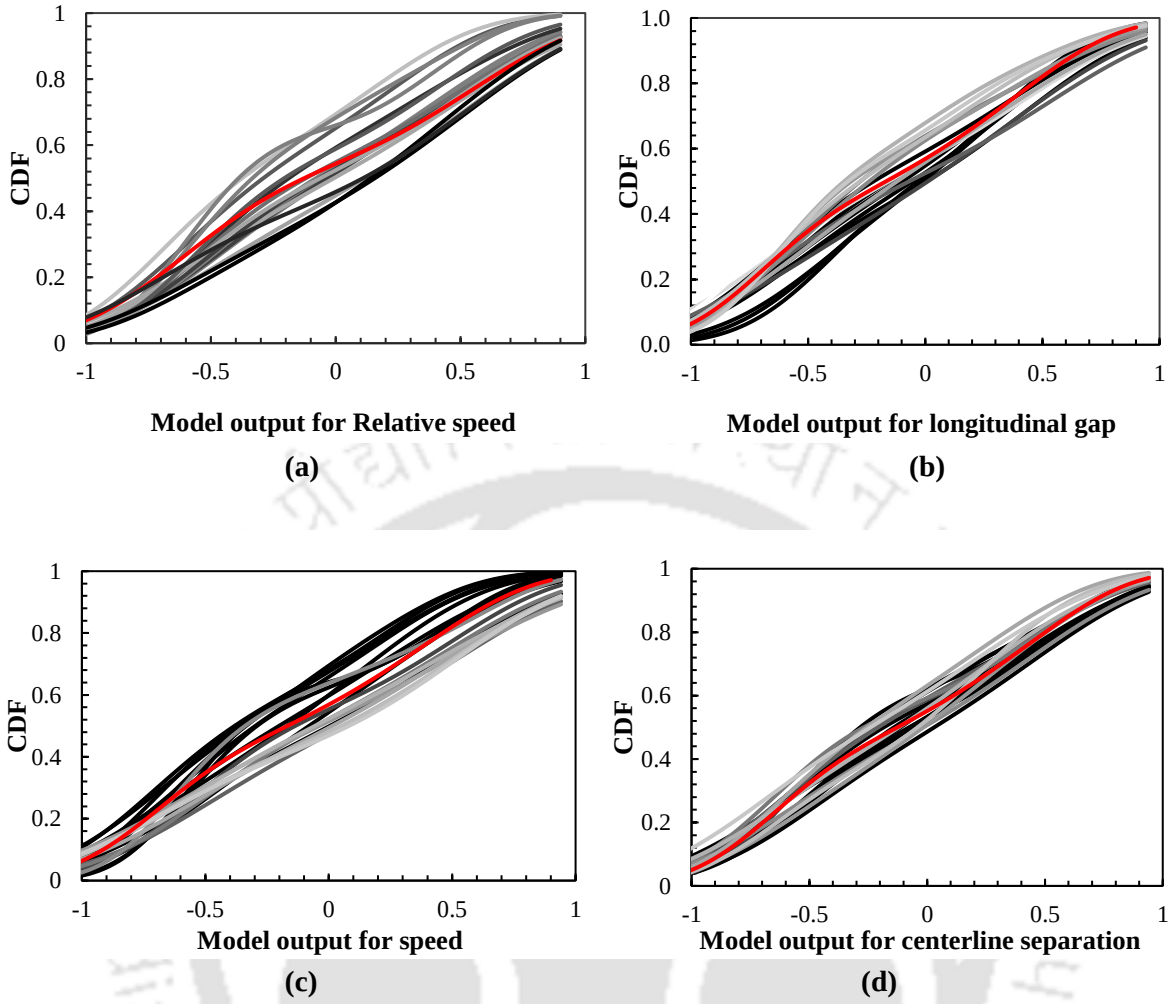

Note: Transition of black to white lines represent the maximum to minimum values of conditionals

Figure 5.11. Cumulative distribution function curves of the model output for each input parameter **(a)** relative speed **(b)** longitudinal gap **(c)** speed and **(d)** centerline separation

As can be observed from the figure, the conditional curves of different input parameters present different discrepancies between the unconditional and conditions CDF functions. A greater separation distance between $F_y(y)$ and observed $F_{y|x_i}(y)$ is observed for relative speed and longitudinal gap while it is comparatively lower for speed and centerline separation. This indicates that relative speed and longitudinal gap have a significant effect on the model response, followed by speed and centerline separation between vehicles.

The figure also provides relevant information about the model behaviour when the levels of conditioning of each input variable are varied. More precisely, the transition of dark lines to clear lines indicate greater to lower values of conditioning respectively. It can be observed that increments in the relative speed, longitudinal gap and centerline separation values increase the model output, indicating acceleration responses. This is in congruent with the actual car-following behavioural phenomena where drivers make the decision to accelerate as soon as they become aware of the positive relative speed and simultaneously, when longitudinal gap increases, drivers make adjustments in their accelerations in order to maintain a desirable

minimum safe longitudinal spacing. Importantly, the model response with respect to centerline separation further signifies that lower the hindrance offered by the leading vehicle at large CS, a wide forward visual field and higher level of safety is apperceived by the following drivers and therefore, more is the acceleration response. On the other hand, from Figure 5.11(d), it is observed that the acceleration of the following vehicle is inversely proportional to the speed. This is quite logical because drivers already proceeding at higher speeds have lesser tendency to accelerate further although they have to be more aggressive while responding to a decelerating leading vehicle in order to avoid possible risks of rear-end collisions. The PAWN sensitivity index is also calculated for each variable and the results are presented in Table 5.7.

Table 5.7. Relative importance of input variables

Parameter	Sensitivity Index, T_i
Relative speed	0.6339
Longitudinal gap	0.5725
Speed	0.4416
Centerline separation	0.3640

The results of the sensitivity index indicate that relative speed is the most significant parameter (0.6339) for predicting response of the following vehicle in car-following scenario, followed by longitudinal speed (0.5725), speed (0.4416) and centerline separation (0.3640). The magnitude of the indices signifies that although the influence of some variables is smaller, their contribution is important for the modelling process. It is therefore important to mention that although RS, LG and speed are the most commonly used input parameters in most of the car-following models, the research work provides enough evidence that the lateral descriptor of vehicle interaction (CS) offers a significant role in predicting the dynamic non-linear behavioural phenomena of drivers in car-following scenario of non-lane based traffic environments.

5.2.4. Evaluation of the proposed model

Fundamentally, a model developed to describe the realistic dynamic car-following behaviour must be dynamically stable for real traffic conditions. For instance, in a close car-following event, an acceleration or deceleration of a vehicle may be small but this small disturbance might be amplified and preserved in the system over time, implying sensitive dependence on the initial conditions, which can even result in potential rear-end collisions. The system is said to be *stable* if the response decays over time while if the response is pure oscillatory or amplified, the system is said to be unstable. The proposed model therefore needs to be checked for traffic stability corresponding to varying initial conditions. This section applies the developed car-following model to the analyses of closing-in and shying-away behaviour, local and asymptotic stability properties in the car-following process.

5.2.4.1. Closing-in and shying-away

The closing-in and shying-away behaviour are essentially related to a pair of vehicles when the driver of the following vehicle tends to close-in if the longitudinal gap is large for a given speed and shies-away if the following vehicle (FV) is closer to the leading vehicle (LV) irrespective of the actions of the leading vehicle. Chakroborty and Kikuchi (1999) provided an elaboration on the philosophical ramifications of a model's inability to describe this behaviour. To illustrate that the proposed model can describe the behaviour of closing-in and shying-away, two cases are considered with respect to different positioning of the following vehicles (that is, at different CS):

Case 1: Initial speed of LV and FV 11m/s, Initial longitudinal gap 24m, LV neither accelerates nor decelerates at different CS levels (0m, 0.5m, 1.5m)

Case 2: Initial speed of LV and FV 11m/s, Initial longitudinal gap 4.5m, LV neither accelerates nor decelerates at different CS levels (0m, 0.5m, 1.5m)

Note that, in both the cases the leading vehicle continues to move at its initial speed (*no perturbations*). The longitudinal gap (LG) versus time plot for different values of CS are presented in Figure 5.12.

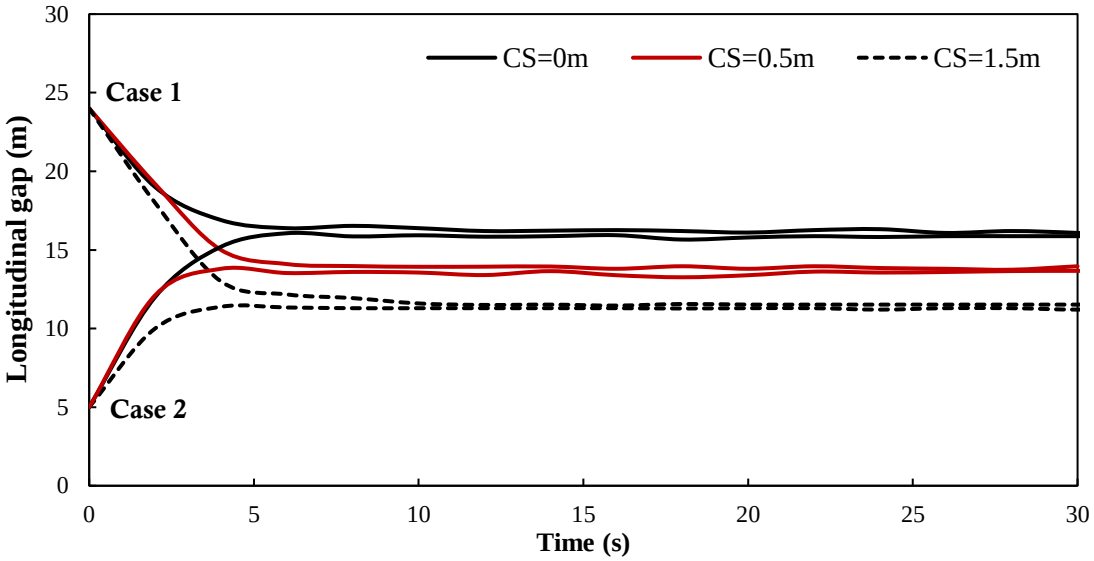

Figure 5.12. Variations in longitudinal gap for different CS values describing the closing-in and shying-away behaviour

From the figure, it is evident that when initial LG is large (*Case 1*), the FV accelerates and then decelerates to reduce the available gap and reach a safe stable distance, despite the fact that the LV maintained a constant speed. This change in the dynamic response from acceleration to deceleration occurred because the driver perceives initial longitudinal gap of 24m to be quite large for a speed of 11m/s. However, when the initial LG is small (*Case 2*), the following vehicle decelerates and then accelerates to increase the space gap to a safe value. This indicates that although the initial relative speed is zero, the driver of the following vehicle

makes continuous adjustments in their accelerations (or, speeds) to achieve a stable longitudinal gap.

Interestingly, the closing-in and shying-away behaviour are also observed at different lateral separations between the cars, indicating that the model can describe the stability at different CSs. While the system stabilizes at about 16m in the actual car-following scenario (CS=0), the stable longitudinal gaps for the staggered-following scenario are achieved at even lower gaps, 13.5m and 11m for CS of 0.5m and 1.5m respectively. It is quite evident because as the lateral separation increases, lower is the hindrance offered by the LVs, drivers are more confident about the anticipated actions of the preceding vehicle, therefore higher is the tendency to follow the LVs closely with lower longitudinal gaps.

5.2.4.2. Local stability

Local stability considers the localized behaviour between a pair of vehicles. More specifically, it is related to how the driver of the following vehicle responds to a fluctuation or unstable motion of the leading vehicle. In general, the actions of the FV should be such that the longitudinal gap eventually stabilizes to a safe stable longitudinal gap after an initial disturbance. This stability criteria is examined for two different cases:

Case 1: different initial longitudinal gaps of 25m, 15m and 10m, initial and final speeds of LV and FV 15m/s, LV decelerates and then accelerates at 0.5m/s^2, CS at 0.5m.

Case 2: same initial longitudinal gap 25m,

(a) different initial speeds of LV and FV 5m/s (LV accelerates at 3m/s^2), 10m/s (LV accelerates at 2m/s^2), 15m/s (LV accelerates at 1m/s^2), final speed of LV and FV 20m/s;

(b) different initial speeds of LV and FV 15m/s (LV decelerates at 1m/s^2), 20m/s (LV decelerates at 2m/s^2), 25m/s (LV decelerates at 2.5m/s^2), final speed of LV and FV 10m/s.

Results from the two considered scenarios are presented though speed profiles of the following vehicle and longitudinal gap versus time plots. The variations in following vehicle's speeds and longitudinal gap over time for *Case 1* corresponding to different initial longitudinal gaps are depicted in Figure 5.13.

It is clear from Figure 5.13(a) and Figure 5.13(b) that in all the three cases (that is, for different initial longitudinal gaps), vehicle speeds and longitudinal gaps have converged to a stable condition. The stability is achieved at a longitudinal gap of about 16m when the LV and FV are laterally separated by 0.5m proceeding at speeds of 15m/s. The observed pattern justifies that the stable longitudinal gap achieved under local stability conditions is independent of initial longitudinal gaps. This is in congruence with the properties of local stability underlined in Chakroborty and Kikuchi's (1999) work.

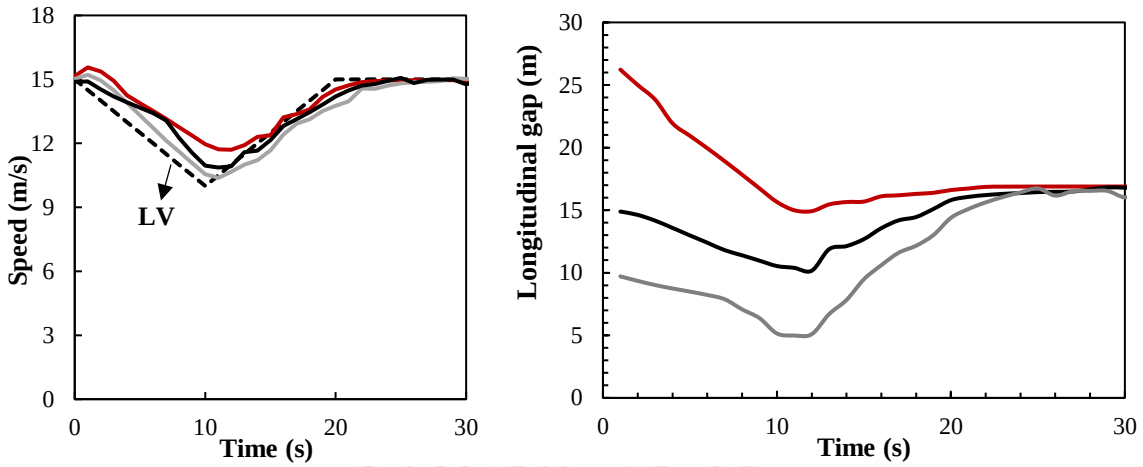

(a) (b)

Figure 5.13. (a) Perturbation in speed and **(b)** Local traffic stability for different initial conditions of longitudinal gap

Moreover, the speed profiles and longitudinal gap versus time plot for *Case 2* corresponding to same initial longitudinal gap, different perturbations in LVs' accelerations and initial and final speeds, are presented in Figure 5.14.

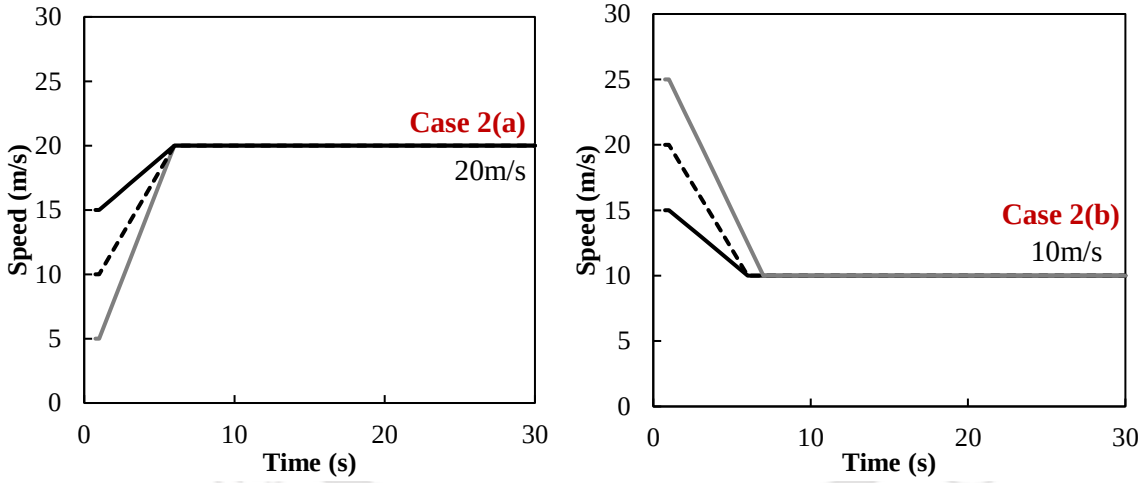

(a)

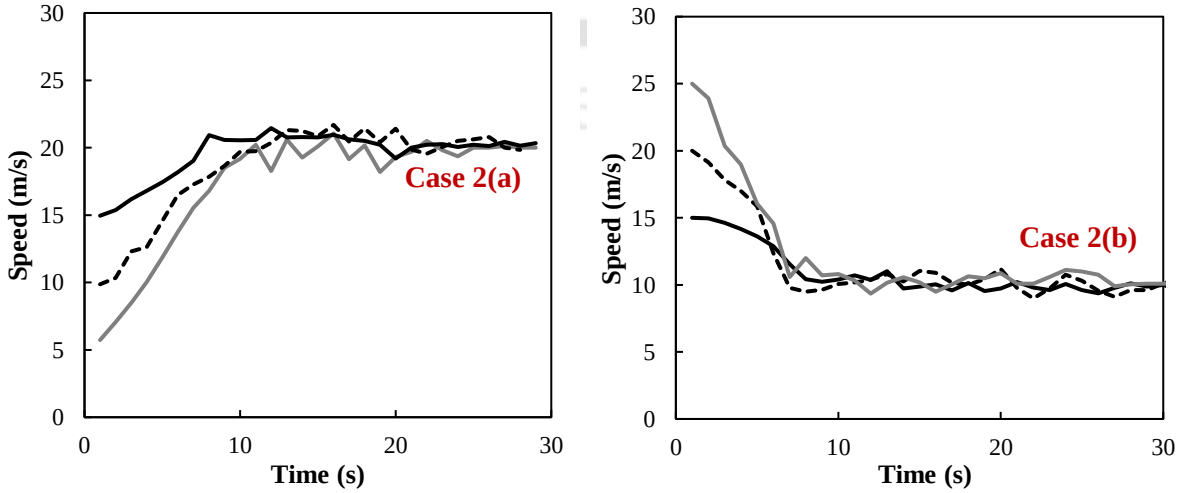

(b)

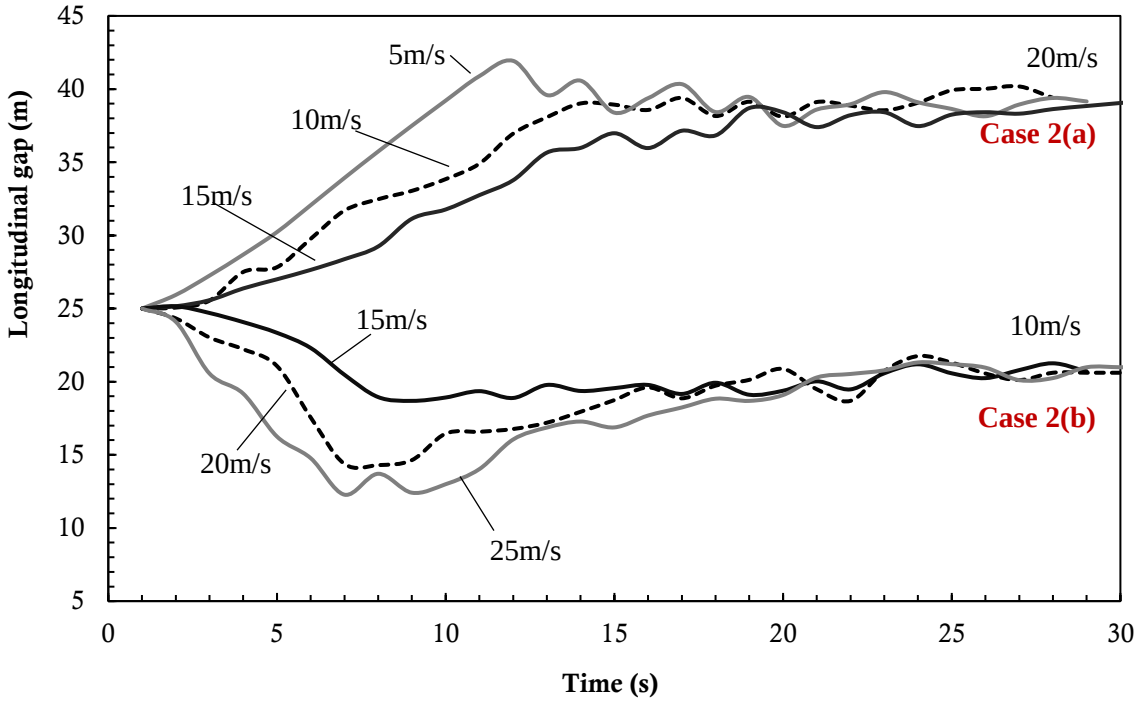

(c)

Figure 5.14. Perturbations in initial speeds and final speeds of **(a)** leading vehicle **(b)** following vehicle and **(c)** Local stability for different considered cases

Results obtained from the developed model justify that in response to different perturbation patterns of the LV and different initial and final speeds of the vehicles, local stability has been attained in both the scenarios. The fluctuations in longitudinal gap in proximity to the stable values are observed to be more for each considered case, suggesting the susceptibility of the FV to the action of the LV. This further concludes that the stable safe longitudinal gap is dependent only on the final speeds of the LV and is independent of the initial LG, initial speed and actions of LV (acceleration/ deceleration). Regardless of the initial speeds, the results show that the stable gap approaches a higher value at a higher speed.

5.2.4.3. Asymptotic stability

Asymptotic stability is related to the manner in which a perturbation in the motion of the leading vehicle propagates through a stream of vehicles. A platoon is said to be asymptotically stable if the perturbation introduced by the leading vehicle gradually reduces as it is transmitted upstream from one vehicle to the next. The aim of this section is to investigate whether the predictions of the proposed model satisfy the property of asymptotic stability. To illustrate such stability property, it is assumed that the platoon consists of 10 cars including the leading vehicle and initial longitudinal gap between any two vehicles is 25m. The first car decelerates from 15m/s to 10m/s in 5s, then accelerates back to 15m/s in 5s, and thereafter travels at a constant speed of 15m/s. Figure 5.15 shows how the longitudinal gap between any two vehicles in a platoon varies when the leading vehicle initially decelerates and then accelerates.

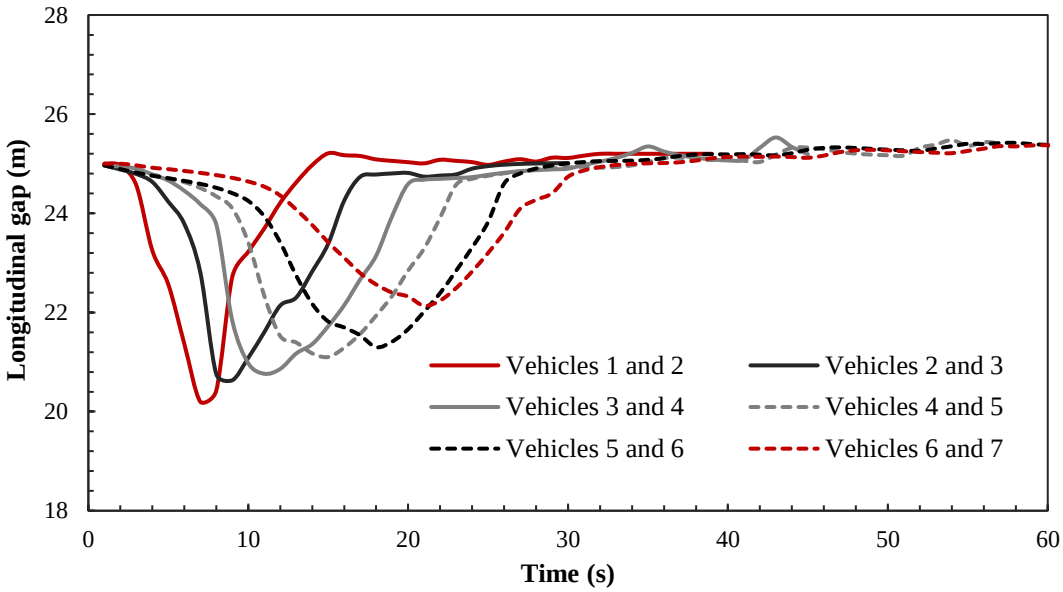

Figure 5.15. Variations in longitudinal gap in a 10-car platoon illustrating asymptotic stability

As can be observed from the figure, the peak in the longitudinal gap variations reduce from the downstream vehicle pair towards the upstream side of the platoon. That is, the perturbation in longitudinal gap variations is much higher for the first LV and the first FV (vehicles 1-2) than that for the first FV and the second FV and gradually, it appears to be the least for eighth FV and ninth FV (vehicles 6-7). This indicates that the asymptotic stability condition is attained and the proposed model is able to predict such behaviour.

5.3. Comparison of the proposed ANN model with existing models

As stated above, a number of prominent work related to the development of car-following models and theories enabled a plausible characterization of human driving behaviour. Over the years, various researchers have recommended several traditional engineering CF models such as Gazis-Herman-Rothery models (Gazis et al., 1961), safe distance models (Kometani and Sasaki, 1958; Gipps, 1981), psychophysical models (Wiedemann and Reiter, 1992), Optimal Velocity model (Bando et al., 1993) and Intelligent driver model (Treiber et al., 2000a) to model CF behaviour. Yet, recent literature has underlined that Gipps' model is more extensively used to depict CF behaviour of both lane-based and non-lane based traffic environments, whereas many researchers argue that acceleration-based models offer more realistic behaviour than the speed-based models. In this light, the traditional acceleration-based CF models that have received considerable attention over the years namely Gazis-Herman-Rothery (GHR) model and Intelligent Driver model (IDM), and the extensively used speed-based model namely Gipps' model, are used as reference models for the comparison with the developed ANN-based car-following model.

This section therefore provides a theoretical basis of each considered engineering mathematical CF models (namely, Gipps', GHR and IDM) with discussion on the calibration process, followed by evaluation of error-based performance measures of the considered

engineering models and the data-driven ANN based model, thus providing evidence about the better predictability of dynamic realistic human driving car-following behaviour.

5.3.1. Estimation of engineering CF models

5.3.1.1. Gipps' model

Gipps' model assumed that the subject vehicle tends to choose the velocity that can avoid rear-end collision if the leading vehicle performs emergent braking (Gipps, 1981). The speed attained by a vehicle based on Gipps' model at a given time instant *(t+ τ)* can be formulated as

$$v_{FV}(t+\tau) = min\begin{cases} v_{FV}(t) + 2.5a_{FV}\tau\left(1-\frac{v_{FV}(t)}{V_{FV}}\right)\sqrt{\left(0.025+\frac{v_{FV}(t)}{V_{FV}}\right)} \\ b_{FV}\tau + \sqrt{b_{FV}^2(\tau)^2 - b_{FV}\left[2(x_{LV}(t)-s_{LV}-x_{FV}(t)) - v_{FV}(t)\tau - \frac{v_{LV}^2(t)}{\hat{b}}\right]} \end{cases}$$

where a_{FV} is the maximum acceleration that the following vehicle (FV) driver wishes to undertake,

b_{FV} is the most severe braking that the FV wishes to undertake

s_{LV} is the effective size (physical size + some margin) of the leading vehicle

V_{FV} is the desired speed of the following vehicle

$\hat{b}$ is the estimation of b_{FV} employed by the driver of FV and

τ is driver's reaction time.

A genetic algorithm (GA) based optimization technique is used to calibrate the parameters of the model, where calibration involved minimizing the percentile error between the observed (v_{obs}) and the predicted speeds (v_{sim}) of the following vehicle expressed as

$$E_P = \frac{\sum_{i=1}^{N}|v_{obs_i} - v_{sim_i}|}{\sum_{i=1}^{N}|v_{obs_i}|}$$

The genetic parameter values used for optimization are population of 100, maximum number of generations 500, crossover probability 0.4 and mutation probability of 0.1. The parameter values yielding minimum percentile errors are considered as calibrated parameters and the GA-based calibration resulted in parameter values of b_{FV}=-2.307, $x_{FV}(t)$=9.656, $\hat{b}$=-2.851, V_{FV}=20.843, τ=0.983, a_{FV}=1.616. A comparison of the observed and predicted speeds is presented in Figure 5.16. The figure depicts good representation of predicted speeds with the observed speeds yielding a mean squared error of 9.30%.

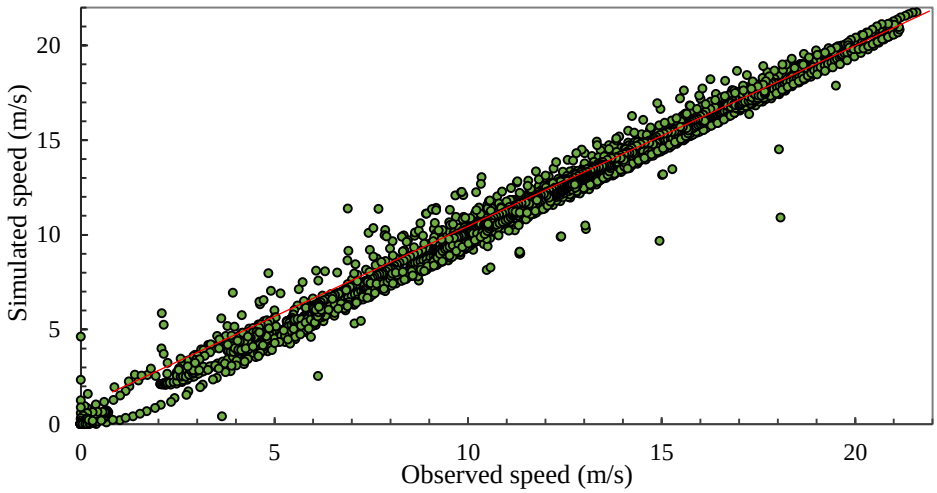

Figure 5.16. Comparison of observed and predicted speeds of Gipps' model

5.3.1.2. Modified GHR model

The general formulation of the GHR-based stimulus-response car-following model is expressed as

$$a_{FV}(t+\tau) = \beta_1 Speed^{\beta_2} RS^{\beta_3} LG^{\beta_4}$$

where $a_{FV}(t+\tau)$ is the acceleration of the following vehicle (FV) at time $t+\tau$
τ is the driver's perception-reaction time,
RS and LG are relative speed and longitudinal gap respectively,
$\beta_1, \beta_2, \beta_3, \beta_4$ are the calibration parameters.

The estimated model is an extension of the model developed by Siuhi and Kaseko (2013). Separate acceleration and deceleration responses of the following vehicle are considered and the parameter estimation for the acceleration and deceleration models are conducted by non-linear least squares regression approach. The estimated parameters of GHR models for acceleration and deceleration responses can thus be expressed as:

$$a_{FV}(t+\tau) = 2.225 Speed^{-0.161} RS^{0.638} LG^{0.439} \quad \text{acceleration}$$

$$a_{FV}(t+\tau) = 0.357 Speed^{0.788} RS^{1.000} LG^{-0.597} \quad \text{deceleration}$$

The estimated model parameters obtained for driver sensitivity constant (β_1) indicate that drivers are more sensitive to a decelerating leading vehicle than an accelerating one because of safety concerns or to avoid possible risks of rear-end collisions. For the speed parameter (β_2), the signs for acceleration and deceleration response indicates that higher the speed of the vehicle, lower will be the tendency to accelerate further but higher will be its response towards a decelerating leading vehicle. Higher magnitude of deceleration response further indicates that drivers are more aggressive towards a decelerating vehicle, therefore the magnitude of decelerating response is higher than acceleration response. In a similar manner, the relative speed parameter (β_3) indicates that larger the relative speed, larger is the response of the following vehicle, irrespective of acceleration and deceleration response; and higher magnitude

of deceleration response justifies that drivers respond with higher magnitude while decelerating. The longitudinal gap parameter (β_4) further suggests that larger the separation between vehicles, larger will be the magnitude of acceleration response while when separation is smaller, drivers will respond with higher deceleration rate to reduce collision risks. A comparison of the observed and predicted responses (acceleration/deceleration) of the GHR model is presented in Figure 5.17 and the corresponding mean squared error in predicting acceleration/deceleration was obtained as 14.24%.

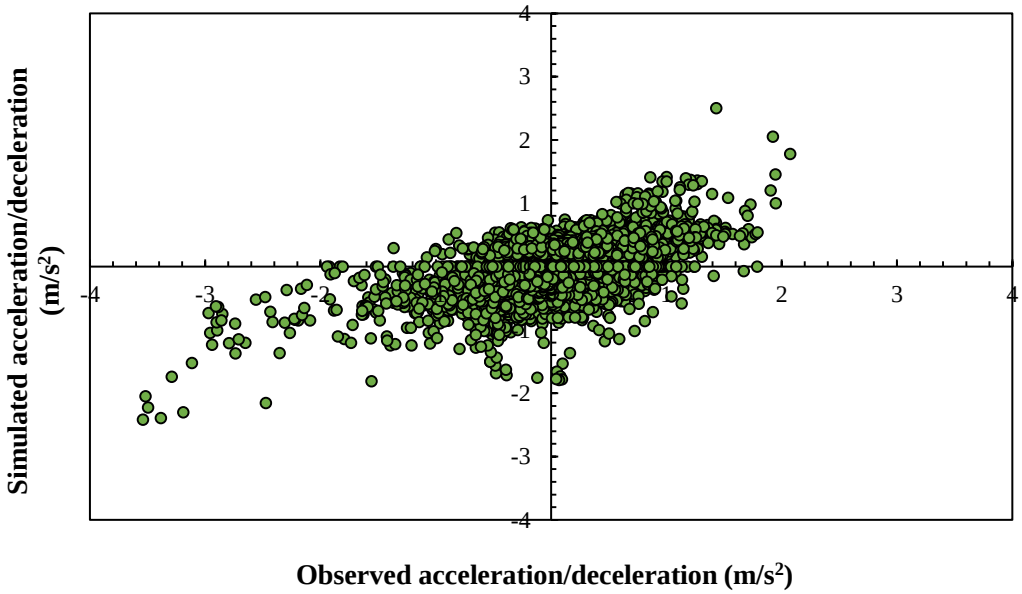

Figure 5.17. Comparison of observed and predicted accelerations of GHR model

5.3.1.3. Intelligent Driver Model

The model combines both free-road acceleration and deceleration strategies of the following vehicle and is a function of the velocity, gap and the velocity difference to the preceding vehicle (Treiber et al., 2000a). The acceleration function is given by

$$a_n = a_{max}\left(1 - \left(\frac{v_n}{v_n^0}\right)^{\delta} - \left(\frac{s_n^0 + T_n v_n - \frac{v_n \Delta v_n}{2\sqrt{a_{max} b_n}}}{s_n}\right)^2\right)$$

Where a_{max} is the maximum acceleration of vehicle *n*,

v_n^0 is the desired velocity of *n*,

δ is a parameter of the model (fixed as 4) which is used to characterize how the maximum acceleration of a vehicle decreases with increase in speed,

s_n is the actual gap available between the front bumper of the following vehicle and the rear bumper of the leading vehicle,

s_n^0 is the desired minimum gap,

b_n is the desired deceleration of the vehicle *n*,

s_n^0 is the jam distance of the vehicle *n* and

T_n is the safety time gap of the vehicle *n*.

The calibration of IDM model is performed using GA based optimization technique considering spacing as a measure of performance (MoP) and root mean square normalised error (RMSNE) as a goodness-of-fit criteria. Punzo and Montanino (2016) confirmed superiority of spacing over speed in model calibration and validation. Conversely, RMSNE has been preferred as a goodness-of-fit criterion for IDM model calibration (Sharma et al., 2019; Ciuffo and Punzo, 2010; Toledo et al., 2003). RMSNE can be mathematically formulated as:

$$RMSNE = \sqrt{\frac{1}{N}\sum_{i=1}^{N}\left(\frac{LG_{obs_i} - LG_{sim_i}}{LG_{obs_i}}\right)^2}$$

Where LG_{obs_i} and LG_{sim_i} denote the observed and simulated spacing at ith time step respectively and N denotes the total time-steps. Accordingly, the calibrated parameters are obtained as a_{max}=0.416, v_n^0=16.592, s_n^0=0.861, T_n=0.395 and b_n=1.965. The acceleration (a_{max}), desired deceleration (b_n) and desired velocity (v_n^0) values are quite in agreement with the calibrated values obtained in Treiber and Kesting's (2013) work but the desired minimum gap and time gap values are quite lower than that obtained in other research work. This is because drivers in disordered systems often tend to follow the preceding vehicles closely maintaining large lateral separation, thereby resulting in lower longitudinal gaps and time gaps (explained elaborately in Chapter 4). Figure 5.18 illustrates the acceleration/deceleration predictions from the IDM model with the observed data, yielding a mean squared error of 19.6%.

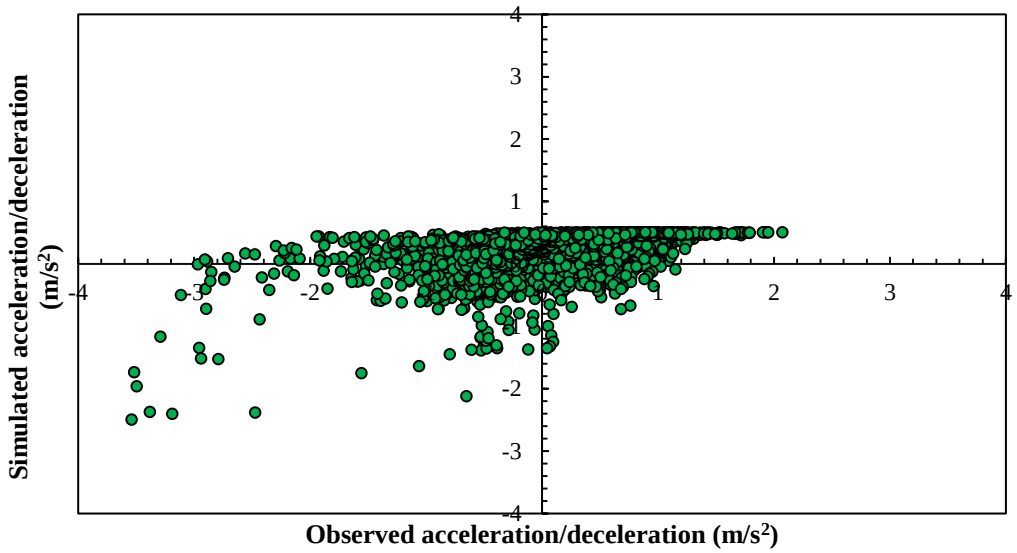

Figure 5.18. Comparison of observed and predicted accelerations of IDM

5.3.2. Results and performance comparison

Since the developed ANN model has different property to analytical car-following models, a comparison of the ANN model with the calibrated Gipps, modified GHR and IDM models is further conducted at a trajectory level. For this purpose, the capability of the developed model is evaluated with the validation data that were not used in the model development. The specification used in this process involved predicting a follower's trajectory based on initial

state of the data-driven leader and follower that includes initial longitudinal gap between leader and follower and initial speed of the follower, and consequently simulating the responses of the following vehicle. The simulated responses from the ANN model and different classical CF models are then further processed to estimate corresponding speeds and distances using basic kinematic equations. The plots of the observed space trajectory of a leader-follower pair and the corresponding follower's trajectory simulated by different models are presented in Figure 5.19.

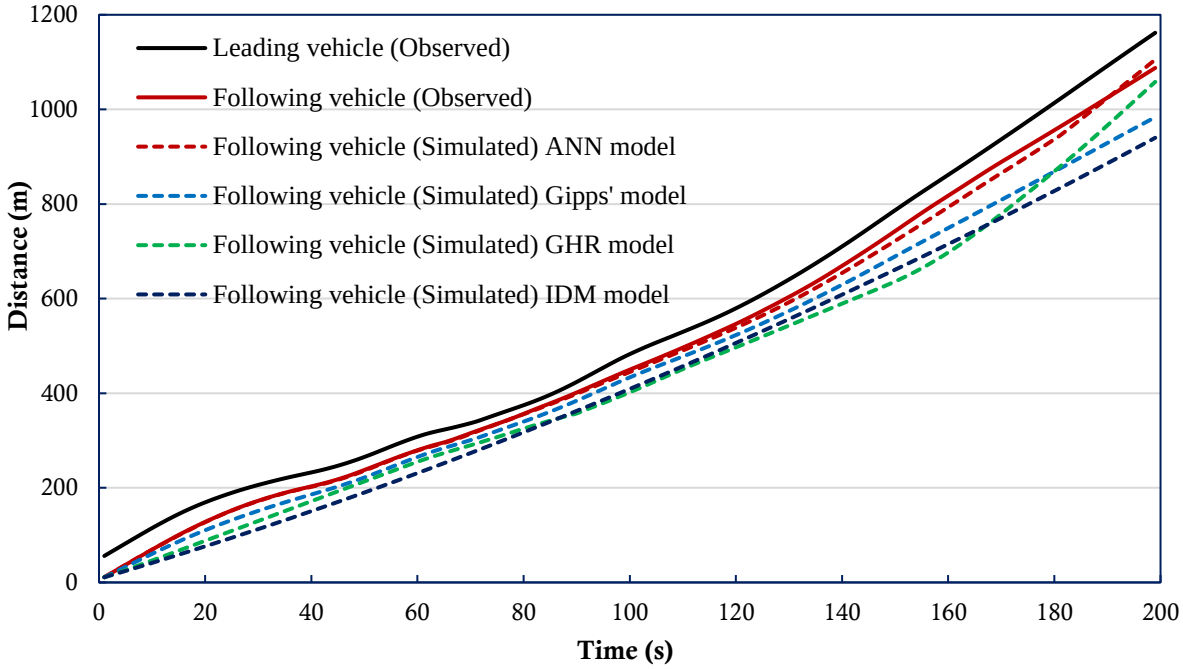

Figure 5.19. Observed and simulated space-time trajectories of the followers for different CF models

Subsequently, the error metrics in observed and simulated accelerations, speeds and distance for the developed ANN model and the considered classical models (Gipps, modified GHR and IDM) are further evaluated (shown in Table 5.8). As illustrated in Figure 5.19, the ANN model fit field data very well as compared to other classical model and predicts responses (acceleration) with MSE 3.1%. Among the classical CF models, the Gipps' model has more accurate predictions in speed and distance estimation, followed by modified GHR and IDM models. However, the modified GHR model has better correspondence with the data than the IDM model. The simulated trajectory of the modified GHR model could represent the acceleration patterns more efficiently than the IDM model, which can also be confirmed from the observed and predicted acceleration patterns of Figure 5.17 and Figure 5.18. The error metrics presented in Table 5.8 further corroborates the results. From the simulated space-time plots and estimated error metrics, it is therefore evident that the developed ANN model outperforms the classical car-following models, with Gipps' model providing better prediction accuracy compared to modified GHR and IDM models.

Table 5.8. Error measures for different models

	Error metrics	ANN	Gipps	GHR	IDM
Acceleration	RMSE	0.176		0.305	0.410
	MAE	0.125		0.228	0.322
	MSE	0.031		0.093	0.167
Speed	MAPE	0.043	0.238	0.451	0.572
	RMSE	0.565	2.085	4.328	4.718
	MAE	0.421	1.642	3.568	4.520
	MSE	0.318	4.348	18.737	22.245
Distance	MAPE	0.012	0.073	0.134	0.152
	RMSE	11.254	45.709	61.644	67.540
	MAE	7.660	35.341	53.541	58.400

Recapitulating the above discussion, a comparison between the predicted responses from Gipps', GHR and IDM models with the observed training data resulted in 9.30% MSE in speed, 14.24% and 19.6% MSEs in accelerations respectively. Conversely, the mean squared error from the ANN based CF model was obtained as 5.70%, which is comparatively lower than the prediction errors obtained in GHR and IDM models, thereby justifying the better predictive capability of the developed ANN model. A stronger performance of the ANN model in predicting the trajectories and lower errors estimated in acceleration, speed and distance estimation, as compared with the classical CF models further corroborated the better performance of ANN-based CF model in predicting realistic car-following human driving behaviour in non-lane-based traffic environments.

5.4. Chapter summary

Early assumptions on core car-following models were primarily rooted in the classical paradigm which gradually embraced exposure to realistic behavioural predictions, yielding a number of widely-used and more influential car-following (CF) models. Characterizing human factors in the model has become an indispensable factor in evaluating model performance. Yet, a significant problem that has become increasingly apparent in model development is the absence of high-fidelity accurate and reliable dynamic time-series data, with which CF behaviour can be realistically modelled and compared. Utilizing dynamic data obtained from an image-based in-vehicle trajectory extracting system, this chapter has illustrated that development of two-dimensional (2D) data-driven single leader-single follower car-following models could substantially improve the complex behavioural predictions of drivers in disordered traffic systems.

Preliminary investigation on the choice of input variables in car-following model development using factor analysis revealed the importance of response variable (following vehicle's acceleration), longitudinal descriptors such as relative speed, longitudinal gap, speed, and lateral descriptor (centerline separation) in explaining the car-following phenomena (or, staggered following behaviour) of non-lane-based systems. Considering complex human driving process associated in disorderly traffic scenario, an artificial neural network (ANN)-

based CF modelling framework is advocated as a powerful tool to deal with uncertainties of human driving process. Prior to the model development, driver's reaction delay was estimated based on *stimulus-response* framework. A comparison of instantaneous delay with fixed delays (0.4s, 0.6s and 0.8s and 1) for the design of an ANN based CF model illustrated the consideration of 0.6s reaction delay as suitable to model the car-following behaviour with an ANN architecture (4-30-1), consisting of four inputs, 30 neurons in the hidden layer and one output.

Results of the global sensitivity analysis indicated that although RS, LG and speed are the most commonly used input parameters in most of the car-following models, CS offers a significant role in predicting the dynamic non-linear behavioural phenomena of drivers. The proposed model could also explain the closing-in and shying-away behaviour, local and asymptotic stability properties in the car-following process, depicting realistic behavioural characterization of the model from traffic stability standpoint. A comparison of the developed ANN model with the classical CF models (such as Gipps, GHR and IDM models) further corroborated that ANN model significantly outperforms the classical models in reproducing trajectories. In this regard, the proposed model can be used to complement classical car-following models in predicting responses of the following vehicle in car-following scenario of disorderly traffic systems.

6

Modelling of Two-Leaders Car-Following Behaviour

Car-following literature has emerged progressively throughout the twentieth century to dynamically document realistic complex human driving behaviour. Research focused on the preceding chapters provided substantial evidence that incorporating lateral descriptor of vehicle interaction in modelling staggered-following behaviour enrich the realism and depiction of dynamic process of human driving behaviour. Usually, drivers in a following regime are subjected to a multitude of complex driving tasks and subsequently based on the notion of *satisficing approach,* they adapt to the prevailing traffic conditions. The driving-related tasks however, become even more complex in disordered systems because of irregular and sporadic behavioural adaptations to varying driving regimes. With single-leader single-follower car-following models forming the cornerstone in the development of many microscopic simulation models, the anticipatory behaviour of drivers in the presence of more than one leader or two nearest vehicles ahead has recently received considerable attention mainly in the context of behavioural modelling of disordered traffic systems.

In the context of multi-leader car-following behaviour, this chapter primarily focusses on the behavioural response of the subject driver considering two leading vehicles ahead. Understanding how drivers apperceive the driving scenario, how they sense stimulus from the vehicles, how they perform control actions against real-time variations in vehicle dynamics and subsequently how the stimulus of leading vehicles affect the behavioural process of drivers in two-leaders following regime deserves symbolic emphasis on modelling such complex dynamic behaviour. The multi-vehicle interactions being poorly delineated in the literature, have causal behavioural sequences influencing their control processes, which if modelled realistically, would substantially enhance the reliability of microscopic simulation models. To address and model such behaviour, this chapter is divided into three broad sections:

1. *Estimation of time-series data for understanding two-leader interaction behaviour*: This section begins with the two-leaders interaction phenomena of drivers, followed by a preliminary analysis on the processed time-series data, describing behavioural differences in the following manoeuvre of drivers in response to multiple sources of stimuli and varying traffic conditions.

2. *Development of data-driven based two-leader single follower car-following model:* An ANN-based modelling framework is proposed to explain the complex non-linear anticipatory behaviour of drivers considering varying reaction delays. A global sensitivity analysis is conducted, justifying the relative contribution of the considered variables, and the proposed model is further evaluated from the model stability standpoint.

3. *Comparison with existing models and its applications:* This section highlights a few work on multiple-leaders car-following behaviour and a comparison of the proposed model is made with the existing classical models.

6.1. Estimation of time-series data for understanding two-leader anticipative behaviour

Existing studies have demonstrated that drivers do not just respond to the vehicle in-front, but also to the nearest vehicles ahead, positioned within the influence zone. While some researchers have highlighted the influence of two direct leaders in the same lane (Hoogendoorn and Ossen, 2006; Lenz et al., 1999), recent literature oriented to behavioural modelling of non-lane based systems has addressed the need to analyze the following behaviour with next-nearest neighbor interaction (Zheng et al., 2012; Li et al., 2015a). Most of the proposed models explaining such multi-leader behaviour are the extensions of Optimal Velocity Models where the stability analysis has been conducted so far through numerical simulations. Yet, a proper, reliable and dynamic time-series database is still lacking that can elucidate the non-linear behavioural process of following drivers in the presence of two leading vehicles ahead. This section aims to explain the multi-leader behavioural phenomena of following drivers, with a preliminary assessment on the descriptive properties of the extracted data and detailed exploration on the behavioural differences of drivers in response to multiple stimuli and varying lateral positions of the vehicles ahead.

6.1.1. Two-leader anticipative behaviour

Drivers in general are active and highly adaptive to changing traffic environments. In a two-leader car-following scenario, the following drivers are assumed to anticipate the actions of both the left-front and right-front interacting vehicles and consequently, based on the dynamics of the leaders, they adjust their speeds and positions in an attempt to obtain a comfortable and safe spacing with the leaders. A graphical representation of the two-leader following scenario considered in this research work is illustrated in Figure 6.1.

Unlike single-leader staggered-following scenario, drivers in a two-leader following regime are associated with more complex driving-related tasks in which they attempt to foresee the behaviour of both the vehicles simultaneously, keep a constant visual record of the forward scenario and maintain certain awareness in order to safely control the vehicle, if in any case,

one (or both) the leaders apply emergency braking. In such scenario, drivers adopt the *satisficing strategy* to maintain a desired and minimum safe longitudinal gap with certain off-centeredness between each of the leaders such that they can apperceive the forward visual field and anticipate leaders' actions with more confidence. Essentially, when more than one leader is present, drivers need to be situationally aware of the anticipated actions of both the leading vehicles, thereby resulting in more complex interactions among the vehicles. Because of the anticipative behaviour, the following driver can react more quickly to changes in the dynamics of the leaders and it will be interesting to evaluate distance-keeping behaviour of drivers in such scenario and provide empirical evidence regarding the same (which will be discussed in detail in later part of the chapter).

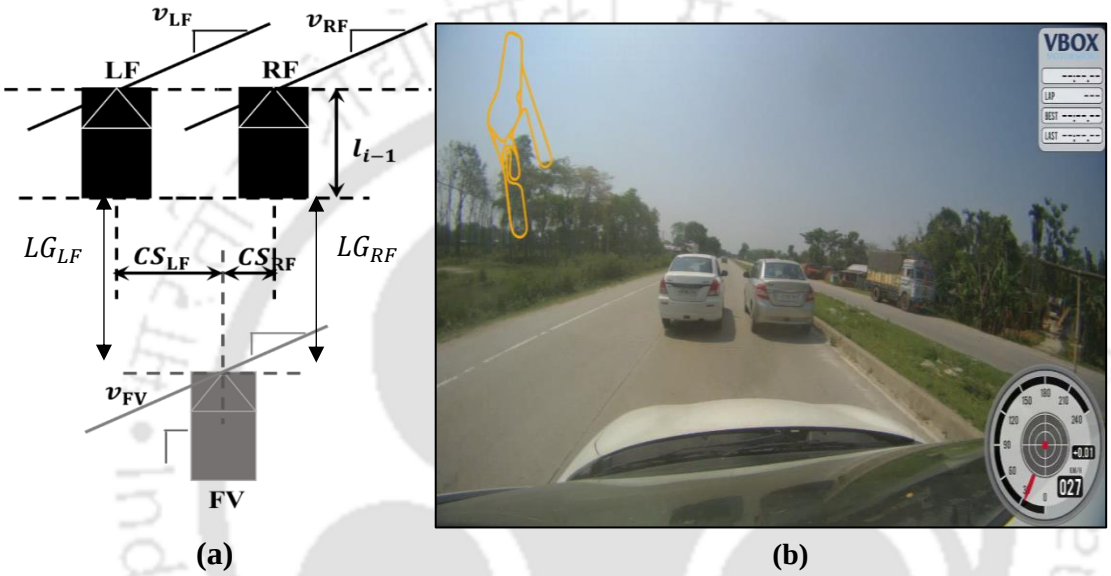

Note: FV- following vehicle, LV- leading vehicle, LF-left-front, RF-right-front, v_{LF}, v_{RF} and v_{FV} representing speeds of left-front, right-front and following vehicles respectively, CS_{LF} and CS_{RF} are the centerline separations of the following vehicles with the left-front and right-front vehicles respectively.

Figure 6.1. (a) Sketch of variables for a typical two-leader single-follower scenario and **(b)** real-time image of the front vehicles recorded from the camera

6.1.1.1. Selection of data

Before analysis can be undertaken, it is important to process the data extracted from the proposed GPS-based in-vehicle trajectory extracting approach such that any case of free-following scenarios are excluded. The experiment was performed in a controlled environment (on a four-lane divided highway) in which both the drivers of the front vehicles were instructed to maintain a specified speed, with significant overlap (in length) between the leading vehicles, and the subject driver had to follow the vehicles ahead by maintaining a safe and comfortable longitudinal and lateral spacing with them. All the vehicles considered in the experiment were of similar vehicle models so as to ensure that vehicle bias could be eliminated from the studied phenomena. Typically, the total duration of interaction for a specified scenario is dependent on how long the subject driver wished to remain behind the vehicles and following that, a range of interactions were captured for a wide variety of speeds. Data collected from the recruited

drivers involved estimating the speeds (v_{LF}, v_{RF} andv_{FV}) and acceleration/deceleration (acc_{LF}, acc_{RF} and acc_{FV}) of left-front (LF), right-front (RF) and subject/following vehicles (FV), measuring longitudinal distances to both the front-vehicles from the subject vehicle ($LG_{LF} = x_{LF} - x_{FV} - l_{LF}, LG_{RF} = x_{RF} - x_{FV} - l_{RF}$; l representing vehicle length) and lateral distances from the subject vehicle to the left-front and right-front vehicles (CS_{LF} and CS_{RF}) (refer Figure 6.1(a)). Based on the methodology discussed in section 3.3.2.3., the extracted two-leader car following data were filtered for further analysis. Only those trajectory data were considered to own significant two-leader following characteristics for which all the three interacting vehicles were jointly observed for a time period of at least 15s (Zheng et al., 2015). Further, to ensure that the dynamic following behavioural process is preserved, the processed data with more than 2m lateral clearance between the LF and RF vehicles are discarded.

6.1.1.2. The two-leader car-following process

Unlike in single-leader car-following process where the follower modulates throttle and brake in order to maintain a desired spacing with the leading vehicle, the control process of subject driver becomes even more complex when more than one vehicle is present in the front. In a two-leader following scenario, the follower not only attempts to keep a safe and comfortable spacing with one leader but she/he has to simultaneously assess the anticipated actions of both the leaders, and accordingly, maintains a desired longitudinal spacing and off-centeredness with each of the leading vehicle. This decision-making process is indeed governed by drivers' perceptions of vehicle speeds, proximity to each of the vehicle ahead, and judgement of available lateral clearance between the two leading vehicles to evaluate the possibility of passing/overtaking or following the vehicles in-front. The dynamics of the decision-making process, typically represented by the relative speed between left-front (LF) or right-front (RF) vehicles and the subject vehicle (SV), and the respective longitudinal spacing between them is illustrated in Figure 6.2.

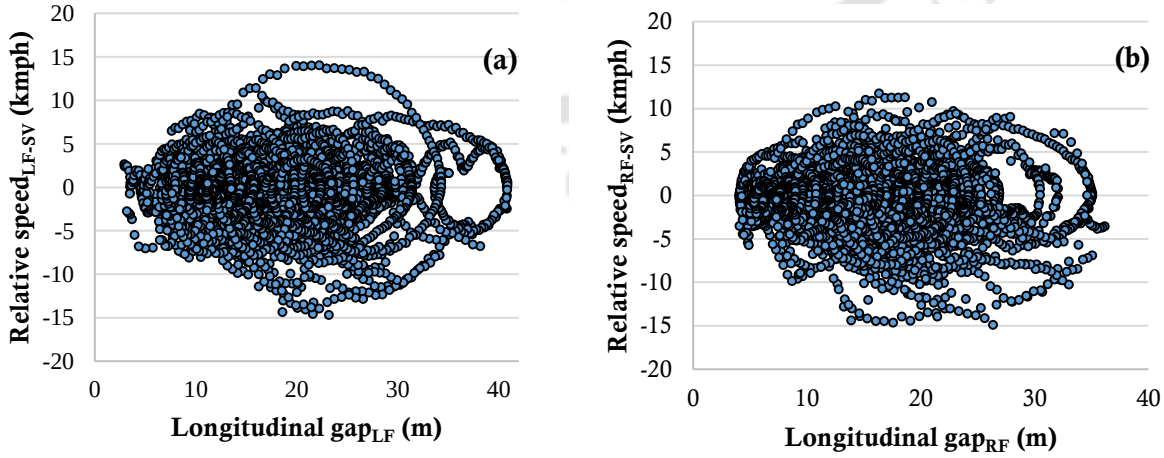

Figure 6.2. A typical following relationship showing relationship between relative speed and longitudinal spacing of subject vehicle with respect to **(a)** left-front vehicle and **(b)** right-front vehicle

An inspection of the time-series data for the two-leader following sequence with respect to LF and RF vehicles confirms that there is a great deal of variation between relative speed and longitudinal spacing for each pair of vehicles (LF/RF with SV), which is best displayed by the following spirals (as in Figure 6.2). These spirals are evocative of the following processes of subject driver interacting with both the left-front and right-front vehicles simultaneously across a variety of speeds, her/his perceptions of maintaining a desired speed, longitudinal and lateral spacing with either of the vehicle, and response time delay in reacting to the anticipated actions of the leaders. The adjustment of the driver to the behaviour of the vehicles in-front occurs at all speeds especially when the available spacing is smaller or larger than the desired and drivers overcompensate for small deviations from the desired spacing. These mini-spirals are an intrinsic part of the following process, carrying essential information on the behavioural process and response of drivers for a specified two-leader following sequence.

The processed dataset covers an entire spectrum of two-leader following interaction with the longitudinal spacing lying within 40m (*x*-axis of the spirals) and relative speeds in between -15kmph and 15kmph. The higher range of longitudinal spacing (40m vs. 30m) and amplifications in the mini-spirals (±15kmph vs. ±10kmph) observed in two-leader scenario as compared to single-leader single-follower regime can be attributed to a wider range of vehicle speeds (lying within 95kmph) considered in two-leader following sequence. A proper consideration of all these dataset would provide a deeper insight into the behavioural aspects of the followers over different sets of two-leader following regime.

6.1.2. Two-leader following data: preliminary exploration

The processed data containing information from initial acquisition to the termination of the following process resulted in a total of 10,743 sets of two-leader following events (at every 0.2s) during the entire observation period. The extracted data involved a sequential arrangement of two-leader following interactions in which the dynamics and behavioural process of the follower were apprehended for different positioning and speeds of the leading vehicles (both left-front and right-front).

Although collection of two-leader following time-series data in real environments proves to be challenging, however the data considered for this work still represents the diffuse nature of the following behaviour, containing a great deal of explanatory information. In particular, the derived trajectory dataset contained a detailed information on spacing-related variables such as longitudinal gap with both left-front (LG_{LF}) and right-front (LG_{RF}) vehicles and lateral spacing or centerline separation between the follower with the left-front (CS_{LF}) and right-front (CS_{RF}) vehicles, speeds (V_{LF}, V_{RF}, V_{SV}), acceleration/deceleration of all the three interacting vehicles, and also relative speeds between the LF ($RS_{LF,SV}$) and RF ($RS_{RF,SV}$) vehicles with the subject vehicle (SV). The basic descriptive statistics of the explanatory data pertaining to the two-leader following interaction regime, are provided in Table 6.1.

Table 6.1. Summary statistics of the extracted multi-leader following data

Considered variables	Range	Mean	Median	Std. dev.	5%ile	95%ile	N*
CS_{LF} (m)	[0, 3.12]	1.05	1.02	0.42	0.62	1.48	
CS_{RF} (m)	[0, 3.32]	1.11	1.09	0.53	0.56	1.69	
LG_{LF} (m)	[0.03, 39.77]	9.66	7.80	6.55	3.86	16.77	
LG_{RF} (m)	[0.02, 39.52]	9.18	7.80	5.92	3.84	15.18	10,743
V_{SV} (kmph)	[12.05, 94.11]	57.32	56.22	16.10	40.25	75.47	
$RS_{LF,SV}$ (kmph)	[-14.69, 14.91]	-0.29	-0.10	3.22	-5.89	4.67	
$RS_{RF,SV}$ (kmph)	[-14.95, 14.66]	-0.26	-0.06	3.28	-5.84	4.68	
Deceleration (m/s^2)	[-4.85, -0.01]	-0.55	-0.42	0.51	-1.49	-0.04	5286
Acceleration (m/s^2)	[0.01, 3.55]	0.47	0.39	0.37	0.04	1.18	5457

Note: * Sample size

Preliminary assessment on the statistical properties of data show that the behavioural aspects of the subject driver in two-leader following scenario could be observed for a wide range of followers' speeds in between 12kmph and 94kmph, with a mean value of 57kmph while only 5 percent of the data lies above 75kmph. Moreover, 95 percent relative speed data were found to be lower than 4.68kmph, indicating steady-state two-leader following sequences in the extracted data. A close inspection on the spacing-related variables reveals that although the maximum longitudinal gap with both LF and RF vehicles in the interaction regime is observed to be 40m, 95 percent data of longitudinal gap lies within 17m. This 95 percentile value is considerably lower (around 43%) than the maximum LG (30m) suggested by different researchers for single-leader single-follower close following behaviour. Further, a comparison of the mean and median values of LG for a two-leader following scenario with a single-leader following case (refer Table 5.1) signifies that drivers prefer to follow the leaders more closely when both left-front and right-front vehicles are present as compared to single leader case. Yet, a detailed exploration on the obtained data is still required to justify this proposition. Conversely, the mean values of centerline separation with both the leaders suggest drivers' preferences of maintaining approximately equal amount of staggeredness with both the leaders. The acceleration and deceleration domains of the following vehicles are further in agreement with realistic acceleration/deceleration asymmetry of drivers (Ahmed, 1999) and the magnitudes indicate higher sensitivity of drivers towards deceleration than acceleration.

6.1.2.1. Driver's perceptions to spacing and speed

In order to understand the behavioural aspects of the drivers in maintaining a desired spacing and speed with both the leading vehicles, it is important to assess the statistical similarities or differences in the adopted longitudinal spacing, centerline separation and relative speeds with respect to left-front and right-front vehicles. This will not only address drivers' preferences in the following process but also form the basis in selecting the determinant variables for the development of two-leader following model. The probability density models of the considered interacting variables namely, longitudinal gap, centerline separation and relative speeds with respect to both LF and RF vehicles are first evaluated as presented in Figure 6.3.

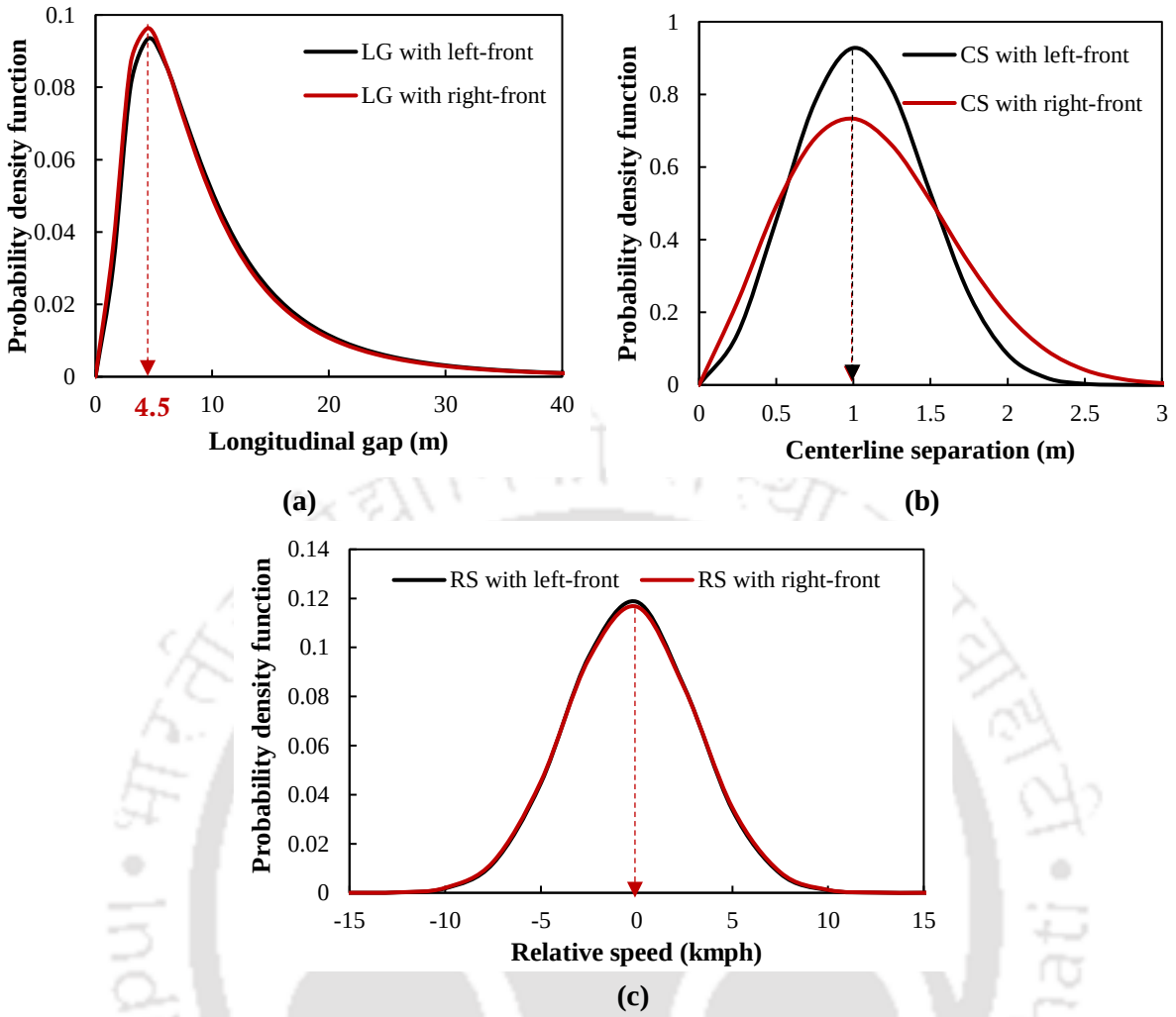

Figure 6.3. Best fitted theoretical distributions for **(a)** longitudinal gap **(b)** centerline separation and **(c)** relative speed with reference to both the leaders

As can be observed from the figure, the longitudinal distance-keeping behaviour of drivers seem to be consistent in the presence of both the leaders, with the peaks being observed at 4.5m for both the cases. Although longitudinal gaps between the leading and following vehicles are characterized by a wide range of data lying within 40m, 23.5% of the data lies below the modal value in both the cases. On the other hand, the distribution patterns of CS appear to be different and the peaks of the distributions are obtained at 1m for both the cases. These modal values are quite similar to the mean and median values of CS maintained with left-front and right-front vehicles (refer Table 6.1), corroborating that the centerline separation data are symmetrically or normally distributed. Considering the case of relative speed with respect to LF and RF vehicles, the statistical models are observed to be similar in nature, with the peaks being obtained at 0kmph, representing stable following behaviour with no differences in the leaders and following vehicles' speeds.

However, to further investigate the statistical differences in the relative speeds, CS and longitudinal gaps maintained by drivers with the left-front and right-front vehicles, two statistical tests, *t*-test (assuming equal means) and *F*-test (equality of variance) are conducted. Results of the statistical tests indicated significant differences in the statistical properties of

longitudinal gap [F(2,10741) =1.446, p<0.001, t-stat=5.475, p<0.001] and centerline separation [F(2,10741) =0.984, p<0.01, t-stat=9.473, p<0.001] while no statistical difference in relative speeds was found [F(2,10741) =0.947, p=0.061, t-stat=0.624, p=0.532]. This can be attributed to stable two-leader following process of the followers, due to which there is no significant difference in the relative speed with the left-front vehicle as well as with the right-front vehicle.

6.1.2.2. Selection of salient input variables: factor analysis approach

Understanding that no clear cut findings is available in the literature regarding the selection of suitable input variables for modelling two-leader following behaviour, an explanatory factor analysis on the considered input parameters is conducted in this section. A more detailed explanation on the analysis procedure is provided in Section 5.1.2.1. To provide additional insights into the explanatory power of the variables in elucidating the two-leader following phenomena, a list of variables including centerline separation with the left-front (CS_{LF}) and right-front (CS_{RF}) vehicles, longitudinal gap with LF (LG_{LF}) and RF (LG_{RF}) vehicles, speed of the following vehicle, acceleration/deceleration of the following vehicle (acc_{FV}) and relative speed between average speed of LF and RF vehicles and speed of the subject vehicle ($RS_{LF,RF-SV}$) are considered for the factor analysis, illustrated in Table 6.2. Because statistical comparisons in relative speeds between LF and RF vehicles with the SV indicated no significant difference in the mean and variance values (refer Section 6.1.2.1), the average value of relative speed between the LF and RF vehicles with the SV is considered ($RS_{LF,RF-SV}$) for further analysis (instead of individual relative speeds, that is $RS_{LF,SV}, RS_{RF,SV}$).

Table 6.2. Results of factor analysis

Variables	Factor structure matrix of principal component analysis				Factor structure matrix of first two factors rotated to Varimax criterion	
	Factor loadings					
	I	II	III	IV	I	II
CS_{LF}	-0.582	-0.214	0.222	-0.360	**-0.594**	-0.221
CS_{RF}	-0.675	-0.093	0.390	0.295	**-0.672**	-0.108
LG_{LF}	0.841	-0.020	0.340	0.262	**0.841**	-0.002
LG_{RF}	0.842	0.057	0.296	0.344	**0.841**	0.074
Speed	0.507	-0.210	-0.063	-0.500	**0.561**	-0.195
$RS_{LF,RF-SV}$	-0.177	0.807	0.050	-0.009	-0.195	**0.803**
acc_{FV}	0.181	0.768	0.194	-0.211	0.164	**0.772**
Eigenvalues	2.532	1.344	0.449	0.698	2.599	1.344
Total variance explained	0.362	0.192	0.064	0.100	0.371	0.192

Note: Bold features indicate higher loaded information

The results of factor analysis indicates that the two retained factors (I and II) could collectively explain 56.3% of the total variance. Factor I accounts for 37.1% of the variance, in which centerline separation with both LF and RF vehicles, longitudinal gap with LF and RF

vehicles and speed of the following vehicle exhibited higher factor loading. This latent factor with implicit information on speed and space-related variables can be attributed to drivers' visual information fidelity and their perceptions towards maintaining a desired longitudinal spacing with certain off-centeredness between the leaders, and their corresponding speeds. The factor loadings further signify that information on longitudinal gap contributes more to visual information fidelity, followed by centerline separation and speed. Conversely, factor II with higher loaded information on average relative speed and acceleration contributes to 19.2% of the variance. This latent factor can be considered as a dynamic aspect related to human sensory modalities of the drivers. When a driver receives stimulus from the vehicles ahead and sense the provided information, a sensory modality transmits the sensory signals to the brain and the driver accordingly modulates the throttle and accelerate or brake in order to ensure safety in presence of both the leaders. Therefore, based on the factor loadings presented in the table, all the seven considered variables are then further evaluated for a detailed comprehension and modelling of the two-leader following phenomena of drivers.

6.1.3. Hypotheses on two-leader following behaviour

Recently, increasing emphasis has been laid to achieve a detailed understanding of two-leader following phenomena that has predominant applications in microscopic simulation modelling of traffic and advanced driver assistance systems, to name a few. Despite its recognized importance, there has been no empirical evidence on how drivers interact with both the leading vehicles for different positional arrangement of the leaders, how drivers apperceive the current scenario, how their preferences in maintaining a desired spacing vary with different situational factors and how they evaluate safety in such scenario. The research work described in this section attempts to answer the proposed questions by examining four hypotheses:

1. *Driver's behavioural characteristics vary with positional arrangement of the leaders*. It is suspected that different arrangement of the leading vehicles, for example, both the leaders moving parallel to each other or left-front vehicle is ahead/behind right-front vehicle, may influence the following behaviour of drivers and their preferences to keep a desired lateral and longitudinal spacing with either of the leading vehicles. Usually, drivers have the urge to occupy the available longitudinal spacing and their preferences to maintain a desired lateral spacing with both the leaders may vary with different positional arrangements of the leaders.

2. *Speed of followers affects the distance-keeping behaviour*. Although it is well-established that speed and longitudinal gap between vehicles are linearly dependent on each other (with adequate evidence has already been provided in chapter 5), still there is a lack of understanding of the adopted longitudinal spacing in a two-leader following scenario and their variations with speed. This, in turn, will also throw light on the safety associated with the drivers when they follow both the leading vehicles simultaneously.

3. *Drivers' control processes depend on the orientation of leaders.* The *stimulus-response* framework forms the basis of the most influential single-leader car-following models. However, in a two-leader scenario, there arises several concerns regarding how actions of the leaders affect the control process of followers, whether positional arrangement of the leaders influence the followers' decisions to accelerate or decelerate. These questions need to be answered to understand the decision making process of the followers in the presence of multiple leaders.

4. *Safety criteria of drivers varies with leaders' positional arrangement.* To suitably assess collision risks in the following scenario, time-to-collision (TTC) is considered as a relevant safety indicator. But, how drivers perceive safety, how close they follow the leaders and how consistent is the safety indicator with respect to varying positions of the leaders in a two-leader scenario still require further elaboration, which has been dealt in this work.

6.1.3.1. Effect of leaders' orientations on the lateral distance-keeping behaviour

Drivers in a two-leader following scenario, maintain a preferable lateral and longitudinal spacing with either of the leaders and based on the positional arrangements of the leaders, drivers' preferences of maintaining a desired spacing also vary. To examine the behavioural characteristics of the followers, three specific cases of leaders' orientations are considered-

Case I: when the leaders are moving parallel to each other, with a maximum 2m clear lateral gap in between and there is approximately 85-100% overlap in length of the leaders

Case II: when the right-front vehicle is ahead of the left-front vehicle with 0% (rear-bumper of the RF vehicle is parallel to front-bumper of LF vehicle with 0m longitudinal gap between them) to 50% (rear-bumper of the RF vehicle is in the midway width of the LF vehicle) overlap in length of the leaders, separated by a maximum of 2m clear lateral gap.

Case III: when the left-front vehicle is ahead of the right-front vehicle with 0%-50% overlap in length, separated by 2m lateral gap in between.

The descriptive statistics of longitudinal spacing and centerline separation maintained by the followers with the left-front and right-front vehicles for different arrangements of the leaders corresponding to 50kmph speed is summarized in Table 6.3.

Table 6.3. Statistical properties of CS and LG for all the three considered cases

Variables	Case I				Case II				Case III			
	Mean	Median	SD	N	Mean	Median	SD	N	Mean	Median	SD	N
CS_{LF}	1.175	1.108	0.383		1.226	1.230	0.272		1.066	1.041	0.359	
CS_{RF}	1.207	1.140	0.393	3771	0.997	0.955	0.456	3694	1.277	1.218	0.489	3278
LG_{LF}	7.185	7.159	3.044		5.281	5.075	4.237		8.048	8.038	6.211	
LG_{RF}	7.241	7.172	4.181		8.231	8.113	4.710		5.038	4.985	5.157	

Note: **SD**-Standard deviation; **N**- Sample size

The distributions of the lateral positions/centerline separations of followers with the LF and RF vehicles for the same speed are also illustrated in Figure 6.4.

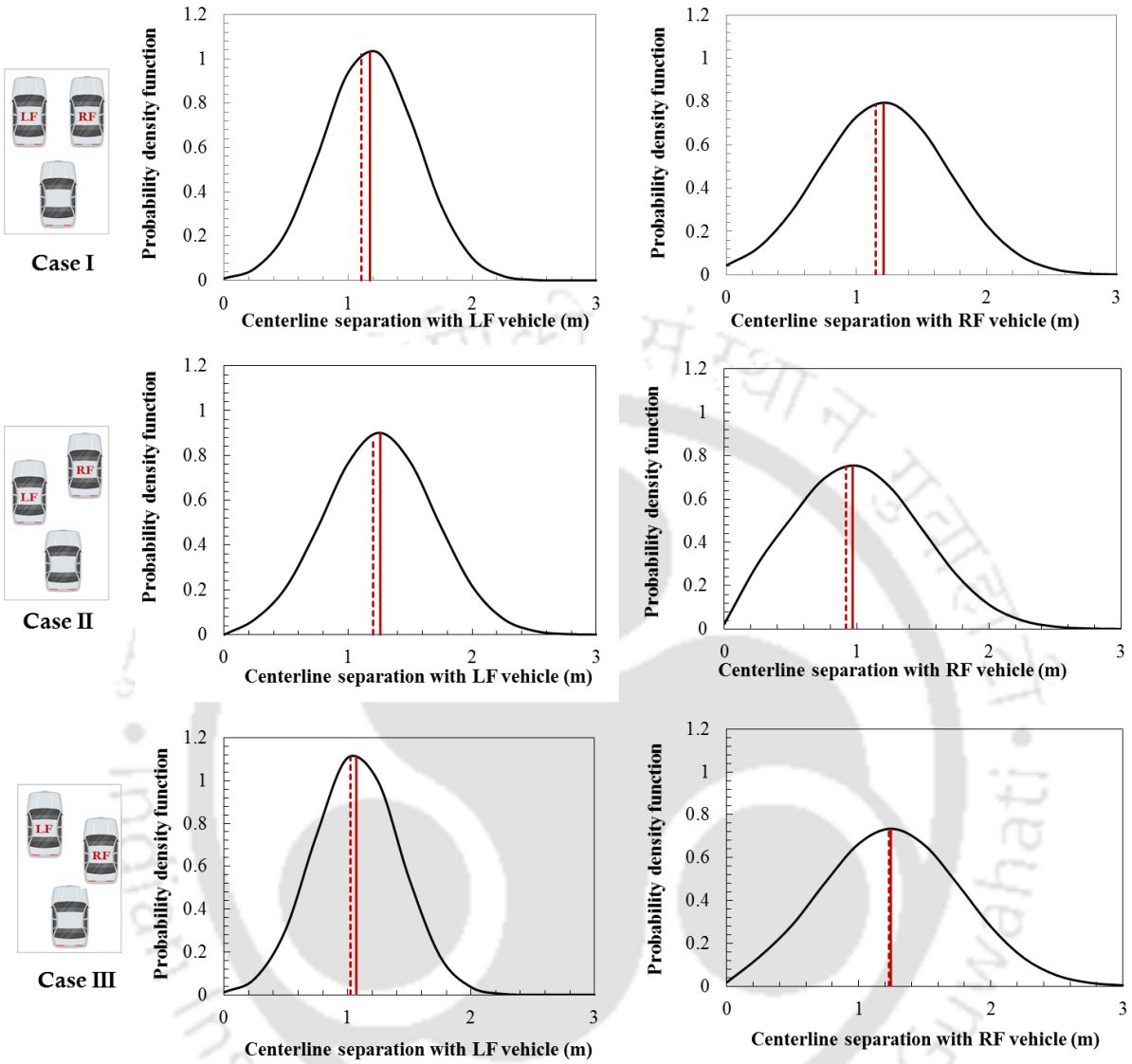

Note: Bold and dotted lines indicate mean and median values respectively.

Figure 6.4. Variation of lateral positions of the subject vehicle for different positional arrangement of the leaders corresponding to 50kmph speed

The descriptive statistics of centerline separation and longitudinal gap reveals an interesting finding- drivers' preferences of maintaining a certain lateral and longitudinal spacing with the leaders are observed to vary with the positional arrangement of the vehicles. Comparing the CS values for all the considered cases, it is found that when the leaders move exactly parallel to each other (case I), the subject drivers follow the leaders by maintaining same amount of lateral separation with both of them. Drivers in such scenario attempt to foresee the behaviour and anticipated actions of both the leaders simultaneously and evaluate possible opportunities to pass through the lateral gaps by keeping a constant visual record, therefore they tend to follow the leaders by positioning themselves in the middle. Conversely, the mean values of CS with LF and RF vehicles for case II and case III indicate that when drivers perceive large longitudinal spacing, they tend to avail the gap by shifting laterally, and therefore the centerline

separations with both the leaders are found to be comparatively different. Comparing the longitudinal gaps, it can be observed that the mean values are slightly larger in case I as compared to minimum longitudinal gaps ($min(LG_{RF}, LG_{RF})$) obtained for case II and case III. This can be attributed to the fact that when drivers perceive larger longitudinal spacing with one of the leaders, they shift their vehicles laterally to avail the space, thereby maintaining lower longitudinal spacing with the other leading vehicle. Conversely, when then they follow both the leaders simultaneously, they maintain comparatively larger longitudinal spacing due to lesser opportunity to initiate lateral shifts. Even if they attempt to shift laterally, the amount of veer needed by the subject driver in case I will be quite higher.

The solid and dotted red lines in the probability density plots of Figure 6.4 represent mean and median values of centerline separation respectively. The distribution patterns clearly signify that although the CS values lie in the range of 0 to 3m, the mean values occur at the peak of the distributions, indicating preferences of the drivers in maintaining the mean values most of the times. To further examine statistical differences in the lateral and longitudinal distance-keeping behaviour of drivers with both the left-front and right-front vehicles, *t*-test (assuming equal means) was initially performed for each considered case separately at 5% significance level and the obtained results are summarized in Table 6.4.

Table 6.4. *t*-test results for CS and LG for each case

	CS_{LF} and CS_{RF}	LG_{LF} and LG_{RF}	Interpretation
Case I	*t*-stat=1.144, *p*=0.126	*t*-stat=1.059, *p*=0.144	No significant difference in means
Case II	*t*-stat=9.911, *p*<0.001	*t*-stat=10.961, *p*<0.001	Significant difference in means
Case III`	*t*-stat=15.668, *p*<0.001	*t*-stat=19.031, *p*<0.001	Significant difference in means

The *t*-test statistical results signify that the longitudinal gaps and lateral separation maintained by the followers with the left-front and right-front leaders are not statistically significant when both the leaders move exactly parallel to each other (Case 1) while significant differences are observed for Case II and Case III. This finding reveals that the distance-keeping behaviour of the drivers depends on the orientation of the leaders. However, it will be more interesting to know whether drivers' preferences to maintain a desired centerline separation with either LF or RF vehicle varies with the leaders' positional arrangement. More precisely, this work further attempts to answer whether statistical differences exist between centerline separations of any two considered cases either with the left or right leading vehicle. Accordingly, the *t*-statistic values are evaluated at 5% significance level and the results are presented in Table 6.5.

Table 6.5. Summary of t-test statistic results

	t-statistic (Significant difference?)				
	$CS_{RF,1}$	$CS_{LF,2}$	$CS_{RF,2}$	$CS_{LF,3}$	$CS_{RF,3}$
$CS_{LF,1}$	N	Y	Y	Y	Y
$CS_{RF,1}$		Y	Y	Y	Y
$CS_{LF,2}$			Y	Y	Y
$CS_{RF,2}$				Y	Y
$CS_{LF,3}$					Y

Note- Subscripts indicate considered cases ($CS_{RF,1}$ representing CS_{RF} for case 1); Y-Yes, N-No

Interestingly, the statistical results reveal significant differences in the mean centerline separations maintained with either of the leaders for any two same or different positional arrangement of the leaders, the only exception being with CS between LF and RF for case I. This justifies that the lateral separations maintained with any leading vehicle (either LF or RF) vary significantly with the orientation/arrangement of the leading vehicles. Empirical evidence has therefore been provided in support to the hypothesis that the preferences or the behavioural characteristics of the drivers in maintaining certain longitudinal and lateral spacing with both the leading vehicles depend to a large extent on the positional arrangement of both the leaders.

6.1.3.2. Effect of speed on the distance-keeping behaviour

Drivers' preferences in maintaining longitudinal spacing with the leading vehicles for different positional arrangement of the leaders and the corresponding variations with vehicle speeds are detailed in this section. The 5th percentile, 95th percentile and mean longitudinal gap values maintained by the drivers with both LF and RF vehicles at different speed groups for each considered case are therefore evaluated and the variations are presented in Figure 6.5.

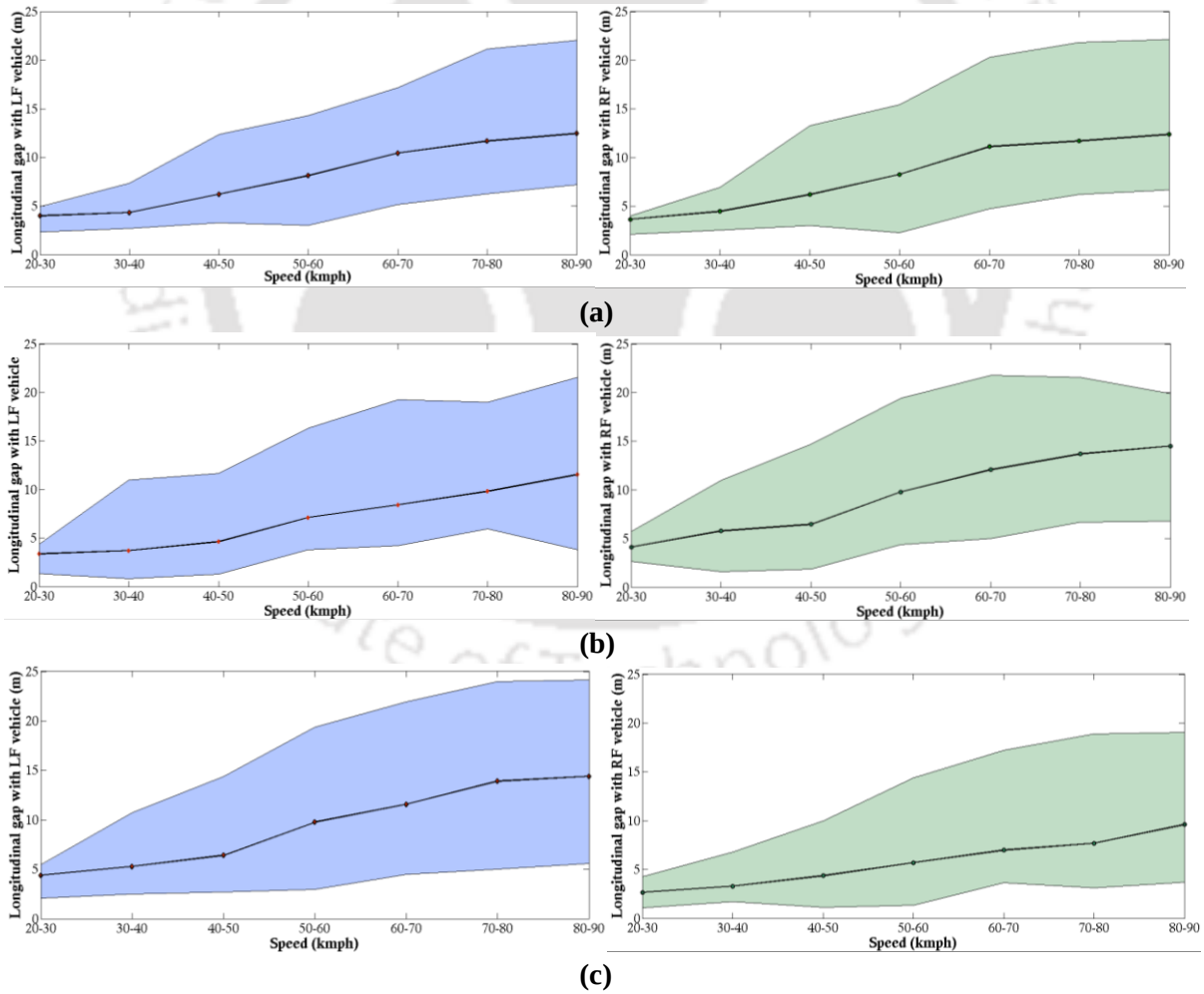

Figure 6.5. Variation of longitudinal gap with speeds for **(a)** Case I **(b)** Case II and **(c)** Case III

The lower and upper bounds of the plots depict the 5th percentile and 95th percentile values for each speed range while the connecting line with red dots lying midway between the lower

and upper bounds represents the average values of longitudinal gap corresponding to different speed groups. An inspection of the figure clearly signifies that the preferred longitudinal gap maintained by the followers with both the left-front and right-front vehicles increases with the speed of the vehicles for all the considered cases. Because drivers travelling at higher speeds are exposed to high risk prone situations, therefore they prefer to maintain a safe large longitudinal gap. On the other hand, drivers proceeding at lower speeds maintain a smaller spacing as they can anticipate the actions of the leaders more precisely with lesser exposure to crash-risks. Considering the statistical plots for each considered case, it can be observed that the minimum longitudinal gaps maintained with either one leading vehicle or both vehicles simultaneously follow a distinct pattern. Comparing all the three cases, the range of longitudinal gaps is found to be minimum for case III (LG with RF vehicle), followed by case II (LG with LF vehicle) and case I. This means that drivers following both the leading vehicles simultaneously (case I) maintain relatively larger longitudinal spacing as compared to case II and case III. This is because drivers in case I mostly prefer to follow the leading vehicles from the middle in order to apperceive the forward visual field and anticipate actions of both the leaders with more confidence and in such scenario, the combined impact of both the leading vehicles pose physical and psychological constraints to the subject drivers. As a result, drivers tend to maintain larger longitudinal spacing with the vehicles ahead. On the other hand, when the left-front vehicle is ahead of the right-front vehicle (case III), the subject drivers shift laterally towards left leader in order to avail the gap and follow the right leader closely with lower spacing. Unlike case I, drivers in case III are more under the influence of LF leader than the right one and they are confident enough to interact with the right leader laterally, as a result of which they maintain even smaller longitudinal spacing with RF vehicle. Moreover, drivers in case II cannot precisely judge the left leader's positions, therefore the minimum longitudinal spacing maintained in case II is larger than that in case III. This further justifies that the positional arrangement of the leaders affect the longitudinal distance keeping behavioural phenomena of the following drivers.

To further investigate the variability in longitudinal gaps between two successive speed groups for a specified positional arrangement of the leaders, F-tests and a one-way Analysis of Variance (ANOVA) test were performed at α=0.05. Results of the statistical tests indicated that drivers' selection of longitudinal gaps in Case I are consistent at speeds above 60km/h [F (2, 3963) = 1.281 < $F_{critical}$=3.03, p=0.274] while for case II and case III, no statistical difference was observed beyond 70kmph vehicle speeds. This finding suggests that the concept of constant headways that is often used in the development of adaptive cruise control systems might be true for a two-leader following scenario with speeds higher than 70kmph for any positional arrangement of the leaders, but is not true for lower speeds.

6.1.3.3. Leaders' orientations on driver's control process

Unlike single-leader following scenario, drivers in a two-leader following regime are associated with more complex driving-related tasks. Having noted that, emphasis needs to be laid to the control processes of subject drivers (in the form of acceleration or deceleration) in

response to the actions of both the leaders in the following scenario. What still remains to be examined is whether the *response* of followers with respect to *stimulus* from the leading vehicles is consistent with different positional arrangement of the vehicles in-front.

This section therefore attempts to investigate the *stimulus* (relative speed)-*response* (acceleration and deceleration) variations for different leaders' orientations. The considered relative speed intervals in kmph were [-17.5,-14.5), [-14.5,-12), [-12,-9.5), [-9.5,-7), [-7,-4.5), [-4.5,-2), [-2,0.5), [0.5,3), [3,5.5), [5.5,8) and [8,10.5). Figure 6.6 illustrates the *stimulus-response* mapping for each considered case, the *x*-axis representing mid-values of the relative speed domains. The upper and lower boundary lines represent 95 percentile and 5 percentile values of acceleration respectively, while the connecting line lying midway in between the upper and lower bounds represents the mean values of responses.

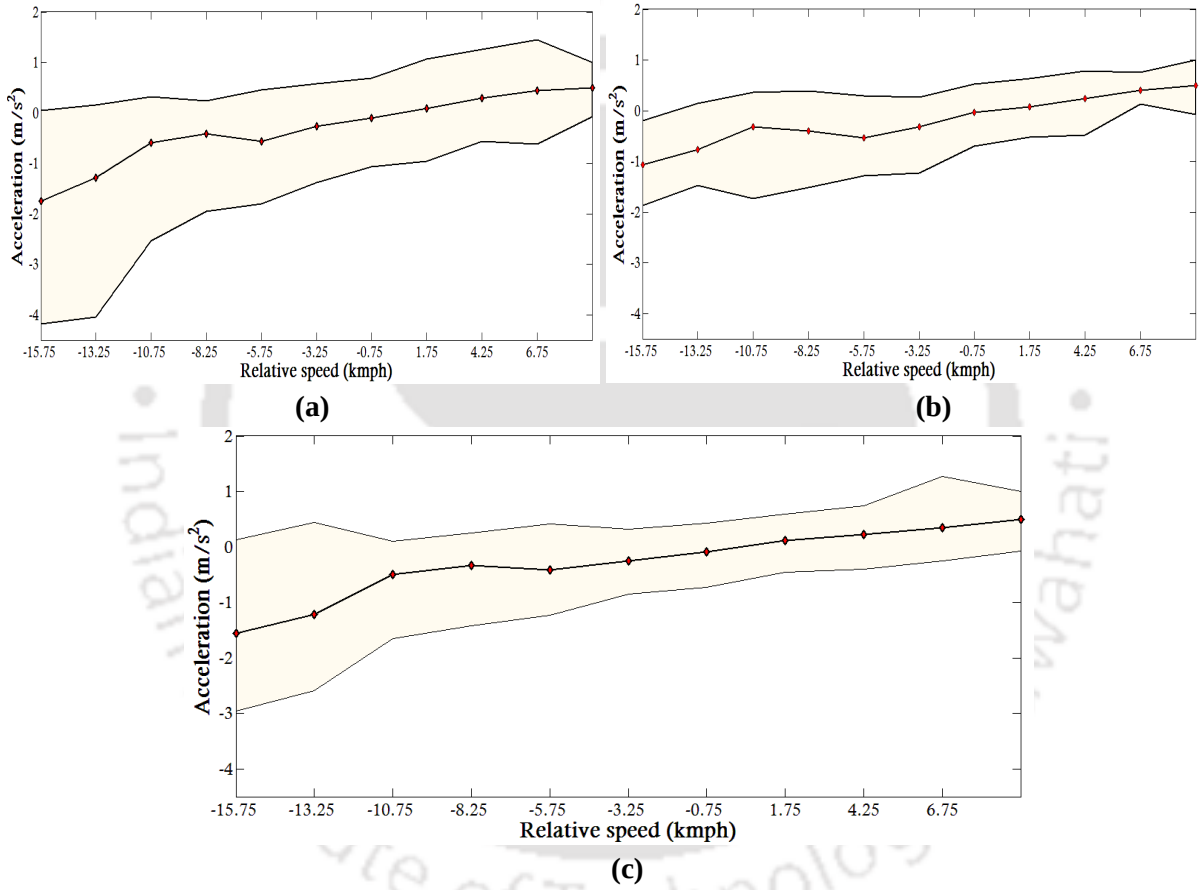

Figure 6.6. Acceleration-relative speed mapping for **(a)** Case I **(b)** Case II and **(c)** Case III

As can be observed, the *stimulus-response* mapping justifies that larger the negative relative speed, larger is the deceleration rate offered by the followers. Although the observed pattern appears to be true for all considered cases, yet the magnitudes are found to be different. A close inspection of the mean values of responses indicates that drivers are more sensitive to the actions of the leaders in case I, followed by case III and case II. The range of acceleration and deceleration values further corroborates the observed trend. For instance, the mean values obtained in case I, case II and case III corresponding to [-12, -9.5) kmph are -0.60m/s^2, -.32m/s^2, -0.39m/s^2 respectively. The underlying reason behind the observed trend is related to drivers' perceptions to relative speed variations and the forward visual angle apperceived by them with respect to varying orientation of the leaders. When the leaders travel exactly parallel

to each other (case I), the subject drivers tend to anticipate the actions of both the leaders simultaneously by maintaining approximately equal CS with both the leaders. In such scenario, drivers are more sensitive to small changes in the stimuli from both the vehicles and in risk-prone situations they control the vehicles by offering comparatively higher deceleration rate to maintain a minimum safe longitudinal spacing such that the associated risks are not compromised. Because the amount of veer required by the subject drivers to avoid any emergency situations is quite large in case I, they are more susceptible to the leading vehicles' actions. Drivers, in general, are confident enough to maintain smaller lateral spacing with the right-side vehicles than the left-side ones because of right-hand driving rule and the corresponding positional arrangement of drivers. As a result when they are in close proximity to RF vehicles (say Case III), they are more susceptible to the actions of the leaders, hence the deceleration rate offered by the drivers are relatively higher in case III than case II.

Moving beyond the observed trend, it still remains unclear if differences in the response values (acceleration and deceleration rates) for a given relative speed range are attributable to the positional arrangement of leaders. To provide evidence on the observed differences, an ANOVA test was performed on the response values corresponding to three different cases for each relative speed and the corresponding results are summarized in Table 6.6.

Table 6.6. Summary of ANOVA test results

Relative speed domain (kmph)	Mid value (kmph)	Case I, Case II and case III	Interpretation
[-17.5, -14.5)	-15.75	Lesser sample size	
[-14.5, -12)	-13.25		
[-12, -9.5)	-10.75	F-stat=0.455< F-cri=3.111, p=0.636	No significant difference
[-9.5, -7)	-8.25	F-stat=0.148< F-cri=3.047, p=0.862	No significant difference
[-7, -4.5)	-5.75	F-stat=1.501< F-cri=3.019, p=0.126	No significant difference
[-4.5, -2)	-3.25	F-stat=7.996< F-cri=3.001, p=0.000	Significant difference
[-2, 0.5)	-0.75	F-stat=10.068< F-cri=2.998, p=0.000	Significant difference
[0.5, 3)	1.75	F-stat=4.016< F-cri=2.999, p=0.018	Significant difference
[3, 5.5)	4.25	F-stat=0.363< F-cri=3.009, p=0.695	No significant difference
[5.5, 8)	6.75	F-stat=0.671< F-cri=3.072, p=0.512	No significant difference
[8, 10.5)	9.25	F-stat=0.561< F-cri=3.001, p=0.526	No significant difference

Interestingly, the test results indicated that the positional arrangement of leaders does not significantly affect the responses of followers when relative speeds lie in the range of -17.5kmph to -4.5kmph and also from 3kmph to 10.5kmph. While for small variations in relative speeds from -4.5kmph to 3kmph, significant differences in the responses were obtained for different leaders' orientations. This can be attributed to the fact that drivers decide to accelerate or decelerate based on the continually changing visual angle apperceived by the drivers at different positional arrangement of the leaders. Because drivers cannot perceive minute variations in relative speeds, the continuous adjustment in acceleration/deceleration responses of the drivers significantly vary according to leaders positional arrangements. To be

more precise, the more perceptible the relative speed is, no significant effect of leaders' orientations is observed on the behavioural responses of followers.

6.1.3.4. Drivers' perceptions to safety

Close-following behaviour of vehicles usually accounts for higher rear-end collision risks. Although the safety aspects of the drivers in a single leader car-following scenario has been documented in the literature, yet the propensity of associated risks in a two-leader car-following scenario has not yet been explored. Congruent to the findings discussed in 6.1.3.1. and 6.1.3.3., the risks associated with the drivers are found to be more predominant in a two-leader following regime when the leaders move exactly parallel to each other (case I) than the other two cases. In such scenario (case I), the followers maintain approximately equal lateral spacing with both the leaders. This proximity with the vehicles ahead increases the rear-end collision risks and in any case of emergency braking, the propensity of collision risks associated with followers becomes drastically high because of the combined impact of both the leaders on the following vehicle. Recognizing that drivers perceive higher collision risks in case I, this section attempts to investigate the applicability of time-to-collision (TTC) measure in a two-leader following scenario (case I) and the corresponding variations in TTC for different lateral positions of the followers.

6.1.3.4.1. Modified time-to-collision

In order to estimate rear-end collision risks in a two-leader following scenario, the TTC is defined as the time taken by the front-end of the following vehicle to reach the rear ends of both the leading vehicles, if both the vehicles proceed at their current speeds. Analytically, the TTC indicator can be expressed as:

$$\mathrm{TTC_{FV}(t)} = \begin{cases} \dfrac{\overline{LG_{LF}(t) + LG_{RF}(t)}}{\overline{RS_{LF}(t) + RS_{RF}(t)}}, & \text{if } v_{FV}(t) > v_{LF}(t) \text{ and } v_{FV}(t) > v_{RF}(t) \\ \infty, & \text{otherwise} \end{cases} \quad (2)$$

Where $\mathrm{TTC}_{FV}(\mathrm{t})$ denotes the TTC value of the following vehicle FV at a time instant t, LG and RS denote the longitudinal gap and relative speeds of the left-front (LF) and right-front (RF) vehicles respectively, the numerator and denominator representing the respective mean values of LG and RS.

As importantly, the underlying reason for considering the mean values lies in the preliminary statistical assessment conducted on longitudinal gaps and relative speeds, in which results of *t*-test and *F*-test confirmed no significant differences in the means and variances of LG and RS with LF and RF vehicles. Smaller the TTC value is, higher is the risk of collision associated with the drivers at a certain time instant.

6.1.3.4.2. Temporal surrogate safety measure: preliminary analysis

In total, the filtered trajectory dataset resulted in 2536 cases of two-leader following events which is speculated to elucidate the characteristics of temporal surrogate safety indicator, TTC, in a two-leader scenario when there is 100% overlap in length of both the left-front and right-front vehicles. With an aim to quantify 'safety' in a two-leader following scenario, the lower 10% values of TTC corresponding to each speed group is considered in this study. The statistical properties of the considered traffic variables (TTC, CS_{LF}, CS_{RF}, LG_{LF} and LG_{RF}) considering the aggregate data and the processed lower 10% data are presented in Table 6.7.

Table 6.7. Summary statistics of traffic variables for the two-leader following case

		Time-to-collision (s)	CS_{LF} (m)	CS_{RF} (m)	LG_{LF} (m)	LG_{RF} (m)
Aggregate data	Mean	4.294	1.071	1.098	7.859	7.948
	Median	3.826	1.045	1.097	6.509	6.732
	Std. dev	3.138	0.374	0.388	5.097	5.189
	Sample	2536	2536	2536	2536	2536
Lower 10% data[#]	Mean	1.014	1.575	1.618	5.027	4.635
	Median	0.841	1.612	1.797	3.751	2.515
	Std. dev	0.587	0.495	0.515	4.596	4.896
	Sample	180	180	180	180	180

[#]Lower 10% TTC values corresponding to each speed range are considered for safety evaluation

The mean and median TTC values obtained for the complete dataset is lower than the 5s-TTC criteria recommended for single-leader car-following scenario in urban areas (Maretzke and Jacob, 1992). While comparing lower 10% TTC values with the recommended TTC thresholds for car-following scenario of lane-based environments, it has been found that the mean TTC value obtained in our study is comparatively lower than the critical values recommended for developing rear-end collision avoidance systems (Hirst and Graham, 1997; Charly and Mathew, 2017), distinguish unsafe car-following manoeuvres (Bella and Russo, 2011) and for identifying the exposure to traffic conflicts (Qu et al., 2014a; Meng and Qu, 2012; Jin et al., 2011; Van der Horst and Godthelp, 1989; Minderhoud and Bovy, 2001). Taking 1s-TTC threshold as the critical value for estimating conflict severity, it can be demonstrated from our study that 10% of data show risky behaviour in a two-leader following scenario.

6.1.3.4.3. Variations of TTC with lateral positions of followers

In an attempt to achieve additional insights into a detailed characterization of the TTC thresholds for different lateral positions of the followers, three scenarios are considered:

Scenario I considers partial overlapping of FV with LF vehicle, $CS_{LF} \in [0, 0.5W)$ and relatively far from RF vehicle, $CS_{RF} \in (LC+0.5W, LC_{max}+W]$

Scenario II involves placement of FV in between LF and RF vehicles separated with equal lateral spacing, CS_{LF} and $CS_{RF} \in [0.5(LC+W), 0.5(LC_{max}+W)]$

Scenario III considers partial overlapping with RF vehicle, $CS_{RF} \in [0, 0.5W)$ and relatively far from LF vehicle, $CS_{LF} \in (LC+0.5W, LC_{max}+W]$; where LC is the clear lateral clearance between the leading vehicles, LC_{max} is the maximum value of LC considered in this study (2m) and W is the width of the leading vehicles (all the three interacting vehicles are of similar vehicle models)

For each scenario, the mean values of TTC considering aggregate data and lower 10% data were further evaluated and the corresponding variations are illustrated in Figure 6.7.

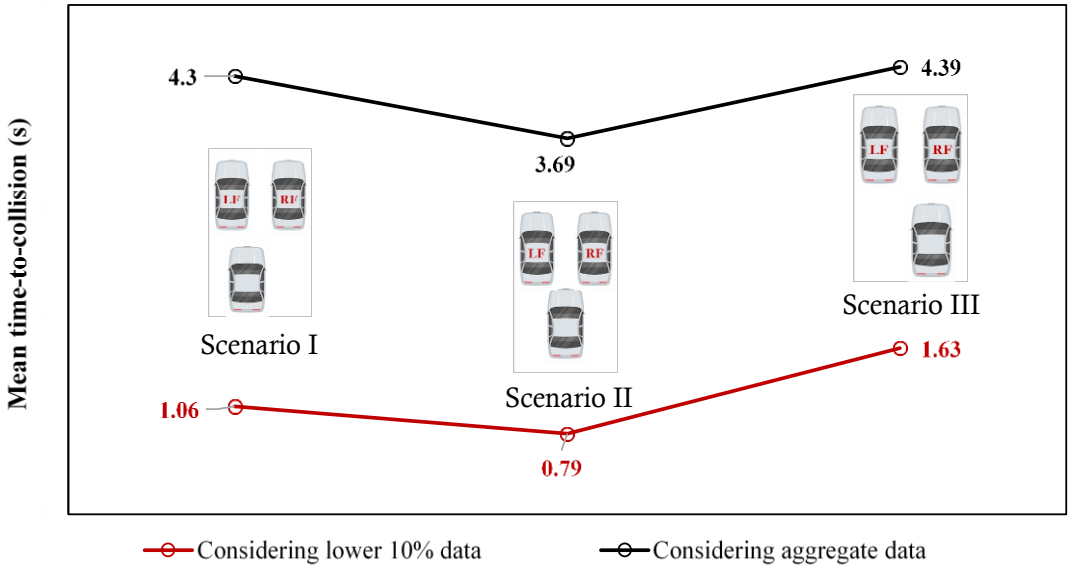

Figure 6.7. Variation of mean time-to-collisions for different positions of the following vehicle.

The observed trend reveals an interesting finding: the mean TTC values are found to be higher for scenario III, followed by scenario I and scenario II. As consistent with the previous discussion, this trend justifies that the perceived risks and the distance-keeping behaviour depend on the apperceived forward scenario and the visual angle available to the driver. For instance, when drivers follow both the leaders by positioning themselves midway in between the vehicles (scenario II), they experience a wide visual field as a result of which, the followers are confident enough to maintain even a smaller safe longitudinal spacing with both the vehicles. But at the same time, this behaviour may account for increased exposure to collision risks, if the leaders apply unprecedented braking in emergency situations. On the contrary, when the followers assign partial leadership with one of the vehicles in-front while maintaining comparatively larger lateral spacing with the other vehicle, they keep a larger longitudinal spacing as compared to scenario II; therefore the mean TTC values are found to be higher in scenario I and scenario III than scenario II. However, an increment in mean TTC value in scenario III than scenario I can be attributed to the extended visual angle available to the driver in scenario I than scenario III. When the positioning of FVs is more towards the right-front vehicle, it somewhat obstructs the visual field of view of the drivers sitting on the right-side of the following vehicle. Followers, therefore prefer to maintain relatively large longitudinal spacing in scenario III. Howbeit, drivers in scenario I experience better apperception of the leaders ahead even by maintaining lower CS with the LF vehicle; the longitudinal spacing maintained by them are therefore even lower, resulting in lower TTC values.

The findings therefore indicates that the recommended TTC thresholds defined for a single leader car-following event may not be applicable to a two-leader following case. Moreover, results further demonstrated that drivers are subjected to different level of risk exposure with different lateral positions of the following vehicles. However, statistical results indicated no significant differences in the mean TTC values across different positions of the followers (t-stat=1.589<t-critical=1.971). This justifies that the actual risk exposure in a two-leader scenario needs further detailed investigation for evaluating safety in such disordered traffic environments, that has direct implications in the design of autonomous systems and in ITS applications.

6.2. Development of data-driven based two-leader car-following model

An accurate and realistic modelling of the car-following dynamics augment the reliability of microscopic traffic simulation models and serve as theoretical references for autonomous car-following systems (Simonelli et al., 2009). While a substantial body of literature has shown the systematic evolution of single leader car-following models, there is still a paucity of research in modelling the behavioural responses of the drivers in a two-leader car-following scenario. In particular, drivers in a two-leader following scenario are subjected to more complex driving tasks in which they integrate several sources of visual information emanating from both the leaders, make numerous decisions, maintain an awareness of the changing environment in order to safely control the vehicle and perform appropriate control actions simultaneously.

Recently, due cognizance has been given to data-driven approaches for modelling the non-linear behavioural responses of drivers more precisely and realistically. Because of good generalization capability, flexibility in modelling, adaptability and inherent propensity of storing multi-dimensional data, an artificial neural network-based data-driven approach is advocated as viable to model and predict the complex dynamics of the subject drivers in a two-leader following scenario. This section therefore details the development of ANN based two-leader car-following model, demonstrating the model performance in terms of both trajectory-reproducing ability and from model stability standpoint, with emphasis being also laid to investigating the relative contribution of different input variables on the model output. A detailed explanation on the neural network methodology advocated in the research work is provided in Section 5.2.1.

6.2.1. Modelling framework and data preparation

The steps involved in the design of artificial neural network model require proper selection of input variables and segmentation of the database, design of neural network architecture and training algorithms, and evaluation metrics for statistical comparisons of the models. As discussed in Section 5.2.1.3., a similar methodology is used in the design of ANN-based two-leader following model, a brief description of which is provided below. The graphical representation of the methodological framework is also illustrated in Figure 6.8.

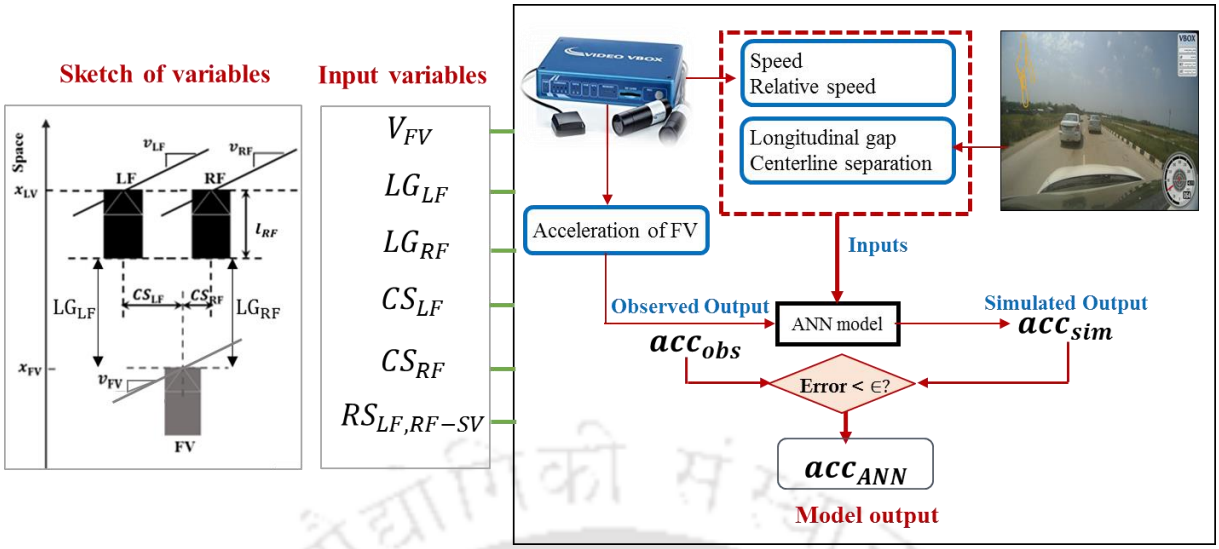

Figure 6.8. Methodological approach for the development of data-driven ANN model

a) *Selection of variables and data segmentation*- Based on the factor analysis results, all the considered variables including centerline separation with the left-front (CS_{LF}) and right-front (CS_{RF}) vehicles, longitudinal gap with LF (LG_{LF}) and RF (LG_{RF}) vehicles, speed of the following vehicle (V_{FV}), acceleration/deceleration of the following vehicle (acc_{FV}) and relative speed between average speed of LF and RF vehicles and speed of the subject vehicle ($RS_{LF,RF-SV}$) were considered as salient variables for elucidating the two-leader following phenomena. Prior to the model development, out of the total 10,743 data, 80% of the data (8595 samples) were used for training and 20% (2148 samples) for model validation.

b) *Design of ANN architecture*- The input layer of the proposed ANN architecture consists of six neurons corresponding to V_{FV}, LG_{LF}, LG_{RF}, CS_{LF}, CS_{RF} and $RS_{LF,RF-SV}$; one neuron corresponding to acceleration of the following vehicle (acc_{FV}) forms the output layer, with one hidden layer in between. The transfer functions used to model the non-linearity of two-leader following behaviour are tangent sigmoid ($Tansig$) and linear transfer functions ($Purline$) for the hidden layer and output layer respectively. Moreover, the Levenberg-Marquardt (LM) back-propagation algorithm was employed to obtain optimum weights and biases for the ANN models.

c) *Evaluation metrics*- The performance for each ANN architecture (with different set of neurons in the hidden layer) is evaluated using mean squared error, root mean square error and correlation coefficient criteria. The architecture fulfilling lower MSE, RMSE and largest R values is considered as the proposed ANN architecture.

6.2.2. The two-leader car-following model

6.2.2.1. Network architecture

To predict complex and non-linear structure of drivers' responses in a two-leader following scenario, several network architecture with different set of neurons (from 10 to 40) in the hidden layer were trained and the performance of each ANN network was evaluated. For the selection of an optimal ANN architecture, the performance of several network configurations were first compared assuming a constant reaction delay of 0.4s, the results of which are summarized in Table 6.8. The study further experimented with neural networks deeper than one hidden layer, but the results showed no significant improvement in the model performance, which demanded only six input variables.

Table 6.8. ANN architecture training results

Input variables	Neurons in HL	MSE	RMSE	R
$RS_{LF,RF-SV}$, LG_{LF}, V_{FV}	3-10-1	0.1134	0.3367	0.5989
$RS_{LF,RF-SV}$, LG_{LF}, LG_{RF}, V_{FV}	4-10-1	0.1009	0.3177	0.6436
$RS_{LF,RF-SV}$, LG_{LF}, LG_{RF}, CS_{LF}, CS_{RF}, V_{FV}	6-10-1	0.0772	0.2786	0.7158
	6-15-1	0.0779	0.2791	0.7479
	6-20-1	0.0745	0.2729	0.7608
	6-25-1	0.0660	0.2569	0.7817
	6-30-1	0.0642	0.2534	0.8081
	6-35-1	**0.0591**	**0.2432**	**0.8258**
	6-40-1	0.0557	0.2361	0.8276
	6-20-10-1	0.0729	0.2700	0.7665

Note: Bold features indicate the final adopted model

The performance metrics for the network configurations with different input neurons indicated that the introduction of CS with left-front and right-front vehicles in addition to, average relative speed, longitudinal gap with both the vehicles and following vehicle's speed, significantly improved the ANN model performance from R=0.6436 to R=0.7158. Moreover, with six neurons in the input layer, an iterative procedure in the hidden neurons resulted in the selection of an optimal ANN architecture with 35 neurons in the hidden layer [6-35-1]. Because increasing the number of neurons from 35 to 40 did not exhibit significant improvement in model performance, an ANN architecture 6-35-1 is therefore advocated as the optimal one for the design of two-leader car-following prediction model.

Furthermore, recognizing that inappropriate selection of reaction delay in a car-following model can contribute to traffic instabilities, rear-end collisions and, affect traffic flow dynamics on a microscopic as well as on a macroscopic scale, the competence of the proposed ANN architecture [6-35-1] was further evaluated considering constant reactions delays of 0.2s, 0.4s, 0.6s, 0.8s and 1s. The performance results of the ANN model for different constant reaction delays are presented in Figure 6.9.

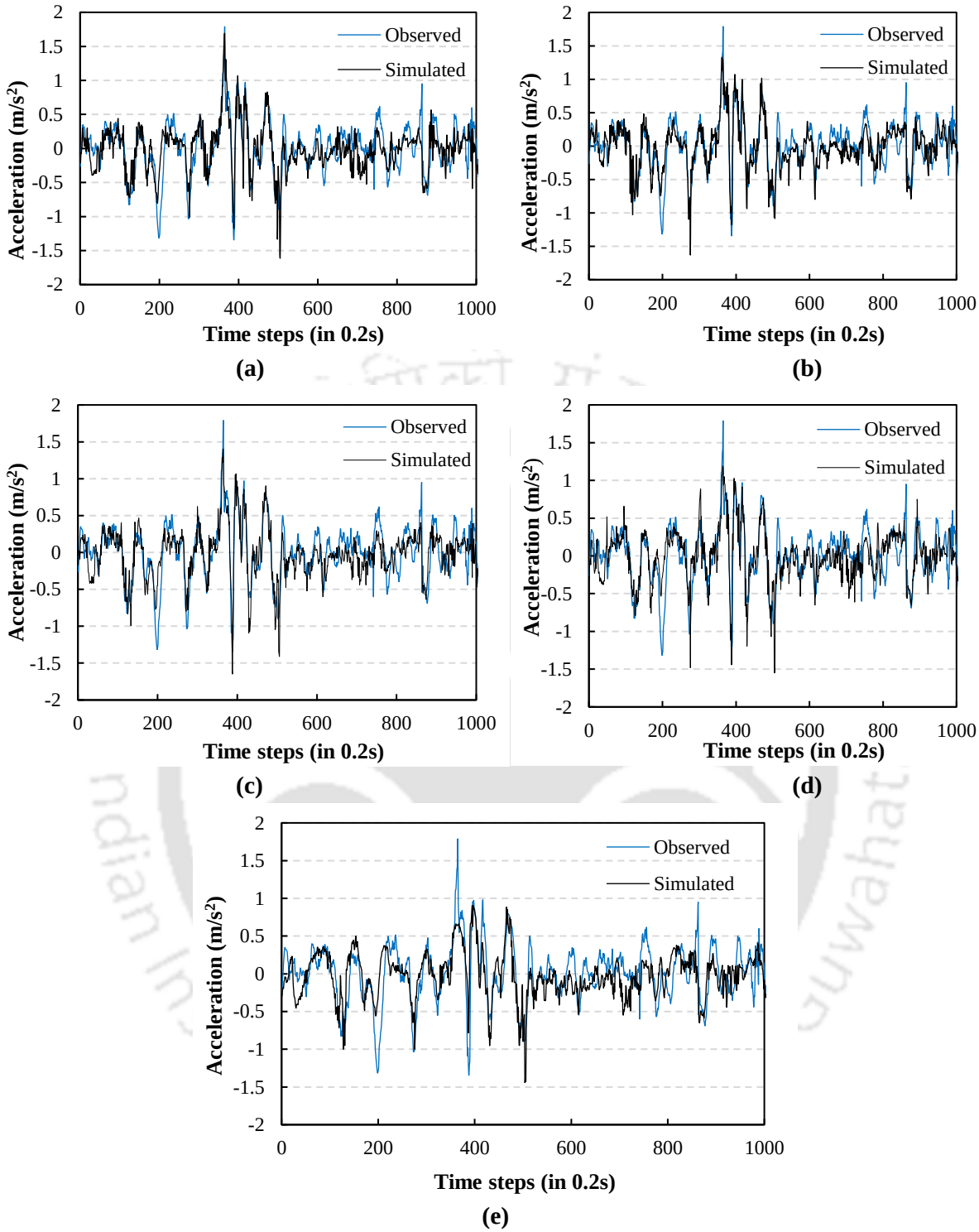

Figure 6.9. ANN prediction results for constant reaction delays of **(a)** 0.2s **(b)** 0.4s **(c)** 0.6s **(d)** 0.8s and **(e)** 1s

The model predictions in Figure 6.9 for different reaction delays show a good representation of the driver responses in most of the cases but a close assessment in the acceleration/deceleration values signify better model predictions with 0.2s reaction delay than 1s delay. A comparison of the error metrics for all the five considered cases was made and the results are presented in Table 6.9.

Table 6.9. Error metrics for ANN two-leader-following model with different reaction delays

ANN two-leader following model	MSE	RMSE	R
Fixed reaction delay of 0.2s	0.0677	0.2602	0.7857
Fixed reaction delay of 0.4s	0.0591	0.2432	0.8258
Fixed reaction delay of 0.6s	0.0605	0.2459	0.8112
Fixed reaction delay of 0.8s	0.0786	0.2804	0.7454
Fixed reaction delay of 1s	0.0847	0.2911	0.7217

The obtained results indicated better performance of ANN based two-leader following model with 0.4s fixed reaction delay, followed by 0.6s delay while the prediction model yielded larger error with 1s fixed reaction delay, which is often considered as an appropriate value in single-leader car-following model development. Recapitulating the main findings of ANN based single-leader car-following model (Section 5.2.3.1.) where the network architecture 4-30-1 with 0.6s reaction delay was advocated as the optimal prediction model, the research presented in this section provided evidence that an ANN based two-leader following model having 6-35-1 network architecture with 0.4s reaction delay yielded minimum errors. This decrease in reaction delay in a two-leader follower scenario can be attributed to the fact that when more than one leader is present, drivers are situationally aware of the anticipated actions of both the leading vehicles, thereby resulting in more complex interactions among the vehicles. Because of the anticipative behaviour, the following driver can react more quickly to changes in the dynamics of the leaders than they actually react in a single-leader case. Further, the observed and predicted responses of the optimal two-leader following ANN model with 0.4s reaction delay are also presented in Figure 6.10. The scatter plots reveal a good correspondence between the observed and predicted drivers' responses.

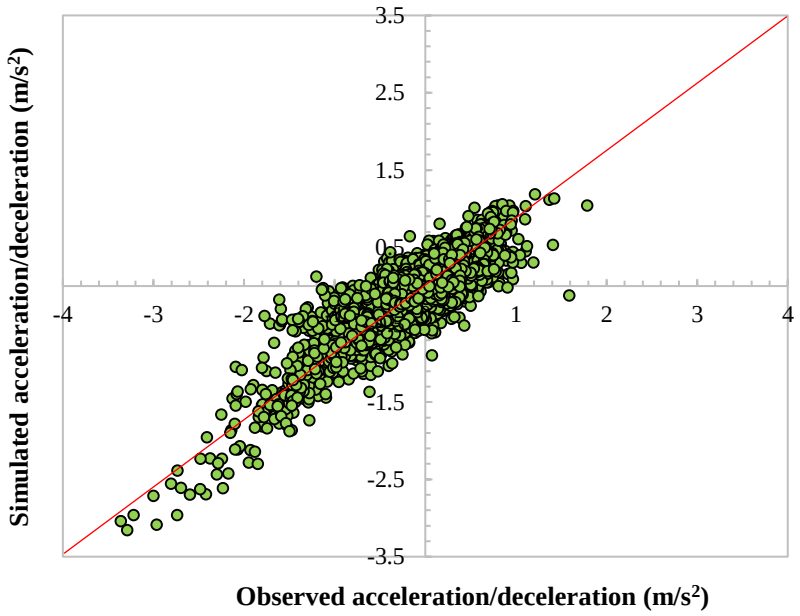

Figure 6.10. Observed and predicted responses based on ANN model with 0.4s reaction delay

6.2.2.2. Global sensitivity analysis

Sensitivity analysis was carried out to investigate the relative contribution of the input variables on the model output, based on different levels of conditioning of the inputs in their entire feasible space. The PAWN sensitivity index was used as a measure to indicate the relative contributions of the input variables: lower value signifies lesser contribution of the considered variable to the model output (detailed description being provided in Section 5.2.3.2.).

For the purpose of the analysis, 1200 random samples of input x, 500 random samples for each conditioning value for x_i and 45 random samples for the fixed input x_i were generated within the entire feasibility space by considering the minimum and maximum values of each variable. Figure 6.11 depicts the unconditional and conditional CDFs of the model output (following vehicle's acceleration) for each input parameter. The red lines represent the unconditional CDFs and the transition of light blue to dark blue lines represent the minimum to maximum values of conditionals.

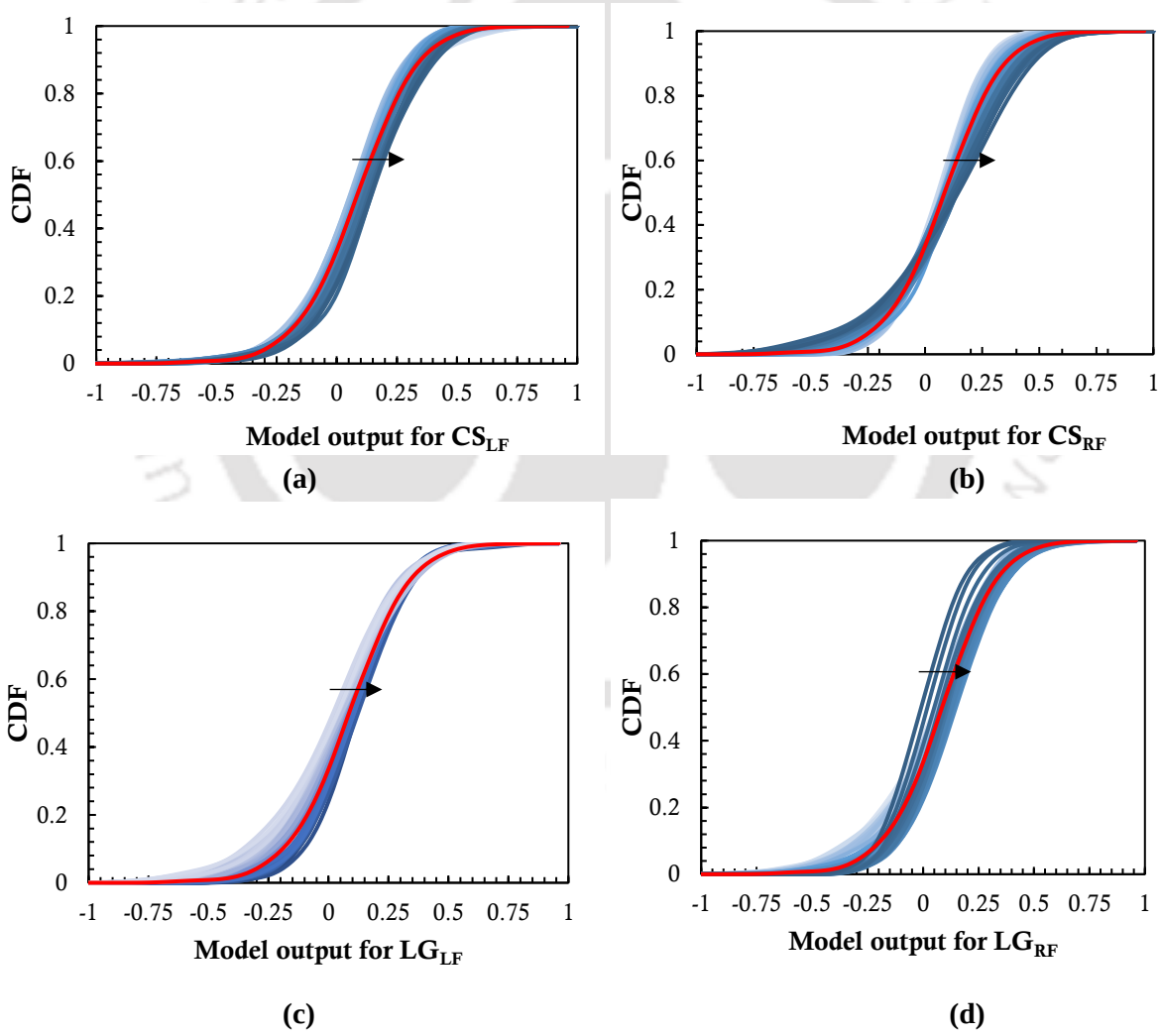

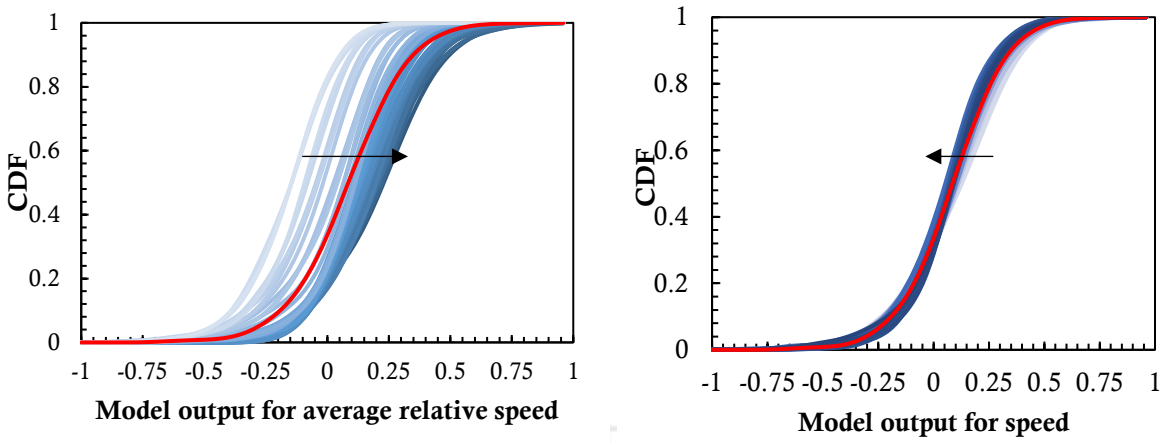

(e) **(f)**

(***Note:*** Transition of light to dark lines represent the minimum to maximum values of conditionals)

Figure 6.11. Cumulative distribution function curves of the model output for **(a)** centerline separation with LF vehicle **(b)** centerline separation with RF vehicle **(c)** longitudinal gap with left-front vehicle **(d)** longitudinal gap with RF vehicle **(e)** average relative speed and **(f)** speed

It is quite evident from the figure that the conditional curves of different input variables exhibit different level of discrepancies between the conditional and unconditional cumulative distribution functions. Comparing the vertical separation distance between the unconditional and conditional CDFs, it can be adjudged that average relative speed has a significant effect on the model output, followed by longitudinal gap with RF vehicle while the remaining considered input variables reveal similar separations. Moreover, corresponding to 0.6 cumulative density function (CDF), it can be observed from the figure that the there is a particular trend in the transition from light to dark conditional curves (as indicated by the direction of arrows) for all the considered input variables. A close assessment of the trends in CDFs for different levels of conditioning of the input variable indicates that increasing centerline separation values with either LF or RF vehicle, longitudinal gaps and average relative speeds increase the model output, indicating acceleration responses. This is because when followers become aware of positive relative speed and larger longitudinal spacing, and simultaneously, when the centerline separations maintained with both the vehicles are more, they apperceive the forward scenario with more confidence and can anticipate the actions of the leaders, as a result of which they avail the longitudinal distance by accelerating the vehicle. Moreover, a reciprocal trend is observed for vehicle speed with the model output because drivers, in general respond with higher accelerations when they proceed at relatively small speeds. The contributions of all the input variables are determined using PAWN sensitivity index as summarized in Table 6.10.

Table 6.10 Relative contribution of input variables

Parameter	Sensitivity Index
Centerline separation with LF	0.1349
Centerline separation with RF	0.1469
Longitudinal gap with LF	0.1371
Longitudinal gap with RF	0.1707
Average relative speed	0.4922
Speed of following vehicle	0.0996

The results of PAWN sensitivity indices indicate that relative speed is the most contributing factor (0.4922) in predicting the responses of the driver in a two-leader following scenario, followed by longitudinal gap with RF vehicle. The magnitudes of the indices signify that centerline separation with both the LF (0.1349) and RF (0.1469) vehicles, longitudinal gap with LF vehicle (0.1371) and speed of following vehicle (0.0996) exhibit similar contributions for the driver behavioural modelling process. Because the indices are close to each other, it determines that although the influence of some variables are smaller, their contributions are equally important for the modelling process. The research work therefore signifies that in addition to relative speed and follower's speed, the longitudinal and lateral separation parameters with both the vehicles in-front offer a significant role in predicting the dynamic non-linear behavioural phenomena of drivers in a two-leader car-following scenario of disordered traffic environments.

6.2.3. Evaluation of the proposed two-leader following model

The developed two-leader following model is then further evaluated to examine stability properties corresponding to varying initial conditions. The system for a particular arrangement of interacting vehicles must be dynamically stable such that the dynamic responses of the drivers decay over time. This section discusses the closing-in and shying-away behaviour and local stability properties in the two-leader following process for different sets of initial disturbances and positional arrangements of the interacting vehicles.

6.2.3.1. Closing-in and shying-away

For a two-leader following scenario, the closing-in and shying away behaviour is examined for case I (Section 6.1.3.1.) that is, when both the leaders move exactly parallel to each other (with 100 percent overlap in length of the leaders) and the lateral positioning of the following vehicle lies midway between the leaders with some longitudinal separation between them. To illustrate that the proposed model can describe the closing-in and shying-away stability properties, three different scenarios are considered with respect to different initial speeds of all the three interacting vehicles and different initial longitudinal gaps with the leaders:

Scenario 1: Different initial speeds of 8m/s, 11m/s, 13.5m/s and 16.2m/s, Initial longitudinal gap with both LF and RF vehicles is 20m, centerline separation with both LF and RF vehicles is 1.5m, LFV and RFV neither accelerates nor decelerates.

Scenario 2: Different initial speeds of 8m/s, 11m/s, 13.5m/s and 16.2m/s, Initial longitudinal gap with both LF and RF vehicles is 5m, centerline separation with both LF and RF vehicles is 1.5m, LFV and RFV neither accelerates nor decelerates.

Scenario 3: Same initial longitudinal gap 15m, different initial and final speeds of the leaders and FV like 13.5m/s (leaders decelerate at 2.5m/s^2), 11m/s (leaders decelerate at 2m/s^2), 8m/s (leaders decelerate at 1m/s^2), final speed of both the leaders and the follower

is 7m/s; different centerline separations with the leaders that is, $CS_{LF} = 1.25m$, $CS_{RF} = 1.25m$ and $CS_{LF} = 1.75m$, $CS_{RF} = 1.75m$.

Both the leading vehicles in Scenario 1 and Scenario 2 proceed at the same initial speeds with no perturbations and the results are presented through longitudinal gap versus time plots, as illustrated in Figure 6.12. The *y*-axis of the plot represents longitudinal gap with both the left-front and right-front vehicles.

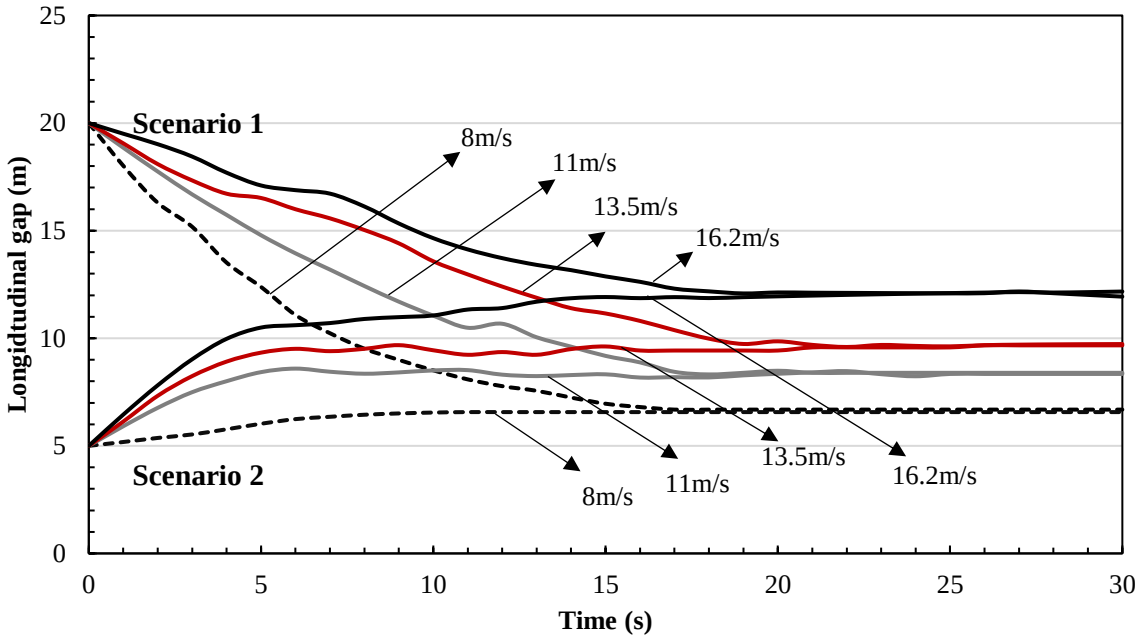

Figure 6.12. Variations in longitudinal gap for different initial speeds describing the closing-in and shying-away behaviour

The plots illustrate that when the initial longitudinal gap is large (20m), the following vehicle positioned at CS_{LF}=CS_{RF}=1.5m accelerates to reach a safe stable longitudinal gap and then adjusts its control process to maintain a desired distance. On the other hand, when the initial longitudinal gap is lower (5m for Scenario 2), the following vehicle first decelerates and shy-away in order to maintain a safe longitudinal separation with the leaders. This indicates that although the initial relative speeds are zero, for a specified positional arrangement of the interacting vehicles, the following vehicle makes adjustments in their accelerations and decelerations to reach a desired safe stable longitudinal gap.

The plots further signify that the stability properties of the model are validated at different initial speeds of the interacting vehicles. Because vehicles travelling at lower speeds have higher tendency to accelerate in the availability of suitable longitudinal gaps, the plot corresponding to 8m/s (Scenario 1) depicts a steep downward fall of longitudinal gap while for scenario 2, the rate of increase of longitudinal gap is not prominent because lower is the tendency to decelerate at 8m/s.

Interestingly, because drivers are more sensitive to deceleration than acceleration, the decrements in longitudinal gap corresponding to Scenario 1 are comparatively larger than the rate of increase in gap for Scenario 2 corresponding to each initial speed of vehicle. While the system stabilizes at 12m for 16.2m/s speed, the stable longitudinal gaps for different initial

vehicle speeds are achieved at even lower longitudinal gaps, 9.6m for 13.5m/s, 8.3m for 11m/s and 6.5m for 8m/s. This trend is quite evident because vehicles travelling at higher speeds maintain large longitudinal gaps in order to safely control the vehicle and to avoid potential rear-end collisions, in the advent of any risk-prone situations.

Further, in order to understand the stability properties for different initial perturbations in the leading vehicles but with same initial longitudinal gap, the longitudinal gap versus time plots corresponding to Scenario 3 for two considered positional arrangements of the leaders, are shown in Figure 6.13.

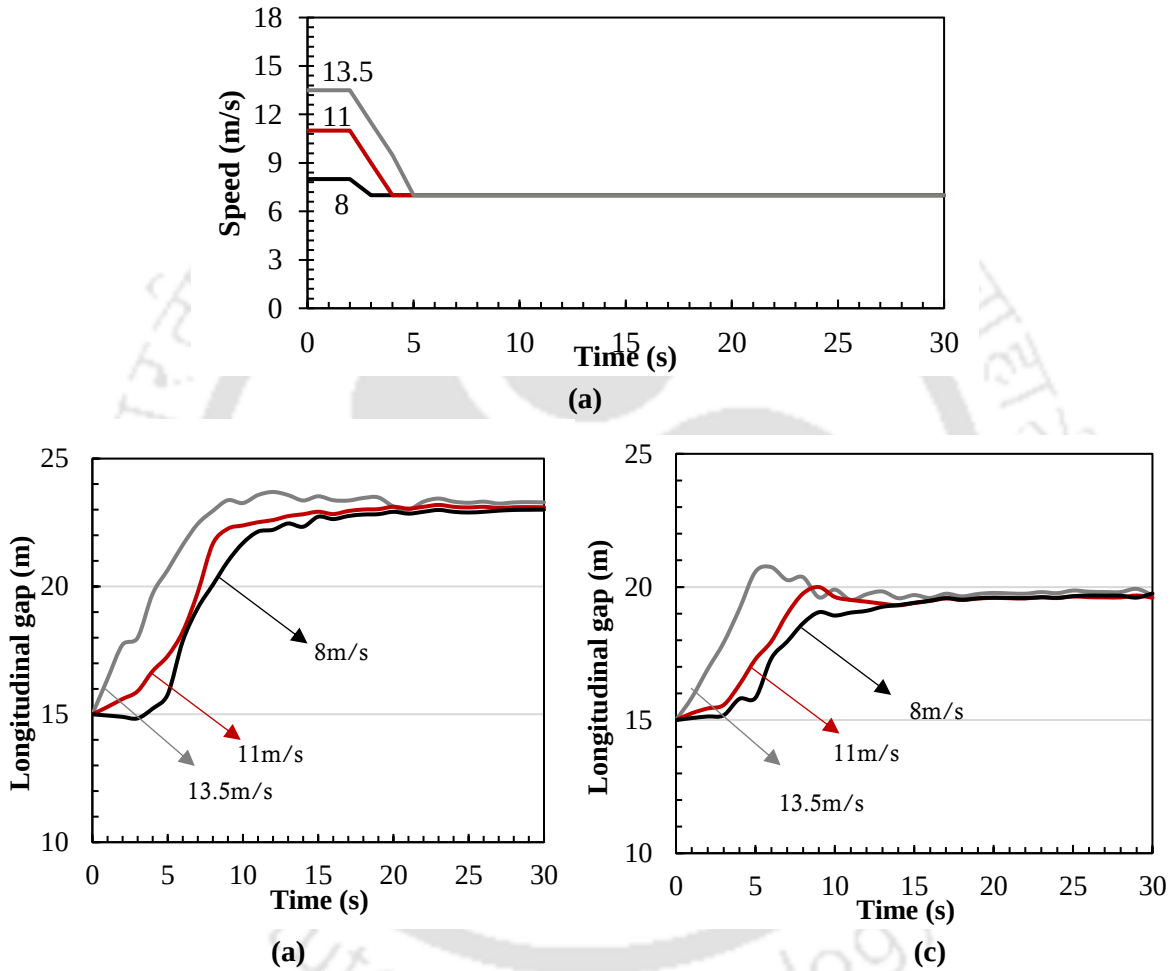

Figure 6.13. **(a)** Perturbation in initial and final speeds of both the left-front and right-front vehicles; Longitudinal gap variations for different lateral separations **(b)** $CS_{LF} = CS_{RF} = 1.25m$ and **(c)** $CS_{LF} = CS_{RF} = 1.75m$

It is evident from the figure that the stability criteria has been attained in both the considered cases, that is, for different positional arrangement of the leaders and initial speeds of the leading vehicles. The fluctuations in longitudinal gap before reaching the stable positions indicates the susceptibility of the followers in making continuous speed adjustments in response to the actions of the leaders. Moreover, the stable longitudinal gaps are achieved at 23m and 19.5m for $CS_{LF} = CS_{RF} = 1.25m$ and $CS_{LF} = CS_{RF} = 1.75m$ respectively. The decrease in stable gaps at larger centerline separation can be related to the fact that when drivers perceive larger lateral gaps in between the leaders, they tend to follow them more closely to get a more wider

visual view of the forward scenario such that they can anticipate the leaders' actions more precisely and subsequently, evaluate possible opportunities to pass in between them.

6.2.3.2. Local stability

Local stability for a two-leader following regime considers the control process of the drivers in response to fluctuations in actions of the leaders. The system is said to be *stable* in such case if the system eventually stabilizes after an unstable motion of the leaders. The local stability criteria is examined for the following scenario:

Scenario: Different initial longitudinal gaps if 15m, 10m and 5m, initial and final speeds of all the three interacting vehicles are 15m/s, both the leaders decelerate after 2s at 3m/s^2 upto 9m/s speed and then again accelerates at 3m/s^2 till it reaches 15m/s speed, and centerline separation with both LF and RF vehicles is 1.5m.

The initial disturbances or speed perturbations applied to the system corresponding to scenario 1 and the corresponding speed profiles as well as longitudinal gap versus time plot results for different initial longitudinal gaps with the leaders is depicted in Figure 6.14.

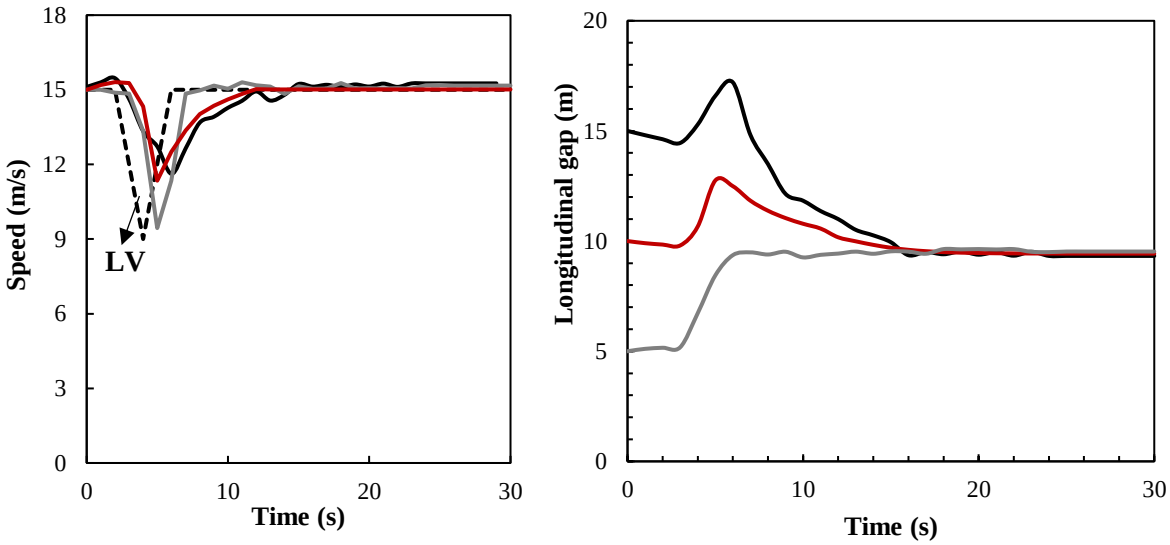

Figure 6.14. (a) Perturbation in initial speeds of both left-front and right-front vehicles and the following vehicle **(b)** Local stability for different initial conditions of longitudinal gap

As can be observed from the figure, irrespective of initial longitudinal gaps with the leading vehicles, the stability is achieved at a longitudinal spacing of about 9.5m when centerline separation of the follower with both the leaders is 1.5m. The plots further illustrate that when the initial spacing is 15m and the leaders proceed at 15m/s speed for 2s, the follower initially applies slight acceleration but after 2s when they perceive perturbations in the leaders, drivers decelerate at first (larger values of longitudinal gap) and then accelerates until they achieve a desired longitudinal spacing. This is in congruence with the local stability properties

highlighted in Chakroborty and Kikuchi's (1999) work for a single-leader car-following model where the stable longitudinal gap was found to be independent of initial gaps.

6.3. Comparison with existing models and its applications

Recently, transport modellers in many European and Asian countries have shown growing concerns to characterize the dynamic responses of drivers in a multiple leader following scenario. Over a decade, many advancements in the existing engineering car-following models have been made, the most prominent one being optimal velocity model amongst all. Although the effect of lateral separation has been incorporated in some of the optimal velocity models, yet empirical calibration of the model has not been explicitly undertaken. This section describes existing optimal velocity models with multiple (two) leaders, followed by model calibration using time-series data and finally, a comparison of the engineering models with the developed ANN-based two-leader following model is conducted.

6.3.1. Optimal velocity model and its modifications

For model comparisons, the widely-used optimal velocity models that incorporate lateral separation effects are considered in this work. These include full velocity difference model (FVDM) and asymmetric optimal velocity car-following model (AOVM).

6.3.1.1. Full velocity difference model

The full velocity difference model (FVDM) was first proposed by Jiang et al. (2001), which was later modified by Jiang and Wu (2003) by substituting the constant sensitive parameter of relative speed with the relative value of spacing. Later, taking into account the lateral separation characteristics, Jin et al. (2010) modified the FVDM. Extending the concept of Jin et al.'s (2010) lateral separation based FVDM model along with the modified model of Jiang and Wu's (2003), the governing equation of the model utilized in this work can be expressed as follows:

$$a_{FV}(t) = \kappa\{V[\Delta x_{FV,LF}(t), \Delta x_{FV,RF}(t)] - v_{FV}(t)\} + \lambda \frac{G[\Delta v_{FV,LF}(t), \Delta v_{FV,RF}(t)]}{[\Delta x_{FV,LF}(t), \Delta x_{FV,RF}(t)]}$$

$$V[\Delta x_{FV,LF}(t), \Delta x_{FV,RF}(t)] = V[(1-p_{FV})\Delta x_{FV,LF}(t) + p_{FV}\Delta x_{FV,RF}(t)]$$

$$G[\Delta v_{FV,LF}(t), \Delta v_{FV,RF}(t)] = [(1-p_{FV})\Delta v_{FV,LF}(t) + p_{FV}\Delta v_{FV,RF}(t)]$$

Where κ is the sensitivity parameter; λ is the sensitivity coefficient related to the speed difference; $\Delta v_{FV,LF}(t)$ is the speed difference between the subject vehicle, FV with the left-front vehicle FV at time t; $V(\Delta x)$ is the optimal speed function with respect to spacing Δx; the lateral separation effect is incorporated in $p_{FV} = \frac{CS_{LF}}{CS_{LF}+CS_{RF}}$; CS_{LF} and CS_{RF}, centerline

separations between the FV with LF and RF vehicles respectively. $p_{FV} = 0$ corresponds to FV following only LF vehicle; whereas $p_n = 1$ indicates that FV follows RF vehicle.

6.3.1.2. Asymmetric optimal velocity model

Considering asymmetry in acceleration and deceleration responses, Xu et al. (2015) developed an asymmetric optimal velocity model (AOVM) by incorporating an asymmetric factor on the velocity difference term. The formulation of the AOV model taking to consideration the lateral separation effects is given as:

$$a_{FV}(t) = \kappa\{V[\Delta x_{FV,LF}(t), \Delta x_{FV,RF}(t)] - v_{FV}(t) + G[\Delta v_{FV,LF}(t), \Delta v_{FV,RF}(t)]\exp(-\mu G[\Delta v_{FV,LF}(t), \Delta v_{FV,RF}(t)])\}$$

Where μ is the asymmetric factor representing the weight of the effect of relative velocity. The numerical simulation results indicated that this model avoids occurrence of unrealistically high acceleration responses and unrealistic negative velocities and headways. Results from the existing literature also demonstrates better performance of FVDM and AOVM than the original optimal velocity model.

6.3.1.3. Selection of optimal velocity functions

Two optimal velocity functions, namely exponential function and the s-shaped function are used for the considered full velocity difference model and asymmetric optimal velocity models. The exponential function was proposed by Newell (1961) and is defined as:

$$V[\Delta x_{FV,LF}(t), \Delta x_{FV,RF}(t)] = v_f\left[1 - exp\left(-\frac{\alpha}{v_f}\left(\left((1-p_{FV})\Delta x_{FV,LF}(t) + p_{FV}\Delta x_{FV,RF}(t)\right) - \Delta x_o\right)\right)\right]$$

Where α the calibrated parameter is positively related to wave speed at traffic jam (Del Castillo and Benitez, 1995); v_f is the desired speed and Δx_o is the unknown parameter represented as jam spacing.

Conversely, the other most widely accepted optimal velocity function is the s-shaped function, which is basically a hyperbolic tangent type function proposed by Bando et al. (1995).

$$V[\Delta x_{FV,LF}(t), \Delta x_{FV,RF}(t)] = 0.5v_f\left[tanh\left(\frac{(1-p_{FV})\Delta x_{FV,LF}(t) + p_{FV}\Delta x_{FV,RF}(t)}{l_{int}} - \eta\right) - tanh(-\eta)\right]$$

Where the interaction length l_{int} and the factor η determine the shape of the optimal velocity function.

6.3.1.4. Comparison between optimal velocity models

In order to find the optimal parameters of the considered FVDM and AOVM models, a genetic-based calibration technique is utilized for model calibration, the idea of which is to minimize the differences in model predictions and actual observations. The optimization was implemented in a MATLAB environment utilizing the GA built-in package. As discussed above, both the exponential and s-shaped functions were used as optimal velocity functions in the full velocity difference model and asymmetric optimal velocity model. A description of the calibrated parameters and the obtained optimal values along with the obtained mean squared error values is presented in Table 6.11.

Table 6.11. Calibration results and estimation performance of FVDM and AOVM models

Model	Parameter	Domains	Optimal values	MSE
FVDM-Exponential	κ	[0,10]	0.48	0.1862
	λ	[0,10]	1.67	
	α	[0.2,5]	3.05	
	Δx_o	[0,5]	0.75	
FVDM- s-shape	κ	[0,10]	0.56	0.1941
	λ	[0,10]	3.34	
	l_{int}	[0.1,40]	4.71	
	η	[0.1,10]	1.92	
AOVM-Exponential	κ	[0,10]	0.62	0.2967
	μ	[0,5]	0.71	
	α	[0.2,5]	3.12	
	Δx_o	[0,5]	1.72	
AOVM-s-shape	κ	[0,10]	0.76	0.336
	μ	[0,5]	0.46	
	l_{int}	[0.1,40]	6.43	
	η	[0.1,10]	1.24	

As presented in Table 6.11, the FVDM with exponential optimal velocity function performs the best in calibration while the FVDM with s-shaped optimal velocity function ranks second, with the mean squared errors being 0.1862 and 0.1941 respectively. On the other hand, the asymmetric optimal velocity model with exponential function ranks third, with the AOVM with s-shape function showing poor performance amongst all with a mean squared error of 0.336. The calibration results further indicate that although s-shaped function is commonly deployed in most of the optimal velocity models and its extensions, the exponential optimal velocity function showed a slight improvement in predictions for the full velocity difference model while in case of AOVM, there is almost 4% reduction in error when the exponential function is used.

Though the AOVM in general, captures the effect of asymmetric acceleration and deceleration responses in the model, a comparison with the other considered models illustrated

a better performance of FVDM with exponential optimal velocity function over AOVM. Considering the calibration results, the FVDM with exponential form is therefore considered as the reference model for comparing drivers' responses with the developed ANN based two-leader following model.

6.3.2. Trajectory reproducing accuracy

In an attempt to examine the driving trajectory-reproducing accuracy of the developed data-driven ANN-based two-leader following model with the full velocity difference optimal velocity model, the performance of the models in terms of errors in acceleration, speed and spacing, is evaluated in detail. A car-following period outside the training dataset was randomly selected from the empirical data and kept for performance evaluation. Based on initial states of the leaders and follower, the driver's responses (accelerations) were predicted from both the data-driven and engineering two-leader car-following model. The simulated responses were then further processed to estimate vehicle speeds and spacing using basic kinematic equations. Figure 6.15 presents the space trajectory of the interacting vehicle pair observed in the empirical data and that obtained from the ANN model and FVDM model with exponential optimal velocity function.

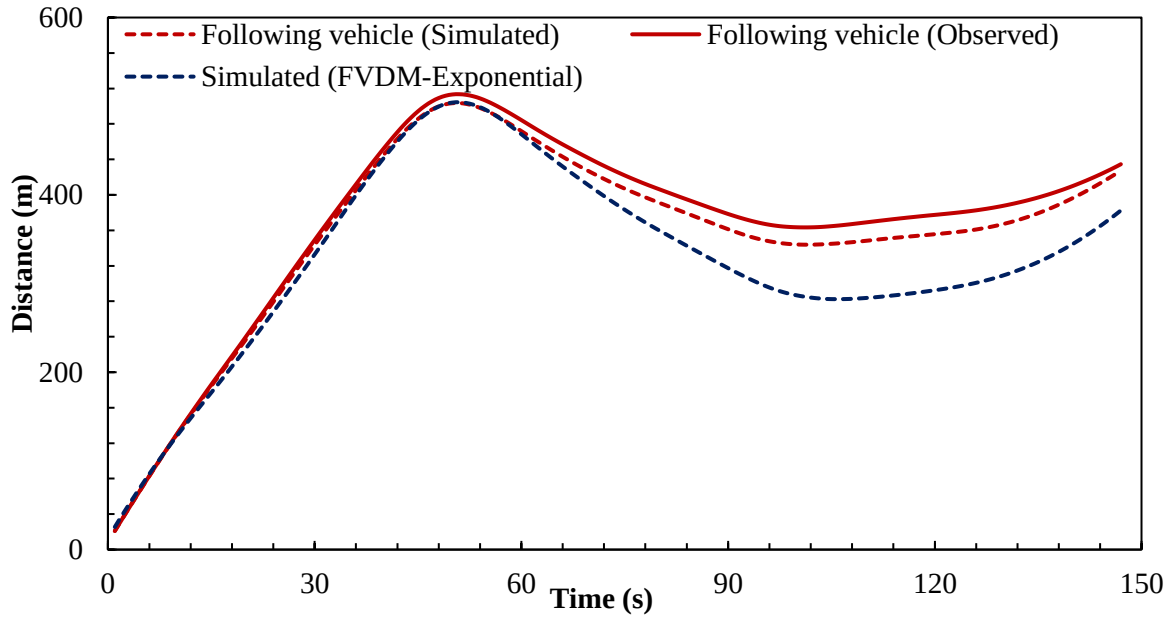

Figure 6.15. Observed and simulated space-time trajectories for the considered two-leader car-following period

The car-following period depicted in the figure considers a scenario when the left-front vehicle initially proceeds at a constant speed till 50s, after which it decelerates and reduces its speed and then again continues moving at higher speeds from t=80s onwards. For the same scenario, the right-front vehicle proceeds at higher speed than the LF vehicle till t=50s after which it moves at reduced speeds and then again accelerates. The responses of the following vehicle in such scenario are predicted from the developed ANN model and the calibrated

FVDM car-following model. Based on the space-time plots, it can be observed that the ANN model is able to predict the responses of follower quite satisfactorily as compared to the FVDM model.

Subsequently, the error metrics in observed and simulated accelerations, speeds and distance for both the models are further evaluated (as presented in Table 6.12).

Table 6.12. Error measures for different models

	Error metrics	ANN	FVDM
Acceleration	RMSE	0.128	0.425
	MAE	0.040	0.199
	MSE	0.016	0.181
Speed	MAPE	0.141	0.256
	RMSE	0.564	1.857
	MAE	0.489	1.593
	MSE	0.318	3.450
Distance	MAPE	0.178	0.291
	RMSE	14.234	38.146
	MAE	12.478	29.262

Results indicate that the simulated trajectory of the ANN model has better correspondence with the empirical data with 17.8% MAPE in distance while for the FVDM model, the MAPE is obtained as 29.1%. The error metrics further confirms that the ANN model has better predictions in acceleration and speed as compared to the non-parametric FVD model. From the simulated space-time trajectory and error measures, it can be concluded that the developed data-driven two-leader car-following model outperformed the non-parametric full velocity difference model in terms of trajectory-reproducing accuracy, thereby demonstrating the ability to reproduce human-like car-following behaviour in a two-leader following scenario.

6.4. Chapter summary

So far, the research conducted on understanding and modelling the two-leader following behaviour has primarily focussed on the theoretical development of classical optimal velocity based models considering effects of lateral separation from numerical simulation standpoint. Besides, recent literature has shed some light on the average distance-keeping behaviour of drivers in a multiple-leader and single-leader following scenario (Budhkar and Maurya, 2017). Yet, a proper understanding of how drivers apperceive the two-leader car-following scenario, how they make decisions and perform control actions against real-time variations in vehicle dynamics, how the stimulus of multiple vehicles affect the behavioural process of drivers and subsequently, how they evaluate safety in such scenario, still remains unclear and unresolved. This chapter has demonstrated that the anticipatory behaviour of drivers in a two-leader following scenario is much more complex than a single-leader following case, enough

symbolic emphasis being laid on the differences in drivers' behavioural characteristics with respect to different situational factors and traffic characteristics.

Utilizing dynamic time-series data collected from in-vehicle camera recorders, preliminary investigation provided evidence that drivers' preferences in maintaining longitudinal and lateral spacing with both the left-front and right-front vehicles depend significantly on the positional arrangement or orientation of the leading vehicles. This is because the perceived risks and the distance-keeping behaviour in such scenario are directly related to the apperceived forward view and visual angle available to the driver. On the contrary, the leaders' positional arrangement is found to significantly affect drivers' responses for small variations in relative speeds from -4.5kmph to 3kmph. That is to say, the more perceptible the relative speed is, lesser is the effect of leaders' orientations on the behavioural responses of followers.

Moreover, to predict the behavioural responses of drivers in a two-leader following scenario, an artificial neural network-based approach is considered in this research. Results indicated that an ANN architecture (6-35-1) consisting of six inputs (average relative speed, longitudinal gaps with LF and RF vehicles, centerline separations with LF and RF vehicles and speed of the following vehicle), 35 neurons in the hidden layer and one output, with consideration of 0.4s reaction delay could illustrate the realistic human-like following behaviour of drivers, much better than the classical optimal velocity based models both in terms of trajectory reproducing accuracy and generalization capability. Results of sensitivity analysis further justified the contribution of all the six input variables in predicting drivers' responses in a two-leader scenario. The proposed model could also explain the closing-in, shying-away behaviour and local stability properties. The two-leader car-following process is comparatively different from a single-leader following case and subsequently, having recognized the differences, if the obtained results are implemented in the microscopic simulation models, it would inherently augment the realistic characterization of drivers' behaviour and development of smarter, safe and user-friendly autonomous vehicles.

7

Modelling Filtering Behaviour of Vehicles

Recognizing that an accurate characterization of different driving regimes in disordered systems constitutes a step towards development of a realistic microscopic simulation model, the complex manoeuvring patterns of vehicles in such traffic systems entail detailed investigation. Research focused on the previous chapters takes due cognizance of the dynamic behavioural aspects of drivers in a single-leader and two-leader following regime. But recently, there has been a great emphasis on modelling the filtering behaviour of vehicles in dense urban heterogeneous traffic environments (FEMA, 2009; Vlahogianni, 2014). Filtering behaviour (also termed as seeping, Agarwal and Lämmel, 2016; Oketch, 2000, 2003) is a commonly observed phenomena for motorized two-wheelers (MTWs) where they attempt to utilize the available lateral spaces (or, pores) described by other surrounding vehicles on the road in order to achieve certain purported benefits such as travel time saving, increased speed and capacity, congestion and emission reduction, etc. On one hand, differences in the physical and dynamic attributes between MTWs and rest of the traffic provide MTW riders/drivers more flexibility in manoeuvring and freedom in choosing high speeds and chaotic trajectories, while on the other, increased exposure and vulnerability of MTW riders inevitably poses serious safety concerns than other means of transportation (Cafiso et al., 2012; Albalate and Fernandez-Villadangos, 2010). Although filtering of motorized two-wheelers (MTWs) is a common practice in developing nations, cars are even observed to exhibit the filtering behaviour in such disordered traffic environments, which still deserves considerable attention from driver behavioural modelling standpoint.

This chapter attempts to provide a detailed investigation of the decision making process of motorized two-wheelers and cars during filtering in urban mid-block sections, describing how this choice is affected by different driver-vehicle characteristics and local traffic conditions. While Chapter 6 shed some light towards the dynamic following behavioural process of cars in the presence of two leaders, the research work undertaken in this chapter intends to investigate the differences in two-leader following and filtering behaviour of both MTWs and cars, with proper emphasis being placed on the assessment and classification of lateral gap (or, pore) acceptance decisions of the drivers during the filtering manoeuvre. The chapter is essentially categorized into three broad sections as described below:

1. *Preliminary assessment of collected data describing filtering behaviour:* A description of the input variables considered in this study, with a preliminary investigation of the

differences in the filtering and two-leader following behaviour for both MTWs and cars have been explored in detail.

2. *Identification of variables affecting the filtering process:* This section addresses various determinant factors that affect the behavioural choice of MTWs and car drivers to filter in between the left and right front vehicles using a binary logit model structure, describing how this choice is affected by different driver-vehicle characteristics and local traffic conditions.

3. *Pore acceptance decisions during filtering:* An attempt has been made in this section to classify and predict the pore acceptance decisions of MTWs and cars during filtering using different methodological approaches, with proper emphasis being laid on understanding the importance and estimation of critical pore size.

4. *Quantifying rider's comfort in filtering:* Understanding that the filtering manoeuvre poses several safety concerns to the MTW riders and they are exposed to higher levels of risks than cars, this section discusses the multivariate aspects of MTWs during filtering using structural equation modelling approach, a detailed exploration of which is believed to apprehend the safety aspects associated with them and their interactions with the surrounding traffic.

7.1. Preliminary assessment of collected data describing filtering behaviour

This section provides a detailed explanation of the microscopic traffic variables considered in this research work for understanding the filtering behaviour of both MTWs and cars in non-lane based traffic environments. Efforts were further made to investigate the differences in the filtering and following manoeuvres of MTWs and cars with respect to kinematic attributes of vehicles and rest of the traffic, such as vehicles' speeds, relative speeds and lateral spacing.

7.1.1. The filtering behaviour

When a vehicle approaches two leading vehicles (left-front and right-front) in her/his direction of travel at a mid-block section, she/he first evaluates the lateral spaces described by the front vehicles and then determines whether the available lateral spaces are adequate to perform the filtering manoeuvre in between the vehicles. Evidently, the decision to filter requires that after accepting the lateral space or pore, the rider should be able to complete the filtering manoeuvre safely. The desire of the rider to perform a filtering manoeuvre is dependent on the minimum traversable lateral width required by the driver to pass in between the two lead vehicles, commonly termed as pore size (Ambarwati et al., 2014) in the literature. A graphical representation of the pore size considered in this study is depicted in Figure 7.1.

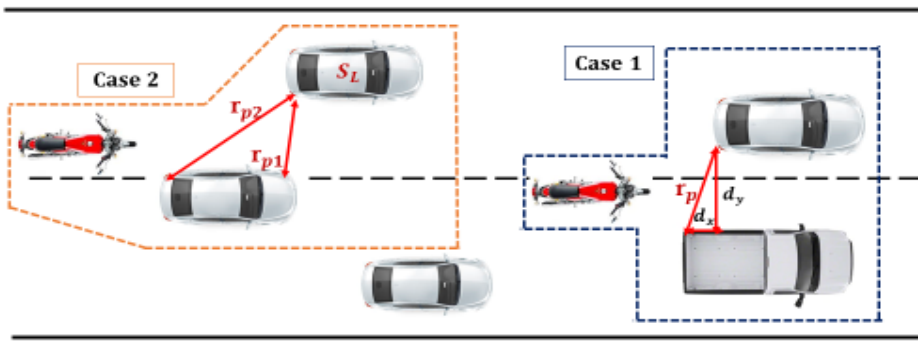

Figure 7.1. Graphical representation of the filtering manoeuvre.

Two different cases are considered to define pore size (measured in *metres*):

Case 1: when both the front vehicles are moving parallel to each other, the subject MTW or car driver perceives the pore size that is described by the parallel edges of both the vehicles in-front. With reference to Figure 7.1, pore size (r_x) can be defined as the minimum lateral width between the two leading vehicles, d_y.

Case 2: when the front vehicles are not moving in parallel (that is, one front vehicle is behind the other with some lateral separation between the leading vehicles), the rider/driver can perceive the pore that is defined by the right edge of the left vehicle's rear bumper with the left edge of the right vehicle's rear/front bumper. In such situation, pore size can be defined as the minimum of r_{p_1} and r_{p_2} (diagonal distances between the edges of the left-front and right-front vehicles, as shown in Figure 7.1).

In essence, when the subject vehicle utilizes the available pore size and filter or pass in between the left-front and right-front vehicles, that particular pore size is then defined as the accepted pore or, she/he has performed the filtering manoeuvre. Conversely, the pore size rejected by the subject vehicle due to her/his inability to pass through the available pore is defined as the rejected pore and consequently she/he is assumed to be in the following state. Each vehicle type perceives the available pores differently. Smaller vehicles can utilize pores that bigger vehicles cannot. The same pore size accepted by a particular driver during filtering may even be rejected by a number of other drivers. Even the same driver may perceive the same pore size differently at different situations. This can be attributed to a variety of traffic and situational factors such as type of front and surrounding vehicles, driver characteristics (age, risk-takers, risk-averters, etc.) as well as other supplementary factors such as perceived safety, risks involved in filtering (Altendorf and Flemisch, 2015), etc. which impedes the desire of drivers to accept a particular pore size. Particularly, the decision of a subject vehicle to filter or follow (accept or reject a particular pore size) the leading vehicles depend to a large extent on a number of variables, which needs to be prudently considered for a better apprehension of the filtering behaviour and its interactions with the surrounding driver-vehicle units.

7.1.2. Selection of data and input variables

Understanding and modelling the filtering behaviour of MTWs and cars and their interactions with the surrounding traffic require a detailed trajectory dataset where the position coordinates, speeds, longitudinal and lateral spacing, vehicle dimensions, type of vehicle involved in filtering, type of interacting vehicles, presence of surrounding vehicles, etc. can be evaluated precisely. For the estimation of pore acceptance and rejection decisions, MTW riders and cars performing the filtering manoeuvre at different time stamps were initially identified from the video footage and the trajectory data was extracted for each filtering case. The minimum pore size that was accepted by the subject vehicle during the filtering process was considered as the accepted pore. Similarly, all the vehicle-following events (when the subject MTW preferred to follow the front vehicles due to their incapability to accept the available pore size) were identified and extracted from the video footage and the corresponding pore size was considered as the rejected pore. In particular, all the observations made on the driver's decision to accept or reject a pore were independent, with the extracted data containing implicit information on the aggregate behavioural decision of a variety of drivers in such urban traffic streams.

The decision of the driver to filter or follow the vehicles in-front is assumed to be affected by several factors such as driver characteristics (such as age, gender, and helmet usage), vehicle characteristics (size of the interacting vehicles), current traffic conditions (speed, spacing, presence of surrounding vehicles, density, etc.) and the history of the past decisions. Several factors were considered to affect the decision making process of the filtering vehicle (MTW and car) and were considered as input variables in the model. Figure 7.2 illustrates a series of variables obtained from the video-based analysis that are considered for a detailed understanding of the filtering behaviour and are defined as follows.

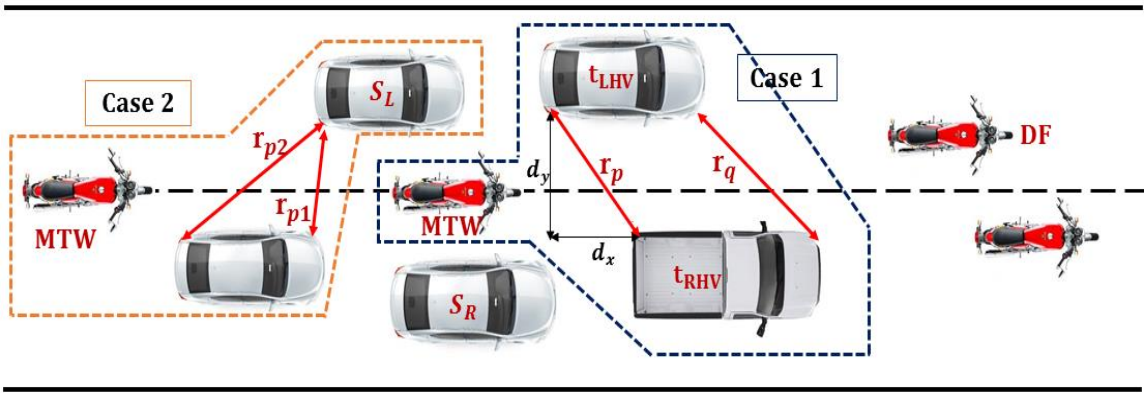

Figure 7.2. Filtering manoeuvre of MTW in urban area under study

Relative speed (km/h): The speed difference between the average leading vehicle speeds and subject vehicle, in km per hour. It can be expressed as $Relative\ speed = 0.5 * (V_{LF} + V_{RF}) - V_{SV}$, where V_{LF}, V_{RF} and V_{SV} are the speeds of the left-front, right-front and subject vehicles respectively.

Pore (m): The minimum traversable lateral width required by the driver to pass in between the two lead vehicles (Ambarwati et al., 2014). Pore size can be calculated as $min(r_p, d_y)$ for Case 1 and $min(r_{p_1}, r_{p_2})$ for Case 2 where $r_p = \sqrt{{d_x}^2 + {d_y}^2}$ (discussed in Section 7.1.1.)

Speed (km/h): The speed of the subject vehicle (V_{MTW} or V_{Car}) involved in the decision making process. A subject vehicle (MTW or car) travelling at higher speed than the leading vehicles is more likely to filter while it rather prefers to follow if the relative speed is comparatively higher (speeds of leading vehicles are higher than the subject vehicle).

Presence of heavy vehicle: The presence of a heavy vehicle (HV) at the left-front side (t_{LHV}) or right-front side (t_{RHV}) of the subject vehicle may affect the driver's filtering choice. It is a categorical variable, considered as '1' if there is presence of any heavy vehicle and '0' otherwise.

Size differential (m): The difference in average vehicle lengths of left-front and right-front vehicles with the subject vehicle, calculated as $Size_D = 0.5(l_{LF} + l_{RF}) - l_{SV}$ where l_{LF}, l_{RF} and l_{SV} are the lengths of the left-front, right-front and subject vehicles respectively. Because the interactions of subject vehicles with several combinations of leading vehicle types are considered in this research, the size differential is introduced in this study to partially capture the heterogeneity in vehicular interactions.

Occupancy: It is a categorical variable representing the number of persons sitting on a motorized two-wheeler. It is defined as '1' if number of persons sitting on the MTW including the rider is two, otherwise '0' (only the rider is sitting). The variable occupancy (Occ) is however not considered for cars performing the filtering manoeuvre.

Presence of a surrounding vehicle: The effect of the presence of a surrounding vehicle just to the immediate right side (S_R) or left side (S_L) of a subject vehicle may affect the filtering choice of the subject vehicle. It is also a categorical variable, considered as '1' if there is presence of any heavy vehicle and '0' otherwise.

Age: The age of the MTW rider is approximated from the video footage and is accordingly categorized into three broad ranges: less than 30 years (categorical variable '0'), between 30 to 50 years (categorical variable '1') and greater than 50 years (categorical variable '2').

Gender: It is a categorical variable and considered as '0' if the subject MTW rider is a female and '1' if the rider is a male.

Hemet usage: The usage of helmet may affect the filtering choice of MTW rider and is assumed as '1' if she/he wears a helmet, else '0'.

Direct front: The presence of MTW in the direct front (DF) of the subject MTWs may attract them to utilize the available pore and perform a filtering manoeuvre ('1' is DF is present else '0').

History: The past decisions of drivers before performing the filtering manoeuvre are represented by the number of lateral movements made by the filtering vehicle in the past trajectories. Because the lateral movement of MTWs is more pronounced than cars, this variable is considered for modelling manoeuvring decisions of only MTWs. A MTW can be considered to have made a lateral movement if the deviation in lateral positions at a time step of 1s is larger than 0.5m, which is commonly adjudged as the minimum lateral gap of a MTW (Minh et al., 2005; Hussain et al., 2005; Minh et al., 2012).

Among all the considered input variables, age, gender and helmet usage are mainly attributed to the MTW rider characteristics, the information of which can be directly processed from a visual assessment of the video footage. Moreover, the variables occupancy and history are also considered for only MTWs. Because information on driver characteristics are not available for the car drivers, these variables are not considered for modelling the filtering behaviour of cars. The available pore size described by the left-front and right-front vehicles during a filtering and a following manoeuvre is estimated when the subject vehicle interacts with the leading vehicles for a minimum of 4s time period. Because the perceived pore size is dependent on the filtering vehicle as well as on the interacting vehicles in-front, the filtering behaviour is studied for those cases for which the available pore size is lower than 3m and 4m for MTWs and cars respectively. For the purpose of the study, a longitudinal distance of 20m from the subject vehicle's position is considered to describe the interactions of subject vehicles with the leading left-front and right-front vehicles. A vast range of traffic conditions ranging from low congestion level to high congestion level were included in the data sample.

The trajectory dataset resulted in a total of 588 observations, 478 of them being filtering (328) and following (150) cases of MTWs and 110 being the filtering (60) and following (50) cases of cars. Each vehicle was tracked at an interval of one-fourth a second making a total of 10,722 position coordinates. The obtained sample size can be considered as adequate for logit modelling purposes (Green, 1991; Minh et al., 2012). These cases cover the entire spectrum of the subject vehicle's action before, during and after filtering and also certain cases when the vehicle tends to follow due to its incapability to pass through the available space. The interactions of the MTW riders and cars with several combinations of the leading left front and right front vehicles (passenger cars, MTWs and trucks) were considered in this work. The plot of spatial pores and relative speeds for both MTWs and cars during filtering (accepted pores) and following (rejected pores) behaviour for the complete dataset are depicted in Figure 7.3.

As can be observed from Figure 7.3, the plots for both filtering and following manoeuvres hold no particular linear relationship, which is indeed evocative of a complex behaviour which requires more number of parameters to be considered to model their manoeuvring patterns. The pore size accepted by a particular driver may even be rejected by a number of other drivers, which can be attributed to the perceived risks associated in filtering, driver characteristics, speeds of the interacting vehicles or other situational factors. Usually, drivers accept large pore sizes and tend to proceed at relatively higher speeds than the leading vehicles to perform a filtering manoeuvre. Hence negative relative speeds and larger pore sizes are observed for the filtering manoeuvre of both the vehicle types as compared to the following case.

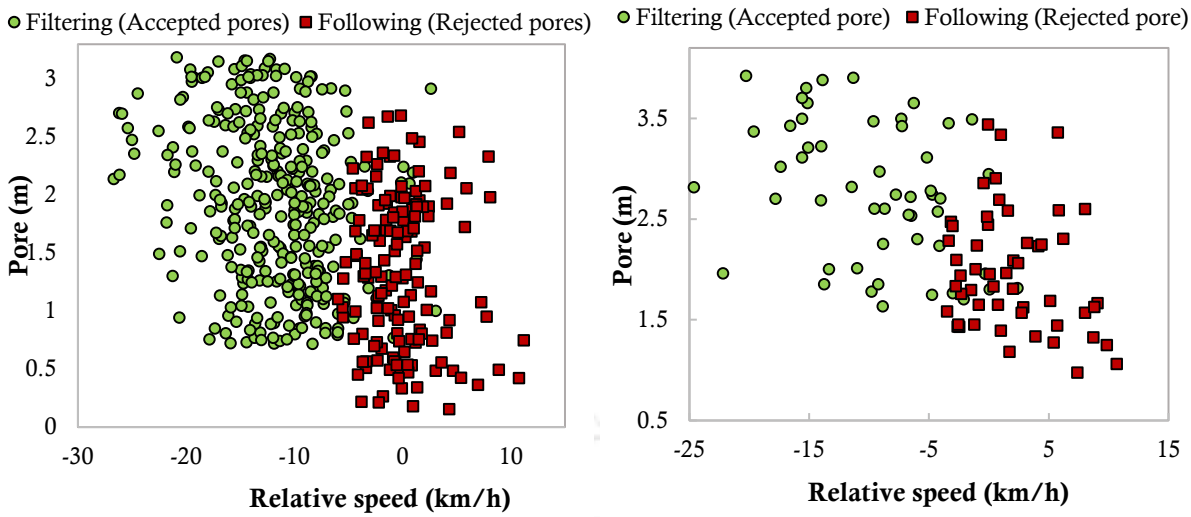

(a) **(b)**

Figure 7.3. Variation of pore sizes and relative speed during filtering and following behaviour of **(a)** MTWs and **(b)** cars

7.1.3. How different are the filtering and following behaviour of MTWs and cars?

In order to comprehend the differences or similarities in the filtering and following manoeuvres of MTWs and cars, the descriptive statistics and the distributional characteristics of pore size (r_p), subject vehicle's speed (V_{MTW}, V_{Car}) and relative speed between average of the lead vehicles' speed and the subject vehicle's speed are evaluated in this section. As discussed in the preceding sections, the available pore sizes accepted or rejected by the subject vehicle are dependent on the vehicle characteristics, driver characteristics and current traffic situations. A detailed understanding of the differences in the filtering and the following manoeuvres can be achieved by representing the best fitted probability density functions with respect to pore size and relative speeds as shown in Figure 7.4.

The figure depicts that MTWs and cars require larger pore sizes and higher speeds than the leading vehicles' speeds (that is, negative relative speeds) to perform a filtering manoeuvre as compared to the following case. The average pore size accepted by MTWs and cars during filtering are 1.91m and 2.55m respectively while the rejected (or following) mean pore sizes for MTWs and cars are obtained as 1.32m and 1.93m respectively. Because cars have bigger vehicle dimensions than MTWs, they usually accept larger pore sizes during filtering as compared to MTWs. Moreover, the distribution patterns indicate that the peaks of the univariate distributions occur at 1.75m for MTWs performing the filtering manoeuvre while for cars, the peak occurs at 2.25m. However, for the vehicle-following case the peaks are observed at 1.25m and 1.75m for MTWs and cars respectively. It is also observed that a majority of the MTW and cars drivers maintain higher speeds than the leading vehicles (the peak of relative speeds being observed at -10km/h for both MTWs and cars) during filtering.

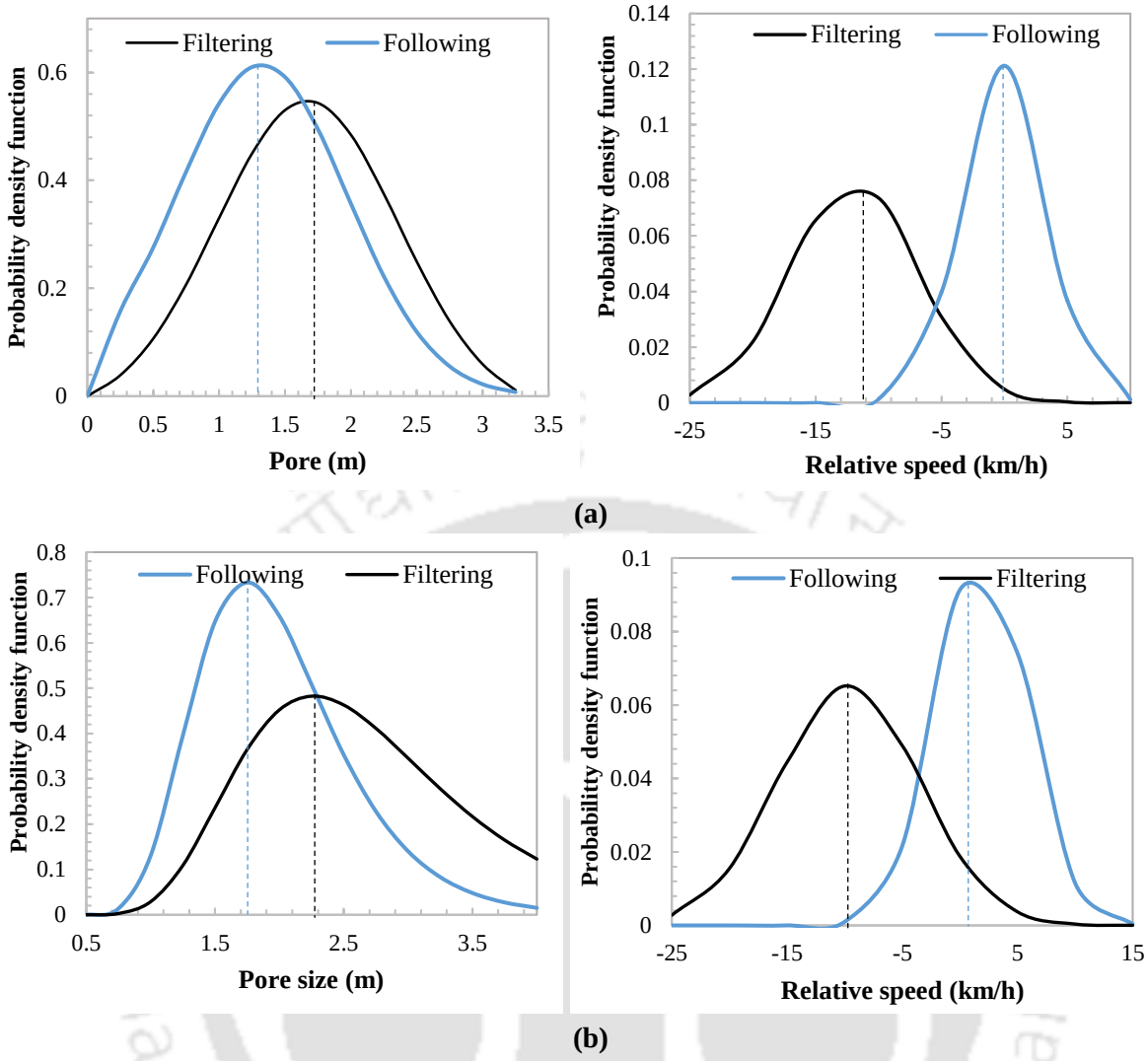

Figure 7.4. Probability density functions of pore size and relative speeds for the filtering and following behaviour of **(a)** MTWs and **(b)** Cars

Considering the ranges of univariate distributions, it can be observed that the pores accepted by the cars (1.5m-3.5m) are even rejected by many MTW drivers. Although MTWs accept pore sizes of 0.7m-3m, the rejected pores lie in the range of 0.25m to 2.5m, the peak being observed at 1.25m. This large difference (0.25m-2.5m) in the rejected pore widths can be attributed to the differences in driver characteristics, traffic characteristics, type of lead and surrounding vehicles, etc. as well as other supplementary factors such as perceived safety, risks involved in filtering, joy of driving, etc. (Altendorf and Flemisch, 2015; Barmpounakis et al., 2017) which impedes the desire of drivers to accept the available pore space. Similar to the observed differences in pore size, the peaks of the probability functions for the relative speed data clearly signify a speed increment of 10kmph in filtering when compared to following, irrespective of the subject vehicle types involved in the filtering process.

To further investigate the differences in filtering and following behaviour of MTWs and cars, two statistical tests, *t*-test (assuming equal means) and *F*-test (equality of variance) are conducted on the explanatory variables such as pore size, speeds and relative speed as presented in Table 7.1.

Table 7.1. Statistical test results for comparing filtering and following manoeuvres

Variables			Mean	Std. dev	
Pore size (m)	MTWs	Filtering	1.671	0.690	F(2,478) =2.52, p<0.001
		Following	1.279	0.654	t-stat=8.80, p<0.001
	Cars	Filtering	2.694	0.840	F(2,55) =0.452, p<0.05
		Following	1.992	0.604	t-stat=4.31, p<0.001
Speed (kmph)	MTWs	Filtering	54.221	19.652	F(2,478) =2.83, p<0.001
		Following	49.660	15.801	t-stat=3.11, p<0.05
	Cars	Filtering	76.320	14.001	F(2,55) =0.866, p<0.001
		Following	66.049	12.628	t-stat=3.37, p<0.001
Relative speed (kmph)	MTWs	Filtering	11.971	4.914	F(2,478) =5.16, p<0.001
		Following	2.486	2.157	t-stat=29.26, p<0.001
	Cars	Filtering	9.474	6.177	F(2,55) =0.290, p<0.001
		Following	1.497	3.675	t-stat=8.705, p<0.001

The statistical results and the obtained p-values signify that the null hypothesis (that is, mean and variance values are equal) can be rejected for all combinations of the input variables at 1% significance level. This indicates that the pore sizes accepted by the subject vehicle, the speeds and relative speed of the vehicles during the filtering manoeuvre differ significantly from that in the following case irrespective of subject vehicle type. In addition, statistical tests were further conducted on the considered variables to comprehend whether the subject vehicle type has any effect on the filtering and following manoeuvre. Interestingly, the results indicated that there is a significant difference in the pore sizes accepted by MTWs and cars during filtering (F-stat =1.52, p<0.001, t-stat=8.15, p<0.001) and following (F-stat =1.24, p<0.05, t-stat=6.31, p<0.001) manoeuvres. Although the peaks of the univariate distributions illustrated same modal values of relative speeds for both MTWs and cars, significant differences in the mean and variance values were obtained for relative speed for both filtering (F-stat =0.66, p<0.10, t-stat=2.94, p<0.05) and following scenarios (F-stat =0.69, p<0.05, t-stat=3.68, p<0.001). This signifies that the decision of the drivers to accept or reject the perceived pores in their direction of travel and the relative speeds significantly differ according to the type of subject vehicle involved in the decision making process. Empirical evidence has therefore been provided to justify that the filtering and following behaviour of MTWs and cars are significantly different and show distinct manoeuvring characteristics, thereby necessitating the need to model their manoeuvring patterns separately.

7.2. Factors affecting drivers' decisions to perform filtering manoeuvre

Modelling filtering behaviour and the risks associated with vehicles during filtering have recently spurred a growing response from transport researchers of many countries to model their dynamic behaviours realistically. A previous study by Nikias et al. (2012) underlined that filtering is the most frequent manoeuvre of MTWs in urban arterials. In recently published

research, Vlahogianni (2014) evaluated several determinants that affect MTW riders' decision to accept critical virtual lane widths during filtering, in which relative speed, spacing, heavy vehicle's presence and occurrence of platoon of moving vehicles were found as significant parameters. Yet, other parameters such as surrounding traffic conditions and driver characteristics, may affect the riders' decision during filtering, which indeed needs further detailed exploration. While the filtering behaviour of MTWs has been an ongoing research topic in recent years, cars are even observed to perform a filtering manoeuvre in disordered systems which has not yet received enough scholarly attention.

Till date, no clear cut findings is available in the literature regarding identification of suitable input variables for modelling the filtering behaviour of motorized two-wheelers and cars in disordered traffic systems. This section is devoted to the development of binary logit model for evaluating the subject vehicle's decision to perform a filtering manoeuvre, describing how this choice is affected by different driver-vehicle characteristics and local traffic conditions. Further, suitable emphasis has also been laid to investigate the relative contribution of the influential variables on the filtering likelihood of vehicles.

7.2.1. Binary logit model structure

A binary logit model structure is developed in this section to describe the determinant factors affecting the choice of filtering manoeuvre for MTWs and cars in mid-block sections. It is assumed that the decision of the driver to perform a filtering manoeuvre is affected by driver characteristics, vehicle characteristics (size of the interacting vehicles and the subject MTW), current traffic conditions (presence of surrounding vehicles, heavy vehicles presence, density, etc.) and the history of the past decisions. The tendency of the vehicle to filter is dependent on the minimum traversable pore width required for the subject vehicle to pass in between the two front lead vehicles. This minimum traversable pore width, commonly termed as pore size varies depending on the interacting vehicle types. Each vehicle requires sufficient pores to accommodate the filtering movement. Different types of front leaders as well as the surrounding traffic may affect driver's likelihood to pass. The driver's decision-making process is indeed complex, and it mostly involves logical components as well as some emotional and supplementary elements such as joy of driving, comfort level, fear arousal, etc. which are non-logical and may even be considered as irrational. The data utilized in this research work, however, contains information on the aggregate behaviour of individual drivers collected from the real-traffic phenomenon. Therefore it is anticipated that the logit model structure can explain drivers' behaviour that may appear both rational and irrational.

When a subject vehicle approaches two lead vehicles in her/his direction of travel, the driver can have two discrete choices based on the surrounding traffic environments: filter through the available pore size or follow the lead vehicles due to her/his incapability to accept the pore between other vehicles. These two choices are defined as the choice set C. To account for the assumed determinants, the utility of the subject vehicle n to perform a desired manoeuvre i at

a time t can be modelled using a random utility based discrete choice model which can be expressed as:

$$U_{i,n,t} = V_{i,n,t} + \varepsilon_{i,n,t}, \quad \text{for all } i \in C_{n,t}$$

where $U_{i,n,t}$ is the utility of subject vehicle in choosing choice i at time t, $V_{i,n,t}$ is the deterministic component, $\varepsilon_{i,n,t}$ is the error component and $C_{n,t}$ is the subject driver n's available choice set. The probability of the subject vehicle to choose decision i at time t is expressed as follows:

$$P_{n,t}(i) = \frac{e^{V_{i,n,t}}}{\sum_{j \in C_{n,t}} e^{V_{j,n,t}}}$$

The deterministic component of utility can be regarded as a linear function of exogenous variables defined as:

$$\mathrm{V_{i,n,t}} = \beta \mathbf{Z_{i,n,t}} + \gamma \sum_{\mathrm{j=1}} \mathbf{d_{i,n,t-j}}$$

where the exogenous variables $\mathbf{Z_{i,n,t}}$ are a set of the observed factors involved in decision making process such as average speed of the lead vehicles, subject vehicle's speed, pore size, presence of vehicles in the surrounding traffic, type of interacting vehicles, etc.; β is a vector of parameters to be estimated.

The second term of the deterministic utility model represents the effect of the past history of subject vehicle before filtering. This includes the subject drivers' decisions during the past time steps as perceived from the video recorders, where j represents the relative time, and γ is assumed to be constant over time. This term is introduced in the model to capture the effect of past trajectories on the current choice.

Based on the above specifications and the variables assumed in the model, the deterministic component for the subject driver's choice in performing a filtering manoeuvre can be expressed explicitly as

$$\begin{aligned}\mathrm{V_{filter,\,MTW}} = {} & ASC_F + \beta_1 \mathrm{t_{LHV}} + \beta_2 \mathrm{t_{RHV}} + \beta_3 \mathrm{Size_D} + \beta_4 \mathrm{V_{MTW}} + \beta_5 \mathrm{V_{avg}} + \beta_6 \mathrm{r_p} + \beta_7 \mathrm{Occ} \\ & + \beta_8 \mathrm{S_R} + \beta_9 \mathrm{S_L} + \beta_{10} \mathrm{Age} + \beta_{11} \mathrm{Gender} + \beta_{12} \mathrm{Helmet} + \beta_{13} \mathrm{DF} + \gamma \mathrm{History}\end{aligned}$$

$$\mathrm{V_{filter,\,Car}} = ASC_F + \beta_1 \mathrm{t_{LHV}} + \beta_2 \mathrm{t_{RHV}} + \beta_3 \mathrm{Size_D} + \beta_4 \mathrm{V_{Car}} + \beta_5 \mathrm{V_{avg}} + \beta_6 \mathrm{r_p} + \beta_7 \mathrm{S_R} + \beta_8 \mathrm{S_L}$$

where ASC_F: alternative-specific constant to be estimated;

β, γ: Coefficients to be estimated and all the explanatory variables are in accordance with the description provided in Section 7.1.2.

7.2.2. Estimation results of binary logit model

To describe various determinant factors that affect the behavioural choice of MTWs and cars to filter in between the left and right front vehicles, the results of the binary logit model are presented in this section. Prior to the logit model development, a correlation analysis was

performed to exclude any correlated variables from further analysis. Estimation results of the logit model for motorized two-wheelers with respect to different coefficients and the proposed hypotheses are listed in Table 7.2.

As presented in the table, variables such as speed of MTW rider (V_{MTW}), average speed of left and right front vehicles (V_{avg}), pore size (r_p) and history are found as significant at 0.05 level of significance, the coefficient estimates of which are all of plausible signs as per priori assumptions. The Mc-Fadden rho squared (ρ^2) value for the developed model is 0.464 which can be considered as a pretty high value for a discrete choice model.

According to the test results, all the insignificant variables have to be removed. It seems that driver characteristics (age and gender) do not affect the choice of filtering. Also, the presence of left or, right front heavy vehicle and any vehicle adjacent to the left or right side of the subject MTW rider do not significantly affect its intention to make a filtering manoeuvre; albeit, MTWs are more concerned about the presence of adjacent right most vehicles and heavy vehicles at the right front than the vehicles at the left-hand side (S_R and t_{RHV} are statistically significant at α=0.10). The test results further indicate that high occupancy, helmet usage and the presence of other MTWs in the direct front are not found to have a statistical significant effect in the choice. The revised model for MTW riders after removing all the insignificant parameters can be presented as:

$$V_{filter,\,MTW} = \underset{(p<0.01)}{-6.581} \; \underset{(p<0.001)}{+0.272V_{MTW}} \; \underset{(p<0.001)}{-0.218V_{avg}} \; \underset{(p<0.001)}{+0.516r_p} \; \underset{(p<0.01)}{+0.842History}$$

All the estimated coefficients show expected signs and pass the z-test at 5% significance level. The values in parentheses represent the p-values showing the statistical significance of each variable. It seems that MTW riders initially tend to evaluate the available pore sizes by manoeuvring laterally (if required) and when various determinant factors permit, they utilize a suitable pore size and perform a filtering manoeuvre to achieve relatively higher speeds. Overall, the revised model may predict the probability of filtering with an accuracy of 91.8%.

Similar to the modelling results estimated for motorized two-wheelers, the binary logit model was further developed for cars considering the input variables expect those related to motorized two-wheelers such as age, gender, helmet, occupancy of MTW and presence of another MTW in the direct front of the subject vehicle. Because all the information were collected from the video footage, attributes related to driver characteristics could not be considered for modelling the filtering behaviour of cars. Moreover, the parameter 'history' considered in the MTW model development could not be extended for cars as initial assessment of data indicated no significant lateral movements before performing the filtering manoeuvre. Accordingly, the parameter estimates, a description of the parameters along with statistical values obtained for the logit model development of cars are presented in Table 7.3.

Table 7.2. A priori hypotheses and estimation results of binary logit model for MTWs

Variables	Anticipated effect	Coefficient Estimates	p value
ASC_F		-5.185	p<0.001***
t_{LHV}	Filtering through heavy vehicle present at the left front side may lead increased exposure to MTWs risks as MTW riders will be more under the influence of HVs involvement during filtering. Therefore, the tendency to filter may reduce.	-1.893	0.116
t_{RHV}	A HV at the right front side of a MTW may have a more dominating role than a HV at the left side.	-2.507	0.095*
$Size_D$	Anecdotal evidence suggests that MTWs usually maintain least lateral clearance (d_y) with other MTW riders as compared to other bigger-sized vehicles (Budhkar and Maurya, 2017). Larger the size differential, larger pore size will be perceived by the subject MTW riders, hence higher will be the likelihood of MTWs to filter.	0.534	0.059*
V_{MTW}	A vehicle travelling at higher speed is more likely to filter through traffic.	0.407	p<0.001***
V_{avg}	A MTW rider is more likely to filter if the average speeds of both the lead front vehicles are lower.	-0.232	p<0.001***
r_p	Larger the pore space defined by the interacting lead vehicles, higher is the probability of filtering.	0.685	p<0.01***
Occ	The choice of MTW to filter may be dependent on the number of persons sitting in a MTW. Higher the occupancy, lesser will be the mobility of MTW, larger will be the risks involved, hence it may act negatively to the filtering probability.	-0.255	0.700
S_R	The effect of the presence of a surrounding vehicle just to the immediate right of the MTW can be manifold. On one hand, the vehicle characteristics and sensitivity offered by the left and right front leaders will affect the decision choice while the presence of right vehicle in addition to the front leaders will further have a prominent effect on the choice. Therefore due to the combined constrained effect of the leaders and surrounding right vehicle, most drivers may be more inclined to follow the leaders, hence a negative relationship is anticipated.	1.029	0.082*
S_L	MTW riders' decision are usually more dependent on the right vehicle's static and dynamic characteristics. Therefore a MTW rider is more likely to filter if there is lesser hindrance from the right surrounding vehicle.	0.842	0.634
Age	Young riders are more likely to filter than elder riders.	-0.311	0.369
Gender	Some male riders may engage themselves in risky manoeuvres more than female riders, the likelihood to filter may thus increase for male riders.	0.758	0.375
Helmet	Usage of helmet may boost the confidence of riders to filter.	0.449	0.382
DF	The presence of MTW in the direct front of the subject MTWs may increase the likelihood to filter because the grouping behaviour of MTWs is a commonly observed phenomena. For instance, front MTW riders may attract the subject MTWs to utilize the available pore size in order to filter through traffic.	0.348	0.269
History	The number of lateral movements (>0.5m within 1s; 0.5m is commonly considered as the minimum lateral gap of MTW) made by the subject MTW in the past trajectory may affect the filtering choice as most MTWs riders tend to make large lateral movements so as to find a suitable gap size for filtering.	0.4817	p<0.05**

***Note*:** ***Significant at 0.01 level of significance, **Significant at α=0.05, * Significant at α=0.10

Table 7.3. Estimation results of binary logit model for cars

Variables	Variables description	Coefficient Estimates	z value
ASC_F		-6.822	-3.327 (p<0.001***)
t_{LHV}	Presence of HV as left-front vehicle	0.317	0.839 (0.316)
t_{RHV}	Presence of HV as right-front vehicle	0.507	1.192 (0.233)
$Size_D$	Size differential of the leaders with respect to cars	0.204	1.110 (0.253)
V_{Car}	Speed of cars	0.057	2.583 (p<0.01***)
V_{avg}	Average speed of leading vehicles	-0.081	-2.870 (p<0.01***)
r_p	Pore size	0.998	2.566 (p<0.01***)
S_L	Presence of surrounding vehicle adjacent to the left-side of the car	0.242	0.338 (0.735)
S_R	Presence of surrounding vehicle adjacent to the right-side of car	1.247	1.560 (0.118)

***Note*:** ***Significant at 0.01 level of significance

From the estimated coefficients of the developed logit model, it appears that presence of heavy vehicle in the left-front (t_{LHV}) or right-front (t_{RHV}) side of car drivers, size differential and presence of surrounding vehicles on either side of car do not affect the filtering choice; while speed of subject vehicles (V_{Car}), average speed of leading vehicles (V_{avg}) and pore size (r_p) are found as significant parameters at 99% confidence level. The parameter estimates further indicate that cars are more concerned about the presence of right side surrounding vehicle and right-front leader than that present at the left-hand side, although no statistical significant effect is observed in the filtering choice. After removing all the insignificant variables, the revised systematic utility equation is expressed as

$$V_{filter,\,Car} = \underset{(p<0.001)}{-6.125} \quad \underset{(p<0.001)}{+0.126V_{Car}} \quad \underset{(p<0.001)}{-0.188V_{avg}} \quad \underset{(p<0.001)}{+2.808r_p}$$

All the estimated coefficients show expected signs and the p-values in parentheses indicate the statistical significance of each variable checked at 5% significance level. Comparing the signs of coefficients estimated for the filtering choice of MTWs and cars, except for t_{LHV} and t_{RHV}, all other variables are of plausible signs and a priori assumptions. It is interesting to note that presence of heavy vehicle either as left-front or right-front leader increase the likelihood of filtering for cars while the reverse trend is observed for MTW riders. This can be attributed to the fact that because of increased vulnerability and high exposure of MTW riders, they do not prefer to interact with heavy vehicles for a longer duration as larger will be the duration of filtering and higher will be the risks involved with the riders. In contrary to that, car drivers possess proper physical protection and when they perceive larger available pores, they tend to

filter in between them. These results further support the hypothesis that the filtering behaviour depends on the subject vehicle type, available pore size and speeds of the interacting vehicles.

7.2.3. Sensitivity analysis of the developed logit model

In order to evaluate the sensitivity of the filtering likelihood with speeds of motorized two-wheelers and cars, three different cases of pore sizes are considered; (i) the most favourable case for filtering (r_p=2.5m), (ii) favourable case (r_p=2m) and (iii) smaller pore size (r_p=1.25m) considered to be the less favourable case. The filtering probability with subject vehicles' speeds for different pore sizes and 10kmph average leading vehicles' speed is illustrated in Figure 7.5.

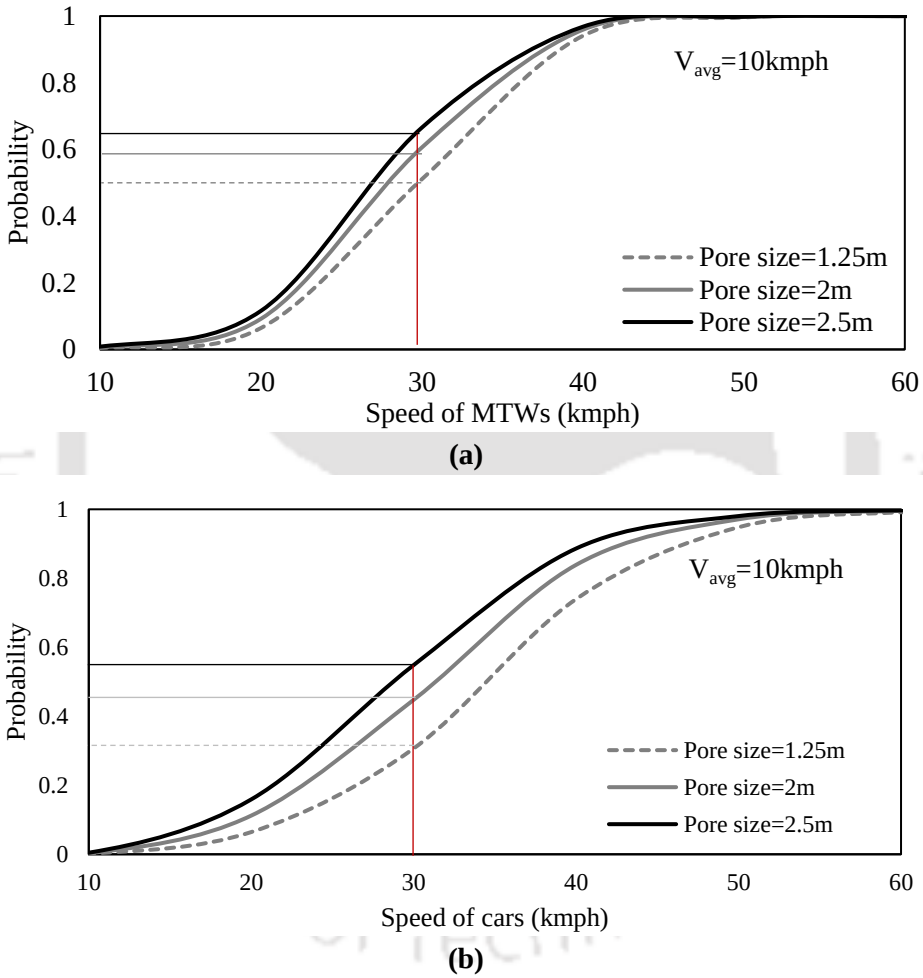

Figure 7.5. Filtering likelihood with respect to subject vehicle's speeds for different levels of conditioning

It is envisaged from the figure that the likelihood to filter increases with the increase in speed of the subject vehicles that is, MTWs and cars are more likely to filter through traffic if they proceed at larger speeds. With 10kmph average speed of leaders, it can be observed that there is an increase in filtering likelihood when the subject vehicles proceed at higher speeds than the leaders. Filtering likelihood is found to be zero for zero relative speed while it increases as the relative speed approaches towards negative values (leaders are slower than subject vehicles). The filtering probability further increases with the corresponding conditional factor

(pore size) increasing, but the relations are non-linear in nature. Larger the available pore size, higher will be the tendency of subject vehicles to avail the pore size and filter through it safely. The filtering probability plots are observed to exhibit a rightward shift in vehicle speeds for cars as compared to MTWs, indicating that cars generally proceed at higher speeds to perform the filtering manoeuvre while MTWs can filter even at lower speeds than that required for cars.

Even for the same subject vehicle's speed of 30kmph, the filtering probability is found to be higher for MTWs than cars. Specifically, 25% increase in pore size (from 2m to 2.5m) leads to 7% and 18% increase in the probability of filtering for MTWs and cars respectively corresponding to a speed difference of -20kmph. Conversely, 60% increase in pore size (from less favourable to favourable pore that is from 1.25m to 2m) results in an increase of 20% and 50% filtering likelihood for MTWs and cars respectively. This observation is indicative of the fact that car drivers are more sensitive to the perceived pore sizes accepted by them during filtering than that of MTW riders. However, it appears that for the most favourable case, subject vehicles' speeds of 40kmph and 50kmph (with relative speeds of -30kmph and -40kmph) are enough for the filtering of MTWs and cars to take place, as the probabilities to filter for MTWs and cars are obtained as 96.8% and 98% respectively.

7.3. Pore acceptance predictions during filtering

With the increasing deployment of Intelligent Transport Systems (ITS) technology in the motorcycle world and automobile industry, the safety aspects of vehicles and their perceptions to safety can be significantly improved in a cognitive architecture. When a subject vehicle approaches two lead vehicles in her/his direction of travel, they may a priori or concurrently have to make a series of decisions: filter through the available lateral space (pore size), or follow the lead vehicles due to its incapability to accept the available pore. The term 'critical pore' has therefore been adopted in this study to represent the minimum pore size accepted by the drivers to comfortably complete the filtering manoeuvre between the two lead vehicles at a mid-block section. That is to say, the driver can filter in between two lead vehicles if the available pore size is larger than critical pore and is called accepted pore, whereas the driver would rather tend to follow if the pore size available is smaller than critical pore and the corresponding pore size is called rejected pore. A proper estimation of critical pore size can suitably improve the representation of overall traffic flow phenomenon, provide a wider perspective in understanding the filtering process and risks associated with MTW riders and car drivers.

Although critical gap analysis is a burgeoning topic within gap-acceptance behavioural research at unsignalized intersections, there is still a paucity of research related to critical pore size determination in the filtering process at mid-block sections. The academic literature on gap acceptance studies has documented different methods for estimating critical gap at unsignalized intersections (Hewitt, 1985; Amin and Maurya, 2015; Pawar et al., 2015), yet the prospect of these developed methods in the estimation and classification of pore acceptance decisions during filtering has not been systematically assessed.

Therefore, in an attempt to understand the filtering/following decisions of MTWs and cars and their perceptions to safety in a dense urban traffic system, this section aims to evaluate the applications and performance of the developed methods popularly used for gap acceptance studies (such as Raff method, logit method, Support Vector Machines and decision trees), for classifying and predicting pore acceptance decisions during filtering at urban mid-block sections. This section firstly provides a description of the considered models, following which empirical results along with model comparisons are summarized.

7.3.1. Estimation methods of critical pore

As critical pores are difficult to acquire from the field directly, it can usually be estimated by evaluating the accepted pores and rejected pores. Accordingly, four methods are selected in this study to evaluate the critical pore: Raff's method, binary logit method (BLM), support vector machines (SVM) and decision tree models.

7.3.1.1. Raff's method

Owing to its simplicity and practicality, the classical Raff's method was selected by many researchers in performing gap-acceptance analyses at unsignalized intersections. According to Raff and Hart (1950), the critical lag L is defined as the size lag for which the number of accepted gaps shorter than L is the same as the number of rejected lags longer than L. So, critical gap can be derived from the intersecting point between the curves of accepted gaps and rejected gaps.

Similar methodology has been translated in this study to define critical pore accepted by the riders in the filtering process at mid-block sections. Based on the proposed methodology, critical pore r_x is defined as that value of r at which the two functions $1 - F_r(r)$ and $F_a(r)$ intersect; where $F_a(r)$ is the cumulative probability of accepted pore, and $F_r(r)$ is the cumulative probability of rejected pore.

7.3.1.2. Binary Logit method

A binary logit model (BLM) is extensively used to model the decision making processes. It offers immense flexibility in handling different factors as explanatory variables. Each vehicle approaching the two leading vehicles in her/his direction of travel has two alternatives: accept the pore to perform the filtering manoeuvre or reject the pore.

A driver in her/his decision situation,d, usually makes those decisions that provide them with the highest utility. This utility can be considered as a combination of safety and the tendency of the drivers to achieve higher speeds than the leading vehicles so as to minimize delay. The deterministic component of utility $V_{i,n,d}$ is assumed to be a linear function of a set of exogenous variables defined as:

$$V_{i,n,d} = \alpha + \beta_1 X_1 + \beta_2 X_2 + \beta_3 X_3 + \cdots + \beta_K X_K$$

where α = alternative specific constant representing the random error term in the utility function

$\beta_1, \beta_2, \beta_3, \ldots, \beta_K$ = vector of coefficient estimates of the explanatory variables to be estimated

$X_1, X_2, X_3, \ldots, X_K$ = vector of the observable factors involved in the decision making process

K = number of attributes

The probability of the driver to choose an alternative i is expressed as follows:

$$P_{n,d}(i) = \frac{1}{1 + e^{-(\alpha + \beta_1 X_1 + \beta_2 X_2 + \beta_3 X_3 + \cdots + \beta_K X_K)}}$$

The logistic function or the probability can be easily linearized with the following transformation

$$P_{n,d}{}'(i) = log_e \frac{P_{n,d}(i)}{1 - P_{n,d}(i)} = \alpha + \beta_1 X_1 + \beta_2 X_2 + \beta_3 X_3 + \cdots + \beta_K X_K \qquad (2)$$

where $P_{n,d}{}'(i)$ is the transformed probability. The critical pore is then calculated as that pore size for which the probability of pore acceptance, $P_{n,d}(i)$ is 0.50.

7.3.1.3. Support Vector Machines

Support vector machine (SVM) is a supervised non-parametric learning method based on Statistical Learning Theory for solving pattern classification problems, clustering and regression (Vapnik, 1998). It combines the fundamental concepts related to learning, concisely-defined formulation and self-consistent mathematical theory (Gryllias and Antoniadis, 2012). Considering high accuracy and good generalization of SVMs for a small number of training datasets (Burges, 1998; Gunn, 1998), SVMs can be considered as an efficient approach in the estimation of critical pore sizes.

In essence, SVM separates the underlying data into two decision classes by an optimal hyperplane. The hyperplane defines the boundary between the two decision classes through a subset of the data points that correspond to the closest accepted and rejected values for both the decision classes (known as support vectors). For a two-dimensional case, the basic form of SVM can be explained in Figure 7.6.

The optimal separating hyperplane in the m-dimensional space can be expressed with the use of support vectors as $(\mathbf{w}.\mathbf{x}) + b = 0$ where $w^T = \{w_1, w_2, .., w_m\}$ defines the boundary, $\mathbf{x}$ is the input vector of dimension m and b is a scalar threshold. The equations for the accepted and rejected pores at the margins (where the support vectors are located) can be expressed as $(\mathbf{w}.\mathbf{x}) + b = +1$ and $(\mathbf{w}.\mathbf{x}) + b = -1$ respectively.

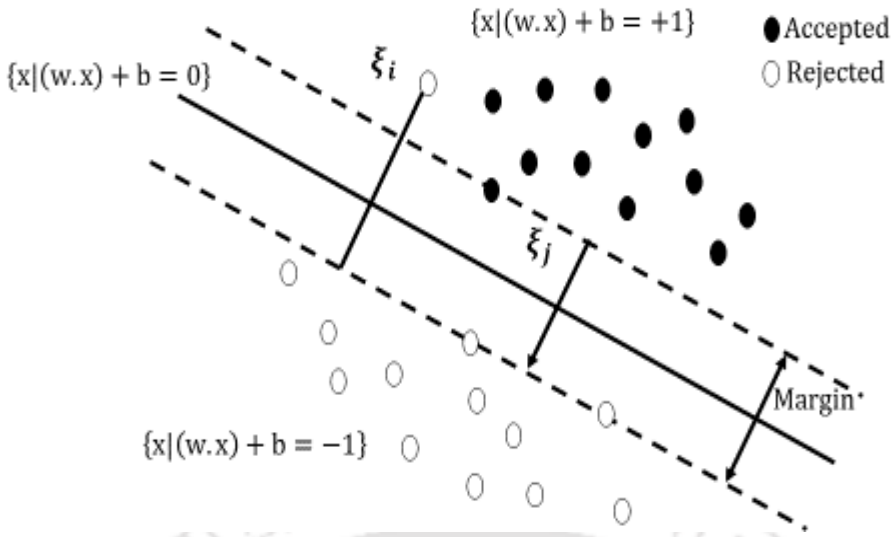

Figure 7.6. Classification of data by support vector machine.

The optimal hyperplane can be calculated by maximizing the margins (minimum $\|w\|$) between the two hyperplanes representing the extremities of the decision classes and minimizing the training error (represented by the slack variables) as given by

$$\min\big(\mathrm{J}(\mathrm{w},\xi)\big) = \min\left(\frac{1}{2}\|w\|^2 + C\sum_{i=1}^{n}\xi_i\right)$$

subject to $y_i(\mathbf{w}.\mathbf{x_i}) + \mathrm{b} \geq 1 - \xi_i$ for all $\mathrm{i} = 1,2,\ldots,N$

To account for noisy and non-separable data, the factor C and the slack variable $\xi_i \geq 0$ are introduced in the above equation where the purpose of C is to control a trade-off between the model complexity and the empirical risk or separating error. For instance, infinite value of C represents a linearly separable case while for non-separable case, C may vary depending on the errors in the trained solution. In order to take into account the linearly non-separable data, a kernel function is used to transform the data into a higher dimension space where the data is linearly separable. The minimization problem can then be solved by introducing a Lagrange multiplier $\{\alpha_i\}$, the decision boundary for which can be expressed as

$$f(x) = \sum_{i=1}^{n}\alpha_i\, y_i k\big(x_i, x_j\big) + b$$

where $k\big(x_i, x_j\big)$=kernel function;

n =set of support vectors

Various kernel functions can be used for constructing optimal separating hyperplane for different types of non-linear input data. Some examples are as follows: linear kernel $k\big(x_i, x_j\big) = \big(x_i.\, x_j\big)$, polynomial kernel $k\big(x_i, x_j\big) = \big(\langle x_i.\, x_j\rangle + 1\big)^p$, and Gaussian radial basis function kernel $k\big(x_i, x_j\big) = exp\left(-\frac{\|x_i - x_j\|^2}{2\delta^2}\right)$ where p is the power of the polynomial

kernel and δ^2 is the bandwidth of the Gaussian kernel. In the present study, the linear kernel function was used.

7.3.1.4. Decision tree model

Decision tree method is one of the most widely used data mining techniques used for classification and prediction of class variables. This method achieves a classification decision by posing a sequence of questions on the feature vectors in a node. Each internal node provides the following question 'Is feature $A_i \leq t$?' where t is a threshold value. The binary answer to the question corresponds to a descendent node and each branch represents one of the possible values of the testing attribute. Unlike other approaches, decision tree models exhibit superior performance in prediction accuracy and interpretation power, and can calculate the relative importance of each explanatory variable contributing to response variables. Moreover, this method does not require prior information on the probability distributions of the explanatory variables and are also capable of modelling non-linear relationships. Prior to the decision tree model development, a balanced dataset is recommended because if a tree grows too large, it could overfit the training data and perform poorly on testing data. The most typical and commonly used decision-tree learning algorithm is C4.5 which primarily supports both discrete and continuous attributes, dealing with unknown attribute values and many other optional features (Yang and Chen, 2016). Although decision trees have been implemented to decision-making process of drivers in overtaking, lane-changing phenomena, (Hou et al., 2014; Barmpounakis et al., 2017) etc., yet this method has not been applied to the modelling of filtering behaviour of MTWs and cars in non-lane based traffic systems.

Construction of decision tree

C4.5 employs a divide-and-conquer strategy to construct a decision tree, in which the algorithm selects all the attributes to be tested at the decision nodes. For a set of cases T belonging to a possible class C_j, the test on the continuous attribute A_i has two possible outcomes $A_i \leq t$ and $A_i > t$, where t is the threshold. At each node of the tree, C4.5 chooses the attribute of the data that most effectively splits its set of samples into subsets enriched in one class or the other using the concept of information entropy or normalized information gain. The information gain for a discrete attribute is calculated as follows:

$$gain = info(T) - \sum_{i=1}^{s} \frac{|T_i|}{|T|} \text{ x } info(T_i)$$

Where $T_1, T_{2,\ldots,} T_s$ are the subsets of T corresponding to cases with different known values for that attribute and the entropy function is given by:

$$info(T) = -\sum_{j=1}^{Nclass} \frac{freq(C_j, T)}{|T|} \text{ x } log_2\left(\frac{freq(C_j, T)}{|T|}\right)$$

The attribute with the highest normalized information gain is then chosen to make the decision.

Tree pruning

The learning algorithm may reduce the training set error so well that it becomes too specific to correctly specify the test dataset. To avoid this problem of overfitting, pruning a decision tree is a fundamental step in optimizing the computational efficiency and classification accuracy (Patel and Upadhyay, 2012). It can significantly reduce the complexity of a model by cutting down branches that contribute less to its predictive accuracy and improve the overall performance of the model.

The C4.5 algorithm applies the error-based pruning method, which is executed from the leaf of the tree to the top based on error in misclassification rates. This method assumes that the error made at a node of the tree on the training set in an estimate of the test set error of that node follows a binomial distribution. Specifically, a confidence interval $\left[L_{CF}(t), U_{Cf}(t)\right]$ for the probability of misclassification for each leaf t (that is, the error occurring over the population at a leaf) can be defined and the certainty factor (Cf) then controls the pruning by using Cf as confidence limit for the binomial distribution $P\left(\frac{e(t)}{n(t)} \leq U_{Cf}\right) = Cf$. With the upper limit and considering the error estimates of the new tree and the original tree and comparing the error rates between leaves, branches and larger branches of a tree, the decision of pruning a certain branch of a tree can be made. In particular, lower values of Cf incur more pruning because progressively more errors are predicted to occur at the leaf for the same number of training samples or, in other words, the errors are overestimated while higher values of Cf would rather indicate no pruning.

7.3.2. Pore acceptance analysis: Empirical results

Although there is no general rule on the number of observations to be assigned for training and testing, the processed dataset was divided into two groups for the prediction of critical pore size: 80% of the observations for each case of filtering and following set were used for training and 20% were used for testing the considered models.

7.3.2.1. Raff's Method

Based on Raff's methodology, critical pore can be defined as that size of pore for which the number of pores shorter than it is equal to the number of pores longer than it. In other words,

critical pore can be obtained from the intersecting point of the cumulative probabilities of accepted and rejected pores as shown in Figure 7.7.

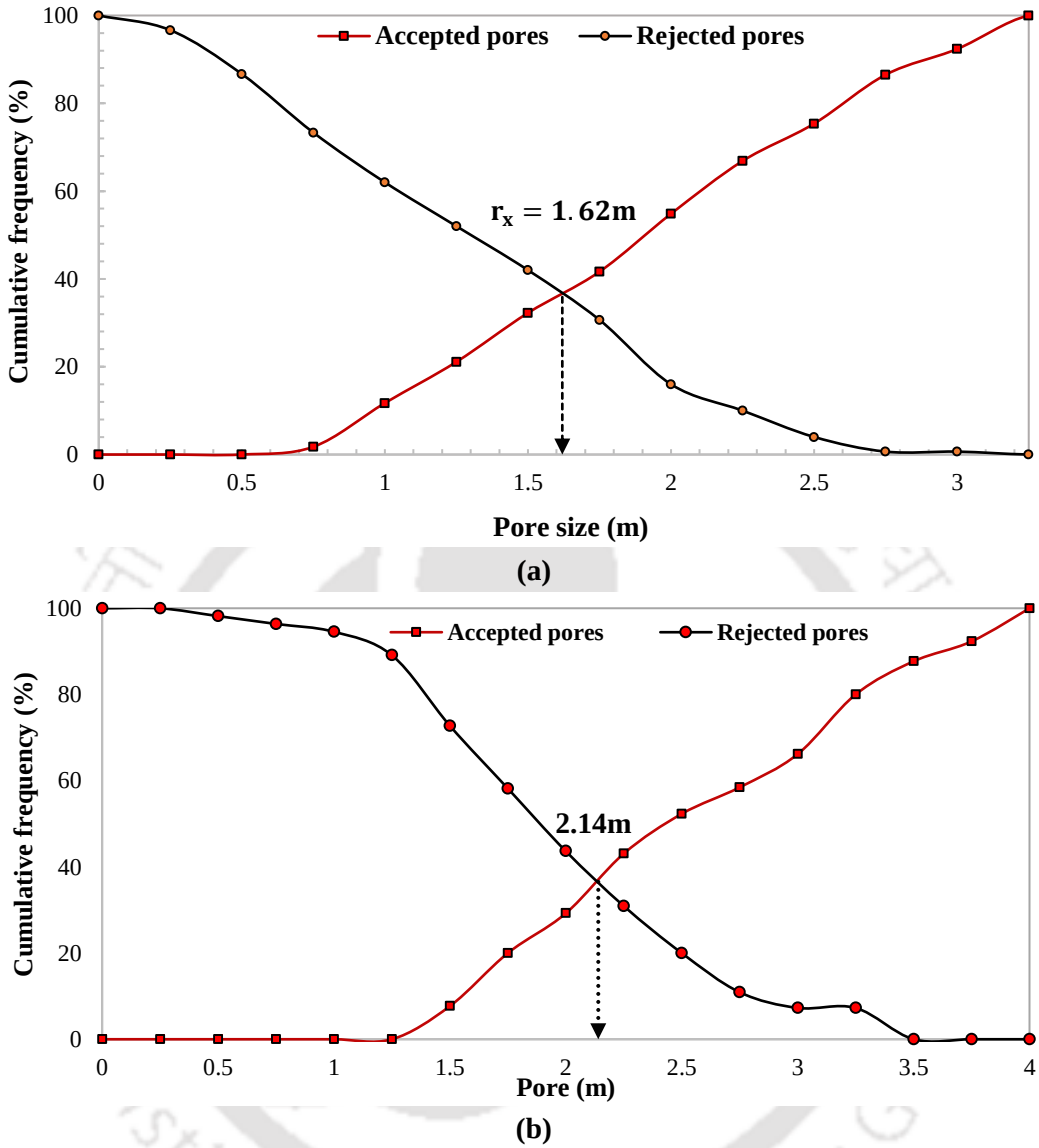

Figure 7.7. Critical pore estimation from the cumulative probability plot of accepted and rejected pores for **(a)** MTWs and **(b)** cars.

The critical pore size for the MTW riders and car drivers are estimated as 1.62m and 2.14m respectively irrespective of the speeds of subject vehicles as well as the leading vehicles. Because of bigger dimensions of cars than MTWs, the pore sizes accepted by cars are much higher than that accepted by MTW riders. Although this method is considered to be popular in the field of gap acceptance studies at unsignalized intersections, yet the prospect of this method in critical pore estimation is quite inexplicit. The decision making process of a driver in accepting/rejecting a pore is believed to be governed by the available pore size and speeds of the leading vehicles and the subject vehicle. Hence, this method may lead to inaccurate estimation of critical pore size if the speeds of the interacting vehicles are not considered; a comparative assessment of the considered four methods will further uphold the proposition.

7.3.2.2. Binary logit method

This method assumes that the pore acceptance behaviour can be represented using a utility function, which can be regarded as a trade-off between safety and travel time saving. As identified previously, the decision of the driver in accepting a pore may depend on the available pore size defined by the leading left front and right front vehicles, speed of the subject vehicle and average speeds of the leading vehicles. While history of past trajectories is obtained as a significant parameter in understanding the filtering choice of MTWs, in an attempt to compare the pore acceptance predictions of both MTWs and cars, all the common significant variables are considered in this study. A binary logit model is therefore developed in this section by considering the assumed variables. Prior to the logit model development, a correlation analysis among the explanatory variables was performed to exclude any cases of correlated variables. In all the cases, correlation value was found to be lower than 0.4. Table 7.4 presents the estimation results of the developed binary logit model for both MTWs and cars in which the coefficients are estimated using the maximum-likelihood method.

Table 7.4. Binary logit model development considering the selected variables

	Variables	Coefficient Estimates	Std. Error	z value	p-value
MTW	Constant	-3.219	0.892	-3.609	0.003
	MTW speed	0.681	0.081	8.399	0.000
	Average speed of front vehicles	-0.711	0.080	-8.835	0.000
	Pore size	1.265	0.392	3.228	0.001
Car	Constant	-6.124	1.050	-3.327	0.001
	Car speed	0.126	0.021	2.583	0.009
	Average speed of front vehicles	-0.188	0.047	-2.87	0.004
	Pore size	2.808	0.289	2.566	0.011

According to the test results, speed of the subject vehicle, average speeds of the leading vehicles and available pore size were found as significant parameters checked at 99% confidence interval. As can be observed, the variables 'MTW/Car speed' and 'pore size' are positively related while average speed of front vehicles is negatively related to the decision of filtering. This implies that the subject vehicle travelling at higher speed is more likely to filter and larger the pore size defined by the interacting lead vehicles, the higher is the probability of pore acceptance. Conversely, the negative coefficient indicates that lower average speeds of the lead vehicles increase the probability of pore acceptance by the vehicles at mid-block sections.

The two decision classes accepted and rejected pores are separated by substituting 0.5 for $P_{n,d}$ in Equation 2 (Section 7.3.1.2.) with the developed logit model structure, from which the separating plane can be obtained for different sets of MTW/Car speed, pore size and average lead vehicles speeds. Figure 7.8 represents the plane separating the accepted and rejected pores for both MTWs and cars.

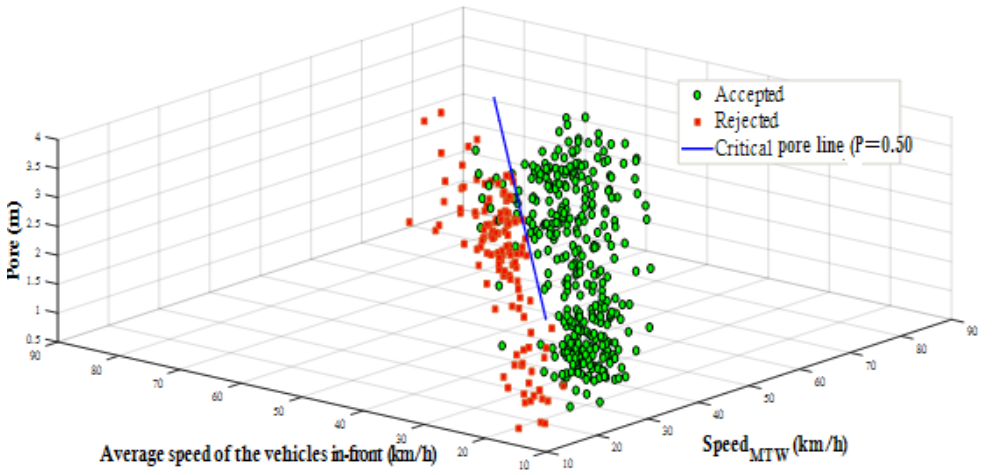

(a)

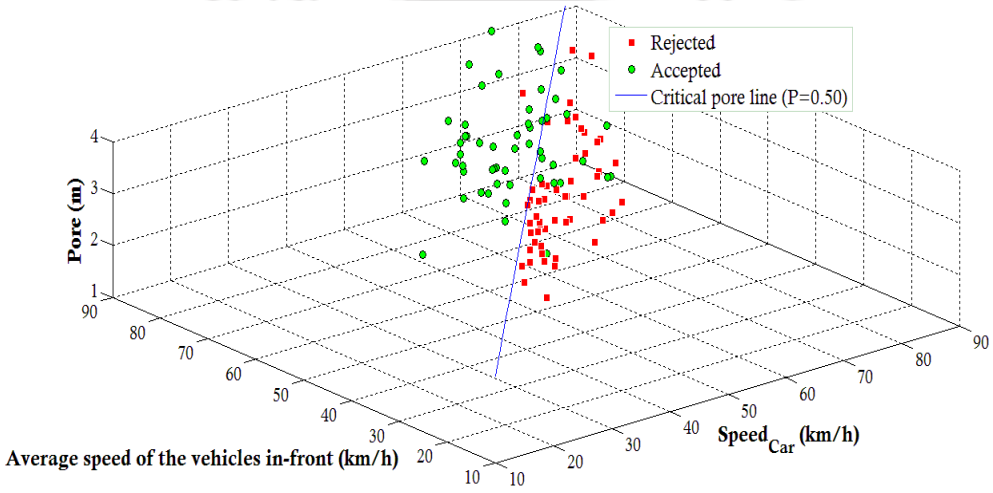

(b)

Figure 7.8. Separating line for BLM considering 50 percent probability for **(a)** MTWs and **(b)** cars

It can be observed that the critical pore increases with the increase in relative speed between the leading vehicles and the subject vehicle. A visual assessment of both the figures reveals that the critical pore values for cars are much higher than MTWs for all combinations of leading vehicles and subject vehicles' speeds. For instance, the critical pores required by the MTWs and cars travelling at 50km/h for a relative speed of -5km/h are observed to be 0.92m and 2.95m respectively. This large difference in the critical pore values justify that the minimum pore sizes accepted by car drivers will be comparatively larger than that accepted by MTWs, which is because of bigger dimensions of cars than MTWs.

7.3.2.3. Support Vector Machines

As identified above, SVMs construct an optimal separating hyperplane which separates the accepted and rejected pores by maximizing the margins between the two hyperplanes representing the extremities of the decision classes. The classification of pore acceptance decision is represented by +1 denoting accepted pores and -1 denoting the rejected pores (see Figure 7.6). For the purpose of SVM model development, three features namely, pore size,

speed of the subject vehicle and average speeds of the leading vehicles are selected and the MATLAB software has been used for the same. A 10-fold cross validation technique was employed to obtain the optimal parameter values of the SVM classifier. Although SVM cannot describe the characteristics of the developed model but it offers flexibility in generating complex linear decision boundary with a simple linear kernel function. The optimal separating hyperplane obtained from the SVM model is depicted in Figure 7.9.

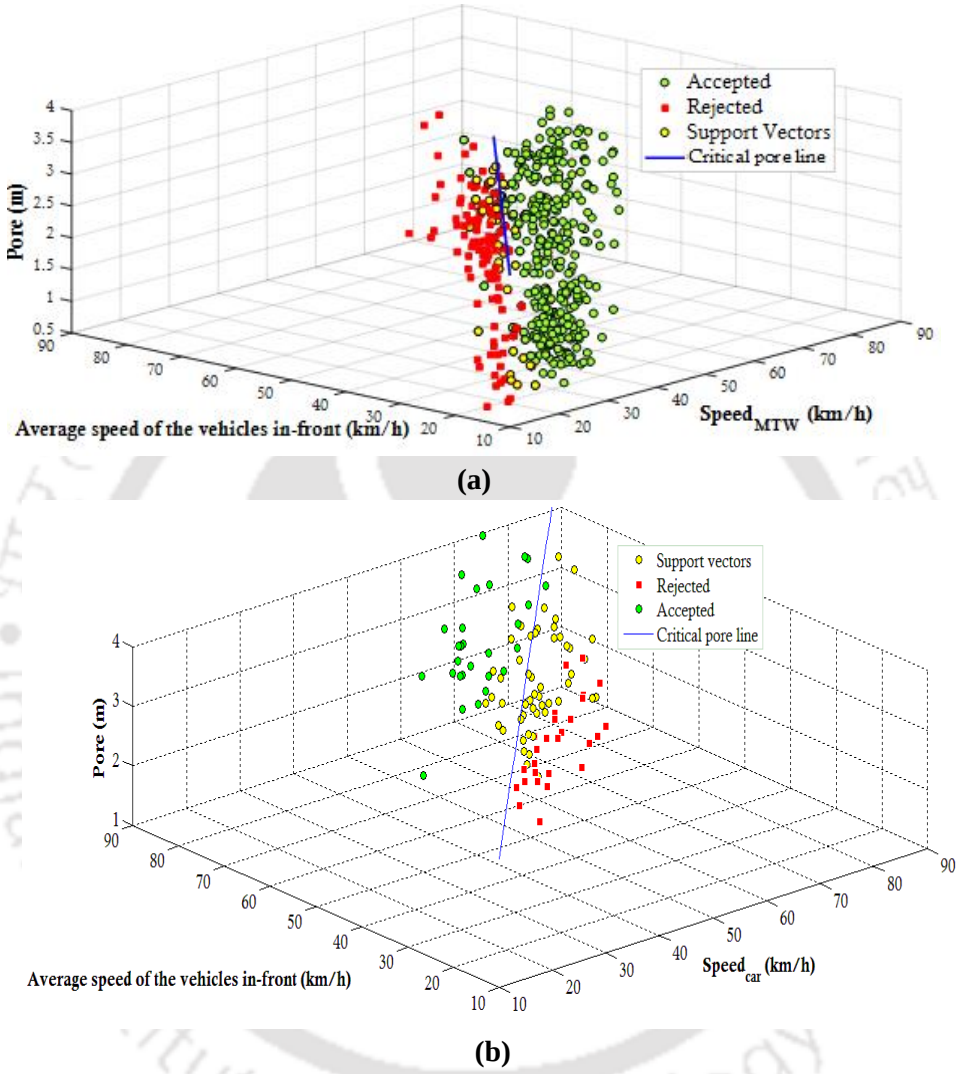

Figure 7.9. Optimal separating hyperplane for **(a)** MTW and **(b)** cars

The optimal hyperplane obtained for the overlapping profiles of accepted and rejected pores can be interpreted as the critical pore line. The green and red profiles of Figure 7.9 are indicative of the accepted pores and rejected pores respectively while the yellow circular profiles represent the support vectors. Further, as expected, the trend of critical pore line reveals a pragmatic increasing relationship for cars than MTWs. Concerning the predictability of the developed SVM model, corresponding to 50km/h speed, the critical pores for MTWs are observed to be 1.07m and 2.01m for a relative speed of -5km/h respectively. These critical pore values for MTWs are observed to be slightly higher than that obtained from the BLM while the critical pores for cars obtained from SVM are relatively lower than that obtained from BLM.

7.3.2.4. Decision tree model

The proposed decision tree model aims to detect under what conditions, the subject vehicles that is, MTW and car will filter in between the vehicles in-front or follow them. It is basically a classification problem where a set of input variables are used to predict the outcome (filter/follow of MTW/car). The three attributes considered in the study that is speed of the subject vehicle, average speed of leading vehicles and available pore size, were selected as predictors in the model with the nominal outcome variable showing whether the MTW rider or car driver did filter in between the lead vehicles (Class 1) or not (Class 0). The prediction accuracy of the developed model is then evaluated by comparing the actual class with the predicted values.

The C4.5 algorithm was implemented in a machine learning software by applying 0.25 confidence factor for pruning. The decision tree structures for MTWs and cars are presented in Figure 7.10.0 and Figure 7.11.1, where terminal nodes are represented by dotted rectangles and decision nodes are represented by bold rectangles.

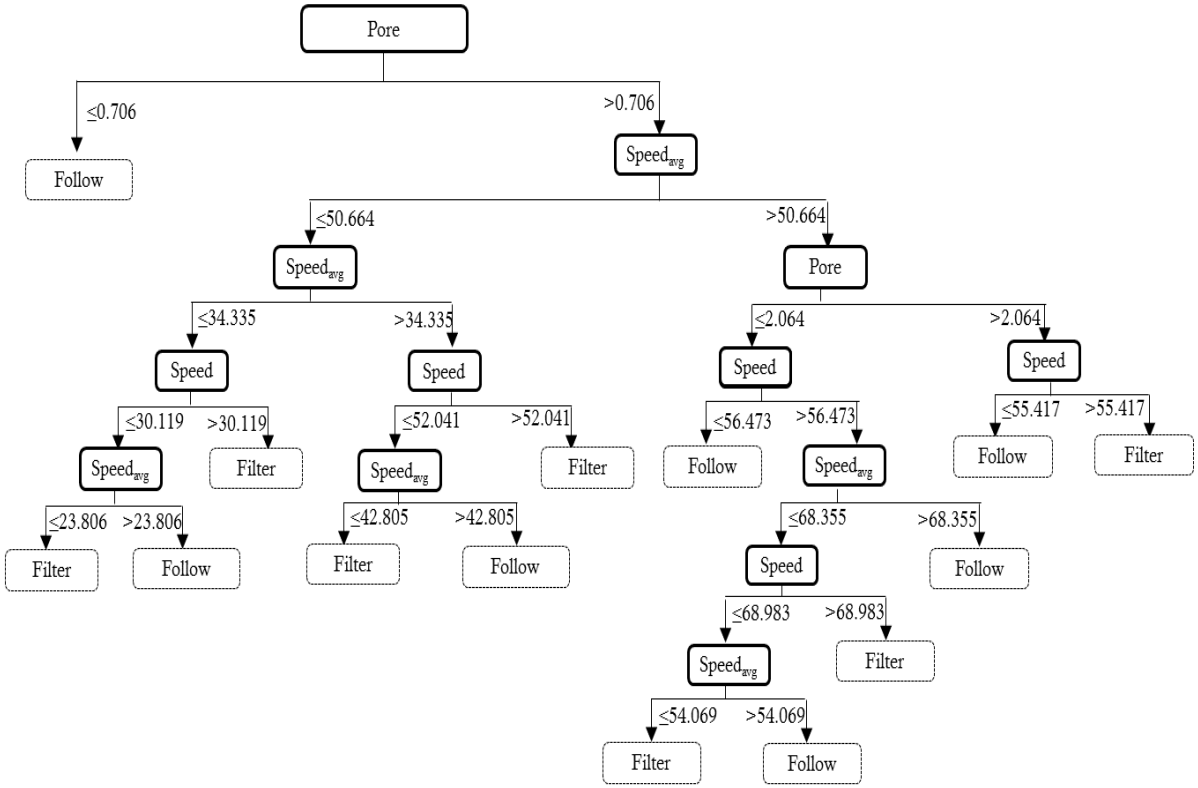

Figure 7.10. Decision tree model structure for motorized two-wheelers

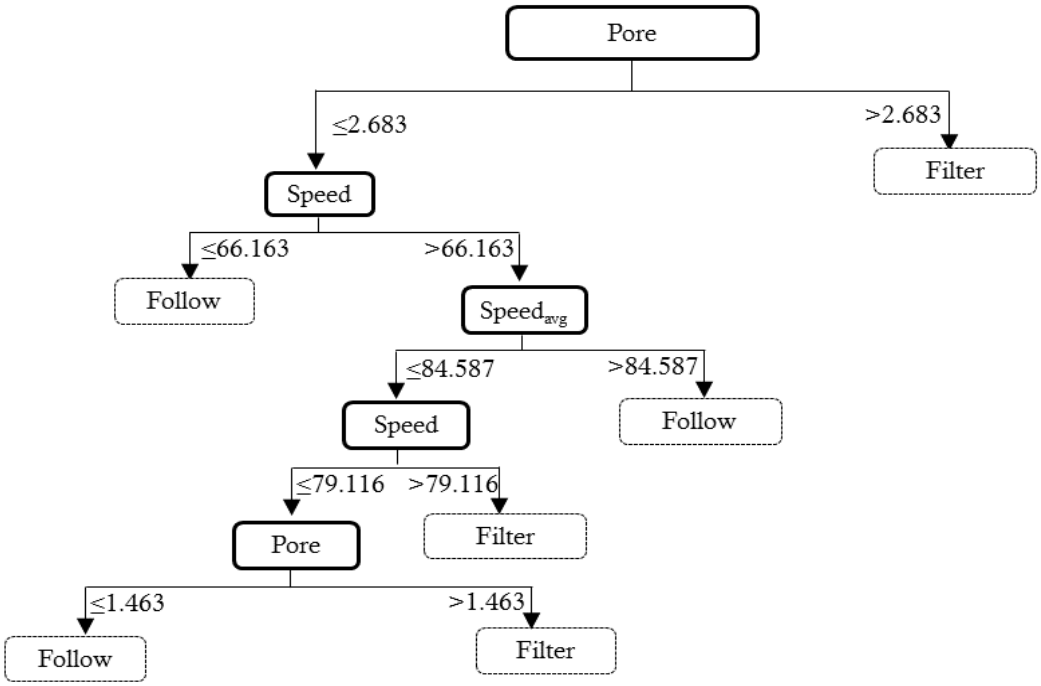

Figure 7.11. Decision tree model for cars

The developed model for motorized two-wheelers indicated that pore size is the most relevant variable in making filtering decisions which is followed by average speed of leading vehicles and subject vehicle's speed. As can be observed, Node 1 was first split by the pore size described by the left-front and right-front vehicles. Under suitable traffic conditions, the MTW riders examine whether the available pore size is greater than 0.71m (or, width of the subject MTWs) and then the average leading vehicles' speeds and subject vehicles speed are examined. For instance, if the pore size is greater than 0.706m, if average leading vehicle's speed lies between 34kmph and 50kmph and subject vehicle travels at speeds higher than 52kmph, the MTW riders decide to filter; following which average leading vehicle's speed criteria is again considered. Subsequently, if the average speed of leading vehicles is greater than 50kmph and available pore size is greater than 2.06m, then the subject MTW's speed is considered, in which the MTW rider decides to filter if speed is greater than 55kmph and follow otherwise. Even when the available pore size lies in the range of 0.71m to 2.06m, the rider's decision to accept or reject the pore depend to a large extent on the leading vehicles' speeds and speeds of the subject vehicle.

From the decision tree model developed for cars, it can be observed that car drivers prefer to filter through the space described by leading vehicles when the available pore size exceeds 2.68m. In contrast, when the pore size is smaller than 2.68m and subject vehicle's speed is lower than 66kmph, car driver prefer to follow the leading vehicles. Furthermore, if the speed of the subject vehicle is large ($66.16 < \text{Speed} \leq 79.12$km/h), average leaders' speed is less than 84.59kmph and pore size is smaller than the car's width (pore < 1.46m), then the car driver decides to follow and filter otherwise (pore > 1.46m).

In particular, the availability of a large pore size does not necessarily guarantee the filtering behaviour of vehicles, this indeed depends on the average speed of leading vehicles, subject vehicle's speed and available pore size. These rules generated by the decision tree are representative of the decision making process of the MTWs and cars while driving in urban roads. Yet, a comparative assessment of all the four considered critical pore estimation models will help in evaluating the better performance and predictions of realistic pore acceptance behaviour.

7.3.3. Comparison of Raff, BLM, SVM and decision tree methods

Recapitulating the above discussion, Raff's methodology resulted into a critical pore of 1.62m and 2.14m for MTWs and cars respectively irrespective of the speeds of interacting vehicles, the developed BLM and SVM methods estimated a critical pore line, while the decision tree model classified the pore acceptance decisions for different combinations of pore size, MTW and car speeds and leading vehicles' speeds. Therefore, in an attempt to assess the prediction success rates of the four methods, a 2x2 confusion matrix is developed from the outcomes of each of the method. A complete set of 20% data which were not utilized for the model development has been used to test the actual performance of the developed methods with the observed dataset. The prediction success values for all the developed methods for both MTWs and cars are presented in Table 7.5.

Table 7.5. Prediction results according to Raff, BLM, SVM and decision tree

Methods	Observed decision	Predicted decisions			
		MTWs		Cars	
		Rejected	Accepted	Rejected	Accepted
Raff's method	Rejected	28 (z)	18 (f)	11 (z)	7 (f)
	Accepted	22 (m)	37 (h)	4 (m)	10 (h)
BLM	Rejected	41 (z)	5 (f)	17 (z)	1 (f)
	Accepted	2 (m)	57 (h)	6 (m)	8 (h)
SVM	Rejected	44 (z)	2 (f)	16 (z)	2 (f)
	Accepted	2 (m)	57 (h)	2 (m)	12 (h)
Decision tree	Rejected	38 (z)	4 (f)	15 (z)	3 (f)
	Accepted	2 (m)	57 (h)	2 (m)	12 (h)

Note: z, f, m and h values represent the number of correct negatives, number of false alarms, number of misses and number of hits respectively.

From the prediction table, the overall prediction success rates can be obtained by adding the correct predictions for both accepted and rejected pores that is by calculating $(z + h)/(z + f + m + h)$; accordingly the respective prediction values for Raff, BLM, SVM and decision tree methods for MTWs are found to be 61.90%, 93.33%, 96.19% and 94.1% respectively while for cars the respective prediction accuracy are obtained as 65.6%, 78.1%, 87.5% and 84.4% for Raff, BLM, SVM and decision tree respectively. The results indicate that the SVM model performs reasonably better than the decision tree, BLM and Raff's

method, although the prediction success rates of SVM and decision methods differ by a marginal amount for both MTWs and cars.

The performance of the four pore acceptance prediction methods is further evaluated from the developed 2x2 confusion matrix by computing various categorical statistics and skill scores such as, bias, precision, recall, F1-score, misclassification rate and False Alarm Ratio (FAR). Bias represents the proportion of total accepted pores predicted by the model relative to total observed accepted pores. Precision represents the proportion of correctly predicted accepted pores in contrast to total predicted accepted pores. On the other hand, recall denotes the proportion of correctly predicted accepted pores relative to total observed accepted pores. F1-score is a weighted harmonic mean of precision and recall. Misclassification rate is the proportion of incorrectly classified accepted and rejected pores relative to total observations. The false alarm ratio (FAR) is the proportion of incorrectly classified pores predicted by the model in contrast to total accepted pores predicted by the model. A detailed explanation on the categorical statistics can be found in Wilks (2011). The skill scores for all the developed four methods along with the formulation of each statistic are presented in Table 7.6.

Table 7.6. Skill Scores for Raff's Method, BLM, SVM and decision tree methods

Skill scores	Formulae	Vehicle	Raff	BLM	SVM	Decision tree	Criteria
Accuracy	$\frac{(z+h)}{(z+f+m+h)}$	MTW	0.619	0.933	0.962	0.941	
		Car	0.656	0.781	0.875	0.844	
Bias	$\frac{(f+h)}{(m+h)}$	MTW	0.932	1.051	1.000	1.030	<1Underestimation 1 Unbiased estimation >1Overestimation
		Car	1.214	0.643	1.000	1.071	
Precision	$\frac{h}{(h+f)}$	MTW	0.673	0.919	0.966	0.934	Percent of correct predictions
		Car	0.588	0.889	0.857	0.800	
Recall	$\frac{h}{(m+h)}$	MTW	0.627	0.966	0.966	0.966	1 Correct estimation of all accepted pores
		Car	0.714	0.571	0.857	0.857	
F1-score	$2\frac{Precision * Recall}{Precision + Recall}$	MTW	0.649	0.942	0.966	0.949	1 Best score 0 Worst score
		Car	0.645	0.695	0.857	0.827	
Misclassification rate	$\frac{(f+m)}{(z+f+m+h)}$	MTW	0.381	0.067	0.038	0.057	1 Highly inaccurate 0 Best score
		Car	0.343	0.218	0.125	0.156	
False Alarm Ratio (FAR)	$\frac{f}{(h+f)}$	MTW	0.327	0.081	0.034	0.065	0 Best score 1 Worst score
		Car	0.412	0.111	0.143	0.200	

It is evident from the table that the SVM model performs reasonably well than the decision tree, BLM and Raff's method, although there is a marginal difference in the prediction rates of decision tree and SVM. The bias score for SVM is 1 indicating that the SVM model provides an accurate estimate of pore acceptance. The precision and recall values for SVM are also higher than decision tree, BLM and Raff methods while the misclassification rate of SVM is the least of all, which indicates that the SVM method predicts the 'accepted' events more accurately than the other three methods. Conversely, the FAR value shows that Raff method

predicts more 'accepted' pores that are actually observed to be rejected; however the SVM has a lower FAR indicating the better performance of SVM model. Concisely, the skill scores indicated the better performance of SVM model than Raff, logit and decision tree methods for both MTWs and cars, although a slight improvement in the skill scores was obtained for the SVM model as compared to decision tree model.

7.3.4. Implementation of the pore acceptance prediction model

With the increasing penetration of MTWs and cars in urban networks, more efficient driver assistance systems are now set to move into the motorcycle and automobile industry in recent years. Some vehicles are now equipped with Adaptive Cruise Control (ACC) that accord to the partial automation of its longitudinal control, in which the ACC modulates adaptively the speed and headway to a front vehicle pre-determined by the users. For an efficient MTW and car oriented intelligent system design, the complex manoeuvring patterns of MTWs and cars on road need to be modelled, which could essentially assist and support the drivers in detecting upcoming safety hazards and risky situations in a convenient manner. While intelligent systems with on-air warnings can identify risky situations considering data from only one vehicle, the intended manoeuvres of MTWs and cars, and their decisions to filter through traffic can be better identified in a cooperative intelligent transport systems environment. With the recent advancements in ITS applications and various sensors and new technologies, the machine learning algorithm can suitably advance the design of Advance Driver Assistance Systems (ADAS). Vehicle dynamics play a crucial role in the design of ADAS that could optimize the filtering manoeuvres using different thresholds of speeds and available pore sizes.

A proper estimation of critical pore size can suitably improve the representation of overall traffic flow phenomenon, provide a wider perspective in understanding the filtering process and risks associated with MTW riders and car drivers. The use of wireless vehicle-to-vehicle communication and data transmission may well benefit from improving the safety and efficiency of the road network, reduce congestions and emissions by delivering accurate warnings to the vehicles. As far as the implementation of the results is concerned, a proper estimation of critical pore size can essentially guide and assist the subject vehicle whether the available pore size, current traffic conditions and the subject vehicle's speed are adequate to accept the pore and conduct a safe filtering manoeuvre. At the same time, the vehicle-to-vehicle communication systems can inform the front vehicles and guide drivers before and during the manoeuvre. Cooperation of the leading vehicles in terms of reducing their speeds with the subject vehicle may allow a successful and safe filtering manoeuvre to take place, however the implementation is still crucial for this part. In cases if the available pore is less than the critical pore size, the system can warn the driver of risky situations ahead and would rather guide to follow the leading vehicles.

Although the filtering manoeuvre delivers many purported benefits such as increased capacity, reduced emissions, travel time saving, etc., if the results generated by the SVM model can be fed into the advanced driver assistance systems, it will not only improve driver's safety but also optimize traffic flow. This calls for the real-time implementation of vehicle-to-vehicle

technologies and pore acceptance prediction models in a cognitive architecture, for increasing the capacity, providing safer driving environment to both MTW riders, car drivers and the surrounding vehicles, where all drivers communicate and cooperate with each other for a safe yet smooth flow of traffic.

7.3.5. Application of 'critical pore' in lane-based scenario

The concept of 'critical pore' is introduced to evaluate the transition regime from vehicle-following to filtering scenario in disorderly traffic environments. This concept can however be extended to model the lane changing decisions of drivers in lane-based scenario. Lane-changing decisions are often modelled using random utility theory. A comprehensive review of the lane changing models is presented in Moridpour et al. (2010). Ahmed (1996, 1999) defined critical gap in gap acceptance models. In essence, lane changing is feasible if a gap or pore of sufficient size is available and speed of the target lag vehicle allows the subject driver to execute the lane-change manoeuvre in the target lane. The subject driver can move into the target lane if the available pore size is not less than the critical pore size. Figure 7.12 illustrates a scenario where the subject vehicle in the current lane interacts with the front vehicle in the same lane and target lag vehicle in the right adjacent lane for the possibility to execute a lane changing manoeuvre.

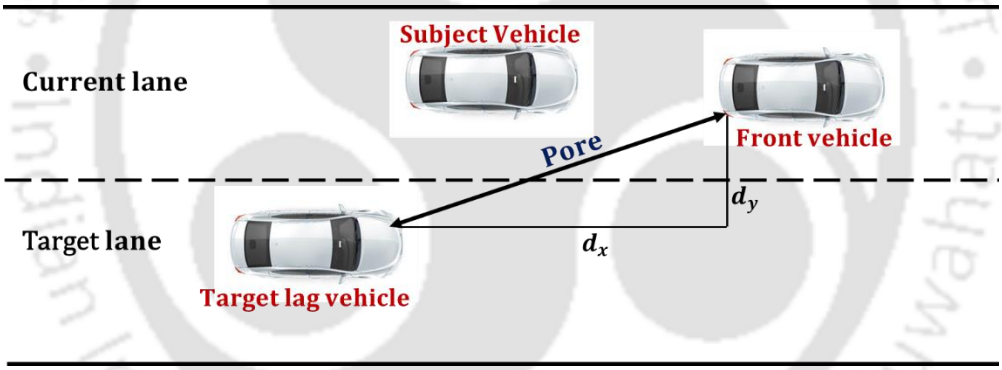

Figure 7.12. Interaction of subject vehicle with surrounding vehicles in lane-based scenario

As discussed in Section 7.3.2., the pore acceptance/rejection decisions in a filtering scenario depend on the speed of the subject vehicle, average speed of the vehicles in-front and available pore size described by the leading vehicles. These findings are also applicable for predicting lane changing decisions in lane-based scenario. Depending on the average speeds of the front vehicle and target lag vehicle and speed of the subject vehicle, if the available pore size is larger than the critical pore size, the subject vehicle will accept the available pore to execute lane-changing manoeuvre in the target lane. This indicates that the concept of critical pore can be extended for modelling lane-changing decisions in lane-based traffic, which can still be explored in future.

7.4. Quantifying comfort associated in filtering

In recent years, researchers have focused more on the safety aspects of MTW riders as compared to other modes of transportation, due to their increased exposure to crash risks and

lesser physical protection. Concerning the safety benefits of MTW riders, a consistent theme emerging from the peer-reviewed literature is that the filtering behaviour of MTWs can be considered as safer, which has indeed emerged as a contentious issue since decades. Implicit in many of the purported safety benefits of MTW-filtering, such as reduction in the risk of rear-end collisions (ACEM, 2009), improved visibility of hazards and traffic (Hurt et al., 1981), is an assumption that the filtering manoeuvre poses several safety concerns and may result in heightened risk of collisions because bigger-sized vehicles often fail to notice the presence of MTWs in traffic due to their compact sizes (Clarke et al., 2004; Sexton et al., 2004; Hublart and Durand, 2012; Rogé et al., 2010). Rogé et al. (2010) highlighted that one of the primary reasons of collisions involving an MTW is lack of attention and/or perception on the part of car driver to detect the MTW in time. Understanding that the filtering manoeuvre poses several safety concerns to the MTW rider, despite copious purported benefits, this section attempts to investigate the multi-variate aspects of MTW riders during filtering and their associated comfort or risk levels.

To suitably elucidate the spatio-temporal aspects of interactions between MTW riders and other surrounding vehicles, quantify the gain of a MTW rider during filtering and the associated risks involved in filtering, the crucial factor which may significantly affect MTW's decision to perform a filtering manoeuvre should be identified and modelled. Recent literature has emphasized the importance of different supplementary factors such as Time-to-Collision (TTC), driving comfort during overtaking (Barmpounakis et al., 2017), perceived safety, joy of driving and social welfare in comprehending the interaction of several driver-vehicle units (Altendorf and Flemisch, 2015; Arbis et al., 2016; Barmpounakis et al., 2017).

Among all the factors identified in the literature, a latent measure termed as Comfort at Filtering (CaF) is defined in this study, which jointly considers the safety measures and the desire of MTW riders to utilize the available pore space defined by the front vehicles in order to achieve higher speeds than the surrounding vehicles. The introduced measure CaF is a non-observable variable (latent variable), a detailed exploration of which will lead to an enhanced comprehension of the interaction of different driver-vehicle units with rest of the traffic.

7.4.1. Structural Equation Modelling Concept

A structural equation model (SEM) is constructed in this section in order to quantify the latent variable CaF for the MTW rider. SEM is a comprehensive advanced statistical modelling approach used to test the hypothesis on the simple and complex relations among observed and unobserved (latent) variables (Hoyle, 1995; MacCallum and Austin, 2000); test and estimate a theoretical framework (assuming linear relationships among the variables) and also to understand the pattern of correlations among the variables (Suhr, 2010). The model consists of two components: a measurement model and structural model. The measurement model deals with the relations between the latent variables and their indicators while the structural model defines the potential causal relationships between exogenous and endogenous variables and their causal effects.

The fundamental equation of the structural model is described as (Bollen, 1989):

$$\eta = \beta\eta + \Gamma\xi + \zeta$$

where η and ξ are a (u x 1) vector of the endogenous latent variables and a (v x 1) vector of the exogenous latent variables respectively; β and Γ are a (u x u) coefficient matrix for the latent exogenous variables and a (u x v) coefficient matrix for the latent exogenous variables respectively; and ζ is a (u x 1) vector of random variables. The basic equations of the models for exogenous and endogenous variables are described as follows:

$$x = \Lambda_x\xi + \delta$$

$$y = \Lambda_y\eta + \varepsilon$$

where x and δ are related to the observed exogenous variables and residuals respectively; y and ε are related to the observed endogenous variables and residuals respectively; Λ_x and Λ_y are the coefficients to be estimated for latent exogenous and endogenous variables respectively to their observed indicator variables.

The Maximum Likelihood Estimation (MLE) approach is adopted in this study to estimate the coefficients in the SEM. The goodness-of-fit of the developed model is assessed by implementing likelihood ratio tests for comparing the model with the saturated one (the model that reproduces variances, covariance and means of the observed variables perfectly) and baseline model (the model which encompasses the means and variances of all observed variables and also covariance of all observed exogenous variables). In addition, various tests such as root mean square error of approximation (RMSEA), the standardized root mean square residual (SRMR) and the coefficient of determination of various models are also evaluated.

7.4.2. Estimation and assessment of SEM

For estimating the latent CaF parameter for the MTW rider, four variables are defined as indicators in the SEM model:

a) Relative speed between average of the lead vehicle speeds and subject MTW (Diff) expresses the desire of MTW riders to achieve higher speeds than the front lead vehicles,
b) Average speed difference of left front and right front vehicles before and during filtering (Diff_{int}) expresses the cooperativeness of the front leaders with the subject MTW rider by reducing their vehicle speeds during the filtering manoeuvre,
c) Pore size (r_p) expresses the desire to utilize the available space during filtering, and
d) Duration, the desire of MTWs to avoid the presence of the surrounding lead vehicles for a long duration.

Table 7.7 shows the statistics for goodness-of-fit tests of the estimated SEM model for the riding comfort of MTW riders in filtering. The χ^2 statistics for the saturated and the baseline models are 9.561 (p-value=0.921) and 169.912 (p-value=0.000) respectively. Based on the suggestion by Schermelleh-Engel et al. (2003), a model with RMSEA of less than 0.08, SRMR

less than 0.05, CFI of above 0.95 and TLI of less than 3.00 can be considered as acceptable. Accordingly, the obtained goodness-of-fit indices suggest that the developed SEM model is acceptable (RMSEA=0.000, SRMR=0.009, CFI=1.000, TLI=1.371).

Table 7.7. Goodness of fit evaluation for SEM models

	Fit statistic	Estimated Values	Criteria
Likelihood ratio	$\chi^2(P > \chi^2)$-Saturated	9.561 (0.921)	
	$\chi^2(P > \chi^2)$-Baseline	169.912 (0.000)	
Population error	RMSEA	0.000	<0.05- Close <0.08- Good <0.10- Reasonable
	90% CI, Lower Bound	0.000	<0.05-Close
	90% CI, Upper Bound	0.023	>0.10 Poor
	pclose	0.992	>0.05
Size of residuals	Standardized Root Mean Square Residual (SRMR)	0.009	<0.10- Favourable <0.05- Good
Baseline comparisons	Comparative Fit Index (CFI)	1.000	>0.90- Good fit
	TLI	1.371	<3.00

Figure 7.12. presents the estimated SEM for the comfort associated in filtering for the MTW rider. Rectangles in the figure are indicative of the observed variables and ellipses represent the latent variable. The curved line (double-headed arrows) between the two exogenous variables depict the non-directional degree of association between them, while the directional arrow indicates the direction of influence from the exogenous to endogenous variables (Washington et al., 2010) and the numbers in the arrows are the estimated parameters.

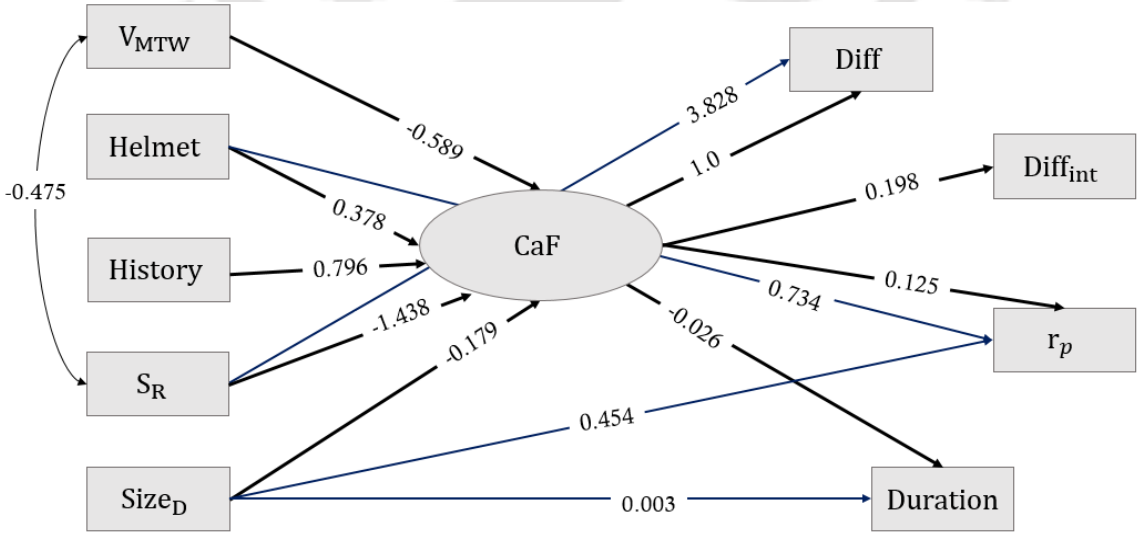

Figure 7.13. Final SEM for the MTW riders' comfort in filtering

The various predictors for the SEM model are considered as: MTWs' speed (V_{MTW}), usage of helmet (Helmet), number of lateral movements made by the MTW rider in the past trajectory

before attempting to filter (History), presence of surrounding right vehicle adjacent to the MTW rider (S_R) and size differential of the lead vehicles' dimensions with respect to the subject MTW rider ($Size_D$). As can be observed, the predictors V_{MTW}, S_R and $Size_D$ are negatively related to the comfort at filtering while Helmet and History are positively related. This may be attributed to the fact that MTW riders perceive increased risks at filtering when they move at higher speeds and are under the influence of bigger-sized front leaders and as a result, the riding comfort level reduces. On the contrary, the usage of helmet boosts the confidence of the rider in performing a filtering manoeuvre and hence his comfort level also increases; on the other hand, history of trajectories considerably increases the riders desire to filter because they usually tend to look for appropriate available pore spaces by making large number of lateral movements in order to undergo the filtering manoeuvre smoothly. Moreover, a strong negative degree of association between V_{MTW} and S_R is revealed which clearly indicates that the presence of surrounding right vehicle results in a reduction of the subject MTW rider's speed.

Table 7.8 presents the results of the estimated model. The coefficients of the predictors show that speed of the MTW rider (V_{MTW}) and the presence of surrounding right vehicle adjacent to the MTW (S_R) are significant parameters for calculating the comfort of MTW riders at filtering (significant at 5% significance level), while the number of lateral movements made by the MTW in the past trajectory, the MTW rider wearing a helmet or not and the size differential are also of importance when estimating CaF.

Table 7.8. Results of the estimated model

Variables	Coefficient	Std. error	z-statistic	p>|z|
CaF				
V_{MTW}	-0.589	0.069	-8.618	0.000
Helmet	0.378	0.622	1.638	0.104
History	0.796	0.488	1.742	0.092
S_R	-1.438	1.427	-1.969	0.047
$Size_D$	-0.179	0.679	-1.701	0.083
Diff				
CaF	1 (Constrained)			
S_R	3.828	2.206	2.035	0.043
$\boldsymbol{Diff_{int}}$				
CaF	0.198	0.094	2.470	0.014
$\boldsymbol{r_p}$				
CaF	0.125	0.067	2.070	0.038
Helmet	0.734	0.377	2.031	0.042
$Size_D$	0.454	0.122	3.905	0.000
Duration				
CaF	-0.026	0.041	-1.664	0.096
$Size_D$	0.003	0.068	1.046	0.408

As far as the indicators are concerned, the available pore size (r_p), average speed difference of left front and right front vehicles before and during filtering ($Diff_{int}$) are critical parameters for defining CaF while the duration required for the rider to complete the filtering manoeuvre is found to be significant at 10% significance level; the coefficient of r_p is 0.734 and more influential than the coefficient of $Diff_{int}$ (0.198) and Duration (-0.026). Usage of helmet, presence of surrounding right vehicle and size differential of the lead vehicles with the subject MTW have a positive relationship with the pore size. Duration was found to be higher with the increase in size differential, although size differential was found to be insignificant. The coefficients of the indicators indicate that the desire of MTWs to filter through traffic increases with the availability of a large pore size while it decreases when MTWs are more under the influence of the leading vehicles during filtering for a longer time. Furthermore, the estimated coefficient for $Diff_{int}$ signifies that the front leaders are usually more cooperative with the MTW riders as they tend to slow down their speeds for a successful MTW filtering manoeuvre to take place.

7.5. Chapter summary

Recent MTW-oriented literature has underlined filtering of MTWs as the most frequent manoeuvre in dense urban areas, which has systematically received considerable attention by transport modellers of many countries. Nevertheless, vehicles including motorized three-wheelers and cars are even observed to filter through traffic in disorderly traffic. This chapter attempted to demonstrate the differences in filtering and following manoeuvre of vehicles in urban mid-block sections, addressing how the decision-making process of drivers to accept or reject the available pore sizes are dependent on several factors, followed by an evaluation of pore acceptance predictions both from driver's safety point of view and from driver behavioural modelling standpoint. Essentially, the behavioural aspects of MTW riders and car drivers are considered in this research work.

Preliminary investigation on the behavioural differences of MTWs and cars indicated that filtering and following behaviour of vehicles are significantly different and show distinct manoeuvring characteristics according to the type of subject vehicle involved in the decision making process. The binary logit models resulted into a set of spatial and kinematic parameters that were significant in determining the driver's likelihood to perform a filtering manoeuvre. Speed of the subject vehicle, average speed of both the leading vehicles and available pore size are the common significant factors affecting the filtering choice of both MTWs and cars. Howbeit, history of the past trajectories of MTWs was found as an additional factor affecting the MTW rider's choice of filtering, indicating that number of lateral movements made in the past trajectory affect the filtering likelihood.

In the estimation of critical pore sizes for both motorized two-wheelers and cars, the support vector machines method was found to outperform the decision tree model, binary logit model and Raff's method, although a marginal improvement in the overall performance was attained for SVM as compared to decision tree model. In particular, considering the high accuracy and

good generalization of SVM for a small number of samples (Burges, 1998), this technique was considered as efficient tool for estimating the pore acceptance and rejection predictions. Moreover, an assessment on quantifying the MTW riders' comfort associated in filtering corroborated significant dependent relationships between different parameters. Particularly, it seemed that MTWs riding at higher speeds preferred to perform a filtering manoeuvre (under suitable traffic conditions), although it reduced their riding comfort levels. As importantly, this research can be a new impetus in the development of autonomous vehicles in developing nations, in which the filtering/following decisions can be fed into the system based on the developed support vector machine learning algorithms, the implementation of which is indeed a crucial task.

8

Conclusions and Avenues for Future Research

This chapter aims to summarize the main findings of the dissertation and to give an outlook for future research. The context of this dissertation is towards understanding driver behaviour in vehicle-following and filtering scenario of disordered traffic systems that can capture interdependencies between both longitudinal and lateral vehicle interactions simultaneously. Drivers' preferences in maintaining certain lateral separation with the preceding vehicles are commonly observed in disordered traffic systems where they often look for possible lateral gaps while progressing longitudinally. Such an integrated driving behaviour adds more complexity to the realistic representation of disorderly traffic, giving rise to various driving phenomena/regimes (Lee et al., 2009). Attaining a comprehensive understanding and a detailed investigation of different driving regimes in the following scenario such as car-following, staggered-following and two leader following, and filtering scenario will not only improve reliability of the models but will indeed contribute a major step towards development of a full-fledged integrated driving behaviour model of disorderly traffic systems more realistically. This research has outlined a modelling framework to capture behavioural aspects of drivers in vehicle-following and filtering scenario of disorderly traffic, and has subsequently attempted to address the key research questions.

The main results from the previous chapters are summarized in this chapter, with a discussion on how the research questions and the objectives are addressed, following which several scientific recommendations and practical implications of the findings are discussed. Finally, the last section in this chapter outlines the avenues for future research and directions for their extensions.

8.1. Research findings and conclusions

The main findings and conclusions of the dissertation are summarized in this section. The structure of the research questions is followed to present concluding remarks on the research conducted in this thesis. A discussion on how each research question has been attempted to fulfil the proposed objective is further provided.

1. Why is modelling different driving regimes important for the development of an integrated model?

Development of an integrated driving behaviour model requires detailed characterization of driving regimes such as car-following, staggered-following, two-leader following, filtering, information on drivers' behavioural responses, longitudinal and lateral distance keeping behaviour, deterministic values of regime boundaries such as transition from two-leader-following to filtering and so forth. The research work undertaken in this thesis attempted to address this question by providing a detailed investigation on the behavioural aspects of drivers in the operational and control process in each driving regime. While Chapter 4, 5 and 6 provide an elaborate investigation on modelling single leader and two-leader vehicle following scenario, Chapter 7 is devoted to modelling the filtering behaviour of vehicles. An amalgamation of the major findings obtained from these chapters can address this research question and the concluding remarks are briefly listed below-

i. ***Characterization of driving regimes:*** Although existing literature suggests threshold values for defining longitudinal interaction, the extent of lateral influence of the leading vehicles in different driving regimes is still lacking. To describe lateral interaction in a single leader following scenario, centerline separation (CS) lower than 0.34m has been assumed as a replication of car-following event (Gunay, 2003). However, in case of staggered-following regime, results from Chapter 4 indicated that vehicles' interactions are not prominent beyond 2m centerline separation. Conversely, considering drivers' manoeuvring pattern in a two-leader following and filtering scenario, a maximum clear lateral clearance of 2m between the leading vehicles was assumed to describe lateral interaction in a two-leader following regime; whereas pore sizes of 3m and 4m were considered as maximum thresholds for defining filtering regimes of motorized two-wheelers (MTWs) and cars respectively.

ii. ***Longitudinal and lateral distance keeping behaviour:*** Findings of Chapter 4, 5, 6 and 7 indicate that the desired lateral position of drivers depend to a large extent on the relative positions (both longitudinal and lateral) of the interacting leading vehicles. In this context, the major findings from all the four chapters can be briefly summarized as:

- As the extent of off-centeredness between the interacting vehicles increases, vehicles in staggered-following scenario tend to follow the leading vehicle closely, either to have a better field of view or to avoid the encumbrance of the leader.
- The modal values of bivariate time-headway centerline separation (TH-CS) plots developed for different combinations of leader-follower vehicle-pairs, as discussed in Chapter 4, represent preferred lateral and longitudinal positions of the followers. The selection of following headways and CS in a single-leader vehicle-following scenario depends on the dimensions of the leading vehicles as well as operational capabilities of the following vehicles. Vehicles having

poor dynamic characteristics maintain larger headway and lesser CS with the leaders. For instance, the modal values of TH-CS plots for truck-car and car-truck pairs occurred at (1.125s, 0.625m) and (1.75s, 0.25m) respectively. Moreover, the bivariate TH-CS plots depicted a gradual rightward shift (that is, increase in time headway) with increasing dimensions of the interacting vehicles.

- Concerning two-leader car-following driving regime, the findings of Chapter 6 indicated that preferences of following driver in maintaining certain lateral and longitudinal spacing with the leading vehicles depend on the positional arrangement of both the leaders. When both the leaders move parallel to each other with 100% overlap in length, most of the times drivers prefer to position their vehicles midway in between both the vehicles with a CS of 2m. The results further demonstrated that as centerline separation between the leaders increase from 1.25m to 1.75m, the stable longitudinal gaps decrease from 23m to 19.5 m respectively (Section 6.2.3.1.). On the contrary, when one of the leaders move ahead of the other, the followers tend to avail the longitudinal gap by shifting laterally, with different CSs with the left-front and right-front leaders.

iii. ***Driver's control process in the following regime:*** Drivers' behavioural responses in terms of acceleration/deceleration in the following regime are characterized by adopting an artificial neural network (ANN) based modelling approach. Chapter 5 and 6 are devoted to modelling the response of the followers in a single-leader and two-leader car-following regime considering inputs as longitudinal gap and CS with the leading vehicle(s), relative speeds and speeds of the following vehicle. Real life acceleration/deceleration asymmetries were observed in the data and the domains confirmed that drivers are more sensitive to deceleration than acceleration in both single-leader and two-leader following regimes. Interestingly, drivers in a two-leader following regime were found to be more susceptible to leading vehicles' actions when there is 100% overlap in length between the leaders. The results from Chapter 6 further indicated that the more perceptible the relative speed is, no significant effect of leaders' orientation is observed on the behavioural responses of followers.

iv. ***Transition from two-leader following to filtering scenario:*** The term 'critical pore' has been introduced in this work to represent the transition regime from following to filtering manoeuvre for MTWs and cars. Estimation results of critical pore are summarized in Chapter 7. In the estimation of critical pore sizes, considering high accuracy and good generalization of support vector machines (SVM) for a small number of samples (Burges, 1998), this technique was considered as efficient tool for estimating the pore acceptance and rejection predictions. Corresponding to 50kmph speed of subject vehicles and 45kmph average leading vehicles' speeds, the critical pores for MTWs and cars are obtained as 1.07m and 2.01m respectively.

To summarize, results of this research attempted to address this question by underlining the differences in behavioural aspects of drivers and modelling their behaviour in each driving

regime such as car-following, staggered-following, two-leader following and filtering scenario. Results from these chapters indicated that drivers' control processes and their preferences to follow a single/two leader(s) or filter through traffic depends to a large extent on the longitudinal and lateral positions of the interacting leading vehicle(s), dimensions and operational capabilities of the interacting vehicles, available pore size between leading vehicles and speeds of the interacting vehicles. Estimation of critical pores further demonstrated deterministic values of regime boundaries from vehicle-following to filtering scenario for MTWs and cars. Information on such drivers' behavioural responses in each driving regime and characterization of regime boundaries would contribute towards detailed understanding of behavioural processes of drivers in each driving regime of disorderly traffic, leading towards development of a comprehensive integrated driving behaviour model.

2. Are the existing data collection techniques appropriate for modelling different driving regimes observed in disorderly traffic?

This question was addressed in Chapter 2 and 3 by reviewing the existing video-based data collection techniques and demonstrating the need to develop image-based on-board data collection technique for modelling detailed vehicle-following responses in disordered traffic environments. While static video recording technique is found suitable to collect data for staggered-following and filtering regimes involving interactions with diverse vehicle types, such technique cannot be directly utilized for the collection of dynamic time-series data in the following regime. Although the efficacy of GPS receivers has been elucidated in the existing literature of disorderly traffic, the estimation of lateral separation may produce unreliable results. Therefore, an image-based in-vehicle trajectory data collection technique is developed in this work (Chapter 3) to process dynamic time-series single-leader and two-leader car-following data (such as longitudinal gap, CS, vehicle speeds, acceleration, etc.) using camera calibration and in-vehicle GPS information on straight roads. The real-time of sampling, the global coordinates and speed of each vehicle involved in the experiment are directly obtained from the GPS receivers at 10Hz frequency while the positional data of the vehicle in-front are extracted from the video recorders at each 5Hz frequency level. After suitable calibration process, the GPS data and the extracted video-data are then synchronized to obtain the desired parameters at each 0.2s-intervals. A detailed description on the proposed methodology is discussed in Chapter 3. This research therefore attempted to develop an image-based in-vehicle trajectory data collection technique for collecting detailed time-series data in a single-leader and two-leader vehicle-following scenario.

3. Data requirements for driver behaviour modelling are stringent. What attributes need to be selected for modelling?

Selection of suitable attributes required for driver behaviour modelling in each driving regime depends on the level of information available as well as on the studied phenomena such as single/two leader following and filtering scenario. Attempts have been made in Chapter 4, 5, 6 and 7 to address this question. The major findings from these chapters can be illustrated as:

- Preliminary investigation on the staggered-following behaviour indicated that mean time headways reduce with the increase in road widths (Section 4.1.3.1.), but the reduction is not statistically significant.
- Vehicle-type specific headways and CS need to be considered for modelling disorderly traffic systems.
- Several microscopic traffic variables such as longitudinal gap, centerline separation, relative speeds and speeds of the following vehicles need to be considered for modelling drivers' responses (in terms of acceleration/deceleration) in a single-leader car-following scenario. As highlighted in chapter 5 (Section 5.2.3.2.), the PAWN global sensitivity analysis also indicated the relative contribution of these considered variables in modelling behavioural responses of drivers. More precisely, relative speed is the most significant parameter (0.6339) for predicting responses, followed by longitudinal speed (0.5725), speed (0.4416) and centerline separation (0.3640).
- As summarized in Chapter 5 (Section 5.2.2.3.), drivers' reaction delays for deceleration responses are found to be lower than that when responding to an accelerating vehicle in the following scenario, with significant differences being obtained in mean values of acceleration and deceleration responses. Estimation results of ANN based models indicated better performance with 0.6s reaction delay for a single-leader car-following scenario and 0.4s reaction delay for a two-leader car-following case. This justifies the importance of reaction delay in modelling realistic drivers' responses in a single/two leader(s) car-following scenario.
- Modelling drivers' responses in a two-leader car-following scenario requires consideration of longitudinal gap and centerline separation with the left-front and right-front vehicles, relative speed between average leading vehicles and subject vehicle and speed of the following vehicle. The global sensitivity analysis (discussed in Section 6.2.2.2 of Chapter 6) further corroborated the importance of these variables.
- Speeds of the leading vehicles and subject vehicle and available pore size are the common variables that need to be considered for understanding the filtering and following manoeuvres of MTWs and cars. From the sensitivity analysis of the binary logit model (Section 7.2.3. of Chapter 7), it appeared that following vehicles travelling at speeds of 40kmph and 50kmph (with relative speeds of -30kmph and -40kmph with the front vehicles) are enough for the filtering of MTWs and cars to take place, as the probabilities to filter for MTWs and cars are obtained as 96.8% and 98% respectively.

Results from these chapters indicated the relative contributions of centerline separation, longitudinal gap with the leading vehicle(s), relative speeds and speeds of following vehicles in modelling drivers' responses in a single/two leader(s) car-following scenario. Estimation results of ANN based models further demonstrated the importance of driver's reaction delay in modelling single-leader and two-leader car-following process. Moreover, speeds of the leading vehicles and subject vehicle and available pore size are the common variables that need to be considered for understanding the filtering behaviour of both MTWs and cars.

4. Why is the integration of longitudinal and lateral interaction important in traffic flow modelling?

The importance of lateral descriptor in understanding the behavioural phenomena of disorderly traffic in the vehicle-following scenario has been attempted in Chapter 4, 5 and 6. Major concluding remarks addressing this research question are listed below:

- The choice of time headways (longitudinal descriptor) in the staggered-following scenario is found to be strongly related with the lateral descriptor of vehicle interaction (or centerline separation, CS). The correlation coefficients (Kendall's tau, τ and Spearman's rho, ρ_S) between TH and CS revealed significant dependence structure in the range of $\tau \in [-0.487, -0.009]$ and $\rho_S \in [-0.672, -0.021]$ for different leader-follower vehicle-pairs.
- Having identified significant correlation between TH and CS, a copula-based modelling framework is developed in this research to capture the dependence structure by accommodating both the longitudinal and lateral descriptors of traffic.
- Bivariate Frank copula, with lognormal and Weibull distributions for TH and CS respectively, was found suitable to model the joint TH-CS distribution for different leader-follower combinations, only exception being with 3W-car and MTW-car where Gaussian copula provided the best fit.
- Modelling results of Chapter 5 (Section 5.2.3.) indicated that the introduction of CS as input variable in a single-leader car-following model improved the model performance from R=0.6841 to R=0.7464. The sensitivity analysis further indicated the contribution of CS in modelling acceleration of following vehicles.
- Results of the ANN based single-leader car-following model further indicated that the stable longitudinal gaps were achieved at about 16m, 13.5m and 11m at CS of 0m, 0.5m and 1.5m respectively for 11m/s speed of leading and following vehicles (Figure 5.12.). This indicates the importance of CS in depicting the behavioural phenomena of drivers.
- As discussed in Chapter 6, model estimation results for a two-leader car-following scenario also revealed an improvement in model performance from R=0.6436 to R=0.7158 when centerline separations with both the leaders are incorporated in addition to longitudinal gap, relative speed and speed of subject vehicles.

To summarize, this research demonstrated that the lateral descriptor of vehicle interaction (or, centerline separation) has a significant effect in modelling the longitudinal descriptors of traffic (time headways, acceleration of following vehicles, etc.), making the lateral dimension an important concept in driver behaviour modelling of disorderly traffic. Capturing such inter-dependencies between the longitudinal and lateral vehicle interactions will provide a detailed understanding of driver behaviour and augment the predictability and reliability of microsimulation models developed for such disordered traffic systems.

5. Can the existing models be applied for modelling disorderly traffic flows?

This question was addressed in Chapter 5 and 6 by developing a data-driven artificial neural network based single/two leader(s) car-following model and comparing its performance with the widely-used car-following models. Results from chapter 4 and 5 underlined that the lateral descriptor, although being poorly represented in the existing car-following models, offers a significant role in predicting behavioural aspects of drivers. Some important findings obtained from these chapters are listed as:

- As summarized in Chapter 5, an ANN architecture (4-30-1), consisting of four inputs (such as relative speed, speed of subject vehicle, centerline separation and longitudinal gap), 30 neurons in the hidden layer and one output (acceleration of following vehicle), with 0.6s reaction delay is found suitable to model normative human driving responses in a single-leader car-following model.
- A comparison of the developed ANN model with the classical single-leader CF models (such as Gipps, GHR and IDM models) further corroborated that ANN model significantly outperforms the classical models in reproducing trajectories (with 3.1% mean squared error in acceleration prediction). Among the classical CF models, the Gipps' model has more accurate predictions in speed and distance estimation, followed by GHR and IDM models. On the other hand, the GHR model was found to have better correspondence with the data than the IDM model.
- For modelling complex dynamics of subject drivers in a two-leader car-following scenario, an ANN architecture (6-35-1) consisting of six inputs (average relative speed, longitudinal gaps with LF and RF vehicles, centerline separations with LF and RF vehicles and speed of the following vehicle), 35 neurons in the hidden layer and one output (acceleration of following vehicle), with 0.4s reaction delay was found suitable to illustrate realistic human-like following behaviour of drivers.
- Comparing error measure of ANN model with the existing optimal velocity models indicated that the ANN model had better correspondence with empirical data (with 17.8% MAPE in distance) than the full velocity difference model (29.1% MAPE).

Results from these chapters indicated that the data-driven ANN-based single-leader and two-leader car-following model outperformed the existing classical models in terms of trajectory-reproducing accuracy, thereby demonstrating the ability to reproduce human-like car-following behaviour in the vehicle-following scenario.

6. Can the safety aspects of drivers be evaluated in such systems?

For the assessment of rear-end collision risks or safety in the vehicle-following scenario of disorderly traffic, the temporal surrogate indicator namely time-to-collision (TTC) has been considered to distinguish between safe and unsafe encounters. While a constant TTC warning threshold is used for lane-based traffic, the results from Chapter 4 demonstrated that a pragmatic decreasing relationship prevails for TTC with increasing CS and decrease in lead vehicle size for single-leader vehicle-following scenario. For instance, the warning thresholds

for MTW-car, 3W-car, car-car, LCV-car and truck-car in pure car-following scenario (CS≤0.34m) are found to be 1.58s, 2.12s, 3s, 3.22s and 3.77s respectively. On the other hand, as the CS increases from 0.5m to 2m, the minimum TTC thresholds for car-car decreases from 2.77s to 2.16s respectively. These findings indicate that the collision avoidance systems should incorporate different TTC-thresholds corresponding to the interacting lead vehicle type and CS between the interacting vehicles, to evaluate and enhance traffic safety, rather than considering a constant TTC_{min} threshold across all centerline separations and lead vehicle types. In parallel, findings from Chapter 6 further demonstrated that the recommended TTC thresholds defined for a single leader car-following event may not be applicable to a two-leader following event.

Moreover, considering increased risk exposure of MTW riders in the filtering regime as compared to cars, a latent measure termed as comfort at filtering is defined in Chapter 7 for evaluating driver's comfort or risk levels. As summarized in Chapter 7, results of the structural equation modelling indicated that the riding comfort level of MTW riders decreases when they move at higher speeds and are under the influence of surrounding vehicles. Particularly, it seemed that MTWs riding at higher speeds preferred to perform a filtering manoeuvre (under suitable traffic conditions), although it reduced their riding comfort levels.

8.2. Contributions of the thesis

The main scientific contributions of the dissertation are described in brief below.

8.2.1. Lateral descriptor in traffic flow modelling

The main contribution of this work comes from its cognizance of considering lateral separation of the interacting vehicles (centerline separation) in modelling the longitudinal descriptors of traffic. Empirical evidence suggests that CS has a prominent effect on the drivers' selection of headways, on defining time-to-collision thresholds and also in modelling behavioural responses of drivers (in terms of acceleration) in the staggered-following scenario. Even the lateral position of the subject vehicles depend on the positional arrangement of the leaders in a two-leader following regime, signifying the importance of incorporating lateral descriptor in driver behaviour modelling. Results of the dissertation have demonstrated that what has traditionally been thought to be a simple vehicle-following process depends, in fact, to a large extent on the lateral descriptor of traffic, making the lateral dimension or centerline separation an important concept in traffic flow modelling.

8.2.2. Joint distribution modelling in staggered-following scenario

Traditionally, longitudinal descriptors of traffic flow (such as time headway, time-to-collision, etc.) were modelled independently via univariate models. But such models describing the staggered-following behaviour did not fully consider the lateral dimension of human driver behaviour. This research contributes to the existing literature by developing a copula-based joint distribution modelling framework that can accommodate the dependence structure between the longitudinal and lateral descriptors of traffic in the staggered-following scenario. Bivariate copula models of CS and time headways were developed for different combinations

of leader-follower vehicle-pairs, justifying the need to consider bivariate vehicle-type specific behavioural models for describing headways in staggered-following scenario. Similarly, the minimum TTC thresholds across different CSs and leading vehicle-types were also defined from the developed bivariate copula models.

8.2.3. Dynamic in-vehicle trajectory data collection technique

An image-based in-vehicle trajectory data collection technique is developed to extract and process dynamic time-series data in a single-leader and two-leader car-following scenario. Considering the importance of lateral descriptor in modelling disorderly traffic flows, collection of time-series data from only GPS receives may lead to inaccurate and unreliable results. While reliable information on vehicle speeds and acceleration can be obtained from GPS receivers, information on longitudinal and lateral separation between the vehicles cannot be directly obtained from the GPS receivers.

This research work, therefore, proposes and establishes an image-based in-vehicle trajectory data collection system to process the microscopic variables (such as longitudinal gap, centerline separation, vehicle speeds, accelerations, etc.) using camera calibration and in-vehicle GPS information on straight roads. Such dynamic video-tracking technique can prove to be adequate for understanding detailed behavioural responses of drivers in a single-leader as well as two-leader car-following scenario.

8.2.4. Artificial neural network methodology for modelling drivers' responses in disorderly flows

The research work proposes an artificial neural network model for predicting acceleration responses of drivers in a single-leader and two-leader car-following scenario. The proposed ANN models could illustrate realistic following behaviour of drivers, much better than the existing classical models (commonly used in non-lane based traffic systems) both in terms of trajectory reproducing accuracy and generalization capability. The ANN models could also explain the closing-in, shying-away behaviour and local/asymptotic stability properties. In this regard, the ANN models can be considered to complement the existing classical models by embracing more realistic human driving behaviour in vehicle-following regimes.

8.2.5. Behavioural phenomena in a two-leader following regime

The behavioural aspects of drivers in a two-leader car-following scenario, which have remained unexplored, are investigated in this research. This work has attempted to answer how drivers apperceive the two-leader car-following scenario, how they perform control actions and how the positional arrangement of the leading vehicles affect the lateral position of the followers. Drivers' preferences in maintaining longitudinal and lateral spacing with the leading vehicles were found to depend on the positional arrangement of the leaders. The anticipatory behaviour of drivers in a two-leader following scenario is much more complex than a single-leader following case, with symbolic emphasis being laid on the differences in drivers' behavioural characteristics with respect to different situational factors and traffic characteristics.

8.2.6. Filtering behaviour in urban areas

A detailed investigation of the decision making process of motorized two-wheelers and cars during filtering in urban mid-block sections is elaborated in this research, describing how this choice is affected by different driver-vehicle characteristics and local traffic conditions. A binary logit model is developed to describe the determinant factors affecting the choice of filtering manoeuvre, with suitable emphasis being laid on investigating the relative contribution of these variables on the filtering likelihood. A latent measure termed as comfort at filtering is also defined in this work for investigating the comfort or risks associated with MTW riders while filtering on urban roads.

8.2.7. Critical pore describing transition regime from vehicle-following to filtering scenario

The concept of critical pore is introduced in this research to evaluate the transition regime from vehicle-following to filtering scenario of cars and MTWs. That is to say, the subject vehicles will filter if the available pore size is larger than the critical pore and they will follow otherwise. The performances of raff method, logit method, support vector machines and decision tree are evaluated for classifying and predicting pore acceptance decisions at urban mid-block sections. Results indicated an improved performance of support vector machines in estimating the pore acceptance and rejection predictions.

8.3. Applications and practical implications of the research

The practical implications of the obtained results are briefly discussed in this section.

Results obtained in modelling drivers' behavioural aspects in the vehicle-following and filtering scenario, by capturing interdependencies between longitudinal and lateral vehicle interactions, can contribute a major step towards development of a comprehensive integrated driving behavioural model for disordered traffic streams. This dissertation has attempted to focus more on understanding the micro-level behavioural aspects of drivers and modelling drivers' responses in each driving regime. Having recognized the differences in driving behaviour in each driving regime, if the results obtained in this research are implemented in the microscopic simulation models, it would inherently augment the realistic characterization of drivers' behaviour and improve the reliability and predictability of the simulation model more realistically. A realistic development of such models would enhance the development of smarter and user-friendly autonomous cruise control systems, intelligent traffic operation studies, traffic safety evaluation, congestion mitigation, capacity estimation and so forth.

With the advent of driving-assistance systems, vehicles are now equipped with adaptive cruise control (ACC)/ collision avoidance systems (CAS) in which the system maintains a safe headway to the vehicle in-front according to the settings predefined by the users, and also warns the drivers of upcoming potential threats and imminent collisions. While intelligent systems with on-air warnings can identify risky situations considering data from only one vehicle, the intended manoeuvres of subject drivers and their decisions to follow a single/two leader(s) or filter through traffic can be better identified in a cooperative intelligent transport systems environment. The use of wireless vehicle-to-vehicle communication and data transmission may

well benefit from improving the safety and efficiency of the road network, reduce congestions and emissions by delivering accurate warnings to the vehicles. Concerning safety aspects of the drivers in disorderly traffic flows, the results of this research work demonstrated that the collision avoidance decision model generally developed for describing only longitudinal vehicle dynamics should incorporate the lateral descriptor of traffic and the lead vehicle type as well, to evaluate the safety performance in non-lane based traffic environments.

As far as the implementation of the critical pore estimation results is concerned, a proper estimation of critical pore size can essentially guide and assist the subject vehicle whether the available pore size, current traffic conditions and the subject vehicle's speed are adequate to conduct a safe filtering manoeuvre. At the same time, the vehicle-to-vehicle communication systems can inform the front vehicles and guide drivers before and during the manoeuvre. Cooperation of the leading vehicles in terms of reducing their speeds with the subject vehicle may allow a successful and safe filtering manoeuvre to take place. In cases if the available pore is less than the critical pore size, the system can warn the driver of risky situations ahead and would rather guide to follow the leading vehicles.

This research can be the new impetus in the target of providing advanced collision warning system adaptation databases in vehicle following and filtering scenario of disorderly traffic environments, which will not only improve driver's safety but also optimize traffic flow. This calls for the real-time implementation of vehicle-to-vehicle technologies and driver behavioural prediction models in a cognitive architecture, for increasing the capacity, providing safer driving environment to the drivers and the surrounding vehicles, where all drivers communicate and cooperate with each other for a safe yet smooth flow of traffic.

8.4. Directions for future research

The research work presented in this dissertation provide ample scope and directions for future research endeavors. Still, much more remains to be learned, tested and explored in detail. As a final outlook, some of the future research directions derived from the present work are illustrated below:

- Development of a full-scaled integrated driving behaviour model for disorderly traffic flows still remains a subject for further exploration. Although recent driving behaviour model formulations allow for improvements in the car-following regime, results at the disaggregated level such as incorporating lateral dimension, accounting for anticipatory actions in a multiple-leader following case and filtering decisions of drivers, are not well replicated. The availability of open-source detailed trajectory datasets will be a source for potential improvements in the development of integrated driving behaviour model.

- Implementing data-driven artificial neural network models to analyze the dynamic responses of drivers in a vehicle-following regime can provide a more general

framework in improving reliability of simulation models. Combining neural network models with statistical methods is another aspect of future research.

- Several enhancements regarding the specific formulation of the proposed models, traffic interactions and driver behaviour modelling features may be introduced. These include: consideration of vehicle-type specific interactions in the neural network models, addition of multiple driver interactions with diverse vehicle types and consideration of multiple leaders in the following regime. The transferability of the proposed models on describing different traffic-states and modelling driver behaviour of different vehicles provides an interesting topic for future research.

- The proposed models still need validation using different trajectory datasets at mid-block sections. Performing this task, however, depends on the availability of such data. The vehicle-following ANN models were developed with dynamic time-series data being collected in a controlled environment. A validation still needs to be performed to validate the robustness of the model.

- Time-to-collision thresholds in the staggered-following events were defined in this research based on the recommended minimum thresholds for lane-based scenario. Therefore it cannot be interpreted as an actual outcome of the situation; further investigation needs to be conducted by analyzing accidents in terms of TTC thresholds, which might possibly improve the conflict-severity estimation of the safety critical event. Moreover, defining minimum TTC thresholds for a two-leader following scenario could be further explored.

Bibliography

Conference/Journal Publications

Abtahi, S. M., Tamannaei, M., & Haghshenash, H. (2011). Analysis and Modeling Time Headway Distributions under Heavy Traffic Flow Conditions in the Urban Highways: Case of Isfahan. Transport, 26: 375–382.

Agarwal, A., & Lämmel, G. (2015). Seepage of smaller vehicles under heterogeneous traffic conditions. 4th International Workshop on Agent-based Mobility, Traffic and Transportation Models, Methodologies and Applications, ABMTRANS 2015, Procedia Computer Science, 52: 890-895. doi:10.1016/j.procs.2015.05.147

Agarwal, A., & Lämmel, G. (2016). Modeling seepage behaviour of smaller vehicles in mixed traffic conditions using an agent based simulation. Transportation in Developing Economies, 2: 1-12.

Agarwal, A., Zilske, M., Rao, K. R., & Nagel, K. (2015). An elegant and computationally efficient approach for heterogeneous traffic modelling using agent based simulation. 4th International Workshop on Agent-based Mobility, Traffic and Transportation Models, Methodologies and Applications, ABMTRANS 2015, Procedia Computer Science, 52, 962-967. doi:10.1016/j.procs.2015.05.173

Aghabayk, K., Sarvi, M., & Young, W. (2016). Including heavy vehicles in a car-following model: modelling, calibrating and validating. Journal of Advanced Transportation, 50(7): 1432-1446.

Ahmed, K., Ben-Akiva, M., Koutsopoulos, H., & Mishalani, R. (1996). Models of freeway lane changing and gap acceptance behavior. Transportation and traffic theory, 13, 501-515.

Akaike, H. (1974). A New Look At the Statistical Model Identification. IEEE Transactions on Automatic Control, 19(6): 716–723. doi:10.1109/TAC.1974.1100705.

Albalate, D., & Fernández-Villadangos, L. (2010). Motorcycle injury severity in Barcelona: the role of vehicle type and congestion. Traffic injury prevention, 11(6): 623-631.

Al-Ghamdi, A. S. (2001). Analysis of Time Headways on Urban Roads: Case Study from Riyadh. Journal of Transportation Engineering, 127(4): 289–294.

Alhassan, H. M., & Ben-Edigbe, J. (2012). Effect of Rain on Probability Distributions Fitted to Vehicle Time Headways. International Journal on Advanced Science, Engineering and Information Technology, 2(2): 144–150.

Altendorf, E., & Flemisch, F. (2014). Prediction of driving behaviour in cooperative guidance and control: a first game-theoretic approach. Kognitive Systeme, 2015(1): 1-10. doi. 10.17185/duepublico/37693

Ambarwati, L., Pel, A. J., Verhaeghe, R., & van Arem, B. (2014). Empirical analysis of heterogeneous traffic flow and calibration of porous flow model. Transportation Research Part C: Emerging Technologies, 48: 418-436.

Ambarwati, L., Pel, A.J., Verhaeghe, R. & van Arem, B. (2013). Empirical Analysis of Heterogeneous Traffic Flow. Proceedings of the Eastern Asia Society for Transportation Studies, 9: 1-15

Amin, H. J., & Maurya, A. K. (2015). A review of critical gap estimation approaches at uncontrolled intersection in case of heterogeneous traffic conditions. Journal of Transport Literature, 9(3): 5-9.

Anand, P. A., Atmakuri, P., Anne, V. S. R., Asaithambi, G., Srinivasan, K. K., Sivanandan, R., & Chilukuri, B. R. (2019). Calibration of Vehicle-Following Model Parameters Using Mixed Traffic Trajectory Data. Transportation in Developing Economies, 5(2): 18.

Arbis, D., Dixit, V. V., & Rashidi, T. H. (2016). Impact of risk attitudes and perception on game theoretic driving interactions and safety. Accident Analysis & Prevention, 94: 135-142.

Arnold, T. B., & Emerson, J. W. (2011). Nonparametric Goodness-of-Fit Tests for Discrete Null Distributions. R Journal, 3(2): 34–39.

Aron, M. (1988). Car following in an urban network: Simulation and experiments. Proceedings of Seminar D, 16th PTRC meeting, Bath, Somerset, England, UK, 27–39.

Asaithambi, G., & Basheer, S. (2017). Analysis and modeling of vehicle following behaviour in mixed traffic conditions. Transportation Research Procedia, 25: 5094-5103.

Asaithambi, G., Kanagaraj, V., & Toledo, T. (2016). Driving behaviours: Models and challenges for non-lane based mixed traffic. Transportation in Developing Economies, 2(2): 19.

Asaithambi, G., Kanagaraj, V., Srinivasan, K. K., & Sivanandan, R. (2018). Study of traffic flow characteristics using different vehicle-following models under mixed traffic conditions. Transportation letters, 10(2): 92-103.

Ashalatha, R., & Chandra, S. (2011). Critical Gap through Clearing Behaviour of Drivers at Unsignalised Intersections. KSCE Journal of Civil Engineering, 15(8): 1427–1434.

Aycin, M. F., & Benekohal, R. F. (2004). Performance of the Generalized Car-Following Model Obtained from Macroscopic Flow Relationships in Simulating Field Data. 83rd Annual Meeting of the Transportation Research Board, Washington, D.C.

Ayres, T. J., Li, L., Schleuning, D., & Young, D. (2001). Preferred Time-Headway of Highway Drivers. Proceedings of Intelligent Transportation Systems, IEEE, 826–829.

Bando, M., Hasebe, K., Nakanishi, K., & Nakayama, A. (1998). Analysis of optimal velocity model with explicit delay. Physical Review E, 58(5): 5429–5435.

Bando, M., Hasebe, K., Nakayama, A., Shibata, A., & Sugiyama, Y. (1995). Dynamics model of traffic congestion and numerical simulation. Physical Review E, 51(2): 1035–1042.

Bando, M., Kugo, T., Maekawa, N., & Nakano, H. (1993). Improving the effective potential. Physics Letters B, 301(1): 83-89.

Barceló, J. (2002). Dynamic Network Simulation with AIMSUN. Proceedings of International Symposium on Transport Simulation, Yokohama, Japan.

Barmpounakis, E. N., Vlahogianni, E. I., & Golias, J. C. (2016). Vision-based multivariate statistical modeling for powered two-wheelers manoeuvreability during overtaking in urban arterials. Transportation Letters: The International Journal of Transportation Science, 8: 167-176.

Barmpounakis, E. N., Vlahogianni, E. I., & Golias, J. C. (2017). Modeling cooperation and powered-two wheelers short-term strategic decisions during overtaking in urban arterials. International Journal of Transportation Science and Technology, 5(4): 227-238.

Bella, F., & Russo, R. (2011). A collision warning system for rear-end collision: a driving simulator study. Procedia-social and behavioural sciences, 20: 676-686.

Bella, F., Calvi, A., & D'Amico, F. (2014). An Empirical Study on Traffic Safety Indicators for the Analysis of Car-following Conditions. Advances in Transportation Studies, 1: 5–16. doi:10.4399/97888548735442.

Bham, G. H., & Benekohal, R. F. (2004). A high fidelity traffic simulation model based on cellular automata and car-following concepts. Transportation Research Part C: Emerging Technologies, 12(1): 1-32.

Bhat, C. R., & Eluru, N. (2009). A Copula-Based Approach to Accommodate Residential Self-Selection Effects in Travel Behaviour Modeling. Transportation Research Part B: Methodological, 43(7): 749–765. doi:10.1016/j.trb.2009.02.001.

Bhat, C. R., & Sener, I. N. (2009). A Copula-Based Closed-Form Binary Logit Choice Model for Accommodating Spatial Correlation Across Observational Units. Journal of Geographical Systems, 11(3): 243–272. doi:10.1007/s10109-009-0077-9.

Bingham, E. (2001). Reinforcement learning in neurofuzzy traffic signal control. European Journal of Operational Research, 131(2): 232-241.

Boer, E. R. (1999). Car following from the driver's perspective. Transportation Research Part F: Traffic Psychology and Behaviour, 2(4): 201-206.

Bonabeau, E. (2002). Agent-based modeling: Methods and techniques for simulating human systems. Proceedings of the National Academy of Sciences of the United States of America, 99: 7280-7287. doi: 10.1073/pnas.082080899

Brackstone, M., & McDonald, M. (1999). Car-following: a historical review. Transportation Research Part F: Traffic Psychology and Behaviour, 2(4): 181-196.

Brackstone, M., & McDonald, M. (2007). Driver headway: How close is too close on a motorway?. Ergonomics, 50(8): 1183-1195

Brackstone, M., Sultan, B., & McDonald, M. (2002). Motorway driver behaviour: studies on car following. Transportation Research Part F: Traffic Psychology Behaviour, 5(1): 31-46

Brackstone, M., Waterson, B., & McDonald, M. (2009). Determinants of following headway in congested traffic. Transportation Research Part F: Traffic Psychology Behaviour, 12(2): 131-142

Brilon, W., Koenig, R., & Troutbeck, R. (1999). Useful Estimation Procedures for Critical Gaps. Transportation Research Part A: Policy and Practice, 33(3-4): 161–186.

Brown, T. L., Lee, J. D., & McGehee, D. V. (2001). Human performance models and rear-end collision avoidance algorithms. Human Factors, 43(3): 462-482.

Budhkar, A. K., & Maurya, A. K. (2017a). Characteristics of lateral vehicular interactions in heterogeneous traffic with weak lane discipline. Journal of Modern Transportation, 25(2): 74-89.

Budhkar, A. K., & Maurya, A. K. (2017b). Multiple-leader vehicle-following behaviour in heterogeneous weak lane discipline traffic. Transportation in developing economies, 3(2): 20.

Burges, C. J. C. (1998). A tutorial on support vector machines for pattern recognition. Data Mining and Knowledge Discovery, 2: 955–974.

Cafiso, S., La Cava, G., & Pappalardo, G. (2012). A logistic model for Powered Two-Wheelers crash in Italy. Procedia-social and behavioural sciences, 53: 880-889.

Cantin, V., Lavallière, M., Simoneau, M., & Teasdale, N. (2009). Mental workload when driving in a simulator: Effects of age and driving complexity. Accident Analysis & Prevention, 41(4): 763-771.

Ceder, A., & May, A. D. (1976). Further evaluation of single and two regime traffic flow models. Transportation Research Record: Journal of Transportation Research Board, 567: 1–30.

Chakroborty, P., & Kikuchi, S. (1999). Evaluation of the General Motors based car-following models and a proposed fuzzy inference model. Transportation Research Part C: Emerging Technologies, 7(4): 209-235.

Chand, S., Dixit, V., & Waller, S. T. (2016). Evaluation of fluctuating speed and lateral movement of vehicles: comparison between mixed traffic and homogeneous traffic. Transportation Research Record: Journal of Transportation Research Board, 2581(1): 104-112.

Chandler, R. E., Herman, R., & Montroll, E. W. (1958). Traffic dynamics: Studies in car following. Operations Research, 6(2): 165–184.

Chang, M., & Kim, Y. (2000). Development of capacity estimation method from statistical distribution of observed traffic flow. Transportation Research Board, Transportation Research Circular, 299-309.

Charly, A., & Mathew, T. V. (2017). Estimation of modified time to collision as surrogate for mid-block crashes under mixed traffic conditions. 96th Transportation Research Board Annual Meeting, Washington, DC.

Cho, H. J., & Wu, Y. T. (2004). Modeling and simulation of motorcycle traffic flow. International Conference on Systems, Man and Cybernetics, IEEE, 7: 6262-6267.

Choudhury, C. F., & Islam, M. M. (2016). Modelling acceleration decisions in traffic streams with weak lane discipline: A latent leader approach. Transportation Research Part C: Emerging Technologies, 67: 214-226.

Chowdhury, D., Wolf, D. E., & Schreckenberg, M. (1997). Particle hopping models for two-lane traffic with two kinds of vehicles: Effects of lane-changing rules. Physica A: Statistical Mechanics and its Applications, 235(3): 417-439. doi:10.1016/S0378-4371(96)00314-7

Ciuffo, B., Punzo, V., & Torrieri, V. (2008). Comparison of Simulation-Based and Model-Based Calibrations of Traffic Flow Microsimulation Models. Transportation Research Record: Journal of the Transportation Research Board, 2088: 36–44.

Clabaux, N., Fournier, J. Y., & Michel, J. E. (2017). Powered two-wheeler riders' risk of crashes associated with filtering on urban roads. Traffic Injury Prevention, 18(2): 182-187.

Clabaux, N., Fournier, J. Y., Michel, J. E., & Perrin, C. (2019). Does filtering by powered two-wheelers present a risk for pedestrians in city centers?. Journal of Transport & Health, 13: 224-233.

Colombaroni, C., & Fusco, G. (2014). Artificial neural network models for car following: experimental analysis and calibration issues. Journal of Intelligent Transportation Systems 18(1): 5-16

Daganzo, C. F. (1981). Estimation of Gap Acceptance Parameters within and Across the Population from Direct Roadside Observation. Transportation Research Part B: Methodological, 15(1): 1–15.

Das, S., & Maurya, A. K. (2017). Time Headway Analysis for Four-Lane and Two-Lane Roads. Transportation in Developing Economies 3: 9. doi:10.1007/s40890-017-0039-8.

Das, S., & Maurya, A. K. (2018a). Multivariate analysis of microscopic traffic variables using copulas in staggered car-following conditions. Transportmetrica A: Transport Science, 14(10): 829-854.

Das, S., & Maurya, A. K. (2018b). Bivariate modeling of time headways in mixed traffic streams: a copula approach. Transportation Letters, 1-11.

Das, S., & Maurya, A. K. (2018c). Modelling of motorised two-wheelers: a review of the literature. Transport reviews, 38(2): 209-231.

Das, S., Maurya, A. K., & Budhkar, A. K. (2019a). Dynamic data collection of staggered-following behaviour in non-lane-based traffic streams. SN Applied Sciences, 1(6): 591.

Das, S., Budhkar, A., Maurya, A. K., & Maji, A. (2019b). Multivariate Analysis on Dynamic Car-Following Data of Non-lane-Based Traffic Environments. Transportation in Developing Economies, 5(2): 17.

Das, S., Maurya, A. K., & Budhkar, A. K. (2019c). Determinants of time headway in staggered car-following conditions. Transportation Letters, 11(8): 447-457.

Das, S., & Maurya, A. K. (2019d). Defining Time-to-Collision Thresholds by the Type of Lead Vehicle in Non-Lane-Based Traffic Environments. IEEE Transactions on Intelligent Transportation Systems, 1-11.

Das, S., & Maurya, A. K. (2019e). Modeling maneuverability of motorized two-wheelers during filtering in urban roads. Transportation research record, 2673(5): 637-647.

Das, S., & Maurya, A. K. (2020). Pore acceptance predictions of motorised Two-Wheelers during filtering at urban Mid-Block sections. Journal of Intelligent Transportation Systems: Transport, Planning and Operations, 1-13.

Del Castillo, J. M., & Benitez, F. G. (1995). On the functional form of the speed-density relationship—II: empirical investigation. Transportation Research Part B: Methodological, 29(5): 391-406.

Derbel, O., Peter, T., Zebiri, H., Mourllion, B., & Basset, M. (2012). Modified Intelligent Driver Model. Periodica Polytechnica Transportation Engineering, 40(2): 53-60.

DeTienne, K. B., Detienne, D. H., & Joshi, S. A. (2003). Neural networks as statistical tools for business researchers. Organizational Research Methods, 6(2): 236–265.

Dougherty, M. (1995). A review of neural networks applied to transport. Transportation Research Part C: Emerging Technologies, 3(4): 247-260.

Duan, J., Li, Z., & Salvendy, G. (2013). Risk Illusions in Car following: Is a Smaller Headway Always Perceived as More Dangerous? Safety Science, 53: 25–33.

Dubey, S. K., Ponnu, B., & Arkatkar, S. S. (2012). Time gap modeling under mixed traffic condition: A statistical analysis. Journal of Transportation Systems Engineering and Information Technology, 12(6): 72-84.

Dubey, S. K., Ponnu, B., & Arkatkar, S. S. (2013). Time Gap Modeling Using Mixture Distributions under Mixed Traffic Conditions. Journal of Transportation Systems Engineering and Information Technology, 13 (3): 91–98.

Durrani, U., Lee, C., & Maoh, H. (2016). Calibrating the Wiedemann's vehicle-following model using mixed vehicle-pair interactions. Transportation Research Part C: Emerging Technologies, 67: 227-242.

Elliott, M. A., Baughan, C. J., & Sexton, B. F. (2007). Errors and violations in relation to motorcyclists crash risk. Accident Analysis and Prevention, 39(3): 491–499.

Embrechts, P., Höing, A., & Juri, A. (2003). Using copulae to bound the value-at-risk for functions of dependent risks. Finance and Stochastics, 7(2): 145-167.

Farah, H., Bekhor, S., & Polus, A. (2009). Risk evaluation by modeling of passing behaviour on two-lane rural highways. Accident Analysis & Prevention, 41(4): 887-894.

Feng, X., Wang, X. F., & Xie, D. F. (2016). Lateral drift behaviour analysis in mixed bicycle traffic: A cellular automaton model approach. Mathematical Problems in Engineering, 1-10. doi. 10.1155/2016/7962171

Flexer, A. (1996). Statistical evaluation of neural network experiments: minimum requirements and current practice. Proceedings of the 13th European Meeting on Cybernetics and Systems Research, Austrian Society for Cybernetic Studies, Vienna, 2: 1005–1008.

Fung, G. S., Yung, N. H., & Pang, G. K. (2003). Camera calibration from road lane markings. Optical Engineering, 42(10): 2967-2977.

Gashaw, S., Goatin, P., & Härri, J. (2018). Modeling and analysis of mixed flow of cars and powered two wheelers. Transportation Research Part C: Emerging Technologies, 89: 148-167.

Gattis, J. L., & Low, S. T. (1999). Gap Acceptance at Atypical Stop-Controlled Intersections. Journal of Transportation Engineering, 125(3): 201–207.

Gazis, D. C., Herman, R., & Potts, R. B. (1959). Car following theory of steady state traffic flow. Operations Research, 7(4): 499–505.

Gazis, D. C., Herman, R., & Rothery, R. W. (1961). Nonlinear follow the leader models of traffic flow. Operations Research, 9: 545-567.

Ge, H. X., Dai, S. Q., Dong, L.Y., Xue, Y. (2004). Stabilization effect of traffic flow in an extended car-following model based on an intelligent transportation system application. Physical Review E, 70(6): 066134.

Ge, H. X., Cheng, R. J. & Li, Z. P. (2008). Two velocity difference model for a car following theory. Physica A, 387: 5239-5245.

Genest, C., & Rivest, L. P. (1993). Statistical Inference Procedures for Bivariate Archimedean Copulas. Journal of the American Statistical Association, 88(423): 1034–1043.

Genest, C., Ghoudi, K., & Rivest, L. P. (1995). A Semiparametric Estimation Procedure of Dependence Parameters in Multivariate Families of Distributions. Biometrika, 82(3): 543–552. doi:10.1093/biomet/82.3.543.

Ghaedi, A. M., Ghaedi, M., Pouranfard, A. R., Ansari, A., Avazzadeh, Z., Vafaei, A., Tyagi, I., Agarwal, S., & Gupta, V. K. (2016). Adsorption of Triamterene on multi-walled and single-walled carbon nanotubes: Artificial neural network modeling and genetic algorithm optimization. Journal of Molecular Liquids, 216: 654-665.

Gipps, P. G. (1981). A behavioural car following model for computer simulation. Transportation Research B: Methodological, 15(2): 105–111.

Govindaraju, R. S. (2000). Artificial neural networks in hydrology II: hydrologic applications. Journal of Hydrologic Engineering, 5(2): 124-137.

Green, M. (2000). How long does it take to stop? Methodological analysis of driver perception-brake times. Transportation Human Factors, 2(3): 195-216.

Green, S. B. (1991). How many subjects does it take to do a regression analysis? Multivariate Behavioural Research, 26(3): 499-510.

Gryllias, K. C., & Antoniadis, I. A. (2012). A Support Vector Machine approach based on physical model training for rolling element bearing fault detection in industrial environments. Engineering Applications of Artificial Intelligence, 25(2): 326-344.

Gunay, B. (2003). Methods to quantify the discipline of lane-based driving. Traffic Engineering and Control, 44(1): 22–27.

Gunay, B. (2004). An investigation of lane utilisation on Turkish highways. ICE-Transport Journal, 157(1): 43–49.

Gunay, B. (2007). Car following Theory with Lateral Discomfort. Transportation Research Part B: Methodological, 41(7): 722–735.

Gunay, B. (2009). Rationality of a non-lane-based car-following theory. Transport, 162: 27-37.

Gupta, A. K., & Dhiman, I. (2014). Analyses of a continuum traffic flow model for a non lane-based system. International Journal of Modern Physics C, 25(10): 1450045.

Gurusinghe, G. S., Nakatsuji, T., Azuta, Y., Ranjitkar, P., & Tanaboriboon, Y. (2002). Multiple Car-Following Data Using Real-Time Kinematic Global Positioning System. Transportation Research Record: Journal of Transportation Research Board, 1802: 166–180.

Hale, S., Myerson, J., Smith, G. A., & Poon, L. W. (1988). Age, variability, and speed: between-subjects diversity. Psychology and aging, 3(4): 407.

Hamed, M. M., Easa, S. M., & Batayneh, R. R. (1997). Disaggregate Gap Acceptance Model for Unsignalized T-Intersections. Journal of Transportation Engineering, 123(1): 36–42.

Han, C., Luan, B. C., & Hsieh, F.C. (2014). Development of autonomous emergency braking control system based on road friction. International Conference on Automation Science and Engineering (CASE), Taipei, Taiwan, 933-937. DOI: 10.1109/CoASE.2014.6899438

Hasebe, K., Nakayama, A., & Sugiyama, Y. (2003). A dynamical model of cooperative driving system for freeway traffic. Physical Review E, 70: 026102.

Hatipkarasulu, Y., Wolshon, B., & Quiroga, C. A. (2000). Global Positioning System Approach for the Analysis of Car-Following Behaviour. 79th Annual Meeting of the Transportation Research Board, Washington, D.C.

He, Z. C., Wang, Y. M., Sun, W. B., Huang, P. Y., Zhang, L. C., & Zhong, R. X. (2015). Modelling car-following behaviour with lateral separation and overtaking expectation. Transportmetrica B: Transport Dynamics, DOI: 10.1080/21680566.2015.1083911.

Helbing, D. & Tilch, B. (1998). Generalized force model of traffic dynamics. Physical Review E, 58(2): 133-138.

Helly, W. (1959). Simulation of bottlenecks in single lane traffic flow. Proceedings of the symposium on theory of traffic flow, Research Laboratories, General Motors, New York, 207–238.

Herman, R., & Rothery, R. W. (1965). Propagation of disturbances in vehicular platoons. Proceedings of the Third International Symposium on the theory of traffic flow, Research Laboratories, General Motors, New York, 14-25.

Hewitt, R. H. (1985). A comparison between some methods of measuring critical gap. Traffic Engineering & Control, 26(1): 13-22.

Heyes, M. P., & Ashworth, R. (1972). Further research on car following models. Transportation Research, 6(3): 287–291.

Hirst, S., & Graham, R. (1997). The format and perception of collision warnings. Ergonomics of intelligent vehicle-highway systems: Ergonomics and safety of intelligent driver interfaces, 203-220, ISBN: 080581955X, 0805819568.

Hoogendoorn, S. P., & Ossen, S. (2006). Empirical analysis of two-leader car-following behaviour. European journal of transport and infrastructure research, 6(3). doi: 10.18757/ejtir.2006.6.3.3447.

Hosseini, S., Murgovski, N., de Campos, G. R., & Sjöberg, J. (2016). Adaptive forward collision warning algorithm for automotive applications. American Control Conference (ACC) Boston, MA, USA, 5982-5987.

Hou, Y., Edara, P., & Sun, C. (2014). Modeling mandatory lane changing using Bayes classifier and decision trees. IEEE Transactions on Intelligent Transportation Systems, 15(2): 647-655.

Houenou, A., Bonnifait, P., Cherfaoui, V., & Yao, W. (2013). Vehicle trajectory prediction based on motion model and maneuver recognition. 2013 IEEE/RSJ International Conference on Intelligent Robots and Systems, Tokyo, Japan, 4363-4369.

Hsu, C. C., Lin, Z. S., Chiou, Y. C. & W. Lan, L. (2007). Exploring traffic features with stationary ad moving bottlenecks using refined cellular automata. Journal of the Eastern Asia Society for Transportation Studies, 7: 2502-2516.

Hublart, A., & Durand, J –F. (2012). Risks for Powered Two-wheelers and Filtering Between Lanes on Urban Motorways. European Transport Conference, Glasgow, Scotland.

Hussain, H., Farhan, M. A., Umar, R. R., & Dadang, M. M. (2005). Key components of a motorcycle-traffic system: A study along the motorcycle path in Malaysia. International Association for Traffic and Safety Sciences (IATSS) Research, 29(1): 50-56.

Jiang, R., & Wu, Q. S. (2003). First-and second-order phase transitions from free flow to synchronized flow. Physica A: Statistical Mechanics and its Applications, 322: 676-684.

Jiang, R., Hu, M.-B., Zhang, H.-M., Gao, Z.-Y., Jia, B., Wu, Q.-S., Wang, B., & Yang, M. (2014). Traffic experiment reveals the nature of car-following. Journal of PloS one, 9(4): e94351. http://dx.doi.org/10.1371/journal.pone.0094351.

Jiang, Y., & Li, S. (2001). Measuring and Analyzing Vehicle Position and Speed Data at Work Zones Using Global Positioning System. 80th Annual Meeting of the Transportation Research Board, Washington, D.C.

Jiang, R., Wu, Q., & Zhu, Z. (2001). Full velocity difference model for a car-following theory. Physical Review E, 64(1): 017101.

Jin, S., Huang, Z. Y., Tao, P. F., & Wang, D. H. (2011). Car-following theory of steady-state traffic flow using time-to-collision. Journal of Zhejiang University-SCIENCE A, 12(8): 645-654.

Jin, S., Qu, X., & Wang, D. (2011a). Assessment of expressway traffic safety using Gaussian mixture model based on time to collision. International Journal of Computational Intelligence Systems, 4(6): 1122-1130.

Jin, S., Wang, D. H., Xu, C., & Ma, D. F. (2013). Short-term traffic safety forecasting using Gaussian mixture model and Kalman filter. Journal of Zhejiang University SCIENCE A, 14(4): 231-243.

Jin, S.,Wang, D., Tao, P., & Li, P. (2010). Non-lane-based full velocity difference car following model. Physica A: Statistical Mechanics and its Applications, 389(21): 4654–4662.

Jin, S., Wang, D., Xu, C., & Huang, Z. (2012). Staggered car-following induced by lateral separation effects in traffic flow. Physics Letters A, 376: 153-157.

Jin, X., Zhang, Y., Wang, F., Li, L., Yao, D., Su, Y., & Wei, Z. (2009). Departure Headways at Signalized Intersections: A Log-Normal Distribution Model Approach. Transportation Research Part C: Emerging Technologies, 17(3): 318–327.

Johansson, G., & Rumar, K. (1971). Drivers' brake reaction times. Human Factors, 13: 23–27.

Kalogirou, S. A. (2000). Applications of artificial neural-networks for energy systems. Applied energy, 67(1-2): 17-35.

Kalyoncuoglu, S. F., & Tigdemir, M. (2004). An alternative approach for modelling and simulation of traffic data: artificial neural networks. Simulation Modelling Practice and Theory, 12(5): 351-362.

Kanagaraj, V., Asaithambi, G., Kumar, C. N., Srinivasan, K. K., & Sivanandan, R. (2013). Evaluation of different vehicle following models under mixed traffic conditions. Procedia-Social and Behavioural Sciences, 104: 390-401.

Kanagaraj, V., Asaithambi, G., Srinivasan, K., & Sivanandan, R. (2011). Vehicle Classwise Analysis of Time Gaps and Headways under Heterogeneous Traffic. 90th Annual Meeting of Transportation Research Board 4249, Washington, D.C.

Kanagaraj, V., Asaithambi, G., Toledo, T., & Lee, T. C. (2015). Trajectory data and flow characteristics of mixed traffic. Transportation Research Record: Journal of Transportation Research Board, 2491(1): 1-11.

Kanagaraj, V., Srinivasan, K. K., & Sivanandan, R. (2010). Modeling vehicular merging behaviour under heterogeneous traffic conditions. Transportation Research Record: Journal of Transportation Research Board, 2188(1): 140-147.

Karlaftis, M. G., & Vlahogianni, E. I. (2011). Statistical methods versus neural networks in transportation research: Differences, similarities and some insights. Transportation Research Part C: Emerging Technologies, 19(3): 387-399.

Keall, M. D., & Newstead, S. (2012). Analysis of factors that increase motorcycle driver risk compared to car driver risk. Accident Analysis and Prevention, 49: 23–29.

Kerner, B. S., & Rehborn, H. (1996). Experimental features and characteristics of traffic jams. Physical Review E, 53: 1297-1300. doi: 10.1103/PhysRevE.53.R1297

Kesting, A., & Treiber, M. (2008). How reaction time, update time, and adaptation time influence the stability of traffic flow. Computer-Aided Civil and Infrastructure Engineering, 23(2): 125-137.

Khansari, E. R., Tabibi, M., & Nejad, F. M. (2018). Studying Non-coaxiality in Non-lane-based Car-following Behaviour. Civil Engineering Journal, 4(12): 2840-2852.

Khashbat, J., Tsevegjav, T., Myagmarjav, J., Bazarragchaa, I., Erdenetuya, A., & Munkhzul, N. (2012). Determining the driver's reaction time in the stationary and real-life environments (Comparative Study). 7th International Forum on Strategic Technology (IFOST), 1-3.

Khodayari, A., Ghaffari, A., Kazemi, R., & Braunstingl, R. (2011). Modify car following model by human effects based on locally linear neuro fuzzy. Intelligent Vehicles Symposium (IV), IEEE, 661-666.

Khodayari, A., Ghaffari, A., Kazemi, R., & Braunstingl, R. (2012). A modified car-following model based on a neural network model of the human driver effects. IEEE Transactions on Systems, Man, and Cybernetics, 42: 1440–1449.

Kikuchi, C., & Chakroborty, P. (1992). Car following model based on a fuzzy inference system. Transportation Research Record: Journal of the Transportation Research Board, 1365: 82–91.

Kim, G., Silvapulle, M. J., & Silvapulle, P. (2007). Comparison of Semiparametric and Parametric Methods for Estimating Copulas. Computational Statistics & Data Analysis, 51(6): 2836–2850. doi:10.1016/j.csda.2006.10.009.

Kim, J., & Mahmassani, H. S. (2014). A Finite Mixture Model of Vehicle-to-Vehicle and Day-to-Day Variability of Traffic Network Travel Times. Transportation Research Part C: Emerging Technologies, 46: 83–97. doi:10.1016/j.trc.2014.05.011.

Knospe, W., Santen, L., Schadschneider, A., & Schreckenberg, M. (2000). Towards a realistic microscopic description of highway traffic. Journal of Physics A: Mathematical and General, 33: L477. Retrieved from: http://stacks.iop.org/0305-4470/33/i=48/a=103

Kojadinovic, I., & Yan, J. (2010). Comparison of Three Semiparametric Methods for Estimating Dependence Parameters in Copula Models. Insurance: Mathematics and Economics, 47(1): 52–63. doi:10.1016/j.insmatheco.2010.03.008.

Kometani, E., & Sasaki, T. (1958). On the stability of traffic flow. Journal of Operations Research Society of Japan, 2(1): 11-26.

Kometani, E., & Sasaki, T. (1959). Dynamic behaviour of traffic with a nonlinear spacing-speed relationship. Proceedings of the symposium on theory of traffic flow, Research Laboratories, General Motors, New York, 105–119.

Korteling, J. E. (1990). Perception-response speed and driving capabilities of brain-damaged and older drivers. Human Factors, 32(1): 95-108.

Lan, L. W., & Chang, C. W. (2003). Motorbike's moving behaviour in mixed traffic: Particle-hopping model with cellular automata. Journal of the Eastern Asia Society for Transportation Studies, 5: 23-37.

Lan, L. W., & Chang, C. W. (2005). Inhomogeneous cellular automata modeling for mixed traffic with cars and motorcycles. Journal of Advanced Transportation, 39: 323-349. doi: 10.1002/atr.5670390307

Lan, L. W., & Hsu, C. C. (2006). Formation of spatiotemporal traffic patterns with cellular automaton simulation. 85th Annual Meeting Transportation Research Board, Washington, D.C.

Lan, L. W., Chiou, Y. C., Lin, Z. S. & Hsu, C. C. (2009). A refined celular automaton model to rectify impractical vehicular movement behaviour. Physica A: Statistical Mechanics and its Applications, 388: 3917-3930.

Lan, L.W., Chiou, Y.C., Lin, Z.S. & Hsu, C.C. (2010). Cellular automaton simulations for mixed traffic with erratic motorcycles' behaviours. Physica A: Statistical Mechanics and its Applications, 389: 2077-2089. doi:10.1016/j.physa.2010.01.028

Laureshyn, A., Svensson, Å., & Hydén, C. (2010). Evaluation of traffic safety, based on micro-level behavioural data: Theoretical framework and first implementation. Accident Analysis & Prevention, 42(6): 1637-1646.

Lee, T. -C., & Wong, K. I. (2016). An agent-based model for queue formation of powered two-wheelers in heterogeneous traffic. Physica A: Statistical Mechanics and its Applications, 461: 199-216. doi:10.1016/j.physa.2016.05.005

Lee, T. C., Polak, J. W., & Bell, M. G. (2009). New approach to modeling mixed traffic containing motorcycles in urban areas. Transportation Research Record: Journal of the Transportation Research Board, 2140(1): 195-205.

Lees, M. N., & Lee, J. D. (2007). The influence of distraction and driving context on driver response to imperfect collision warning systems. Ergonomics, 50(8): 1264-1286.

Lenorzer, A., Casas, J., Dinesh, R., Zubair, M., Sharma, N., Dixit, V., Torday, A., Brakstone, M. (2015). Modelling and simulation of mixed traffic. Proceedings of the Australian Transport Research Forum 2015, 1-12.

Lenz, H., Wagner, C. K., & Sollacher, R. (1999). Multi-anticipative car-following model. The European Physical Journal B-Condensed Matter and Complex Systems, 7(2): 331-335.

Lerner, N. (1994). Brake perception–reaction times of older and younger drivers. Proceedings of the Human Factors and Ergonomics Society, 38: 206–209.

Li, Y., Zhang, L., Peeta, S., Pan, H., Zheng, T., Li, Y., & He, X. (2015a). Non-lane-discipline-based car-following model considering the effects of two-sided lateral gaps. Nonlinear Dynamics, 80(1-2): 227-238.

Li, Y., Zhang, L., Zheng, H., He, X., Peeta, S., Zheng, T., & Li, Y. (2015b). Evaluating the energy consumption of electric vehicles based on car-following model under non-lane discipline. Nonlinear Dynamics, 82(1-2): 629-641.

Li, Y., Zhang, L., Zhang, B., Zheng, T., Feng, H., & Li, Y. (2016). Non-lane-discipline-based car-following model considering the effect of visual angle. Nonlinear Dynamics, 85(3): 1901-1912.

Li, Y., Li, Z., Wang, H., Wang, W., & Xing, L. (2017). Evaluating the safety impact of adaptive cruise control in traffic oscillations on freeways. Accident Analysis & Prevention, 104: 137-145.

Li, Y., Zhao, H., Zheng, T., Sun, F., & Feng, H. (2017a). Non-lane-discipline-based car-following model incorporating the electronic throttle dynamics under connected environment. Nonlinear Dynamics, 90(4): 2345-2358.

Li, Y., Song, Y., Yang, B., Zheng, T., Feng, H., & Li, Y. (2017b). A new lattice hydrodynamic model considering the effects of bilateral gaps on vehicular traffic flow. Nonlinear Dynamics, 87(1): 1-11.

Li, Y., Zhao, H., Zhang, L., & Zhang, C. (2018). An extended car-following model incorporating the effects of lateral gap and gradient. Physica A: Statistical Mechanics and its Applications, 503: 177-189.

Li, Z., & Zhang, R. (2013). An extended non-lane-based optimal velocity model with dynamic collaboration. Mathematical Problems in Engineering, 2013: 1-8. doi:10.1155/2013/124908.

Liebermann, D., Ben-David, G., Schweitzer, N., Apter, Y., & Parush, A. (1995). A field study on braking responses during driving I. Triggering and modulation. Ergonomics, 38: 1894–1902.

Lubashevsky, I., Wagner, P., & Mahnke, R. (2003). Bounded rational driver models. The European Physical Journal B-Condensed Matter and Complex Systems, 32(2): 243-247.

Luo, Y., Jia, B., Liu, J., Lam, W. H., Li, X., & Gao, Z. (2015). Modeling the interactions between car and bicycle in heterogeneous traffic. Journal of Advanced Transportation, 49(1): 29-47.

Ma, X., & Andréasson, I. (2006). Estimation of Driver Reaction Time from Car-Following Data: Application in Evaluation of General Motor–Type Model. Transportation Research Record: Journal of Transportation Research Board, 1965(1): 130-141.

Mahapatra, G., Maurya, A. K., & Chakroborty, P. (2018). Parametric study of microscopic two-dimensional traffic flow models: A literature review. Canadian Journal of Civil Engineering, 45(11): 909-921.

Mallikarjuna, C., & Rao, K. R. (2009). Cellular automata model for heterogeneous traffic. Journal of Advanced Transportation, 43(3): 321-345. doi:10.1002/atr.5670430305

Mallikarjuna, C., Phanindra, A., & Rao, K. R. (2009). Traffic data collection under mixed traffic conditions using video image processing. Journal of Transportation Engineering, 135(4): 174-182.

Mallikarjuna, C., Tharun, B., & Pal, D. (2013). Analysis of the lateral gap maintaining behaviour of vehicles in heterogeneous traffic stream. Procedia-social and behavioural sciences, 104: 370-379.

Maretzke, J., & Jacob, U. (1992). Distance warning and control as a means of increasing road safety and ease of operation. XXIV Fisita Congress, The Automotive Technology Servicing Society. Technical Papers. Safety, the Vehicle and the Road. Volume 1 (Imeche No C389/359 and Fisita No 925214).

Martinie, M.-A., Olive, T., & Milland, L. (2010). Cognitive dissonance induced by writing a counter attitudinal essay facilitates performance on simple tasks but not on complex tasks that involve working memory. Journal of Experimental Social Psychology, 46(4): 587-594.

Mathew, T. V., & Ravishankar, K. V. R. (2012). Neural network based vehicle-following model for mixed traffic conditions. European Transport, 52: 1-15

Mathew, T. V., Munigety, C. R., & Bajpai, A. (2015). Strip-based approach for the simulation of mixed traffic conditions. Journal of Computing in Civil Engineering, 29(5): 04014069.

Maurya, A. K., Dey, S., & Das, S. (2015). Speed and Time Headway Distribution under Mixed Traffic Condition. Journal of the Eastern Asia Society for Transportation Studies, 11: 1774–1792.

May, A. D., & Keller, H. E. (1967). Non integer car following models. Highway Research Record, 199(1): 19–32.

McCulloch, W. S., & Pitts, W. (1943). A logical calculus of the ideas immanent in nervous activity. The bulletin of mathematical biophysics, 5(4): 115-133.

McGehee, D. V., Dingus, T. A., & Horowitz, A. D. (1992, October). The potential value of a front-to-rear-end collision warning system based on factors of driver behaviour, visual perception and brake reaction time. Proceedings of the Human Factors and Ergonomics Society Annual Meeting, 36(13): 1003-1005.

Mehmood, A., & Easa, S. M. (2009). Modeling reaction time in car-following behaviour based on human factors. International Journal of Applied Science, Engineering and Technology, 5(14): 93-101.

Meng, J., Dai, S., Dong, L., & Zhang, J. (2007). Cellular automaton model for mixed traffic flow with motorcycles. Physica A: Statistical Methods and its Applications, 380: 470-480.

Meng, Q., & Qu, X. (2012). Estimation of rear-end vehicle crash frequencies in urban road tunnels. Accident Analysis & Prevention, 48: 254-263.

Michael, P. G., Leeming, F. C., & Dwyer, W. O. (2000). Headway on Urban Streets: Observational Data and an Intervention to Decrease Tailgating. Transportation Research Part F: Traffic Psychology and Behaviour, 3(2): 55–64.

Michaels, R. M. (1965). Perceptual factors in car-following. Proceedings of second International Symposium on the Theory of Road-Traffic Flow, 44-59.

Miller, A. J. (1974). A Note on the Analysis of Gap-Acceptance in Traffic. Journal of the Royal Statistical Society. Series C (Applied Statistics), 23(1): 66–73.

Minderhoud, M. M., Bovy, P. H. (2001). Extended time-to-collision measures for road traffic safety assessment. Accident Analysis & Prevention, 33(1): 89-97.

Minh, C. C., Sano, K., & Matsumoto, S. (2005). The speed, flow and headway analyses of motorcycle traffic. Journal of the Eastern Asia Society for Transportation Studies, 6: 1496-1508.

Minh, C. C., Sano, K., & Matsumoto, S. (2012). Manoeuvres of motorcycles in queues at signalized intersections. Journal of advanced transportation, 46(1): 39-53.

Moghadam, M. P. A., Pahlavani, P., & Naseralavi, S. (2016). Prediction of car following behaviour based on the instantaneous reaction time using an ANFIS-CART based model. International Journal of Transportation Engineering, 4(2): 109-126.

Mohan, M., & Chandra, S. (2016). Review and Assessment of Techniques for Estimating Critical Gap at Two-way Stop-controlled Intersections. European Transport-Trasporti Europei, 61(8): 1-18.

Moridpour, S. (2014). Evaluating the Time Headway Distributions in Congested Highways. Journal of Traffic and Logistics Engineering, 2(3): 224–229.

Moridpour, S., Sarvi, M., & Rose, G. (2010). Lane changing models: a critical review. Transportation letters, 2(3), 157-173.

Muhrer, E., & Vollrath, M. (2011). The effect of visual and cognitive distraction on driver's anticipation in a simulated car following scenario. Transportation Research Part F: Traffic Psychology and Behaviour, 14(6): 555-566.

Munigety, C. R., & Mathew, T. V. (2016). Towards behavioural modeling of drivers in mixed traffic conditions. Transportation in Developing Economies, 2(1): 6.

Munigety, C. R., Vicraman, V., & Mathew, T. V. (2014). Semiautomated tool for extraction of microlevel traffic data from videographic survey. Transportation Research Record: Journal of Transportation Research Board, 2443(1): 88-95.

Nagatani, T. (1999). Stabilization and enhancement of traffic flow by the next-nearest-neighbour interaction. Physical.Review E, 60(6): 6395–6401.

Nagel, K. (1996). Particle hopping models and traffic flow theory. Physical review E, 53: 4655-4672. doi:10.1103/PhysRevE.53.4655

Nagel, K., & Schreckenberg, M. (1992). A cellular automaton model for freeway traffic. Journal de physique I, 2(12): 2221-2229.

Nagel, K., Wolf, D. E., Wagner, P., & Simon, P. (1998). Two-lane traffic rules for cellular automata: A systematic approach. Physical Review E, 58: 1425-1437.

Nair, R., Mahmassani, H. S., & Miller-Hooks, E. (2011). A porous flow approach to modeling heterogeneous traffic in disordered systems. Transportation Research Part B: Methodological, 45(9): 1331-1345.

Naranjo, J. E., Jiménez, F., Anaya, J. J., Talavera, E., & Gómez, O. (2017). Application of vehicle to another entity (V2X) communications for motorcycle crash avoidance. Journal of Intelligent Transportation Systems, 21(4): 285-295.

Neville, J., & Jensen, D. (2007). Relational Dependency Networks. Journal of Machine Learning Research, 8: 653–692.

Newell, G. F. (1961). Nonlinear effects in the dynamics of car following. Operations research, 9(2): 209-229.

Nguyen, L.X., Hanaoka, S., & Kawasaki, T. (2012). Describing non-lane-based motorcycle movements in motorcycle-only traffic flow. Transportation Research Record: Journal of the Transportation Research Board, 2281: 76-82.

Nguyen, L. X., Hanaoka, S., & Kawasaki, T. (2014). Traffic conflict assessment for non-lane-based movements of motorcycles under congested conditions. IATSS Research, 37: 137-147.

Nikias, V. A., Vlahogianni, E. I., Lee, T. C., & Golias, J. C. (2012). Determinants of powered two-wheelers virtual lane width in urban arterials. 15th International IEEE Conference on Intelligent Transportation Systems, 1205-1210.

Oketch, T. (2000). New modeling approach for mixed-traffic streams with nonmotorized vehicles. Transportation Research Record: Journal of the Transportation Research Board, 1705: 61-69.

Oketch, T. (2003). Modeled performance characteristics of heterogeneous traffic streams containing non-motorized vehicles. 82nd Annual Meeting of the Transportation Research Board, Washington, D.C.

Olson, P. L., & Sivak, M. (1986). Perception-response time to unexpected roadway hazards. Human factors, 28(1): 91-96.

Ossen, S., & Hoogendoorn, S. P. (2011). Heterogeneity in car-following behaviour: Theory and empirics. Transportation Research Part C: Emerging Technologies, 19(2): 182-195.

Ota, H. (1994). Distance Headway Behaviour between Vehicles from the Viewpoint of Proxemics. IATSS Research, 18 (2): 5–14.

Ozaki, H. (1993). Reaction and anticipation in the car following behaviour. Proceedings of the 12th international symposium on traffic and transportation theory, 349–366.

Pal, D., & Chunchu, M. (2019). Modeling of lateral gap maintaining behaviour of vehicles in heterogeneous traffic stream. Transportation Letters, 11(7): 373-381.

Panwai, S., & Dia, H. (2007). Neural agent car-following models. IEEE Transactions on Intelligent Transportation Systems, 8: 60–70.

Papathanasopoulou, V., & Antoniou, C. (2015). Towards data-driven car-following models. Transportation Research Part C: Emerging Technologies, 55: 496-509.

Papathanasopoulou, V., & Antoniou, C. (2018). Flexible car–following models for mixed traffic and weak lane–discipline conditions. European Transport Research Review, 10(2): 62.

Papathanaspoulou, V., & Antoniou, C. (2019). Towards an integrated longitudinal and lateral movement data-driven model for mixed traffic. Transportation Research Procedia, 37: 489-496.

Pariota, L., Galante, F., & Bifulco, G. N. (2016). Heterogeneity of driving behaviours in different car-following conditions. Periodica Polytechnica Transportation Engineering, 44(2): 105-114.

Patel, N., & Upadhyay, S. (2012). Study of various decision tree pruning methods with their empirical comparison in WEKA. International journal of computer applications, 60(12): 20-25.

Pawar, D. S., Patil, G. R., Chandrasekharan, A., & Upadhyaya, S. (2015). Classification of gaps at uncontrolled intersections and midblock crossings using support vector machines. Transportation Research Record: Journal of Transportation Research Board, 2515(1): 26-33.

Pekkanen, J., Lappi, O., Rinkkala, P., Tuhkanen, S., Frantsi, R., & Summala, H. (2018). A computational model for driver's cognitive state, visual perception and intermittent attention in a distracted car following task. Royal Society open science, 5(9): 180-194.

Peng, G. H., Cai, X. H., Cao, B. F., & Liu, C. Q. (2011). Non-lane-based lattice hydrodynamic model of traffic flow considering the lateral effects of the lane width. Physics Letters A, 375(30-31): 2823-2827.

Pianosi, F., & Wagener, T. (2015). A simple and efficient method for global sensitivity analysis based on cumulative distribution functions. Environmental Modelling & Software, 67: 1-11.

Piao, J., & McDonald, M. (2003). Low Speed Car following Behaviour from Floating Vehicle Data. Proceedings of Intelligent Vehicles Symposium, IEEE, 462–467.

Pipes, L. A. (1953). An operational analysis of traffic dynamics. Journal of Applied Physics, 24(3): 274-281.

Ponnu, B., & Coifman, B. (2015). Speed-spacing dependency on relative speed from the adjacent lane: New insights for car following models. Transportation Research Part B: Methodological, 82: 74-90.

Probst, T., Krafczyk, S., Brandt, T., & Wist, E. R. (1984). Interaction between perceived self-motion and object-motion impairs vehicle guidance. Science, 225(4661): 536-538.

Pucher, J., Peng, Z. R., Mittal, N., Zhu, Y., & Korattyswaroopam, N. (2007). Urban transport trends and policies in China and India: impacts of rapid economic growth. Transport Reviews, 27(4): 379-410.

Punzo, V., Borzacchiello, M. T., & Ciuffo, B. (2011). On the assessment of vehicle trajectory data accuracy and application to the Next Generation SIMulation (NGSIM) program data. Transportation Research Part C: Emerging Technologies, 19(6), 1243-1262.

Punzo, V., & Simonelli, F. (2005). Analysis and comparison of microscopic traffic flow models with real traffic microscopic data. Transportation Research Record: Journal of Transportation Research Board, 1934: 53-63

Purucker, C., Rüger, F., Schneider, N., Neukum, A., & Färber, B. (2014). Comparing the perception of critical longitudinal distances between dynamic driving simulation, test track and Vehicle in the Loop. Proceedings of the 5th Advances in human aspects of transportation (AHFE) Conference, 19(23.07): 421-430.

Qingyi, A. I., Zhuo, Y. A. O., Heng, W. E. I., & Zhixia, L. I. (2010). Identifying Characteristics of Freeway Traffic Headway by Vehicle Types Using Video Trajectory Data. Tenth International Conference of Chinese Transportation Professionals (ICCTP), American Society of Civil Engineers. doi:10.1061/41127(382)214.

Qu, D., Chen, X., Yang, W., & Bian, X. (2014). Modeling of car-following required safe distance based on molecular dynamics. Mathematical Problems in Engineering, 2014: 1-7. doi: 10.1155/2014/604023

Qu, X., Kuang, Y., Oh, E., Jin, S. (2014a). Safety evaluation for expressways: a comparative study for macroscopic and microscopic indicators. Traffic injury prevention, 15(1): 89-93.

Qu, X., Yang, Y., Liu, Z., Jin, S., Weng, J. (2014b). Potential crash risks of expressway on-ramps and off-ramps: a case study in Beijing, China. Safety science, 70: 58-62.

Radwan, A. E., & Sinha, K. C. (1980). At Stop Controlled Intersections On Multi- Lane Divided Highways. ITE journal, 3: 38–44.

Rahman, A., & Lownes, N. E. (2012). Analysis of Rainfall Impacts on Platooned Vehicle Spacing and Speed. Transportation Research Part F: Traffic Psychology and Behaviour, 15(4): 395–403.

Raju, N., Arkatkar, S., & Joshi, G. (2018). Study of Vehicle-Following Behaviour Under Heterogeneous Traffic Conditions. International Conference on Traffic and Granular Flow, Springer, Cham, 87-95.

Raju, N., Arkatkar, S., & Joshi, G. (2019). Methodological framework for modeling following behaviour of vehicles under Indian traffic scenario. Innovative research in transportation infrastructure, Springer, Singapore, 1-11.

Rakha, H., & Wang, W. (2009). Procedure for calibrating Gipps car-following model. Transportation Research Record: Journal of the Transportation Research Board, 2124(1): 113–124.

Ravishankar, K. V. R., & Mathew, T. V. (2011). Vehicle-type dependent car-following model for heterogeneous traffic conditions. Journal of Transportation Engineering, 137(11): 775-781.

Reiter, U. (1994). Empirical Studies as Basis for Traffic Flow Models. Proc. of the Second International Symposium on Highway Capacity, 2: 493-502

Reuschel, A. (1950). Fahrzeugbewegungen in der Kolonne. Osterreichisches Ingenieur Archiv, 4: 193-215.

Riad, S., Mania, J., Bouchaou, L., & Najjar, Y. (2004). Rainfall-runoff model usingan artificial neural network approach. Mathematical and Computer Modelling, 40(7-8): 839-846.

Richardson, M., & Domingos, P. (2006). Markov Logic Networks. Machine Learning, 62 (1-2): 107–136. doi:10.1007/s10994-006-5833-1.

Rogé, J., Ferretti, J., & Devreux, G. (2010). Sensory Conspicuousness of Powered Two-wheelers during Filtering Manœuvre, According to the Age of the Car Driver. Le travail humain, 73: 7-30.

Rossi, R., Gastaldi, M., & Pascucci, F. (2014). Gamma-GQM Time Headway Model: Endogenous Effects in Rural Two-Lane Two-Way Roads. Procedia-Social and Behavioural Sciences, 111: 859–868.

Saha, P., Mahmud, H. I., Hossain, Q. S., & Islam, M. Z. (2009). Passenger Car Equivalent (PCE) of through Vehicles at Signalized Intersections in Dhaka Metropolitan City, Bangladesh. IATSS Research, 33 (2): 99–104.

Saifuzzaman, M., & Zheng, Z. (2014). Incorporating human-factors in car-following models: a review of recent developments and research needs. Transportation Research Part C: Emerging Technologies, 48: 379-403.

Sangole, J. P., & Patil, G. R. (2014). Modeling vehicle group gap acceptance at uncontrolled T-intersections in Indian traffic. 93rd Annual Meeting of Transportation Research Board, 14-4866, Washington D.C., USA.

Sarvi, M. (2013). Heavy commercial vehicles-following behaviour and interactions with different vehicle classes. Journal of advanced transportation, 47(6): 572-580.

Sayed, T., Brown, G., & Navin, F. (1994). Simulation of traffic conflicts at unsignalized intersections with TSC-Sim. Accident Analysis & Prevention, 26(5): 593-607.

Sayer, J. R., Mefford, M. L., & Huang, R. (2003). The Effect of Lead Vehicle Size on Driver Following Behaviour: Is Ignorance Truly Bliss? Proceedings of the 2nd international driving symposium on human factors in driver assessment, training and vehicle design, Park City, Utah.

Schermelleh-Engel, K., Moosbrugger, H., & Muller, H. (2003). Evaluating the fit of structural equation models: tests of significance and descriptive goodness-of fit measures. Methods of Psychological Research Online, 8(2): 23–74.

Schmidt, R. (1993). Unintended acceleration: Human performance considerations. Automotive Ergonomics, 431-451.

Schweitzer, N., Apter, Y., Ben-David, G., Liebermann, D., & Parush, A. (1995). A field study on braking responses during driving II. Minimum driver braking times. Ergonomics, 38: 1903–1910.

Sermpis, D., & Spyropoulou, I. (2007). Parameters related to modelling motorcycle movement. 86th Annual Meeting of Transportation Research Board, Washington, D.C.

Sermpis, D., Spyropoulou, I., & Golias, J. (2005). Investigation of the two-wheel vehicle movement at urban signal-controlled junctions. 84th Annual Meeting of Transportation Research Board, Washington, D.C.

Shekleton, S. (2002). A GPS study of car following theory. Conference of Australian Institutes of Transport Research (CAITR). http://www.sidrasolutions.com/documents/CAITR2002_SimonShekletonPaper.PDF

Siebert, F. W., Oehl, M., & Pfister, H. R. (2014). The Influence of Time Headway on Subjective Driver States in Adaptive Cruise Control. Transportation Research Part F: Traffic Psychology and Behaviour, 25: 65–73.

Simon, P. M., Esser, J., & Nagel, K. (1999). Simple queueing model applied to the city of Portland. International Journal of Modern Physics C, 10(05): 941-960.

Simonelli, F., Bifulco, G. N., De Martinis, V., & Punzo, V. (2009). Human-like adaptive cruise control systems through a learning machine approach. Applications of Soft Computing, Springer, Berlin, Heidelberg, 240-249.

Siuhi, S., & Kaseko, M. (2013). Nonlinear acceleration and deceleration response behaviour in stimulus-response car-following models. Advances in Transportation Studies, 31: 81-96.

Siuhi, S., & Kaseko, M. (2016). Incorporating vehicle mix in stimulus-response car-following models. Journal of Traffic and Transportation Engineering, 3(3): 226-235.

Sivak, M., Post, D., Olson, P., & Donohue, R. (1981a). Automobile rear lights: Effect of the number, mounting height, and lateral position on reaction times of following drivers. Perceptual and Motor Skills, 52: 795–802.

Sivak, M., Post, D., Olson, P., & Donohue, R. (1981b). Driver responses to high-mounted brake lights in actual traffic. Human Factors, 23: 231–235.

Sklar, A. (1973). Random Variables, Joint Distribution Functions, and Copulas. Kybernetika, 9(6): 449–460.

Sklar, M. (1959). Fonctions de répartition à n dimensions et leurs marges. Publications de l'Institut Statistique de l'Université de Paris, 8: 229–231.

Srinivasan, D., Choy, M. C., Cheu, R. L. (2006). Neural networks for real-time traffic signal control. IEEE Transactions on Intelligent Transportation Systems, 7(3): 261–272.

Srinivasan, D., Jin, X., & Cheu, R. L. (2004). Evaluation of adaptive neural network models for freeway incident detection. IEEE Transactions on Intelligent Transportation Systems, 5(1): 1-11.

Srivaree-Ratana, C., Konak, A., & Smith, A. E. (2002). Estimation of all-terminal network reliability using an artificial neural network. Computers & Operations Research, 29(7): 849-868.

Stephenson, S., Meng, X., Moore, T., Baxendale, A., & Ford, T. (2011). Accuracy requirements and benchmarking position solutions for intelligent transportation location based services. Proceedings at the 8th International Symposium on Location-Based Services, 21-23 November, 2011, Vienna.

Strauss, D., & Ikeda, M. (1990). Pseudolikelihood Estimation for Social Networks. Journal of the American Statistical Association, 85(409): 204–212.

Suweda, I. W. (2016). Time Headway Analysis to Determine the Road Capacity. Jurnal Spektran, 4(2): 71–80.

Taieb-Maimon, M., & Shinar, D. (2001). Minimum and Comfortable Driving Headways: Reality versus Perception. Human Factors: The Journal of the Human Factors and Ergonomics Society, 43(1): 159–172.

Tang, T., Li, C., Wu, Y., & Huang, H. (2011). Impact of the honk effect on the stability of traffic flow. Physica A: Statistical Mechanics and its Applications, 390(20): 3362–3368.

Tao, P., Hu, H., Gao, Z., Li, Z., Song, X., Xing, Y., Wei, F., & Duan, Y. (2015). An Improved General Motor Car-Following Model considering the Lateral Impact. Advances in Mechanical Engineering, 7(2): 894589.

Tao, P., Hu, H., Gao, Z., Liu, X., Song, X., Xing, Y., Wei, F., & Wei, F. (2014). The research of the driver attention field modeling. Discrete dynamics in nature and society, 2014: 1-9. doi: 10.1155/2014/270616

Toledo, T., Koutsopoulos, H. N., & Ben-Akiva, M. E. (2003). Modeling integrated lane-changing behaviour. Transportation Research Record: Journal of theTransportation Research Board, 1857(1): 30-38.

Tordeux, A., Lassarre, S., & Roussignol, M. (2010). An adaptive time gap car-following model. Transportation research part B: methodological, 44(8-9): 1115-1131.

Törnros, J. (1995). Effect of driving speed on reaction time during motorway driving. Accident Analysis & Prevention, 27(4): 435-442.

Treiber, M., Hennecke, A., & Helbing, D. (2000a). Congested traffic states in empirical observations and microscopic simulations. Physical Review E, 62(2): 1805–1824.

Treiber, M., Hennecke, A., & Helbing, D. (2000b). Microscopic simulation of congested traffic. Traffic and Granular Flow'99: 365-376.

Treiber, M., Kesting, A., & Helbing, D. (2006). Delays, inaccuracies and anticipation in microscopic traffic models. Physica A: Statistical Mechanics and its Applications, 360(1): 71-88.

Treiber, M., Kesting, A., & Helbing, D. (2007). Influence of reaction times and anticipation on stability of vehicular traffic flow. Transportation Research Record: Journal of the Transportation research Board, 1999(1): 23-29.

Treiber, M., & Kesting, A. (2013). Traffic Flow Dynamics: Data, Models and Simulation. Physics Today, 67(3): 54.

Treiterer, J., & Myers, J. A. (1974). The hysteresis phenomenon in traffic flow. Proceedings of the sixth International Symposium on Transportation and Traffic Theory, Sydney, 13–38.

Van der Horst, R., & Godthelp, H. (1989). Measuring road user behaviour with an 625 instrumented car and an outside-the-vehicle video observation technique. Transportation Research Record: Journal of Transportation Research Board, 1213: 72-81.

Van der Horst, R., & Hogema, J. (1993). Time-to-collision and collision avoidance systems. In Proceedings of 6th ICTCT Workshop Safety Evaluation of Traffic Systems: Traffic Conflicts and Other Measures, Salzburg, October, 109-121.

Van Winsum, W., & Heino, A. (1996). Choice of time headway in car following and the role of time to collision information in braking. Ergonomics, 39: 579–592

Van Winsum, W. (1999). The human element in car following models. Transportation Research Part F: Traffic Psychology And Behaviour, 2(4): 207-211.

Vlahogianni, E. I. (2014). Powered-two-wheelers kinematic characteristics and interactions during filtering and overtaking in urban arterials. Transportation Research Part F: Traffic Psychology and Behaviour, 24: 133–145.

Vogel, K. (2003). A comparison of headway and time to collision as safety indicators. Accident analysis & prevention, 35(3): 427-433.

Wasielewski, P. (1979). Car-Following Headways on Freeways Interpreted by the Semi-Poisson Headway Distribution Model. Transportation Science, 13(1): 36–55.

Watanabe, Y., & Ito, S. (2007). Influence of vehicle properties and human attributes on neck injuries in rear-end collisions. 20th International Technical Conference on the Enhanced Safety of Vehicles (ESV) National Highway Traffic Safety Administration (No. 07-0160).

Wilde, G. J. (1982). The theory of risk homeostasis: implications for safety and health. Risk Analysis, 2(4): 209-225.

Wilde, G. J. (1998). Risk homeostasis theory: an overview. Injury Prevention, 4(2): 89-91.

Xing, C. F., Yang, L., & Zhang, Y. H. (2015). Study of driver's reaction time (DRT) during car following. Applied Mechanics and Material, 713-715: 2089-2092. doi: 10.4028/www.scientific.net/AMM.713-715.2089

Xu, L., Hu, S., Luo, Q., & Zhang, L. (2015). Research on Car-following model considering lateral offset. International Journal of Engineering Research in Africa, 13: 71-80.

Xu, L., Li, Y., & Feng, H. (2018). Non-Lane-Discipline-Based Car-Following Model Considering the Effects of Full Lateral Gaps. Chinese Automation Congress (CAC), 1146-1150.

Xu, R. G. (2015). Multiple traffic jams in Full Velocity Difference Model with reaction time delay. International Journal of Simulation Models, 14(2): 325-334.

Yang, Y., & Chen, W. (2016). Taiga: performance optimization of the C4.5 decision tree construction algorithm. Tsinghua Science and Technology, 21(4): 415-425.

Ye, F., & Zhang, Y. (2009). Vehicle Type-Specific Headway Analysis Using Freeway Traffic Data. Transportation Research Record: Journal of the Transportation Research Board, 2124: 222–230.

Yin, S., Li, Z., Zhang, Y., Yao, D., Su, Y., & Li, L. (2009). Headway Distribution Modeling with Regard to Traffic Status. Intelligent Vehicles Symposium, IEEE, 1057–1062. doi:10.1109/IVS.2009.5164427.

Young, S. (2012). Ergonomics issues with advanced driver assistance systems (ADAS). Automotive Ergonomics, 810: 55-76.

Zhang, X., & Bham, G. H. (2007). Estimation of Driver Reaction Time from Detailed Vehicle Trajectory Data. Proceedings of the 18th IASTED international conference, Montreal, Canada, 574–579.

Zhao, P., & Lee, C. (2017). Analysis and Validation of Surrogate Safety Measures by Types of Lead and Following Vehicles. Transportation Research Record: Journal of the Transportation Research Board, 2659(1): 137-147.

Zheng, J., Suzuki, K., & Fujita, M. (2013). Car-following behaviour with instantaneous driver–vehicle reaction delay: A neural-network-based methodology. Transportation Research Part C: Emerging Technologies, 36: 339-351.

Zheng, L., Jin, P. J., Huang, H., Gao, M., & Ran, B. (2015). A vehicle type-dependent visual imaging model for analysing the heterogeneous car-following dynamics. Transportmetrica B: Transport Dynamics, 4(1): 68-85. DOI: 10.1080/21680566.2015.1055618

Zheng, L., Zhong, S., Jin, P. J., & Ma, S. (2012). Influence of lateral discomfort on the stability of traffic flow based on visual angle car-following model. Physica A: Statistical Mechanics and its Applications, 391(23): 5948-5959.

Zhou, J., Shi, Z. K., & Cao, J. -L. (2014). Nonlinear analysis of the optimal velocity difference model with reaction time delay. Physica A: Statistical Mechanics and its Applications, 396: 77-87.

Zou, Y., Zhang, Y., & Zhu, X. (2014). Constructing a Bivariate Distribution for Freeway Speed and Headway Data. Transportmetrica A: Transport Science, 10(3): 255–272. doi:10.1080/18128602.2012.745099.

Zou, Y., & Zhang, Y. (2016). A Copula-based Approach to Accommodate the Dependence among Microscopic Traffic Variables. Transportation Research Part C: Emerging Technologies, 70: 53–68. doi:10.1016/j.trc.2015.11.003.

Zou, Y., Yang, H., Zhang, Y., Tang, J., & Zhang, W. (2017). Mixture Modeling of Freeway Speed and Headway Data Using Multivariate Skew-t Distributions. Transportmetrica A: Transport Science, 13 (7): 657–678. doi:10.1080/23249935.2017.1318973.

Theses

Ahmed, K. I. (1999). Modeling drivers' acceleration and lane changing behaviour. Doctoral dissertation, Department of Civil and Environmental Engineering, Massachusetts Institute of Technology, Massachusetts, USA.

Brown, D. (2012). A comparison of drivers' braking responses across ages. Master's Thesis, East Carolina University, North Carolina, USA.

Budhkar, A. K. (2017). Modelling of Inter-vehicular Gaps and Driver Behaviour in Heterogeneous Traffic Stream with Weak Lane Discipline. Doctoral Dissertation, Indian Institute of Technology Guwahati, Guwahati, India.

Chen, R. (2016). Driver Behaviour in Car Following-The Implications for Forward Collision Avoidance. Doctoral Dissertation, Virginia Tech, Virginia, USA.

Choudhury, C. F. (2007). Modeling driving decisions with latent plans. Doctoral Dissertation, Massachusetts Institute of Technology, Massachusetts, USA.

Dickie, D. A. (2010). The effects of trust on the use of adaptive cruise control. Master's Thesis, University of Iowa, Iowa, USA.

Kesting, A. (2008). Microscopic modeling of human and automated driving: Towards traffic-adaptive cruise control. Doctoral Dissertation, Technische Universität Dresden, Dresden, Germany.

Lee, T.-C. (2008). An Agent-Based Model to Simulate Motorcycle Behaviour in Mixed Traffic Flow. Doctoral Dissertation, Imperial College London, United Kingdom. Retrieved from: www.cts.cv.ic.ac.uk/documents/theses/LeePhD.pdf.

Maurya, A. K. (2007). Development of a Comprehensive Microscopic Model for Simulation of Large Uninterrupted Traffic Streams without Lane Discipline. Doctoral Dissertation, Indian Institute of Technology Kanpur, India.

Nguyen, X. L. (2012). A concept of safety space for describing non-lane-based movements of motorcycles. Doctoral Dissertation, Tokyo Institute of Technology, Japan.

Siddique, M. (2013). Modeling Drivers' Lateral Movement Behaviour under Weak-Lane-Disciplined Traffic Conditions. Master's Thesis, Bangladesh University of Engineering and Technology, Bangladesh.

Subramanian, H. (1996). Estimation of car following models. Master's thesis. Massachusetts Institute of Technology, Massachusetts, USA.

Van der Horst, R. (1990). A time-based analysis of road user behaviour in normal and critical encounters. Doctoral Dissertation, Delft University of Technology, Netherlands.

Books/Reports/Manuals

ACEM (Association des Constructeurs Européens de Motocycles) (2009). In-depth investigations of accidents involving powered two-wheelers (MAIDS). Retrieved from http://www.maids-study.eu/pdf/MAIDS2.pdf

Akbar, P. A., Couture, V., Duranton, G., Ghani, E., & Storeygard, A. (2018). Mobility and congestion in urban India. The World Bank.

Austroads Research Report (2013). Vehicle positioning for C-ITS in Australia. AP-R431-13, Austroads Ltd, Sydney.

Baber, C. (1994). Psychological aspects of in-car warning devices. In Stanton, N. (Ed.), Human Factors in Alarm Design. Taylor &Francis, London.

Bollen, K. A. (1989). Structural equations with latent variables, John Wiley & Sons, New York.

Bovik, A. C. (2010). Handbook of image and video processing. Academic press.

Braun, M., Coleman, C. S., & Drew, D. A. (1983). Modules in Applied Mathematics: Volume 1 Differential Equation Models, Springer-Verlag New York Inc, ISBN:13:978-1-4612-5429-4, doi: 10.1007/978-1-4612-5427-0

Clarke, D. D., Ward, P., Bartle, C., & Truman, W. (2004). In-depth study of motorcycle accidents. Road Safety Research Report, Department for Transport, London, UK.

CPCB (1999). Central Pollution Control Board – auto emissions, Parivesh Newsletter. 6(1), New Delhi, June.

DeSilva, H., & Forbes, T. (1937). Driver testing results. Cambridge, MA: Harvard Traffic Bureau.

Fausett, L. (1994). Fundamentals of neural networks. Prentice Hall, Englewood Cliffs, N.J

FEMA (2009). A european agenda for motorcycle safety: The motorcyclists' point of view. Technical report, Federation of European Motorcyclists Associations.

Franklin, S. & Graesser, A. (1997). Is it an agent, or just a program?: A taxonomy for autonomous agents. In J. P. Müller, M. J. Wooldridge & N. R. Jennings (Eds.), Intelligent Agents III: Agent Theories, Architectures, and Languages, 21-35, Springer, London.

Fuller, R. G. C. (1986). Reflections on risk homeostasis theory. In New Directions in Research on Decision Making (Edited by B. Brehmer, H. Jungermann, P. Lourens and G. Sevgn). North-Holland, Amsterdam, 263-273.

German Federal Statistical Office (2009). Verkehrsunfälle. Fachserie 8, Reihe 7.

Greenshields, B. D., Shapiro, D., & Ericksen, E. L. (1947). Traffic performance at urban street intersections, Technical Report No. 1.Bureau of Highway Traffic, Yale University.

Gunn, S. R. (1998) Support Vector Machines for Classification and Regression. Technical Report. Department of Electrical and Computer Science, University of Southampton.

Harman, H. H. (1976). Modern factor analysis. University of Chicago press, Chicago and London.

Hayward, J. (1972). Near misses as a measure of safety at urban intersections. Pennsylvania Transportation and Traffic Safety Center.

Highway Capacity Manual (2000). Transportation Research Board, National Research Council, Washington D.C., USA.

Hogema, J.H., & Janssen, W.H. (1996). Effects of Intelligent Cruise Control on Driving Behaviour. TNO Human Factors, Soesterberg, the Netherlands, Report tm-1996-c-12.

Hoyle, R. H. (1995). The Structural Equation Modelling Approach: Basic Concepts and Fundamentals Issues (Edited by R. H. Hoyle), Structural Equation Modelling: Concepts, Issues, and Applications.

Hurt, H. H., Ouellet, J. V., & Thom, D. R. (1981). Motorcycle accident cause factors and identification of countermeasures. DOT-HS-5-01160, Volume 1. National Highway Traffic Safety Administration, US Department of Transportation.

Hydén, C. (1996). Traffic conflicts technique: state-of-the-art. Traffic safety work with video processing, 37: 3-14.

International Organization for Standardization [ISO] (2010). ISO 15622: 2010: Intelligent transport systems — Adaptive Cruise Control systems — Performance requirements and test procedures. Geneva.

Joe, H. (1997). Multivariate Models and Dependence Concepts. Monographs on Statistics and Applied Probability, Vol. 73. Boca Raton, FL: Chapman & Hall.

Kraay, J. H., & van der Horst, A. (1985). Trautenfels–study: a diagnosis of road safety using the Dutch Conflict observation technique. DOCTOR (Report R–85–53), Institute for Road Safety Research SWOV, Leidschendam.

Langton, C.G. (1989). Artificial life. In Artificial Life. C. Langton (ed.). Addison-Wesley.

Liu, R. (2010). Traffic Simulation with DRACULA. In Fundamentals of Traffic Simulation (J. Barceló, ed.), Springer.

MacCallum, R. C. (1995). Model specification: Procedures, strategies, and related issues. (Edited by R. H. Hoyle), Structural equation modeling: Concepts, issues, and applications, Thousand Oaks, CA: Sage Publications, 16-36.

Miller, A. J. (1972). Nine Estimators of Gap-Acceptance Parameters. In Traffic Flow and Transportation, G.Newell, ed., American Elseview Publ. Co. Inc., New York, 215–235.

MoRTH (2017). Road accidents in India- 2017. http://www.indiaenvironmentportal.org.in/files/file/road%20accidents%20in%20India%202017.pdf

MoRTH (2019). Annual Report 2018-2019. Ministry of Road Transport and Highways, Government of India, New Delhi.

PREVENT (2006). Code of practice for the design and evaluation of ADAS. Deliverable D11.2, Integrated Project PREVENT.

Racelogic Video VBox lite with cameras- User Manual (2011). VBox motorspot, Racelogic Ltd.

Raff, M. S., & Hart, J. W. (1950). A volume warrant for urban stop signs. Eno Foundation for Highway Traffic Control, Bureau of Highway Traffic, Saugatack, USA.

Sexton, B., Fletcher, J., & Hamilton, K. (2004). Motorcycle accidents and casualties in Scotland 1992–2002. Research Findings No. 194/2004. Transport Planning Group, Edinburgh, UK.

Silcock, J. P. (1993). SIGSIM version 1.0 users guide. Working Paper. Centre for Transport Studies, University of London.

Simon, H. A. (1972). Theories of Bounded Rationality, in: Decision and Organization (Edited by C.B. McGuire, R. Radner), North-Holland, Amsterdam, Chapter 8.

Solberg, P. (1964). A Study of LAG and GAP Acceptances at Stop-Controlled Intersections. Joint Highway Research Project, Purdue University.

Suhr, D. (2010). The basics of structural equation modeling. www.lexjansen.com/wuss/2006/tutorials/TUT-Suhr.pdf (Accessed 18th October, 2017).

Svensson, A. (1992). Further development and validation of the Swedish traffic conflicts technique. Dept. of Traffic planning and Engineering. Lund University. Lund, Sweden

Traffic Safety Facts (2013). Publication DOT HS 812 139. NHTSA, U.S. DOT.

Triggs, T. J., & Harris, W. G. (1982). Reaction time of drivers to road stimuli. Monash University Human Factors Group- Report HFR-12

Vapnik, V. N. (1998). Statistical Learning Theory, Vol. 2. John Wiley and Sons, New York.

Wasserman, P. D. (1989). Neural computing: Theory and Practice. Van Nostrand Reinhold, New York.

Wiedemann, R. (1974). Simulation des Strassenverkehrsflusses. Technical report, Institut fur Verkehrswesen, Universitat Karlsruhe, Karlsruhe, Germany.

Wiedemann, R., & Reiter, U. (1992). Microscopic traffic simulation: the simulation system MISSION, background and actual state. Project ICARUS (V1052), Final Report, vol. 2, Appendix A. Brussels: CEC.

Wilks, D. S. (2011). Statistical Methods in the Atmospheric Sciences, Vol. 100, 3rd ed., Academic Press, Boston, Mass.

Web Access

The Boston Consulting Group (BCG) and commissioned by Uber, Unlocking cities: the impact of ridesharing across India. (Accessed on 2nd January 2020)

World Health Organization (2018). https://www.who.int/violence_injury_prevention/road_safety_status/2018/en/ (Accessed on 22nd December 2019)

World Bank (2018). https://data.worldbank.org/indicator/NY.GDP.PCAP.CD?locations=IN&start=1980 (Accessed 2nd January 2020).

List of Publications

Journals

Das, S., & Maurya, A. K. (2018). Modelling of motorised two-wheelers: a review of the literature. Transport Reviews, 38(2): 209-231.

Das, S., Maurya, A. K., & Budhkar, A. K. (2019). Determinants of time headway in staggered car-following conditions. Transportation Letters: The International Journal of Transportation Research, 11(8): 447-457.

Das, S., & Maurya, A. K. (2018). Multivariate analysis of microscopic traffic variables using copulas in staggered car-following conditions. Transportmetrica A: Transport science, 14(10): 829-854.

Das, S., & Maurya, A. K. (2018). Bivariate modeling of time headways in mixed traffic streams: a copula approach. Transportation Letters: The International Journal of Transportation Research, 1-11. doi: 10.1080/19427867.2018.1537209

Das, S., & Maurya, A.K. (2019). Modelling of motorised two-wheelers' manoeuvrability during filtering in urban roads, Transportation Research Record: Journal of the Transportation Research Board. doi:10.1177/0361198119842818

Das, S., Maurya, A. K., & Budhkar, A. K. (2019). Dynamic data collection of staggered-following behaviour in non-lane-based traffic streams. SN Applied Sciences, 1(6), 591. doi: 10.1007/s42452-019-0604-3

Das, S., & Maurya, A.K. (2019). Defining Time-to-Collision Thresholds by the Type of Lead Vehicle in Non-Lane Based Traffic Environments, IEEE Transactions on Intelligent Transportation Systems, 1-11. doi. 10.1109/TITS.2019.2946001

Das, S., Budhkar, A., Maurya, A. K., & Maji, A. (2019). Multivariate Analysis on Dynamic Car-Following Data of Non-lane-Based Traffic Environments. Transportation in Developing Economies, 5(2): 17.

Das, S., & Maurya, A. K. (2020). Pore acceptance predictions of motorised Two-Wheelers during filtering at urban Mid-Block sections. Journal of Intelligent Transportation Systems: Transport, Planning and Operations, 1-13.

Das, S., & Maurya, A. K. (2020). Modelling single-leader car-following behaviour in disorderly traffic: A neural network modelling framework (Under preparation)

Das, S., & Maurya, A. K. (2020). Modelling driver behaviour in a two-leader car-following scenario of disordered systems. (Under preparation)

Conferences

Das, S., Budhkar, A., Maurya, A.K., & Maji, A. (2018). Multivariate Analysis on Dynamic Car-following Data of non-lane based traffic environments, Third National Conference on Recent Advances in Traffic Engineering, August 11-12, Surat, India.

Das, S., & Maurya, A.K. (2018). Dynamic data collection of staggered-following behaviour in non-lane based traffic streams, 2nd International Conference on Sustainability, CESDOC 2018, December 18-19, Guwahati, India.

Das, S. (2019). Modelling filtering behaviour of motorized two-wheelers and cars in disordered traffic systems using decision trees, World Conference on Transport Research - WCTR 2019 May 26-31, Mumbai, India.

Das, S., & Maurya, A.K. (2019). Modeling of motorised two-wheelers' maneuverability during filtering in urban roads, 98th Annual Meeting of Transportation Research Board, January 13-17, Washington D.C., USA.

Das, S., & Maurya, A.K. (2019). Pore acceptance predictions of motorized two-wheelers at urban mid-block sections, 98th Annual Meeting of Transportation Research Board, January 13-17, Washington D.C., USA.